Design and Synthesis of Supramolecular Adducts of Nucleobases and Nucleosides

Thesis submitted to

University of Pune

For the degree of

Doctor of Philosophy

In

Chemistry

By

Sathyanarayana Reddy Perumalla

Division of Organic Chemistry
National Chemical Laboratory
Dr. Homi Bhabha Road
Pune 411 008

September 2008

DEDICATED TO MY BELOVED PARENTS

Shri. Ram Reddy Perumalla & Smt. Narsamma Perumalla

National Chemical Laboratory

Division of Organic Chemistry
Pune – 411008. India
Fax: +91(20) 25902624
Email: ***vr. pedireddi@ncl.res.in***

CERTIFICATE

This is to certify that the work presented in the thesis entitled **"Design and Synthesis of Supramolecular Adducts of Nucleobases and Nucleosides"** submitted by Sathyanarayana Reddy Perumalla, was carried out by the candidate at National Chemical Laboratory, Pune, under my supervision. Such materials as obtained from other sources have been duly acknowledged in the thesis.

September 2008

Dr. V. R. Pedireddi
Research Guide
Division of Organic Chemistry
National Chemical Laboratory
Pune 411 008.

CANDIDATE'S DECLARATION

I here by declare that the thesis entitled **"Design and Synthesis of Supramolecular Adducts of Nucleobases and Nucleosides"** submitted for the degree of Doctor of Philosophy in Chemistry to the University of Pune has not been submitted by me to any other university or institution. This work was carried out at the National Chemical Laboratory, Pune, India.

Sathyanarayana Reddy Perumalla

National Chemical Laboratory
Pune 411 008.
September 2008

Acknowledgements

With deep sense of gratitude and profound respect, I express my sincere thanks to my mentor, **Dr. V. R. Pedireddi** for his inspiring guidance and constant encouragement throughout my Ph.D. He has been my source of inspiration in many aspects. I have been able to learn many things from him and consider my association with him a rewarding experience.

It is my privilege to thank Dr. K. N. Ganesh, former Head of the Division of Organic Chemistry, NCL, and currently director, IISER Pune, for his constant support and encouragement during the progress of this work. I take this opportunity to thank Dr. Ganesh pandey, for his continued support as present Head of the Division.

I thank Dr. S. Sivaram, Director NCL, for giving infrastructure facilities and University grant commission for financial support. I also thank Dr. B. D. Kulkarni, Deputy Director, for his support and encouragement.

My heart felt thanks to Dr. C. V. V. Sathyanarayana for his assistance in powder X-ray diffraction analysis. I also thank Dr. Srinivas Hotha, Dr. Ramana, Dr. P. A. Joy and Dr. C. G. Suresh for fruitful scientific discussions and support in many aspects.

I am grateful to Dr. Mohan Bhadbhade, Dr. Mrs. Vedavathi Puranik Dr. Rajesh Gonnade and Dr. Manoj for their assistance in the single crystal X-ray diffraction. I would like to thank Dr. E. Suresh, Bhavnagar, for his assistance in the collection of X-ray diffraction data.

I take this opportunity to express my heartfelt thanks to my primary and higher secondary school teachers, Ramabrammam, Madusudan Rao, Ashok Reddy, Srinivasa Rao, Ram Reddy, Shashireka and Sarojini devi for their encouragement and motivation.

I am thankful to all the teachers and lecturers, who taught me throughout my career. My sincere thank to Ravinder, Sribabu and Ramachary, Prasanna Kumar and Namrata who ignited my interest in chemistry through excellent chemistry lectures.

I thank to all the faculty members of the School of Chemistry, University of Hyderabad, for their outstanding lectures during my M.Sc. tenure.

I wish to thank my friendly and cooperative labmates, Prakash, Kapil, Sunil, Seetha, Marivel, Manish kumar, Amit, Deepika, Shreeja, Parul, Yogesh, Mayura, Ketaki, Manish, Prince, and Asad for their help in various capacities and providing me with an excellent working ambience.

I am very much thankful to Prof. Poala Spadon, Prof. Lodovico, Prof. Dario Braga, Prof. Fabrizia Grepioni, Prof. Lia Addadi, Prof. Juan J. Novoa and the organizers of the ERICE-2007 meeting for their support and wonderful hospitality during my visit to Italy. I also thank NCL and DST for financial support for attending the ERICE-2007 meeting.

I sincerely thank Prof. Roland Boese, University of Essen, Germany and Prof. Judith Howard, University of Durham, UK for their support in various capacities.

I never thought about the research earlier in my life, but all my friends made me to think and pursue my career as chemistry. I thank all of them for their kind support and friendly environment.

I thank to my brother-Niranjan Reddy, Vadina-Lavanya, Akkalu- Niraja & Ramakka, Bavalu- Prabhakar Reddy and Venkat Reddy for their encouragement and allundlu- Pavan Kumar and Hanu for their smiles and wishes. I also thank to my mamalu and their family members, Sampath Reddy, chinna athamma, Somi Reddy mama, Pedda athamma, Varda Reddy mama, suguna athamma, Devender Reddy mama, Mani athamma, my fathers brothers- Ganapati Reddy and Jayapal Reddy; Narender babai, Baskar babai, Ratnakar babai, Ravinder babai, Linga Reddy mama & athamma, and all their family members.

I thank all my old friends Pulakka, chandraiah thatha, Mallaiah thatha, Sushilammama, Aga Reddy thatha and nanamma, Venkat Reddy thatha and nanamma, Vallapureddy Laxma Reddy mama and athamma, Vallapureddy Janardhan mama and athamma, Kotilingam shavkari, Danakka, Lakkarsu Mallaiah and ammamma, Lakkarsu Chandraiah and Bagyammatha, Lakkarsu Komuraiah and athamma,

Mogilaiah thatha, Rajahamsa nanamma, and all their family members for their cheerful environment as neighbors.

I thank my grand parents- Perumalla Raji Reddy, Linga Reddy, Malla Reddy; Chennuri Buchireddy; nanammalu-Rangamma, Lingareddy thatha nanamma and Mallareddy thatha nanamma and ammamma- Buchamma for their blessings.

The blessings and best wishes of my parents keep me active throughout my life. They made me what I am and I owe everything to them. Dedicating this thesis to them is a minor recognition for their invaluable support and encouragement.

I thank all of you once again for your kind support and cooperation.

Table of contents

Chapter 1

SUPRAMOLECULAR CHEMISTRY: CONCEPTS AND PROGRESS

Chapter 2

NUCLEOBASES IN MOLECULAR RECOGNITION

Chapter 3

CYTOSINE DUPLEXES

CHAPTER 4

MOLECULAR RECOGNITION STUDIES OF NUCLEOSIDES WITH 5-HALOURACILS

The thesis entitled **"Design and Synthesis of Supramolecular Adducts of Nucleobases and Nucleosides"** consists of four chapters. First chapter is an account of the introduction to supramolecular chemistry and its importance in chemical sciences in various aspects. In chapter two, syntheses of supramolecular assemblies of nucleobases with –COOH and triazine functional groups is presented. Chapter three deals with the design and synthesis of cytosine duplexes and co-crystals of 5-fluorocytosine, a bioactive cytosine derivative. Finally, in chapter four, molecular recognition features between halouracils and nucleosides are discussed.

Chapter 1

Noncovalent interactions, such as the hydrogen bonds, play a very important role in many natural processes - for example - stabilization of secondary and tertiary structures of many simple molecules like water (clusters of water in different topological arrangements such as hexagons, tetrahedrons etc.) to complex biomolecules like DNA (double helix), enzymes and proteins (variety of foldings, ribbons, etc.). Thus, utilization of the exotic features of such interactions in chemical sciences has emerged as one of the contemporary research areas that led to the evolution of new branch of science i.e., supramolecular chemistry.

Supramolecular chemistry as illustrated by noble laureate J. M. Lehn is the "*chemistry beyond the molecules*". As the molecules are constructed by atoms with covalent bonds, the supermolecules are due to the aggregation of molecules that are held together by noncovalent interactions. Some of the well known self-assembly patterns of the molecules are shown in Scheme 1, which have been well studied for the creation of exotic supramolecular assemblies. A detailed discussion of the contemporary research work in these areas is compiled in this chapter.

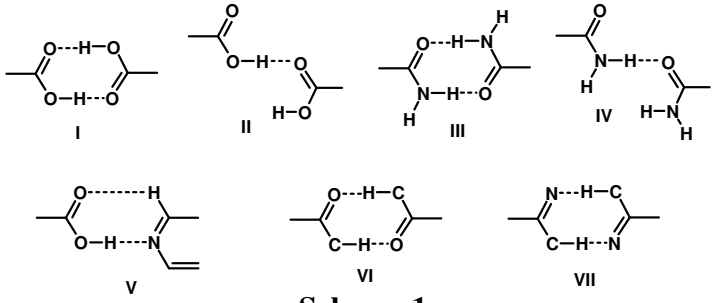

Scheme 1

Chapter 2

Nucleobases in Molecular Recognition

It is well known from the literature that the studies in supramolecular chemistry are dominated by molecules possessing complementary functional groups like –COOH and aza-donors. However, it is rather surprising to note that molecular recognition studies of nucleobases (adenine, thymine, guanine, cytosine and uracil), which are the prime constituents for the formation of different types of base pairs (Watson-Crick, Hoogsteen, etc.) and also possess hetero –N atoms (potential acceptors), are limited and not well explored as evident from the search performed on Cambridge Structural Database (CSD), an eloquent resource for the three-dimensional structural studies of small molecules of organic and organometallics. Thus, necessity of such studies are imminent, with current developments and challenges in the areas of biomimicking of natural systems, protein/enzyme/DNA interaction with drugs, computational aided drug design, etc., which may facilitate a thorough understanding of biological process.

For this purpose, to explore the intermolecular interactions, the natural nucleobases and their derivatives have been chosen and the endeavors have been initiated with the molecular recognition studies of the nucleobases with various derivatives of benzoic acid as shown in Scheme 2.

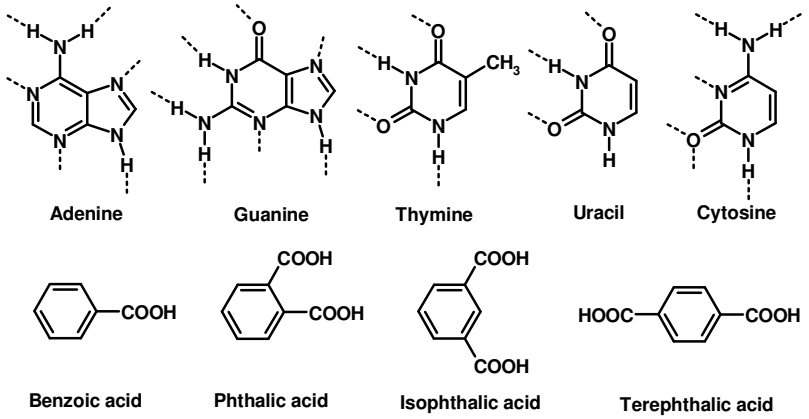

Scheme 2

The results were quite intriguing with the observation of selective recognition between nucleobases and –COOH moiety, with only adenine and cytosine being able

to form adducts with exotic supramolecular assemblies ranging from lamellar to ladder structures as shown in Figure 1, for the cytosine adducts of different benzoic acids.

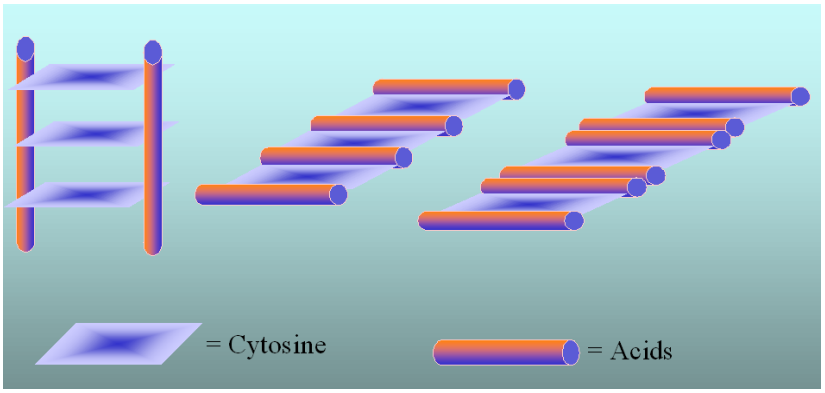

Figure 1. Schematic representation of three-dimensional packing in the complexes of cytosine with different benzoic acids.

Encouraged by the successful selective recognition features observed in the above study with nucleobases, further investigations of cocrystallization studies with different ligands, which are basic in nature, like melamine have been carried out. It has been observed that nucleobases (for example, thymine and uracil) that were inert to –COOH group, as described above, have only shown interaction with melamine. In addition, it is noteworthy to mention that the three-dimensional structures of these complexes are quite exotic, especially the observation of host-guest type assembly with channels, that were occupied by the solvent of crystallization molecules, in the complex of melamine and thymine, as shown in Figure 2. In this chapter, a detailed discussion of all the structural features would be presented.

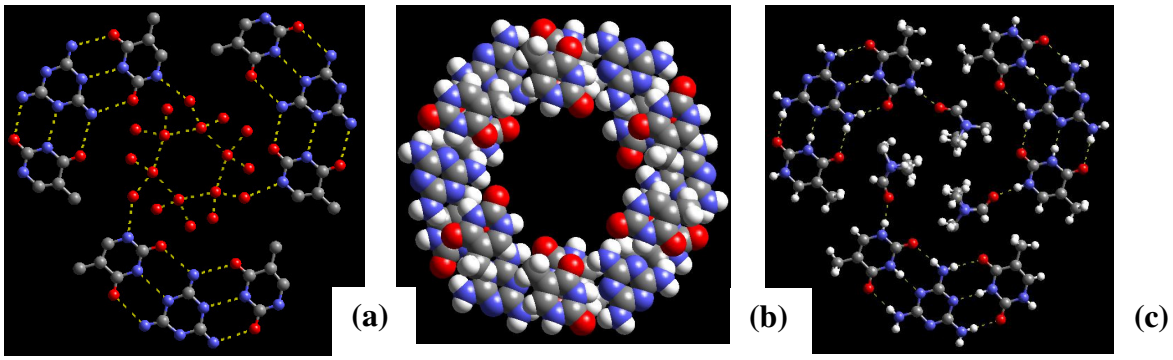

Figure 2. Two-dimensional arrangement of supramolecular units of melamine and thymine. a) water in the channels, b) space filling representation of channels and c) DMF in channels.

Chapter 3

Cytosine duplexes: from understandings to applications

Telomere DNA at chromosome ends has a large number of repeating sequences in which DNA strands typically have guanine or cytosine clusters. While G-rich DNA oligomers are well known to form G-tetrads *via* Watson-Crick and Hoogsteen hydrogen bond mediated cyclic structures, the complementary C-rich sequences in acidic conditions aggregates as tetramers *via* the hemiprotonated cytosine-cytosine base pairs ($C–C^+$), which referred as I-motifs, formed by intercalation processes of parallel double strands.

It is evident from the literature that the importance of G-quartets and $C\text{-}C^+$ interactions have been demonstrated in several biological processes, but studies to mimic such patterns through supramolecular synthesis are not well known, in particular $C\text{-}C^+$ interactions. Hence, to investigate such novel structural features, co-crystallization studies of cytosine with various molecules, possessing acidic hydrogen as shown in the Scheme-3, has been initiated.

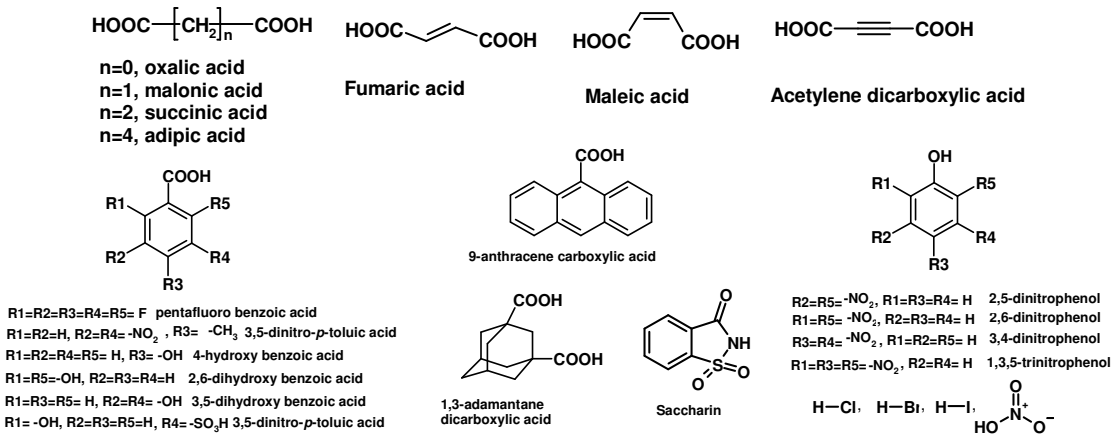

Scheme-3

In all these assemblies the $C\text{-}C^+$ interaction have been observed, irrespective of the nature of the complementary molecules, as illustrated in Figure 3 for some representative examples.

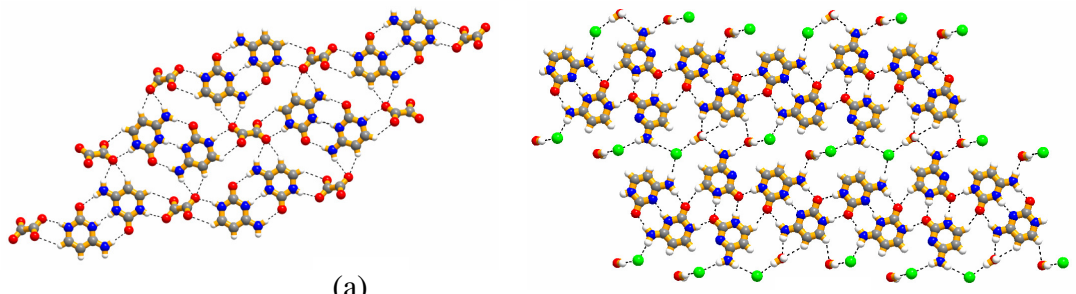

Figure 3: Representative examples of the cytosine duplexes formed in the molecular adducts with a) oxalic acid and b) hydrochloric acid.

Furthermore, such exotic structural motifs have been identified even in the co-crystals of cytosine derivatives, for example, 5-fluorocytosine (FC), an active pharmaceutical ingredient (API) as shown in Figure 4. The structural features of all the complexes are discussed in detail, in this chapter.

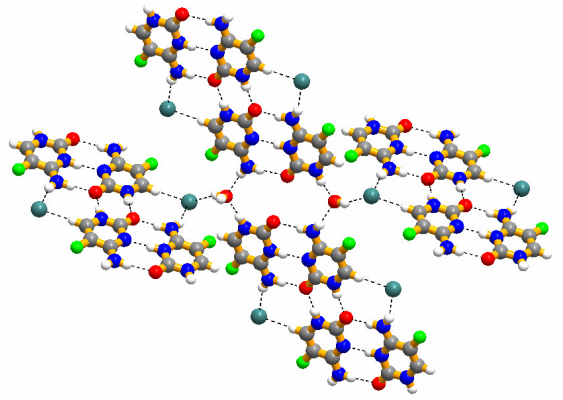

Figure 4: Arrangement of molecules of 5-fluorocytosine and in its hydrochloride salt.

Chapter 4

Molecular recognition studies of 5-halouracils with nucleosides

Understanding the biological properties of various molecules in a chemistry point of view is a long standing research goal for the chemists and

biologists as exemplified by the molecular recognition studies of nucleobases with cis-platinum complexes to simplify the understanding processes of antitumor activity.

On the other hand, the recent new-dimensions in the chemical genetics research front, particularly, the binding studies of DNA with various chemical entities such as drugs and inhibitors emerged as the focus of contemporary research to understand the various biological features like protein-drug interactions, target based design of new chemical entities etc. which proceed through nucleosides and nucleotides. However, mostly, the studies are confined to computational approaches and with a very limited number of experimental studies.

Hence, to understand the intrinsic nature of interaction between the substrates within chemical biological studies, synthesis and structural evaluation of numerous nucleosides with different bioactive compounds, such as halo uracils (5-fuloro (FU), chloro (CU), bromo (BU) and iodouracils (IU)), which are well known as chemical mutagens, antiviral agents, and anticancer drugs, were chosen.

In this direction, adenosine (ADS), uridine (URD), thymidine (TMD), cytidine (CTD) and guanosine (GNS) have been considered to co-crystallize with FU, CU, BU and IU, as shown in the Scheme 4.

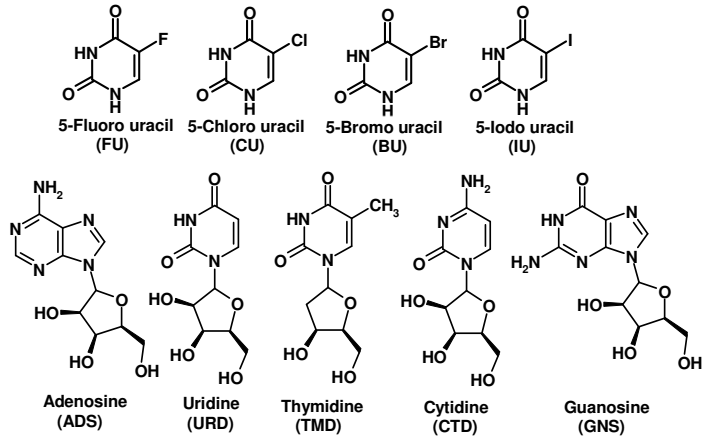

Scheme 4

X-ray diffraction (XRD) analysis of the resulting crystals/precipitates revealed that alike in the study of nucleobases with –COOH group, as discussed in chapter two, nucleosides also did show selectivity in such a manner that ADS, URD and CTD only form complexes with the 5-halouracils, whereas GNS and TMD remain

inert towards the XU. Structural representation of the complex of ADS and 5-Fluorouracil is shown in figure 5. Further interesting feature of this study is that, while ADS form complexes with all the XU, URD and CTD forms adduct only with FU. A detailed discussion of salient features of all the complexes would be compiled in this chapter.

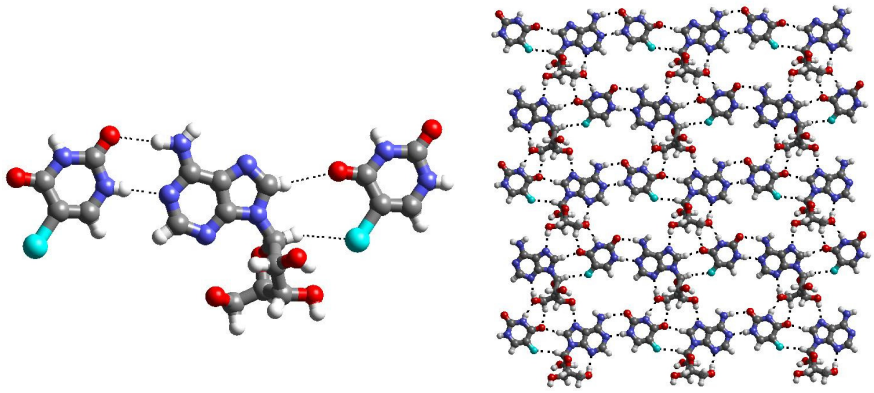

(a) (b)

Figure 5: a) Recognition between adenosine and a 5-fluorouracil b) 2D arrangement of ADS-XU adducts forming sheet like structure.

References:

[1] a) J. D. Watson, F. H. C. Crick, *Nature* **1953,** *171,* 964-967. b) G. A. Jeffrey, W. Saenger, *Hydrogen Bonding in Biological Structures*, Springer-Verlag, Berlin **1991**.

[2] a) J. M. Lehn, *Supramolecular Chemistry: Concepts and Perspectives*, VCH, Weinheim **1995.** b) J. L. Atwood, J. E. D. Davies, D. D. MacNicol, F. Vogtle, *Comprehensive Supramolecular Chemistry*, Pergamon, Oxford, U.K. **1996.**

[3] a) K. K. Arora, V. R. Pedireddi, *J. Org. Chem.* **2003,** *68,* 9177-9185. b) S. Varughese and V. R. Pedireddi, *Chemistry, A European Journal,* **2006,** *12,* 1597-1609.

[4] CSD analysis: a) C. M. Weeks, D. C. Rohrer, W. L. Duax, *Science* **1975,** *190,* 1096-1097; b) D. Voet, A. Rich, *J. Am. Chem. Soc.* **1969,** *91,* 3069-3075.

[5] F. H. Allen.; O. Kennard, *Chem. Des. Automat. News*. **1993**, *8*, 31-37.

[6] S. R. Perumalla, E. Suresh, V. R. Pedireddi, *Angew. Chem. Int. Ed.* **2005,** *44,* 7752-7757.

[7] K. Gehring, J. –L. Leroy, M. Gueron, Nature, 1993, 363, 561-565

[8] P. H. Stahl and G. Wermuth, *Handbook of Pharmaceutical Salts: Properties, Selection, and Use,* Verlag Helvetica Chimica Acta, Zürich, **2002**.

[9] B. Lippert, *Coord. Chem. Rev.* **2000,** *200-202,* 487-516.

[10] a) C.M. Lewis and G.M. Tarrant, *Mutation,* **1971**, *12,* 349. b) P.M. Aebersold, *Cancer Res.,* **1979**, *39,* 808.

CHAPTER ONE

Supramolecular chemistry: concepts and progress

"Where nature finishes producing its own species, man begins, using natural things and with the help of this nature, to create an infinity of species"

- Leonardo da Vinci

1.1 Introduction

An organic molecule is usually understood as a stable collection of atoms, connected by well defined network of covalent bonds. Development of different strategies and methods for constructing these networks is the central focus in many frontier research areas of organic chemistry. Such methods, indeed, has made possible even the preparations of highly complex molecular entities, like vitamin B_{12}, chlorophyll, secondary metabolites etc., demonstrating the extraordinary sophistication of synthetic routes established.[1]

In addition, several biologically important molecules responsible for different biological processes like peptides, proteins etc., also could be easily prepared following the well established protocols of organic synthesis. However, many biological processes undergo through aggregation of molecules that are held together by non-covalent interactions.

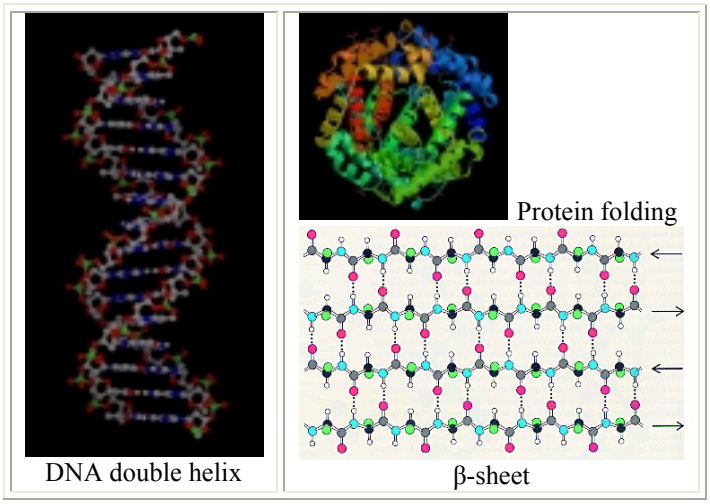

Figure 1.1

These interactions are dynamic in nature and also possibly responsible for most of the processes occurring in living systems such as transduction of signals, the

selective transport of ions and small molecules across membranes, expression and transfer of genetic information, enzymatic reactions, protein folding, recognition between base pairs in DNA, α-helix, β-sheets, etc.[2] Some of representative structures, governed by intermolecular interactions, are shown in Figure 1.1.

In chemical sciences also, such noncovalent interactions have paramount effect, especially, towards the physical properties of molecules. For example, the properties of liquids, the dissolution of solids, or the organization of amphiphillic molecules in larger aggregates such as membranes, micelles and vesicles, etc.

Thus, utilization of the exotic features of such interactions in chemical sciences has emerged as one of the contemporary research areas that led to the evolution of new branch of science i.e., supramolecular chemistry. [3]

1.2 Supramolecular chemistry

Molecular associations have been recognized and studied for a long time and the term "übermoleküle",[4] i.e. supermolecules, was introduced in the mid-1930's to describe entities of higher organization resulting from the association of coordinatively saturated species. In supramolecular chemistry, molecular recognition between the constituents is the fundamental aspect, resembling lock and key model, enunciated by Emil Fischer in 1984,[5] as shown in Figure 1.2. Such high specific interactions also lead to useful supramolecular functions, for example, specific and selective functions of the enzymes, which are, often, encountered in both chemical and biological processes.

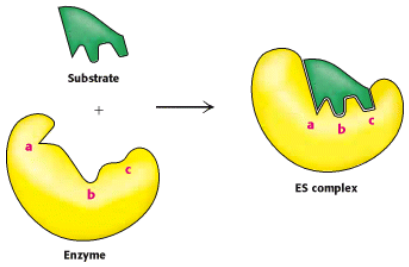

Figure 1.2. Lock and key model

Noble Laureate J. M. Lehn[6] defined supramolecular chemistry as "*the chemistry of the intermolecular bond"*, just as molecules are built by connecting atoms with covalent bonds, supramolecular compounds are built by linking molecules with intermolecular interactions as illustrated in Figure 1.3.

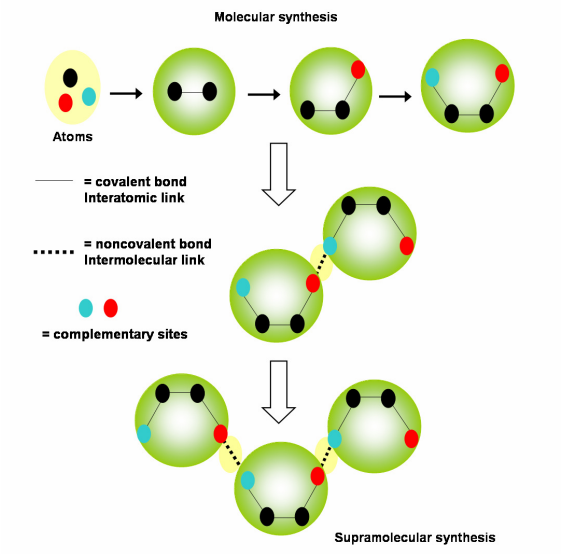

Figure 1.3. Analogy between molecular and supramolecular synthesis.

Supramolecular structures are the resultant of not only additive, but also cooperative interactions and their properties are the representative of the supramolecular character. These properties are important in both material science (magnetism, conductivity, sensors, nonlinear optics) and biology (receptor-protein binding, drug design, protein folding).[7]

In supramolecular synthesis, a large number of intermolecular interactions simultaneously play a significant role, which make it difficult for a directed synthesis of a desired supramolecular structure, as number of possible structural moieties that would evolve are large in number. But this flexibility also means that they are frequently favored in several processes of biological reactions and in crystallization experiments - wherein the ability to form short-lived transition states and to perform trial-and-error correction at ease is essential.

In general, supramolecular chemistry concerns with noncovalents. The term "noncovalent" encompasses an enormous range of attractive and repulsive forces, such as hydrogen bonding, ion-ion, ion-dipole, dipole-dipole, cation-π interactions, π-π and van der Waals interactions, and their energies are given in Table 1.1.[8] However, taken into account the energy and directionality properties, hydrogen bonds have been found to be of great value for effective utilization in different frontier areas of supramolecular chemistry.

Table 1.1. Different types of noncovalent bonds[8]

Type of interaction	Energy range
Ion-ion interactions	100-350 KJ/mol
Ion-dipole interactions	50-200 KJ/mol
Dipole-dipole interactions	5-50 KJ/mol
Hydrogen bonding	4-120 KJ/mol
Cation-π interactions	5-80 KJ/mol
π-π stacking	0-50 KJ/mol
van der Waals forces	< 5 KJ/mol; variable

1.3 Hydrogen bond and Non-covalent synthesis of molecular complexes

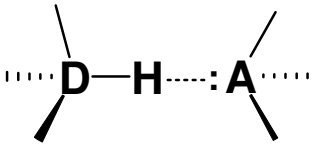

D = F, Cl, O, S, N, C A = F, Cl, O, S, N, π-system

Scheme 1.1. A Hydrogen bond formed between an acidic hydrogen atom and an appropriate acceptor.

Pauling's early definition of the hydrogen bond[9]

"A hydrogen bond is an interaction that directs the association of a covalently bound hydrogen atom with one or more other atoms, groups of atoms, or molecules into an aggregate structure that is sufficiently stable to make it convenient for the chemist to consider it as an independent chemical species."

Table 1.2. Properties of hydrogen bond interactions.

	Strong	Moderate	Weak
Bond energy (KJ/mol)	60-120	16-60	<12
Bond lengths (Å) H···A D···A	 1.2-1.5 2.2-2.5	 1.5-2.2 2.5-3.2	 2.2-3.2 3.2-4.0
Bond angles (º)	175-180	130-180	90-150
Relative IR vibration shift (stretching symmetrical mode, cm^{-1})	25%	10-25%	<10%
^{1}H NMR chemical shift downfield (ppm)	14-22	<14	
Examples	$[F{\cdots}H{\cdots}F]^-$ $[N{\cdots}H{\cdots}N]^+$	O-H···O N-H···O	C-H···O C-H···π

The hydrogen bond, usually denoted as D-H···A (see Scheme 1.1), is an interaction between an hydrogen atom, covalently bound to a proton donor D, and interacting with proton acceptor A. Thus, a continuum of hydrogen bonds with various strengths are observed depending upon the nature of donor and acceptor moieties, and some general properties of these categories are listed in Table 1.2.[8]

Several studies of systematic analysis of hydrogen bonding patterns have been carried out for the development of methodologies to utilize the hydrogen bonds in supramolecular synthesis. For example, Kuleshova and Zorkip applied graph theory to describe organic crystal structures, while Wells, Hamilton and Ibers had developed schemes for hydrogen bonds.[10] The modern interpretation of hydrogen bonding analysis is originated with the formulation of a *graph set analysis* (see Scheme 1.2),[11] proposed by Etter and further refined by Bernstein.[12] The purpose of graph-set assignments is to define the morphology of hydrogen-bonded arrays through numerical codings, following some principles, often, referred as Etter rules, as described below.

Etter Rules:[12a]

1. All good proton donors and acceptors are used in hydrogen bonding.[13a]
2. Six-membered-ring intramolecular hydrogen bonds form in preference to intermolecular hydrogen bonds.
3. The best proton donors and acceptors remaining after intramolecular hydrogen-bond formation form intermolecular hydrogen bonds to one another.[13b]

The process of assigning a graph set begins with identification of number of different types of hydrogen bonds, as defined by the nature of the donors and

acceptors in a hydrogen bond, that are present in the structure. The set of molecules that are hydrogen bonded to one another by repetition of just one of these types of hydrogen bonds is called a motif and is characterized by one of the four designators, which indicate whether the motif is a cyclic, finite, intermolecular, intramolecular etc. For motifs generated from intermolecular hydrogen bonds, these designators are **C** (chain), **R** (ring), and **D** (dimer or other finite set), while **S** denotes an intramolecular hydrogen bond. The number of donors and acceptors used in each motif are assigned as subscripts and superscripts, respectively, and the size or degree of the motif (corresponding to the number of atoms in the repeat unit) is indicated in parentheses. Thus, a hydrogen bond network found by either –COOH or $–CONH_2$, shown in Scheme 1.2, will have a graph set notation as $R_2^2(8)$, which indicates that network is a ring with eight atoms and comprises of two acceptors and two donors each.

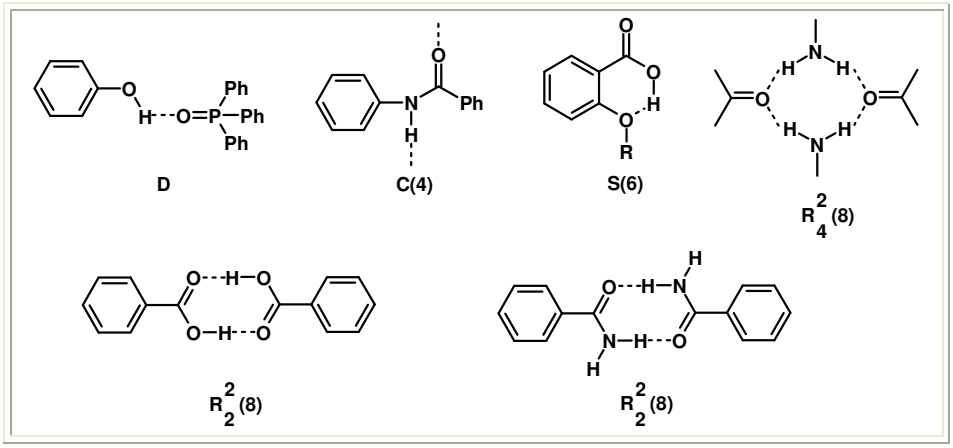

Scheme 1.2. Graph set notations for some hydrogen bonding networks.[11a]

Some of the well known hydrogen bonding patterns of the molecules are shown in Scheme 1.3, which have been well studied for the creation of exotic supramolecular assemblies.

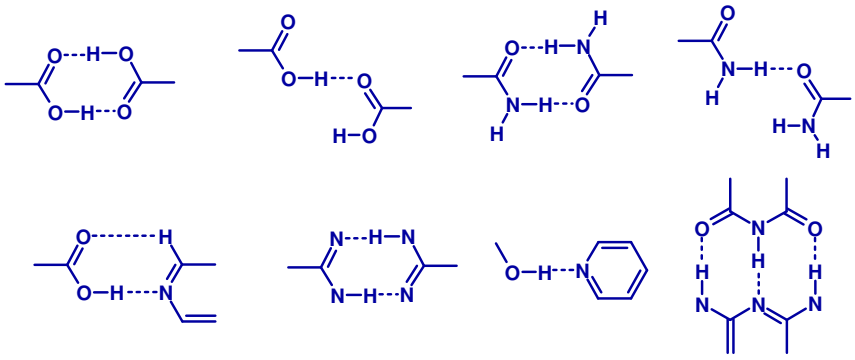

Scheme 1.3

Systematic analysis of these recognition patterns lead to the development of various strategies to use them in supramolecular synthesis by inducing aggregation of complementary compounds that could potentially yield the stable hydrogen bonding patterns. Thus, a wide variety of supramolecular assemblies with varied geometrical architectures have been prepared, which find applications in many frontier areas of supramolecular chemistry. Some of the exotic examples, observed from the literature, are discussed in the following sections.

Jones and Pedireddi identified a pair-wise hydrogen bonding pattern O-H···N/ C-H···O, which is a combination of strong and weak hydrogen bonds illustrating its utility through the supramolecular complex formed by 3,5-dinitrobenzoic acid and its methyl derivative with phenazine molecules, as shown in Figure 1.4.[14]

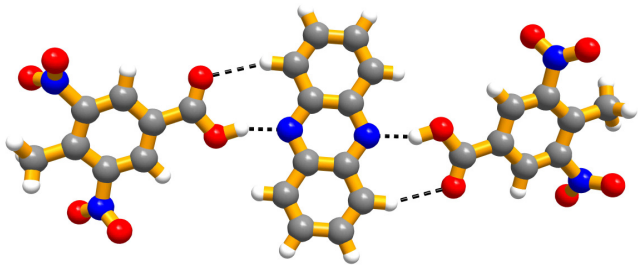

Figure 1.4. Recognition pattern between 4-methyl-3,5-dinitrobenzoic acid and phenazine.

Zaworotko *et al.* have reported a supramolecular assembly of 1,3,5-benzenetricarboxylic acid (**TMA**) and 1,2-*bis*(4-pyridyl)ethane, ***bpyea***, in which ***bpyea*** molecules are inserted between **TMA**, through a pair-wise hydrogen bonding pattern, comprising of O-H···N and C-H···O hydrogen bonds, yielding voids of 39 x 27 $Å^2$, which subsequently undergo extensive interpenetration, as shown in Figure 1.5.[15]

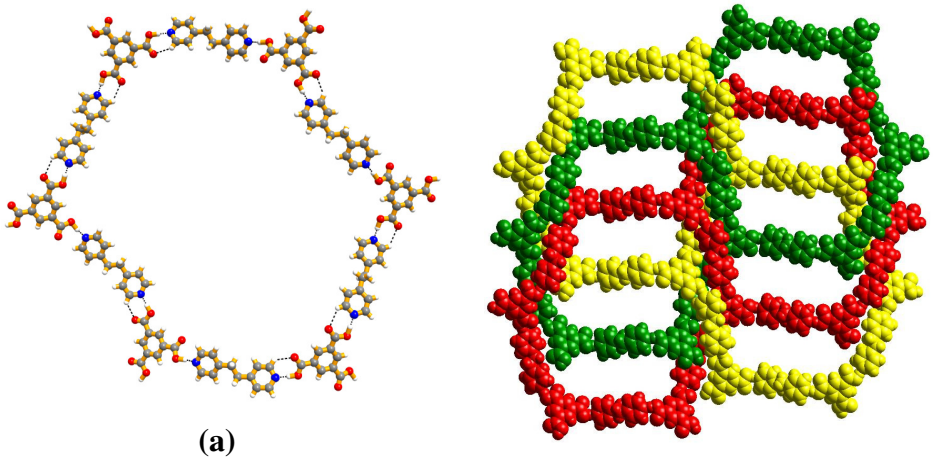

(a) **(b)**

Figure 1.5. (a) Super honeycomb (6,3) network in the molecular complex of **TMA** and ***bpyea***. (b) Space filling view of triply parallel interpenetrated nets.

However, in the presence of suitable guests with appropriate dimension corresponding to the void space, **TMA** was shown to form host-guest type assemblies as well.[16] For example, Zimmerman *et al.* reported a host-guest network structure of **TMA** by co-crystallization of it with pyrene from ethanol. The hexagonal host network is formed by the **TMA** and ethanol molecules with void space, which is being occupied by pyrene as well as ethanol molecules, as shown in Figure 1.6.[17]

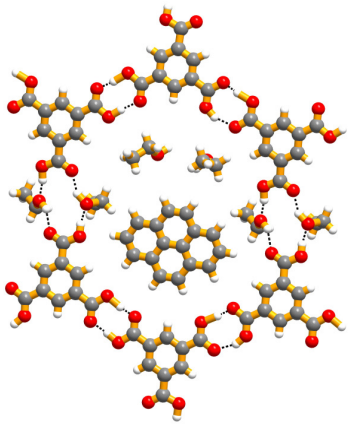

Figure 1.6. **TMA** forming a hexagonal network utilizing the ethanol molecules to accommodate the guest molecules.

Similarly, Coppens and co-workers have also prepared the host-guest complex by reaction of tridentate ligand 1,3,5-tri(4-pyridyl)-2,4,6-triazine (**TPT**) and **TMA** in the presence of pyrene, to obtain a honeycomb framework. The observed three-dimensional structure, with four pyrene molecules in each channel, is shown in Figure 1.7.[18]

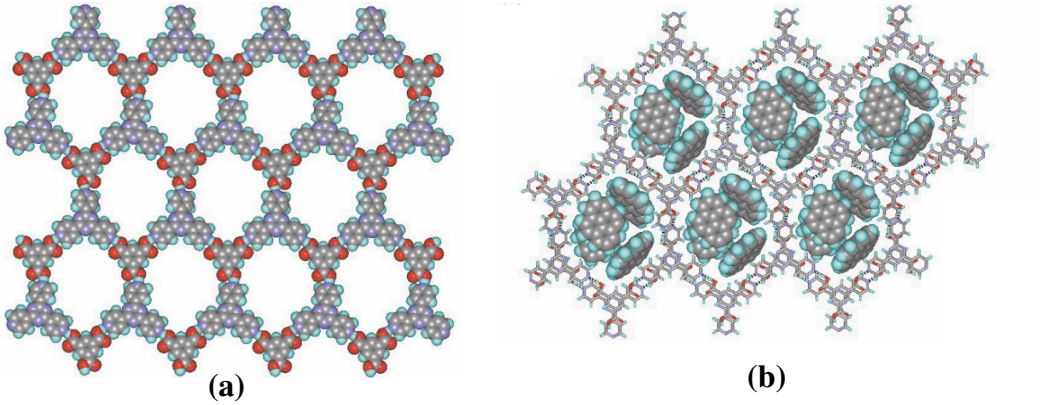

Figure 1.7. (a) Honeycomb framework formed by **TMA** and **TPT** in the adduct. (Pyrene molecules were removed for clarity purpose). (b) Four pyrene molecules are present per cavity.

Recently, Pedireddi *et al*. have shown the significance of interactions between carboxylic acids and various aza donor compounds for the preparation of structures of varied geometries like host-guest, lamellar assemblies etc., depending upon the dimension of the aza-donor compounds, as shown in Figure 1.8. For this purpose, 1,2,4,5-benzenetetracarboxylic acid was co-crystallized with various aza donor compounds, like 4,7-, 1,7-, 1,10- phenanthrolines, 1,2-bis(4-pyridyl) ethene/ethane etc., and it was shown that the acid form host network around phenanthroline molecules that fit well within the void space, while it constituted lamellar assemblies with other pyridyl derivatives, due to incompatibility in the dimensions of void space and the aza-donor compound.[19]

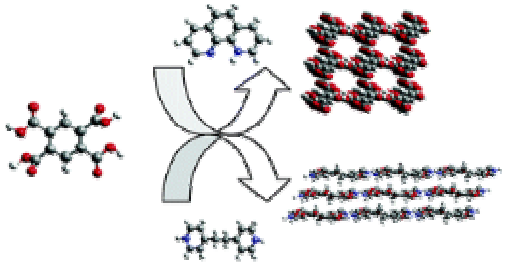

Figure 1.8. Schematic representation of different type of networks, obtained by carboxylic acid and aza-donor molecules.

Apart from carboxylic acid and aza-donor aggregations, Whitesides *et al.* studied the utilization of compounds possessing complimentary groups, such as melamines, cyanuric acid,[20] barbituric acid etc.[21] It was found that the solid-state structures/architectures formed by such compounds are dependent on steric interactions and the dimension of the substituents, etc. For example, Cl, Br, I and CH_3 substituted melamines gave tape structures, where as methyl or ethyl ester substituted self assembled into ribbons. However, when the substituents are bulky, like *t*-butyl

group, a cyclic hexamer is formed. A representative example for each type of motif is given in Figure 1.9. In fact, a great significant impact of this study is the prediction of rosette structures that could be formed between melamine and cyanuric acid (Figure 1.9(d),[22] which was proven by single crystal X-ray diffraction studies by Rao and Pedireddi.[23]

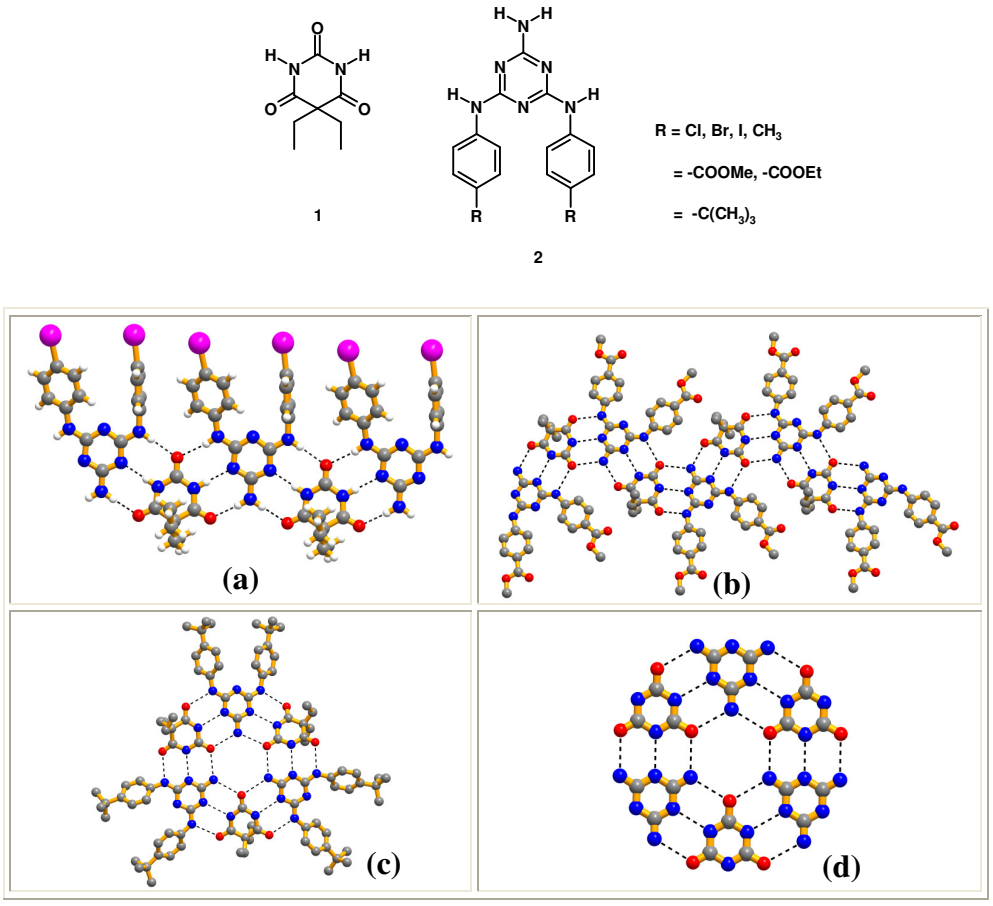

Figure 1.9. (a) Supramolecular tape formed in the crystal structure of *N*,*N*′-bis(4-iodophenyl)melamine 5,5-diethylbarbituric acid adduct, (b) Ribbons like architecture formed in *N*,*N*′-bis(4-Carboxymethylphenyl)melamine 5,5-diethyl-2,4,6(1H,3H,5H)-pyrimidinetrione ethanol solvate, (c) a cyclic hexamer is formed in the crystal structure of *N*,*N*′-bis(4-t-Butylphenyl)melamine 5,5-diethyl-2,4,6(1H,3H,5H)-pyrimidinetrione and (d) rosette structure formed between melamine and cyanuric acid.

Understanding the efficacy of intermolecular interactions from these studies, Bassani and co-workers elegantly utilized it for [2+2] photodimerization of cinnamic esters.[24] In this context, the authors have chosen a cinnamic ester derivative, as shown in Scheme 1.4, and co-crystallized with a barbituric acid (co-ligand) and subjected to photoirradiation. It was found that the conversion to a cyclobutane product is enhanced in the presence of co-ligand than observed in similar experiment without the co-ligand.

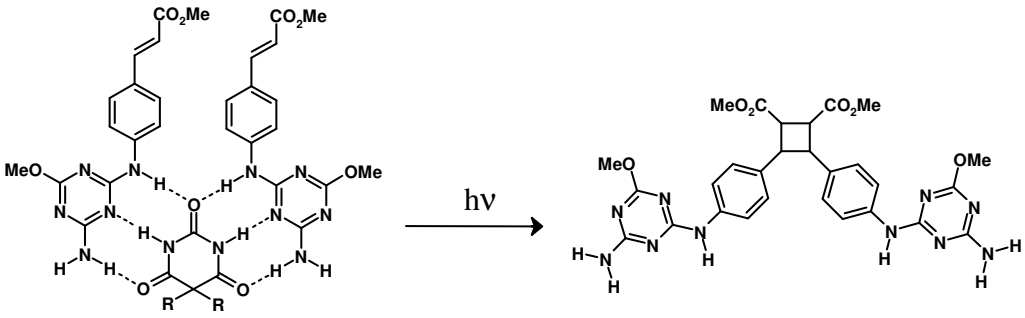

Scheme 1.4. Photoactive hydrogen bonded assembly (reactants) observed in NMR titration experiments.

Similarly, many researchers have utilized noncovalent interactions for [2+2] photodimerization reactions.[25] For example, MacGillivray and co-workers[26] carried out co-crystallization of 1,8-naphthalenedicarboxylic acid with *trans*-1,2-bis(4-pyridyl)ethylene, which gave a discrete four-component molecular assembly formed through noncovalent interactions, as a template, for creating a wide range of cyclobutane products, as the olefin moieties are placed at photoreactive distance to undergo photochemical cycloaddition reaction in the solid state.

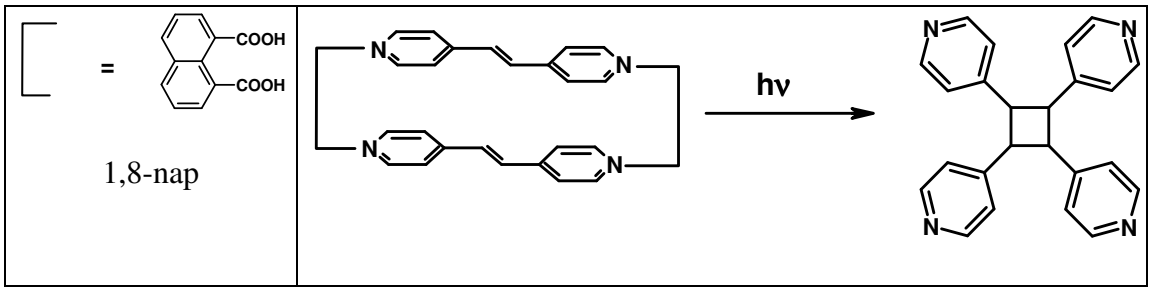

Scheme 1.5

UV irradiation of powdered crystalline samples of such supramolecular assembly for a period of 7 h (Rayonet reactor, 300 nm Hg lamp), produced, stereospecifically (100% yield), *rctt*-tetrakis(4-pyridyl) cyclobutane (4,4A-tpcb), as shown in Scheme 1.5.

Similarly, Wolf and co-workers have also utilized the carboxylic acid aza donor interactions for the preparation of cyclobutane tetracarboxylic acid as shown in Scheme 1.6.[27]

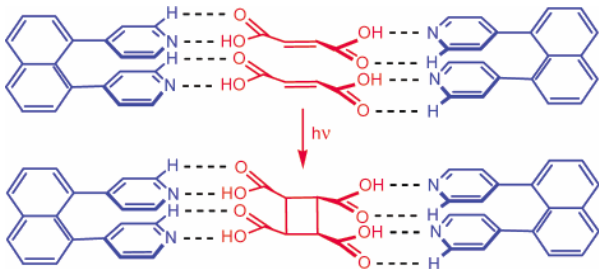

Scheme 1.6. Schematic representation for the preparation of cyclobutane tetracarboxylic acid.[27]

Apart from the synthesis of various cyclobutane derivatives, in fact, the elegance of utilization of co-crystallization concept has been demonstrated by preparing complex molecules like cyclophanes, ladderanes (see Scheme 1.7) by simple template processes.

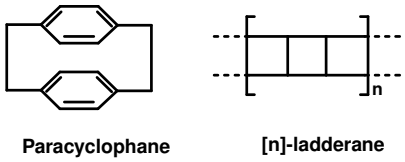

Scheme 1.7. General representation of paracyclophanes and ladderanes.

This approach was resultant of the preliminary studies carried out by MacGillivray and co-workers through co-crystallization of resorcinol derivatives with different aza-donor compounds that can undergo photodimerization, as illustrated in Scheme 1.8.[28]

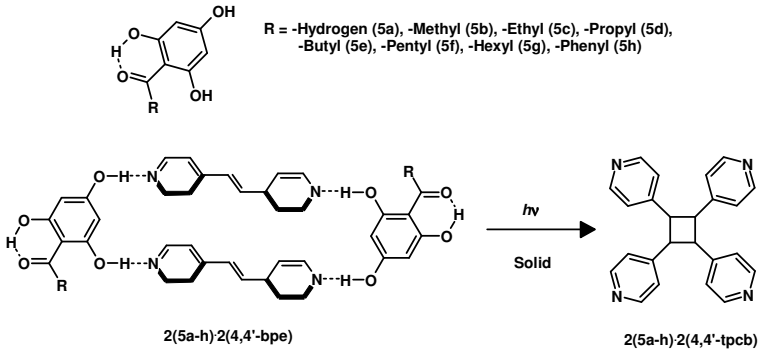

Scheme 1.8. Schematic representation of the experiments.[28]

In extension of these studies, 1,4-bis[2-(4-pyridyl)ethenyl]benzene (**14PEB**) was co-crystallized with 4-benzylresorcinol (**4BRes**), and the obtained co-crystals, in which molecular assembly formed a discrete four-component moiety, through O-H···N hydrogen bonds, (Figure 1.10), was used for photochemical reaction and synthesized the targets shown in Figure 1.11.[29]

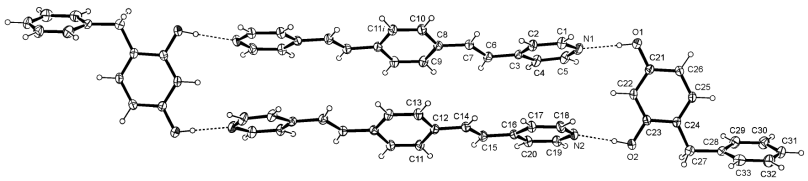

Figure 1.10. ORTEP representation of the structure of the assembly **14PEB·4BRes**. [29]

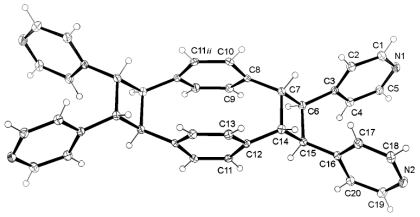

Figure 1.11. An ORTEP representation of corresponding cyclopane**.** [29]

Similarly, when the reactions were carried out between resorcinol derivative and diene/triene molecules, corresponding ladderanes were obtained, as shown in Scheme 1.9.[30]

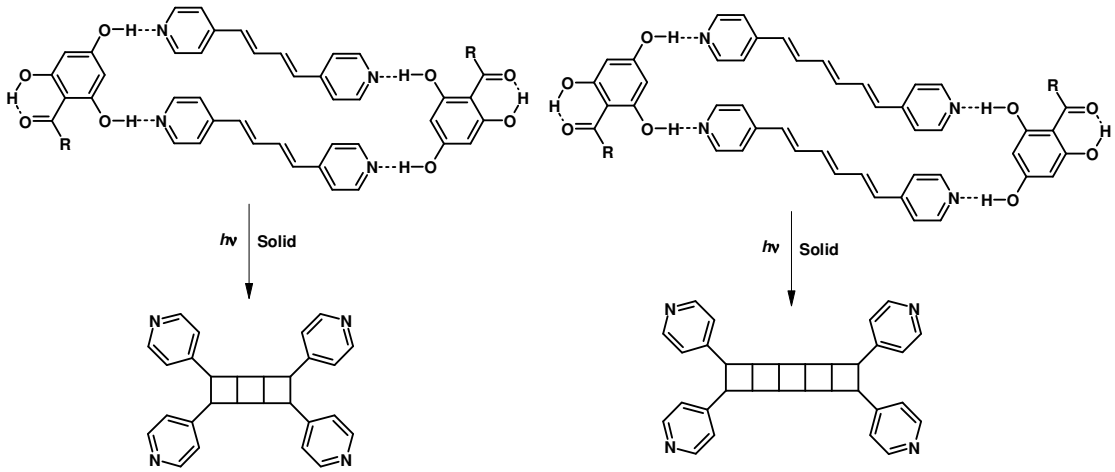

Scheme 1.9. Schematic representation of reactions for ladderane formation.

In addition to organic assemblies, coordination assemblies, often referred as metal-organic frameworks (**MOFs**),[31] have been thoroughly studied in recent years. This is not only due to the exotic structural features of the resultant assemblies but also because of the potential applications in gas storage,[32] separation,[33] catalysis,[34] etc., and some of the representative examples from the literature are discussed here.

For example, Kitagawa and co-workers have utilized the porous coordination polymers for radical polymerization of styrene molecules.[35] For this purpose, a metal-

organic framework, $[Zn_2(1,4\text{-benzenedicarboxylate})_2(\text{triethylenediamine})]_n$, **ZBT**, was chosen, which forms one dimensional nanochannels of dimension, 7.5 x 7.5 $Å^2$. The polymerization of styrene in the channels of **ZBT** was carried out by loading the monomer styrene into the nanochannels by immersion of **ZBT** in liquid styrene followed by removal of excess styrene, under reduced pressure, and subsequently, the loading was estimated by thermogravimetric analysis (TGA). The polymerization of styrene in the adduct was carried out in the presence of 2,2'-azobis(isobutyronitrile) (AIBN), a radical polymerization initiator, at 70 ºC for 48 h (Figure 1.12), and found that 71% of the adsorbed styrene converted to polystyrene.

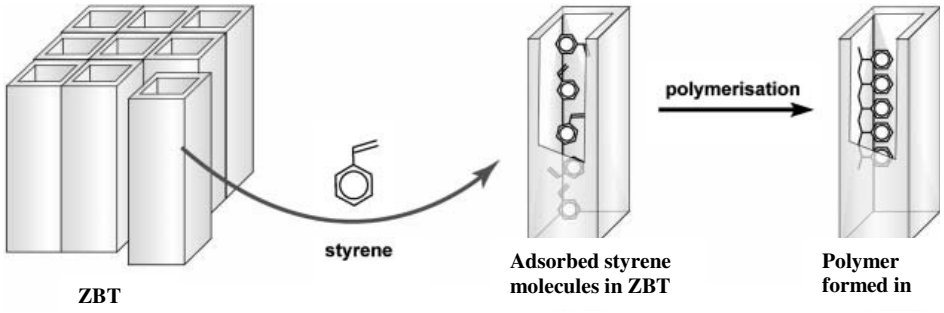

Figure 1.12. Schematic illustration for polymerization of styrene in the nanochannels of **ZBT**.

Apart from the polymerization reactions, these metal-organic frameworks also utilized for some of the well known organic transformations.[36] For example Diels-Alder reaction between 9-substituted anthracenes and *N*-cyclohexylphthalimide was carried out in MOF, as discussed below.[37]

Diels-Alder reaction of anthracenes could yield two types of adducts, i.e., an adduct bridging the center ring (9,10-position) and the terminal ring (1,4-posotion), as shown in Scheme 1.10.

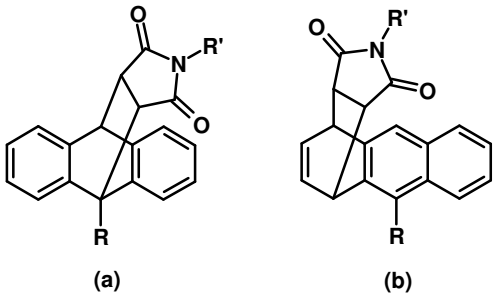

Scheme 1.10. (a) 1,9-isomer and (b) 1,4-isomer.

It was observed from the literature that the adducts formed through usual synthetic methodologies, in general, form an adduct belong to the center ring (9,10-position) of the anthracene framework as a consequence of the high localization of the π-electron density at that site. However, Fujita and co-workers have designed a cage structure (see Figure 1.13) and demonstrated its selectivity with varied substrates such as 9-hydroxymethyl, carboxyl, cyano, vinyl anthracenes coupled with N-cyclohexylphthalimide preferentially yielding 1,4-isomers, as shown in Scheme 1.11.

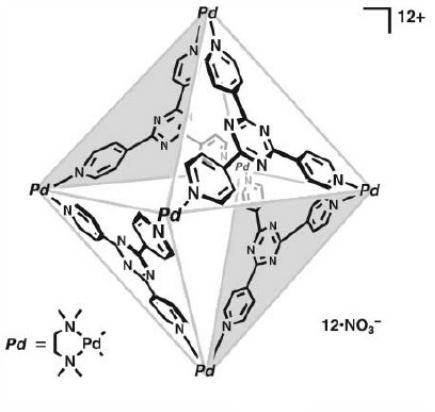

Figure 1.13. Self-assembled coordination cage (1), which was prepared by simple mixing of an exo-tridentate organic ligand and an end-capped Pd(II) ion in a 4:6 ratio in water.

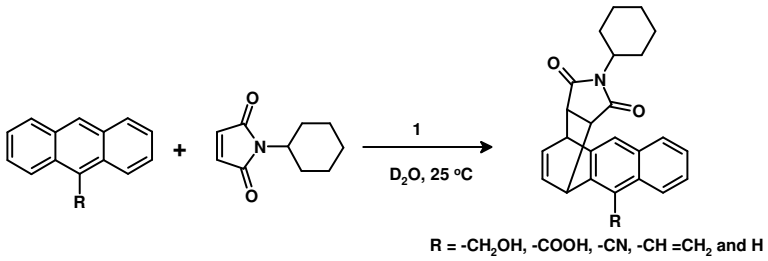

Scheme 1.11.

This selective regioselectivity was rationalized in terms of topochemical control induced by the proximity of the 1,4-position of the anthracene to the dienophile in the cage, as evident from the crystal structure shown in Figure 1.14.

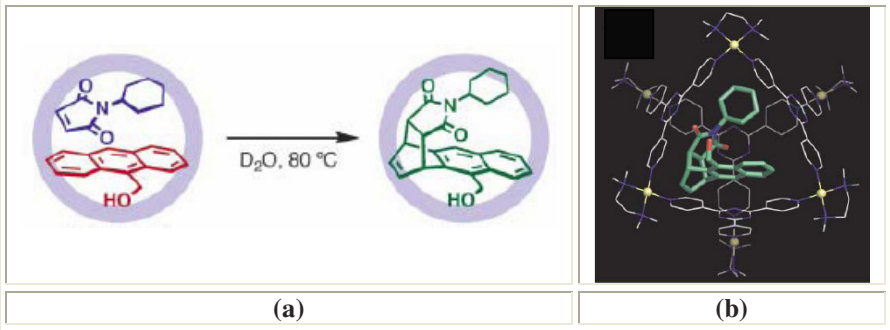

Figure 1.14. (a) Schematic representation for the adduct formation in the cage and (b) Crystal structure of the adduct (encapsulated cage).

Similarly, Vittal and co-workers demonstrated the [2+2] topochemical photodimerization in the co-ordination polymer through single crystal to single-crystal transformation.[38] A reaction between an equimolar ratio of Zn-$(O_2CCH_3)_2{\cdot}2H_2O$, 4,4'-bipyridyl ethene and CF_3CO_2H in *N,N*-dimethylformamide (DMF), gave a complex as $[\{(F_3CCO_2)(m\text{-}O_2CCH_3)Zn\}2(m\text{-}bpyee)_2]_n$. Packing analysis revealed the formation of a molecular ladder (see Figure 1.15a), in which azadonor molecules aligned with olefinic bond distance being 3.747 Å, which was within Schmidt photodimerization

distance. Thus, UV irradiation of single crystals, for about three hours, yielded a complex $[\{(F_3CCO_2)(m\text{-}O_2CCH_3)Zn\}_2(\mu\text{-}tpcb)_2]_n$, as shown in Figure 1.15b.

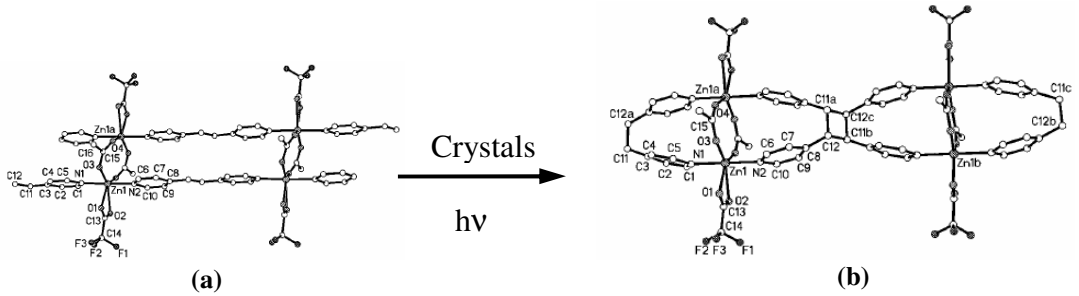

Figure 1.15. (a) A perspective view of a portion of the 1D molecular ladder polymeric structure of $[\{(F_3CCO_2)(m\text{-}O_2CCH_3)Zn\}2(m\text{-}bpyee)_2]_n$ and (b) A view showing a part of the 1D polymeric structure of $[\{(F_3CCO_2)(m\text{-}O_2CCH_3)Zn\}_2(\mu\text{-}tpcb)_2]_n$.

Apart from these applications, metal-organic assemblies were also utilized as gas storage materials for hydrogen, carbondioxide, nitrogen, etc., which will have significant utility in the development of materials that meets the demands of 21st century applications. For example, the widespread use of hydrogen as a fuel is limited by the lack of convenient, safe, and cost-effective methods to develop H_2 storage devices. None of the current H_2 storage options (liquefied or high-pressure H_2 gas, metal hydrides, and adsorption on porous materials) satisfy the criteria of size, recharge kinetics, cost, and safety required for use in transportation. To overcome these problems, it was proposed that adsorbents with porosity at the molecular scale would be effective materials for high adsorption of hydrogen. In this direction, many researchers have prepared porous metal-organic frameworks and evaluated the adsorption properties.

Yaghi and co-workers synthesized the MOF-505 by solvothermal reaction of 3,3',5,5'-biphenyltetracarboxylic acid (H_4bptc) and $Cu(NO_3)_2 \cdot 2.5(H_2O)$ in *N,N*-dimethylformamide (DMF)/ethanol/H_2O (3:3:2 v/v/v) at 65ºC.[39] The compound, thus, obtained was formulated as $[Cu_2(bptc)(H_2O)_2(dmf)_3(H_2O)]$. It was observed that two type of pores are formed. One of the pores is defined by six inorganic SBUs (representing the faces of a cubic NbO subunit) with a spherical volume of 290 $Å^3$ and a pore diameter of 8.30 Å (Figure 1.16a), while the other pore is defined by six organic SBUs (again representing the faces of a cubic NbO subunit) and has a solvent-accessible void of 540 $Å^3$ with a pore diameter of 10.10 Å (Figure 1.16b).

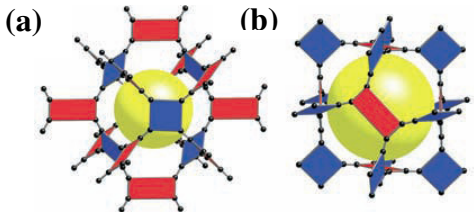

Figure 1.16. (a) Pores formed by six inorganic SBUs (b) Pore formed by six organic SBUs.[39]

It was observed that, total 37% of free space, is available for hydrogen adsorption. The hydrogen isotherms of MOF-505 were measured at 77 K at different stages of activation of the sample as it is shown in Figure 1.17.

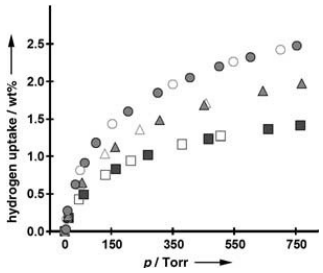

Figure 1.17. H_2 isotherms for MOF-505 (77 K) after three different activation stages: stage I (25 ºC, squares), stage II (70 ºC, triangles), and stage III (120 ºC, circles); filled shapes indicate adsorption and open shapes indicate desorption data points.[39]

Thus, the examples described, herein, so far, highlighted the understanding of interplay of intermolecular interactions, and successful applications to develop targeted supramolecular assemblies, have directed the creation of myriad of exotic supramolecular architectures with tailor-made properties and applications especially in the areas of materials and catalytic industries. In recent times, supramolecular concepts have been extended even in the development of pharmaceutical formulations, which may influence the bioactivity of drug compounds, as illustrated in the following sections.

1.4 Pharmaceutical co-crystallization [40]

In the process of drug developments, exploration of novel methodologies for the delivery of the active pharmaceutical ingredients (API's) is a continuous challenging task.[41] Most API's are crystalline solids at room temperature and are commonly delivered as tablets. However, recent advancements in the areas of supramolecular chemistry, under the umbrella of polymorphism,[42] reveal that different solid forms of the same compound show different chemical and physical properties. Thus, the solid-state chemistry of API's has become a subject of fundamental, practical and legal interest. As a result, polymorphs, solvates, salts, etc., of API's represent extensions of chemical space, with the enhancement or new chemical and physical properties, leading to extended patent coverage and consequent legal protection of products that may be of great concern to innovator and generic pharmaceutical companies.[43] In this process, co-crystals of API's with different co-ligands, generally, approved by FDA, generated considerable interest, as such

complexes have shown varied bioproperties than the native API's. While this concept has initially been introduced by Zaworotko and co-workers, since then tremendous advancements have taken place, as discussed below. The strategies to deal with inadequate solubility, dissolution rate, bioavailability, absorption of neutral crystal forms, physical stabilization of amorphous solids, complexation, or encapsulation of organic solutions etc., are of current interest.[44] In fact, pharmaceutical co-crystals could have broader implications for the formulation of API's, as the important physical properties that play a crucial role in drug delivery processes, i.e., composition can be addressable via a supramolecular retrosynthetic approach.

Zaworotko and co-workers for the first time, reported, the application of the principles of supramolecular chemistry for API's by co-crystallization of ibuprofen, flurbiprofen and aspirin with 4,4'-bipyridine and the molecular recognition between the components is shown in the Figure 1.18.[45] Form this study, it was observed that the nature of the non-pharmaceutical component (4,4'-bipyridine in the above mentioned case) can dramatically affect the crystal packing and hence the physical properties, such as melting point, etc.

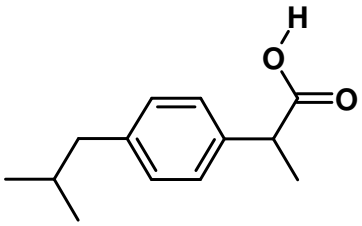

Ibuprofen

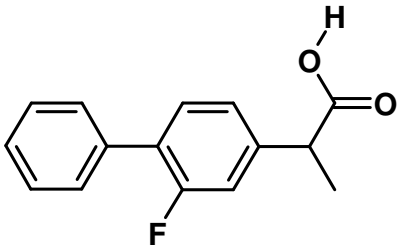

Flurbiprofen

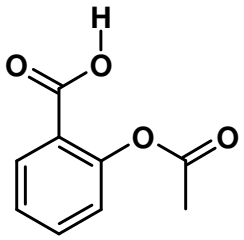

Aspirin

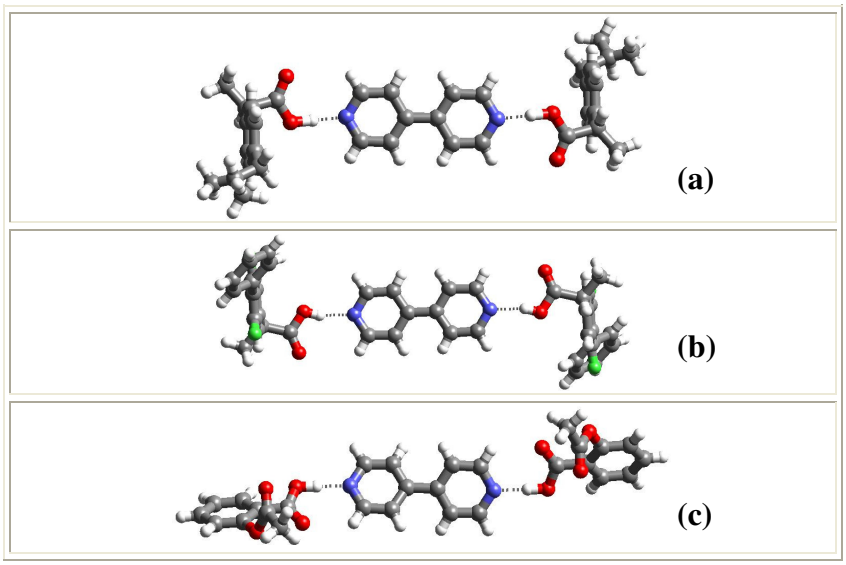

Figure 1.18. Molecular recognition pattern of (a) Ibuprofen **:** 4,4'-bipyridine, (b) Flurbiprofen **:** 4,4'-bipyridine and (c) Aspirin **:** 4,4'-bipyridine.

Piroxicam, which exhibits tautomerism (Scheme 1.12) is a nonsteroidal anti-inflammatory drug (NSAID). Piroxicam is an enolic acid used in the symptomatic relief of rheumatoid arthritis and osteoarthritis. Piroxicam has low solubility at physiological pH and is classified as a Class II API (low solubility and high permeability) based on the Biopharmaceutics Classification System (BCS). It takes more than two hours for piroxicam to reach the maximum concentration after being administered orally. A more rapid onset and increased bioavailability is desirable for analgesics of this type and formulation and delivery of piroxicam with improved bioavailability has been the goal of a number of research studies.[46]

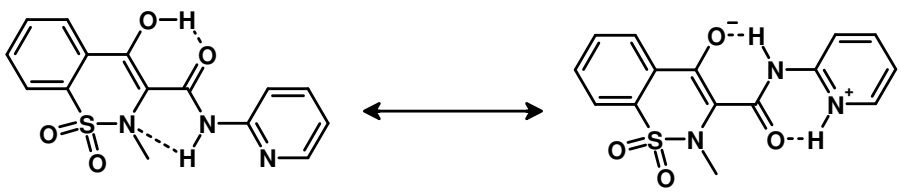

Scheme 1.12. Two possible tautomeric forms of piroxicam.

In this context, Childs and co-workers have investigated the co-crystals of piroxicam with various carboxylic acids to improve the bioavailability. Basic recognition patterns in its adducts with succinic and benzoic acids are shown in Figure 1.19.

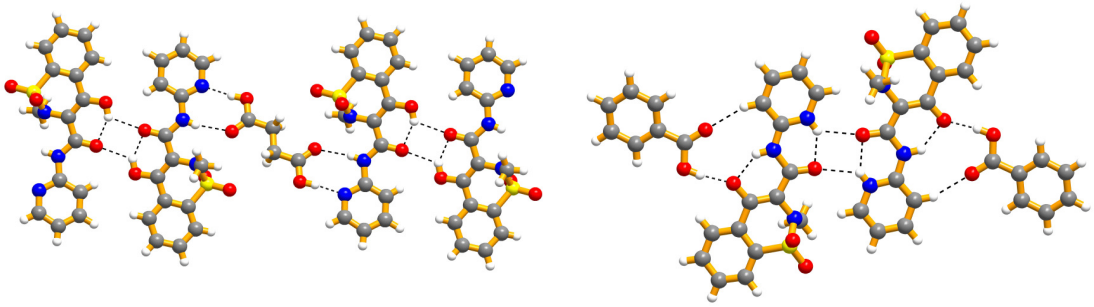

Figure 1.19. (a) Hydrogen-bonding motif in the 2:1 piroxicam/succinic acid cocrystal. (b) Four molecules form an aggregate through hydrogen bonding in the structure of 1:1 piroxicam/benzoic acid.

Caffeine[47] (1,3,7-trimethyl-2,6-purinedione) is a xanthine alkaloid that acts as a psychoactive stimulant drug and a mild diuretic in humans and other animals, known to exhibit instability with respect to humidity, with the formation of a crystalline nonstoichiometric hydrate, etc. To overcome this problem, Jones and co-workers have co-crystallized caffeine with various aliphatic dicarboxylic acids (Scheme 1.13) and studied for their stability. In this study, it was observed that the stability profile of these co-crystals differed from pure crystalline caffeine. A typical molecular recognition pattern in one of the co-crystals, caffeine and oxalic acid adduct is shown in Figure 1.20.

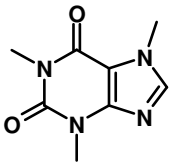

Caffeine

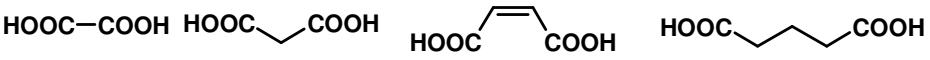

Oxalic acid Malonic acid Maleic acid Glutaric acid

Scheme 1.13

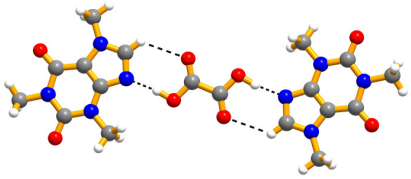

Figure 1.20. Molecular recognition between caffeine and oxalic acid in the adduct.

Norfloxacin is a widely used fluoroquinolone antibacterial compound. In aqueous solution, norfloxacin essentially exists in a zwitterionic form, owing to the acid/base interaction between the basic nitrogen of the piperazine and the carboxylic acid group (Scheme 1.14). Further, the aqueous solubility of norfloxacin at a pH close to 7 (isoelectric point of the molecule) is quite low (0.28-0.40 mg/mL).[48] Therefore, improving the aqueous solubility of norfloxacin through the preparation of cocrystals and new salt forms of the compound is of interest for the design of new dosage forms.

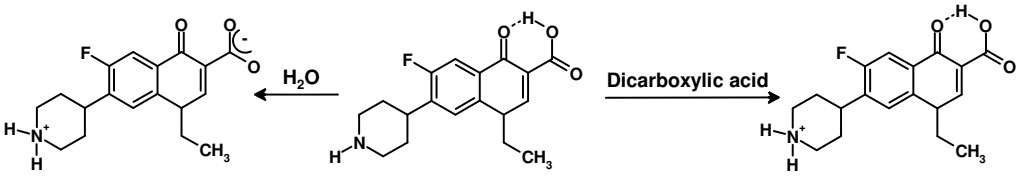

Scheme 1.14. (a) Zwitterionic form of Norfloxacin and (b) Norfloxacin protonated by dicarboxylic acids.

In this context, Velaga and co-workers[49] have prepared salts and co-crystals of norfloxacin with isonicotinamide, malonic acid, succinic acid, maleic acid, etc., and studied their solubility properties. It was observed that cocrystals and salts have shown the increase in the solubility when compared to that of the starting material. Basic recognition pattern between the constituents in one of the representative examples is shown in Figure 1.21.

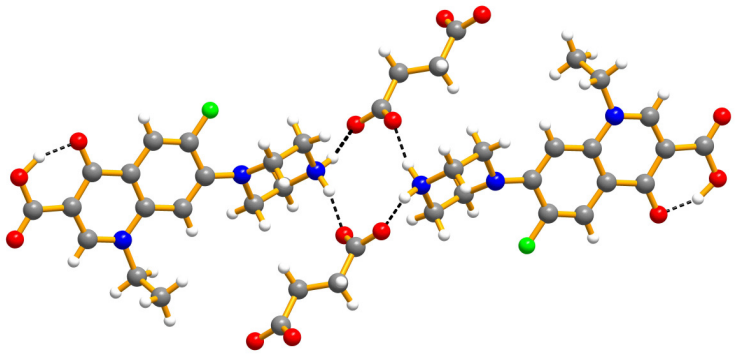

Figure 1.21. Recognition between the constituents in Norfloxacinium succinate.

2-[4-(4-chloro-2-fluorophenoxy)phenyl]pyrimidine-4-carboxamide (**CFPPC**), belongs to the pharmacologic class of sodium channel blockers and was developed as a potential drug candidate useful for treating or preventing surgical, chronic and neuropathic pain (Scheme 1.15).

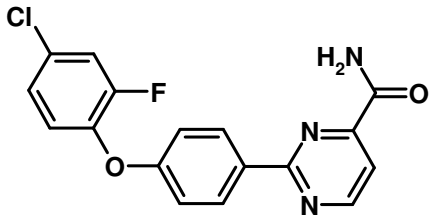

Scheme 1.15. 2-[4-(4-chloro-2-fluorophenoxyl)phenyl]pyrimidine-4-carboxamide, **CFPPC**.

It possesses extremely low solubility characteristics (<0.1 mg/ml) in aqueous systems. Hence, it is classified as a Class II API (low solubility, low in vivo plasma concentrations after oral dosing and high permeability) based on the Biopharmaceutics Classification System (BCS). In order to increase bioavailability, McNamara *et al* have prepared a 1:1 complex with glutaric acid (see Figure 1.22) and, further, studied for its properties.[50]

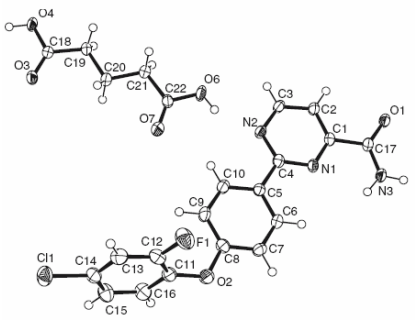

Figure 1.22. ORTEP drawing (ellipsoids at 50% probability level) of the glutaric acid co-crystal.

It was observed that the glutaric acid co-crystal showed 18 times greater intrinsic dissolution rate and three times the plasma area-under-the-curve (AUC) as compared to CFPPC in a single dose dog exposure study. A basic recognition pattern in the complex with glutaric acid is shown in Figure 1.23.

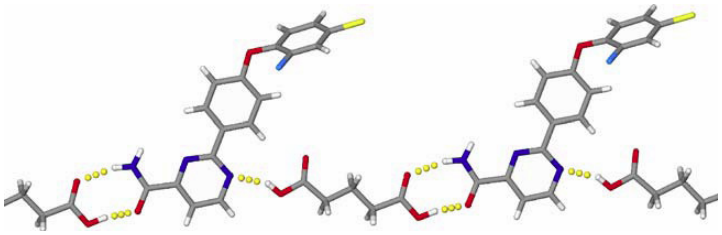

Figure 1.23. Hydrogen bonding in complex consists of interactions between the carboxylic acid groups of the glutaric acid molecule and the amide and pyridine groups on the drug molecule.

Apart from general organic, metal-organic and pharmaceutical compounds, co-crystallization and supramolecular syntheses for the creation of novel molecular ensembles were carried out with many different classes of molecular entities. In this direction, studies pertaining to derivatives of nucleobases are of great significance because of their association with naturally important biological entity, DNA.

In fact, the present advancement in the contemporary supramolecular chemistry may be regarded as being influenced by the exotic DNA double helical structure stabilized by hydrogen bonding formed between complimentary nucleobases, well known as, A-T and G-C base pairs.[2a]

Thus, mimic or modeling of such hydrogen bonding patterns to enhance the understanding of function of macro systems, in biology, indeed, is of great concern of many pioneers in the frontier areas of structural, chemical biology, etc. Hence, some of the experiments were carried out utilizing nucleobase/nucleosides with various compounds possessing complementary functional groups. The results, thus, obtained are compiled in chapter two, three and four. These studies, perhaps, may provide further insight into biomimicking of natural systems, protein/enzyme/DNA interaction with drugs, computational aided drug design, etc., which may facilitate a thorough understanding of biological process.

1.5 References

[1] (a) Corey, E. J.; Cheng, X. -M. *The Logic of Chemical Synthesis*, Wiley, New York, **1989**. (b) Masters, J. J.; Link, J. T.; Synder, L. B.; Young, W. B.; Danishefsky, S. J. *Angew. Chem. Int. Ed.* **1995**, *34*, 1723-1726. (c) Nicolaou, K. C.; Sorensen. E. J. In *Classics in Total Synthesis*; VCH: Weinheim **1996**; p265 and references therein.

[2] (a) Watson, J. D.; Crick, F. H. C. *Nature* **1953**, *171*, 964-967. (b) Barlow, D. J.; Thornton, J. M. *J. Mol. Biol.* **1988**, *201*, 601-619. (c) Fairlie, D. P.; West, M. L.; Wong, A. K. *Curr. Med. Chem.* **1998**, *5*, 29-62. (d) Salemme, F. R. *Prog. Biophys. Mol. Biol.* **1983**, *42*, 95-133. (e) Richardson, J. S. *Adv. Protein Chem.* **1981**, *34*, 167-339. (f) Bryngelson, J. D.; Onuchic, J. N.; Socci, N. D.; Wolynes, P. G. *Proteins* **1995**, *21***,** 167–195. (g) Eaton, W. A.; Munoz, V.; Thompson, P. A.; Chan, C. -K.; Hofrichter, J. *Curr. Opin. Struct. Biol.* **1997**, *7*, 10–14.

[3] (a) Lehn, J. M. *Angew. Chem. Int. Ed.* **1990**, *29*, 1304-1319. (b) Lehn, J. M. *Science* **1993**, *260*, 1762-1763. (c) Lehn, J. M. *Reports on Progress in Physics* **2004**, *67*, 249-265. (d) Supramolecular Chemistry, J.-M. Lehn, Wiley-VCH (**1995**) ISBN-13:978-3527293117. (e) Desiraju, G. R. *Nature* **2006**, *412*, 397-400. (f) J.-M. Lehn, Supramolecular Chemistry: Concepts and Perspectives, VCH, Weinheim, **1995**; (g) J. L. Atwood, J. E. D. Davies, D. D. MacNicol, F. VÖgtle, Comprehensive Supramolecular Chemistry, Pergamon, Oxford, **1996**.

[4] (a) Pfeiffer, R. "Organische Molekülerverbindungen", Stuttgart, 1927. (b) Wolf, K. L.; Frahm, F.; Harms, H. *Z. Phys. Chem. Abt.* **1937**, *36*, 17. (c) Wolf, K. L.; Wolff, R. *Angew. Chem.* **1949**, *61*, 191-201.

[5] Fisher, E. *Ber. Deutsch. Chem. Gesell* **1894**, *27*, 2985.

[6] Lehn, J. M. *Angew. Chem. Int. Ed.* **1988**, *27*, 89-112.

[7] (a) Whitesides, G. M.; Simanek, E. E.; Mathias, J. P.; Seto, C. T.; Chin, D. N.; Mammen, M.; Gordon, D. M. *Acc. Chem. Res.* **1995**, *28*, 37-44. (b) Desiraju, G. R.; *Crystal Engineering: The Design of Organic Solids Elsevier: Amsterdam* **1989**. (c) Schneider, H. –J. *Angew. Chem. Int. Ed. Engl.* **1991**, *30*, 1417-1436.

[8] Steed, J. W.; Atwood, J. L. Supramolecular Chemistry, VCH, Weinheim, **1995**.

[9] Pauling, L. *The Nature of the Chemical Bond*, Cornell University Press, Ithaca, **1939**.

[10] (a) Wells, A. F. Structural Inorganic Chemistry; Clarendon Press: Oxford, **1962**; pp 294-315. (b) Hamilton, W. **C.;** Ibers, J. A. Hydrogen Bonding in Solids; W. A. Benjamin, Inc.: New York, **1968**; pp 19-21.

[11] (a) Etter, M. C. *Acc. Chem. Res.* **1990**, *23*, 120-126. (b) Etter, M. C.; MacDonald, J. C.; Bernstein, J. *Acta Crystallogr.* **1990**, *B46*, 256-263. (c) Etter, M. C. *J. Phys. Chem.* **1991**, *95*, 4601-4606.

[12] (a) Bernstein, J. *Acta Crystallogr.* **1991**, *B47*, 1004-1012. (b) Bernstein, J.; Davis, R. E.; Shimoni, L.; Chang, N. -L. *Angew. Chem. Int. Ed.* **1995**, *34*, 1555-1573.

[13] (a) Donohue, J. *J. Phys. Chem.* **1952**, *56*, 502-510. (b) Etter, M. C.; Adsmond, D. A. *J. Chem. Soc. Chem. Commun.* **1990**, *8*, 589-591.

[14] Pedireddi, V. R.; Jones, W.; Chorlton, A. P.; Docherty, R. *Chem. Commun.,* **1996**, 997-998.

[15] Shattock, T. R.; Vishweshwar, P.; Zaworotko, M. J. *Cryst.Growth Des.* **2005**, *5*, 2046-2049.

[16] (a) Kolotuchin, S. V.; Fenlon, E. E.; Wilson, S. R.; Loweth, C. J.; Zimmerman, S. C. *Angew. Chem., Int. Ed. Engl.*, **1995**, *34*, 2654-2657. (b) Melendez, R. E.; Sharma, C. V. K.; Zaworotko, M. J.; Bauer, C.; Rogers, R. D. *Angew. Chem., Int. Ed. Engl.*, **1996**, *35*, 2213-2215. (c) Kolotuchin, S. V.; Rhiessen, P. A.; Fenlon, E. E.; Wilson, S. R.; Loweth, C. J.; Zimmerman, S. C. *Chem. Eur. J.*, **1999**, *5*, 2537-2547. (d) Herbstein, F. H.; Kapon, M.; Shteiman, V. *Acta Crystallogr., Sect. B*, **2001**, *57*, 692-696. (e) Ermer, O.; Neudorfl, J. *Helv. Chim. Acta*, **2001**, *84*, 1268-1313.

[17] Kolotuchin, S. V.; Fenlon, E. E.; Wilson, S. R.; Loweth, C. J.; Zimmerman, S. C. *Angew. Chem., Int. Ed. Engl*. **1995**, *34*, 2654-2657.

[18] Ma, B. –Q.; Coppens, P. *Chem. Commun.* **2003**, 2290–2291.

[19] Arora, K. K.; Pedireddi, V. R. *J. Org. Chem.* **2003**, *68*, 9177-9185.

[20] (a) Zerkowski, J. A.; Seto, C. T.; Whitesides, G. M. *J. Am. Chem. Soc.* **1992**, *114*, 5473-5475. (b) Zerkowski, J. A.; MacDonald, J. C.; Seto, C. T.; Wierda, D. A.; Whitesides, G. M. *J. Am. Chem. Soc.* **1994**, *116*, 2382-2391.

[21] (a) Zerkowski, J. A.; Seto, C. T.; Wierda, D. A.; Whitesides, G. M. *J. Am. Chem. Soc.* **1990**, *112*, 9025-9026. (b) Zerkowski, J. A.; Whitesides, G. M. *J. Am. Chem. Soc.* **1994**, *116*, 4298-4304. (c) Zerkowski, J. A.; MacDonald, J. C.; Whitesides, G. M. *Chem. Mater.* **1994**, *6*, 1250-1257. (d) Zerkowski, J. A.; Mathias, J. P.; Whitesides, G. M. *J. Am. Chem. Soc.* **1994**, *116*, 4305-4315.

[22] (a) Seto, C. T.; Whitesides, G. M. *J. Am. Chem. Soc.* **1980**, *112*, 6409-6411. (b) Lehn, J. M.; Mascal, M.; Decian, A.; Fischer, J. *J Chem. Soc. Chem. Commun.* **1990**, 479-481.

[23] Ranganathan, A.; Pedireddi, V. R.; Rao, C. N. R. *J. Am. Chem. Soc.* **1999**, *121*, 1752-1753.

[24] Bassani, D. M.; Darcos, C.; Mahony, S.; Desvergne, J. –P. *J. Am. Chem. Soc.* **2000**, *122*, 8795-8796.

[25] (a) Schmidt, G. M. J. *Pure Appl. Chem.* **1971**, *27*, 647-678. (b) Friscic, T.; MacGillivray, L. R. *Chem. Commun.*, **2005**, 5748-5750. (c) Friscic, T.; MacGillivray, L. R. *Zeitschrift fur Kristallographie* **2005**, *220*, 351-363. (d) Moorthy, J. N.; Venkatakrishnan, P. *Cryst. Growth Des*. **2007**, *7*, 713-718. (e) MacGillivray, L. R.; Papaefstathiou, G. S.; Friscic, T.; Hamilton, T. D.; Bucar, D. K.; Chu, Q.; Varshney, D. B.; Georgiev, I. G. *Acc. Chem. Res.* **2008**, *41*, 280-291 and references their in.

[26] Papaefstathiou, G. S.; Kipp, A. J.; MacGillivray, L. R. *Chem. Commun.* **2001**, 2462–2463.

[27] Mei, X.; Liu, S.; Wolf, C. *Org. Lett.,* **2007**, *9*, 2729-2732.

[28] Friscic, T.; Drab, D. M.; MacGillivray, L. R. *Org. Lett.,* **2004**, *6*, 4647-4650.

[29] Friscic, T.; MacGillivray, L. R. *Chem. Commun.*, **2003**, 1306-1307.

[30] Friscic, T.; MacGillivray, L. R. *Supramolecular Chemistry,* **2005**, *17*, 47–51.

[31] (a) PrakashaReddy, J.; Pedireddi, V. R. *Eur. J. Inorg. Chem.* **2007**, 1150-1158. (b) Marivel, S.; Shimpi, M. R.; Pedireddi, V. R. *Cryst. Growth Des.* **2007**, *7*, 1791-1796. (c) Varughese, S.; Pedireddi, V. R. *Chem. Commun.* **2005**, 1824-1826. (d) Rao, C. N. R.; Natarajan, S.; Vaidhyanathan, R. *Angew. Chem. Int. Ed.* **2004**, *43*, 1466-1496. (e) Yaghi, O. M.; Li, H.; Davis, C.; Richardson, D.; Groy, T. L. *Acc Chem.Res.* **1998**, *31*, 474-484. (f) Batten, S. R. *Curr. Opin. Solid State Mater.Sci.* **2001**, *5*, 107-114. (g) Moulton, B.; Zaworotko, M. J. *Chem. Rev.* **2001**, *101*, 1629-1658. (h) Janiak,

C. *Dalton Trans.* **2003**, 2781-2804. (i) Kitagawa, S.; Kitaura, R.; Noro, S. *Angew. Chem., Int. Ed.* **2004**, *43*, 2334-2375. (j) Rosseinsky, M. J. *Microporous Mesoporous Mater.* **2004**, *73*, 15-30.

[32] (a) Eddaoudi, M.; Kim, J.; Rosi, N.; Vodak, D.; Wachter, J.; O'Keeffe, M.; Yaghi, O. M. *Science* **2002**, *295*, 469-472. (b) Kitaura, R.; Kitagawa, S.; Kubota, Y.; Kobayashi, T. C.; Kindo, K.; Mita, Y.; Matsuo, A.; Kobayashi, M.; Chang, H. C.; Ozawa, T. C.; Suzuki, M.; Sakata, M.; Takata, M. *Science* **2002**, *298*, 2358-2361. (c) Ferey, G.; Latroche, M.; Serre, C.; Millange, F.; Loiseau, T.; Guegan, A. P. *Chem. Commun.* **2003**, 2976-2977. (d) Chu, H.; Dybtsev, D. N.; Kim, H.; Kim, K. *Chem. Eur. J.* **2005**, *11*, 3521-3529. (e) Rowsell, J. L. C.; Yaghi, O. M. *Angew. Chem., Int. Ed.* **2005**, *44*, 4670-4679. (f) Matsuda, R.; Kitaura, R.; Kitagawa, S.; Kubota, Y.; Belosludov, R. V.; Kobayashi, T. C.; Sakamoto, H.; Chiba, T.; Takata, M.; Kawazoe, Y.; Mita, Y. *Nature* **2005**, *436*, 238-241. (g) Dinca, M.; Long, J. R. *J. Am. Chem. Soc.* **2005**, *127*, 9376-9377.

[33] (a) Yaghi, O. M.; Li, H. *J. Am. Chem. Soc.* **1996**, *118*, 295-296. (b) Dalrymple, S. A.; Shimizu, G. K. H. *Chem. Eur. J.* **2002**, *8*, 3010-3015. (c) Kosal, M. E.; Chou, J. H.; Wilson, S. R.; Suslick, K. S. *Nat. Mater.* **2002**, *1*, 118-121. (d) Kim, H.; Suh, M. P. *Inorg. Chem.* **2005**, *44*, 810-812.

[34] (a) Fujita, M.; Kwon, Y. J.; Washizu, S.; Ogura, K. *J. Am. Chem. Soc.* **1994**, *116*, 1151-1152. (b) Seo, J. S.; Whang, D.; Lee, H.; Jun, S. I.; Oh, J.; Jeon, Y. J.; Kim, K. *Nature* **2000**, *404*, 982-986. (c) Wu, C. D.; Hu, A.; Zhang, L.; Lin, W. *J. Am. Chem. Soc.* **2005**, *127*, 8940-8941. (d) Lor, B. G.; Puebla, E. G.; Iglesias, M.; Monge, M. A.; Valero, C. R.; Snejko, N. *Chem. Mater.* **2005**, *17*, 2568-2573. (e) Sato, T.; Mori, W.;

Kato, C. N.; Yanaoka, E.; Kuribayashi, T.; Ohtera, R.; Shiraishi, Y. *J. Catal.* **2005**, *232*, 186-198. (f) Dybtsev, D. N.; Nuzhdin, A. L.; Chun, H.; Bryliakov, K. P.; Talsi, E. P.; Fedin, V. P.; Kim, K. *Angew. Chem., Int. Ed.* **2006**, *45*, 916-920. (g) Uemura, T.; Kitaura, R.; Ohta, Y.; Nagaoka, M.; Kitagawa, S. *Angew. Chem., Int. Ed.* **2006**, *45*, 4112-4116.

[35] Uemura, T.; Kitagawa, K.; Horike, S.; Kawamura, T.; Kitagawa, S.; Mizuno, M.; Endo, K. *Chem. Commun.* **2005**, 5968-5970.

[36] (a) J. Kang, J. Santamaria, G. Hilmersson, J. Rebek Jr., *J. Am. Chem. Soc.* **1998**, *120*, 7389-7390. (b) M. L. Merlau, M. P. Mejia, S. T. Nguyen, J. T. Hupp, *Angew. Chem. Int. Ed.* **2001**, *40*, 4239-4242. (c) D. Fiedler, R. G. Bergman, K. N. Raymond, *Angew. Chem. Int. Ed.* **2004**, *43*, 6748-6751.

[37] Yoshizawa, M.; Tamura, M.; Fujita, M. *Science* **2006**, *312*, 251-254.

[38] Toh, N. L.; Nagarathinam, M.; Vittal, J. J. *Angew. Chem. Int. Ed.* **2005**, *44*, 2237-2241.

[39] Chen, B.; Ockwig, N. W.; Millward, A. R.; Contreras, D. S.; Yaghi, O. M. *Angew. Chem., Int. Ed.* **2005**, *44*, 4745-4749.

[40] (a) Stahl, P. H.; Wermuth, G. *Handbook of Pharmaceutical Salts: Properties, Selection, and Use,* Verlag Helvetica Chimica Acta, Zürich, **2002**. (b) Trask, A. V. *Mol. Pharmaceutics* **2007**, *4*, 301-309. (c) Shan, N.; Zaworotko, M. J. *Drug Discovery Today* **2008**, *13*, 440-446. (d) Trask, A. V. *Mol. Pharmaceutics* **2007**, *4*, 301-309. (e) Jones, W.; Motherwell, S.; Trask, A. V. *Mrs Bulletin* **2006**, *31*, 875-879. (f) Trask, A. V.; Motherwell, W. D. S.; Jones, W. *Int. J. Pharm.* **2006**, *320*, 114-123.

[41] (a) Malmsten, M. *Surfactants and Polymers in Drug Delivery. Drugs and the Pharmaceutical Sciences.* Marcel Dekker, Inc.: New York *Vol 122*., 2002. (b) Amidon, G. L. *Chemical Aspects of Drug Delivery Systems* Ed.: Karsa, D. R and Stephenson, R. A. The Royal Society of Chemistry: Cambridge 1996. (c) Son, S. J.; Reichel, J.; He, B.; Schuchman, M.; Lee, S. B. *J. Am. Chem. Soc.* **2005**, *127*, 7316-7317. (d) Kumar, R.; Chen, M.-H.; Parmar, V. S.; Samuelson, L. A.; Kumar, J.; Nicolosi, R.; Yoganathan, S.; Watterson, A. C. *J. Am. Chem. Soc.* **2004**, *126*, 10640-10644.

[42] (a) Special Issue: *Org. Proc. Res. & Dev*. **2003**, *7*, 957-1016. (b) McCrone W. C. in *Physics and Chemistry of the Organic Solid State, Vol. II* (Eds: Fox, D.; Labes, M. M.; Weissberger A.), Interscience, New York, 1965, pp. 725-767. (c) Byrn, S. R. *Solid State Chemistry of Drugs*, Academic Press: New York, 1992. (d) Special Issue: *Polymorphism in Crystals, Cryst. Growth Des*. **2003**, *3*, 867-1040. (e) Threlfall, T. L. *Analyst* **1995**, *120*, 2435-2460. (f) Dunitz, J. D.; Bernstein, J. *Acc. Chem. Res*. **1995**, *28*, 193-200. (g) Davey, R. J. *Chem. Commun*. **2003**, 1463-1467.

[43] (a) Bernstein, J. *Polymorphism in Molecular Crystals*; Oxford University Press: New York, 2002**.** (b) Brittain, H. G. *Polymorphism in Pharmaceutical Solids*; Marcel Dekker Inc.: New York, 1999. (c) Special Issue on Pharmaceutical solid polymorphism in drug development and regulation. *Adv. Drug Delivery Rev.* **2004**, *56*, 235-418. (d) Hilfiker, R. *Polymorphism: in the Pharmaceutical Industry*; Wiley VCH: New York, 2006.

[44] (a) Datta, S.; Grant, D. J. W. *Nat. Rev. Drug Discovery* **2004**, *3*, 42-57. (b) Almarsson, O.; Zaworotko, M. J. *Chem. Commun.* **2004**, 1889-1896. (c) Gardner, C.

R.; Walsh, C. T.; Almarsson, O. *Nat. Rev. Drug Discovery* **2004**, *3*, 926-934. (d) Rodriguez-Spong, B.; Price, C. P.; Jayasankar, A.; Matzger, A. J.; Rodriguez-Horenedo, N. *Adv. Drug Delivery Res.* **2004**, *56*, 241-274. (e) Huang, L. F.; Tong, W. Q. *Adv. Drug Delivery Res.* **2004**, *56*, 321-334.

[45] Walsh, R. B.; Bradner, M. W.; Fleischman, S. G.; Morales, L. A.; Moulton, B.; Rodriguez-Horenedo, N.; Zaworotko, M. J. *Chem. Commun.* **2003**, 186-187.

[46] Childs, S. L.; Hardcastle, K. I. *Cryst. Growth Des*. **2007**, *7*, 1291-1304.

[47] Trask, A. V.; Motherwell, W. D. S.; Jones, W. *Cryst. Growth Des*. **2005**, *5*, 1013-1021.

[48] (a) Tackas-Novak, K.; Noszal, B.; Hermecz, I.; Kerszturri, G.; Podanyi, B.; Szasz, G. *J. Pharm. Sci*. **1990**, *79*, 1023-1028. (b) Rose, D. L.; Riley, C. M. *Int. J. Pharm*. **1990**, *63*, 237-250. (c) Tackas-Novak, K.; Juzan, M.; Hermecz, I., Szasz, G. *Int. J. Pharm*. **1992**, *79*, 89-96.

[49] Basavoju, S.; Boström, D.; Velaga, S. P. *Cryst. Growth Des*. **2006**, *6*, 2699-2708.

[50] McNamara, D. P.; Childs, S. L.; Giordano, J.; Iarriccio, A.; Cassidy, J.; Shet, M. S.; Mannion, R.; O'Donnell, E.; Park, A. *Pharm. Res.* **2006**, *23*, 1888-1897.

CHAPTER TWO

Nucleobases in molecular recognition

2.1 Introduction

DNA is a very important biomolecule, usually, occurs as an antiparallel double helix with complementary nucleobases being held together through hydrogen bonds, i.e., adenine-thymine (A-T) and guanine-cytosine (G-C), as shown in Scheme 2.1, often, being referred as Watson-Crick base pairs.[1] There are 28 base pairing possibilities, which involve at least two hydrogen bonds that could be formed by nucleobases.[2] Because, base pair association is responsible for the unique DNA structure and also due to the specificity, such hydrogen bond patterns have gained a lot of attention for the systematic analysis and to utilize in various branches of chemistry, ranging from small molecules to macromolecules, such as peptide nucleic acids (PNA),[3] DNA based nanotechnology,[4] synthesis of bioactive molecules,[5] liquid crystals,[6] supramolecular polymers,[7] magnetic materials,[8] electron and energy transfer systems,[9] etc. Several exotic examples have appeared in recent literature exemplifying the elegance of the studies and a few representative studies are discussed in the following section.

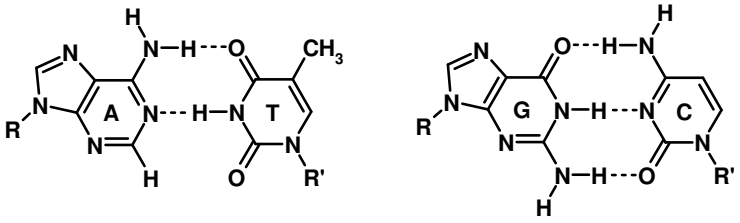

Scheme 2.1. Watson-crick base pairing interactions.

Takui and co-workers for the first time, have utilized, A-T and G-C base pair interactions for the preparation of organic magnetic materials. The resulted magnetic properties associated with the complexes were analyzed based on the molecular

arrangement and complementary hydrogen bonding interactions between the nucleobases.[10]

For this purpose, Nitronylnitroxide (**NN**) substituted adenine, thymine and cytosine and *n*-butyl substituted guanines have been co-crystallized accordingly, to prepare complexes between complementary nucleobases, as shown in Scheme 2.2. The assemblies, thus, formed were confirmed by single crystal X-ray diffraction methods.

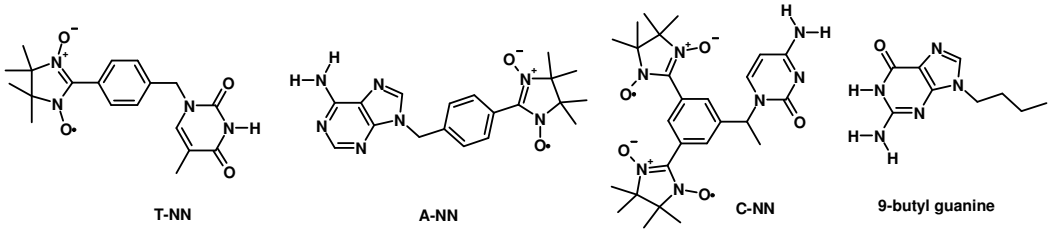

(a)

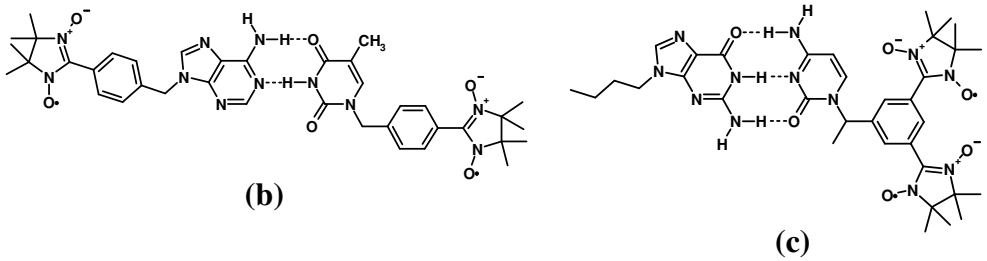

(b) **(c)**

Scheme 2.2. (a) Nitronylnitroxide (**NN**) substituted adenine, thymine and cytosine and n-butyl substituted guanines used in this study. Basic recognition pattern in the complexes of (b) A-NN **:** T-NN and (c) C-NN **:** 9-butyl guanine.

Shimuzu and co-workers have reported the formation of microsized supramolecular fibers directed by internucleobase interactions. Three types of monomeric units were synthesized in which 1-(2-carboxyethyl)thymine or 9-(2-corboxyethyl)adenine were homoditopically or heteroditopically attached to both ends of alkyl chains (see Scheme 2.3).[11]

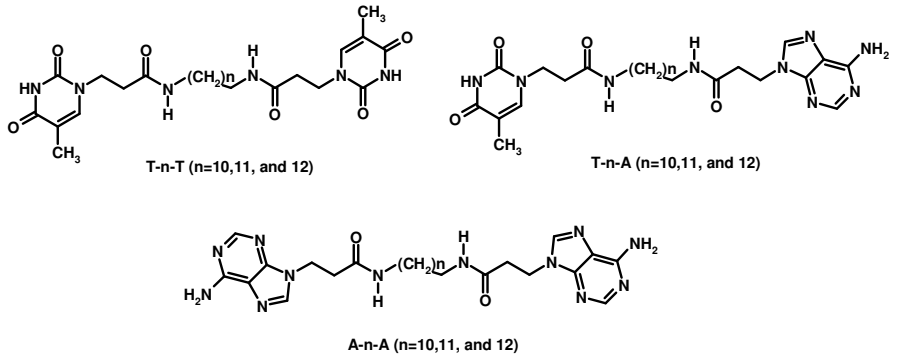

Scheme 2.3. Monomer structures synthesized for preparation of supramolecular polymers.

Supramolecular fibers were formed due to homomeric aggregation of heteroditopic T-n-A (where n denotes the number of methylenes spacing the bases) or homoditopic T-n-T and heteromeric aggregation of a 1:1 mixture of T-n-T and A-n-A, as shown in Figure 2.1.

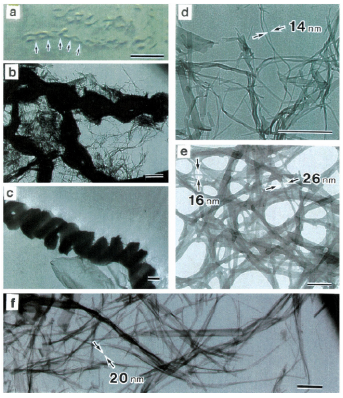

Figure 2.1. (a) Dark-field light micrograph of double-helical ropes formed from the homoditopic **T-10-T** (at 25 °C in 10% ethanolic/aqueous solutions, bar 5 μm). The arrows denote representative interwoven portions of the helical ropes. EF-TEM images of (b, c) the double-helical ropes (bar 1 μm), (d) nanofibers as a constituent of the helical ropes (bar 1 μm), (e) nanofibers formed from an equimolar mixture of **T-10-T** and **A-10-A** (bar 200 nm), and (f) nanofibers formed from the heteroditopic **T-12-A** (bar 1 μm).[11]

Rowan and co-worker have prepared the fluorescent supramolecular liquid crystalline polymers based on A-T base pairing. In this work, they have synthesized four monomers, as shown in Scheme 2.4, and the reaction process was monitored by differential scanning calorimetry (DSC), depicted in Figure 2.2.[12]

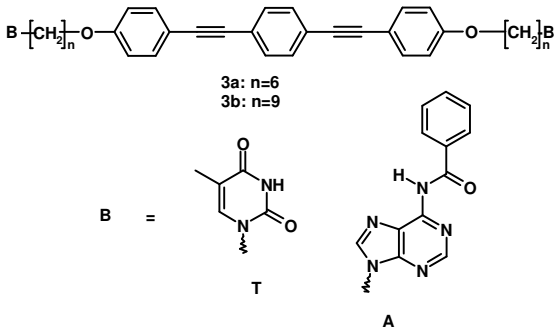

Scheme 2.4

The four monomers, independently, showed no propensity for liquid crystalline behavior and have very high melting points (Figures 2.2(a), 2.2(b) show the DSC thermograms for **A–3a–A** and **T–3a–T**). However, upon mixing and melting these two complementary nucleobase terminated monomers, showed a dramatic decrease in the melting point (see Figure 2.2(c)) along with the concurrent information of viscous phase between 125-154 ºC.

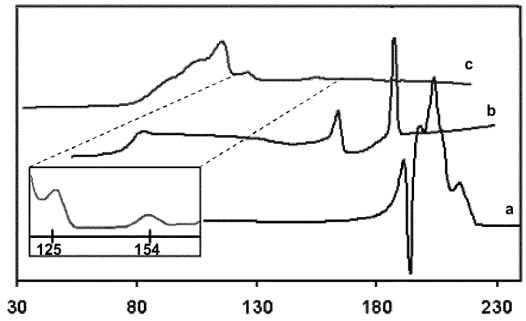

Figure 2.2. DSC thermograms of the second heating of (a) **T–3a–T**; (b) **A–3a–A**; and (c) **A–3a–A**: **T–3a–T** (1: 1 molar ratio) with an expansion of the bifringent region (inset).[12]

Similarly, the other combinations i.e., **A-3a-A** : **T–3b–T**, **A–3c–A** : **T–3a–T and A–3b–A** : **T–3b–T** also yielded viscous phases at different temperatures. Polarized optical micrographs of the resulted liquid crystalline materials are shown in Figure 2.3.

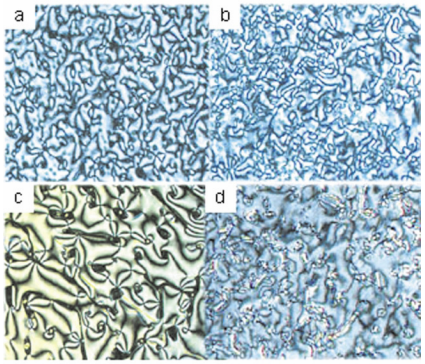

Figure 2.3. Polarized optical micrographs of liquid crystalline materials observed for (a) **A-3a-A** : **T–3a–T** at 130 °C; (b) **A-3a-A** : **T–3b–T** at 160 °C; (c) **A–3c–A** : **T–3a–T** at 155 °C and (d) **A–3b–A** : **T–3b–T** at 120 °C (magnification 5003).[12]

Gokel and co-workers have reported a "molecular box" composed of a dimer of dinucleoside stabilized through A-T base pair interactions, as shown in Scheme 2.5. This duplex is of special interest because, it is stabilized by a combination of intramolecular Hoogsteen base-pairing and intermolecular one-point N-H···O hydrogen bonds.[13]

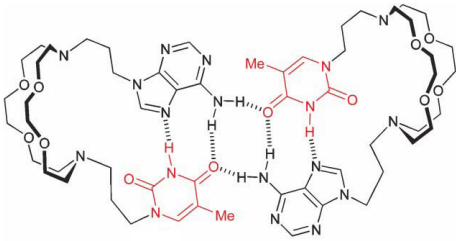

Scheme 2.5. Molecular box formed between adenine and thymine interactions.[13]

Sessler and co-workers have developed a method for transporting nucleosides and their analogous drug molecules with complementary base-pairing agents.[14] To qualify a given molecule as drug, the first requirement is its ability to get transported into the diseased cells through lipophilic membrane barrier. In this direction, lipophilic triisopropyl (Tips) substituted nucleoside derivatives, i.e., A-Tips, U-Tips, C-Tips and G-Tips have been examined as transport agents for a variety of nucleoside derivatives, such as acyclovir (**ACV**), dideoxycytidine (**DDC**), and azidothymidine (**AZT**), (see Scheme 2.6) in a simple (H_2O-$CHCl_3$-H_2O) liquid membrane system.

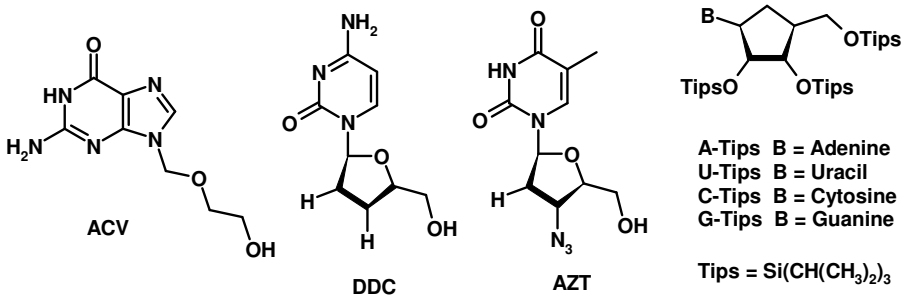

Scheme 2.6

It was observed that, in the presence of complementary lipophilic Tips, nucleoside molecules enhance the transport of the drug molecules across the membrane. These observations were rationalized in term of the known base pairing interactions. For example, acyclovir, which is being used to treat herpes infections, is a guanine derivative having complementary hydrogen bonding site to establish interaction with C-Tips nucleoside, which, enhanced the transportation across membranes. Schematic representation of interaction between acyclovir and C-Tips molecule is shown in Scheme 2.7.

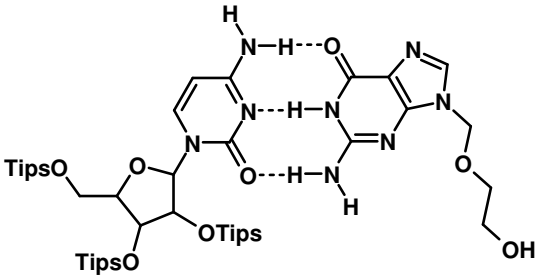

Scheme 2.7. Basic recognition pattern between C-Tips nucleoside and acyclovir.

Mascal and co-workers also have utilized the guanine-cytosine interactions for the preparation of hexameric exotic supramolecular architecture.[15] For this purpose, pyrido[4,3-d]pyrimidine, **PP**, was synthesized, in which one end of the molecule possesses the cytosine with acceptor-acceptor-donor (**AAD**) hydrogen bonding code, while the other possess guanine with donor-donor-acceptor (**DDA**) code, placed at an angle of 120º to each other. Crystallization of it from DMSO yielded an elegant six membered supramolecular unit, as shown in Figure 2.4. In fact, twenty four hydrogen bonds are involved in the obtained hexagonal supramolecular assembly, with structurally close similarity to the cyanuric acid-melamine supramolecular assembly (see Figure 1.8(d) in chapter 1).

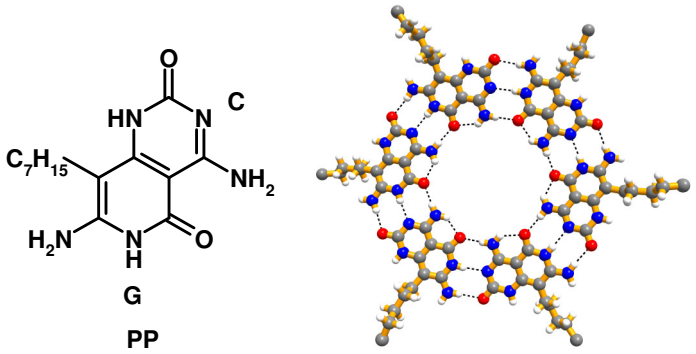

Figure 2.4. Hexameric network formed by **PP**.

Similarly, Sessler and co-workers also have utilized the G-C base pair interactions for the creation of a cyclic trimeric supramolecular unit. Salient features of hydrogen bonding interactions are shown in Scheme 2.8.[16]

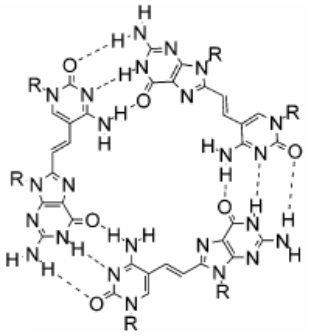

Scheme 2.8. Trimeric supramolecular assembly governed by guanine-cytosine interactions.

Thus, the examples so far been described above emphasized on the utility of hydrogen bonding patterns formed by various derivatives of nucleobases. Indeed, a thorough search made on Cambridge Structural Database (CSD) revealed that only a few structures of molecular complexes of native nucleobases are known.[17] Further, it is interesting to note that most of the **AT** (**U**) base pair interactions observed in the structures retrieved from CSD, belong to the Hoogsteen interactions (see Figure 2.5(b)) rather than Watson-crick base pairing (see Figure 2.5(a)).[18]

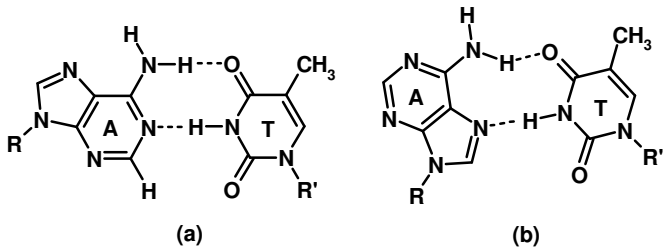

Figure 2.5. (a) Watson-crick base pair (b) Hoogsteen base pair.

Apart from the well known Watson-Crick and Hoogsteen hydrogen bonding patterns, nucleobases could form several other possible types of interactions between them. Necessity of studies of those hydrogen bonding patterns are imminent, with current developments and challenges in the areas of biomimicking of natural systems, for example protein/enzyme/DNA interaction with drugs, computational aided drug design, etc., which are mainly facilitated by the interactions formed by nucleobases. Hence, it would be of great interest to study the molecular recognition properties of native nucleobases, with various substrates.

It is known from the literature that, -COOH functional group has high affinity towards pyridyl –N atoms,[19] by forming O-H···N hydrogen bond, as it was identified by Pedireddi and Jones, which was well explored by several other researchers. Since, nucleobases also have such –N atoms in plenty, molecular recognition studies of native nucleobases with carboxyl compounds would be of appropriate to evaluate the properties of nucleobases in supramolecular chemistry.

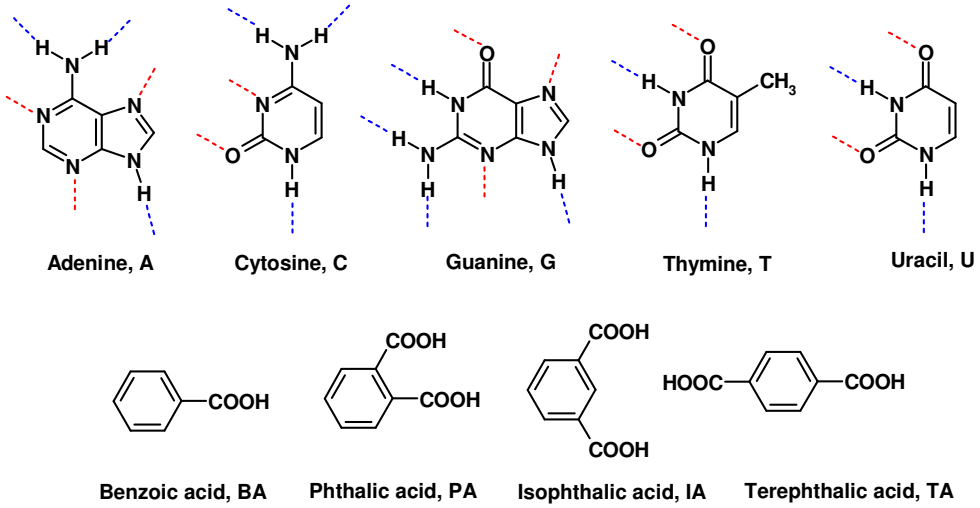

Scheme 2.9

For this purpose, co-crystallization experiments of all natural nucleobases with various derivatives of benzoic acid, as shown in Scheme 2.9, have been carried out.[20]

2.2 Molecular adducts of nucleobases with some aromatic carboxylic acids.

Analysis of the residues obtained from co-crystallization experiments either in the form of crystals or precipitates, by X-ray diffraction methods, revealed that only adenine and cytosine formed complexes with all the aromatic carboxylic acids listed in Scheme 2.9. Complete details of the experiments and characterization methods are given in Table 2.1.

Table 2.1. Co-crystal experiments of nucleobases with different benzoic acids.

	Benzoic Acid	**Phthalic Acid**	**Isophthalic Acid**	**Terephthalic Acid**
Adenine	Complex formed (confirmed by single crystal X-ray diffraction methods)	Complex formed (new peaks in powder X-ray diffractogram)	Complex formed (new peaks in powder X-ray diffractogram)	Complex formed (new peaks in powder X-ray diffractogram)
Thymine	No complex formation is observed from Methanol	No complex formation is observed from methanol	No complex formation is observed from methanol	No complex formation is observed from methanol
Uracil	No complex formation is observed from methanol	No complex formation is observed from methanol	No complex formation is observed from methanol	No complex formation is observed from methanol
Cytosine	Complex formed (confirmed by Single crystal X-ray diffraction methods)	Complex formed (confirmed by Single crystal X-ray diffraction methods)	Complex formed (confirmed by Single crystal X-ray diffraction methods)	Complex formed (new peaks in powder X-ray diffractogram)
Guanine	No complex formed from dimethylformamide	No complex formed from dimethylformamide	No complex formed from dimethylformamide	No complex formed from dimethylformamide

2.2.1 Molecular adduct of adenine with benzoic acid

Co-crystallization of adenine, **A** and benzoic acid, **BA** from a CH_3OH solution gave good quality single crystals. Structure determination by X-ray diffraction methods reveal that an adduct of **A** and **BA** was formed in a 1:2 ratio, as shown in Figure 2.6.

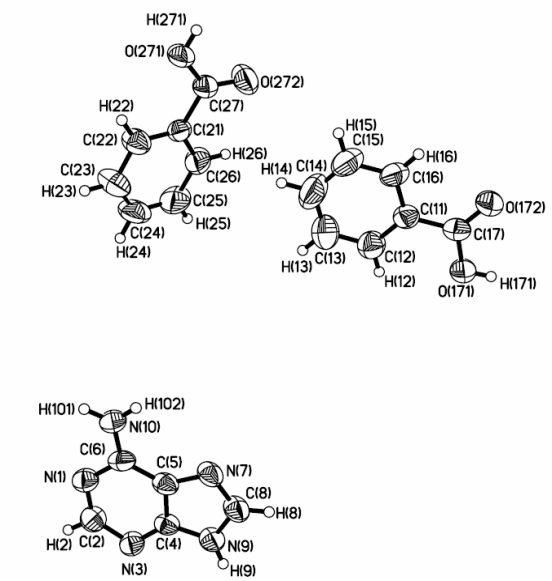

Figure 2.6. ORTEP (50% probability level) drawing of the molecular complex of adenine and benzoic acid.

In the crystal lattice, molecules of **A** and **BA** interact with each other through the formation of cyclic hydrogen bonding pattern through –COOH, $-NH_2$ and hetero –N atoms (N^1 and N^7) like in Watson-Crick and Hoogsteen base pairs. The recognition pattern and the molecular arrangement in two-dimensions is shown in Figure 2.7(a). Thus, **BA** interacts with **A** through both pyrimidine and imidazole rings with the formation of O-H···N (H···N, 1.83 and 1.86 Å) and N-H···O (H···O, 2.10 and 2.15 Å) hydrogen bonds. Further, the 1:2 units are held together by centrosymmetric N-H···N hydrogen bond coupling formed between pyrimidine $–N^3$ atom and imidazole NH at 9-position with an H···N distance of 1.98 Å, as shown in Figure 2.7(b).

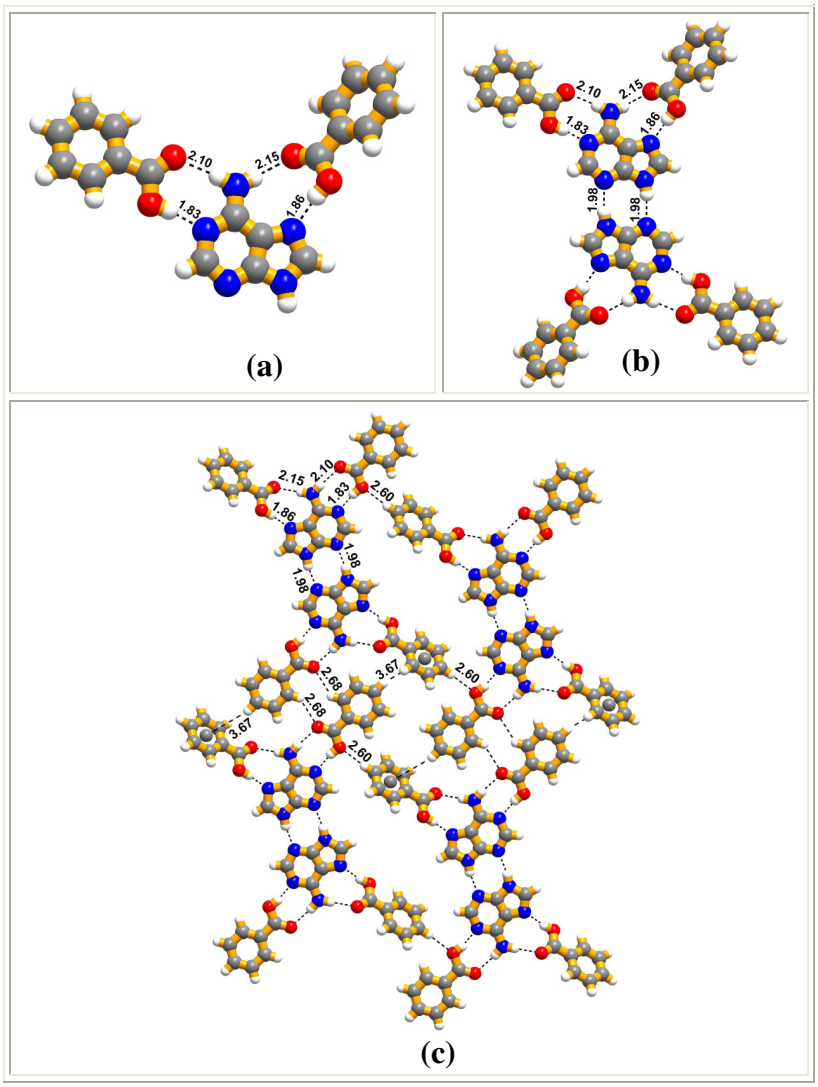

Figure 2.7. (a) Molecular recognition between A and BA in a 1:2 adduct and (b) interaction between 1:2 units through N-H···N centrosymmetric interactions. (c) Arrangement of adenine, **A** and benzoic acid, **BA** in the molecular adduct. Hydrogen bonds are shown in dashed lines. Lines between H-atoms and the centroid of the phenyl moiety of **BA** molecules represent C-H···π interactions.

Such aggregates constituted one-dimensional networks, through cyclic C-H···O hydrogen bonds (H···O, 2.68 Å), formed between **BA** molecules yielding infinite molecular tapes, which, in turn, are further held together by single C-H···O hydrogen

bond (H···O, 2.60 Å) as well as C-H···π interactions (3.67 Å), forming sheet like structure in two dimensions, as shown in Figure 2.7(c).

2.2.2 Molecular adducts of adenine with phthalic acid, isophthalic acid and terephthalic acid

Co-crystallization of adenine with three isomers of dicarboxylic acid (phthalic acid, isophthalic acid and terephthalic acid) from various solvents such as methanol, ethanol, water, dimethyl formamide etc., however, gave only precipitates rather than single crystals. Powder X-ray diffraction patterns of the resulted precipitates have been recorded to characterize the residues, by comparing with the pattern of the reactants.

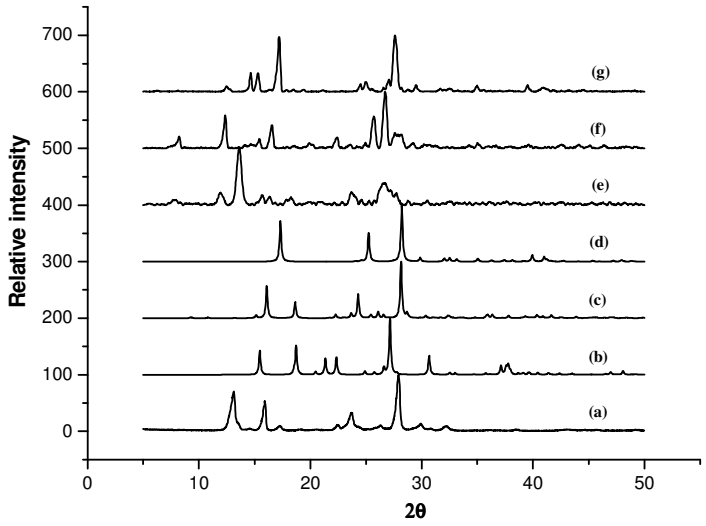

Figure 2.8. Powder X-ray diffraction patterns of (a) adenine, (b) phthalic acid, (c) isophthalic acid, (d) terephthalic acid, (e) adenine-phthalic acid, (f) adenine-isophthalic acid, and (g) adenine-terephthalic acid.

In all the cases, new peaks are formed in the residues, which were not present in either of the reactant phases, as shown in Figure 2.8, thus, conforming the formation of complexes. For example, in the residue of adenine and phthalic acid, new peaks at

11.9, 13.6 and 23.7 º are observed (see Figure 2.8(e)) and also the characteristic peaks corresponding to either of the reactant (phthalic acid, 15.5, 18.8, 21.3, 22.3 and 27.2 º (see Figure 2.8(b)) and adenine 13.1, 15.9 and 28 º (see Figure 2.8(a)) are completely absent. Similarly, for the adducts of isophthalic and terephthalic acids, their characteristic peaks at 16, 18.8, 24.2 and 28.2 º (isophthalic acid) and 17.3, 25.2 and 28.3 º (terephthalic acid) as well as of adenine are absent, while new peaks were observed at 8.1, 12.2, 16.8, 25.8 and 26.8 º and 14.8, 15.2, 17.1 and 27.8 º in the patterns of the corresponding residues (Figure 2.8(f) and (g)).

2.2.3 Molecular adduct of cytosine with benzoic acid

Co-crystallization of cytosine and benzoic acid in 1:1 molar ratio from methanol yielded good quality single crystals. Structure analysis revealed that it formed a 1:1 molecular adduct, but with two molecules of each **C** and **BA** in the asymmetric unit, as shown in Figure 2.9. Further, while one pair of **C** and **BA** show recognition through the proton transfer from –COOH group to pyrimidine N^3, the other pair remains in neutral form.

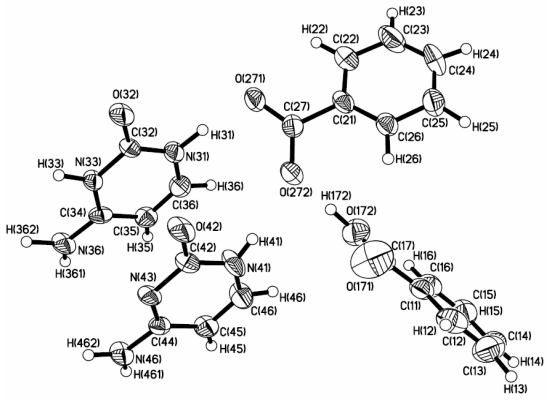

Figure 2.9. ORTEP (50% probability level) drawing of the molecular complex of cytosine and benzoic acid.

In the complex, the interaction between **C** and **BA** is established through N^1, such that each deprotonated acid interacts with both the symmetry independent molecules of **C**, while the adjacent molecules of **C** form dimers by a triple hydrogen bonding involving N^3, carbonyl and the $-NH_2$ groups, resembling pseudo Watson-Crick pattern. A pictorial representation of the interactions between the cytosine and **BA** molecules is shown in Figure 2.10(a). The hydrogen bond distances ($H^{\cdots}O$ and $H^{\cdots}N$) in the cytosine duplex are 1.91, 1.96 and 1.98 Å. Further, the adjacent cytosine dimers are held together by two $N\text{-}H^{\cdots}O$ hydrogen bonds with $H^{\cdots}O$ distances of 2.12 and 2.15 Å, formed by $-NH_2$ groups and carbonyl group (see Figure 2.10(b)). Three-dimensional arrangement of these species is quite intriguing, with the formation of ladder-like structure as shown in Figure 2.11.

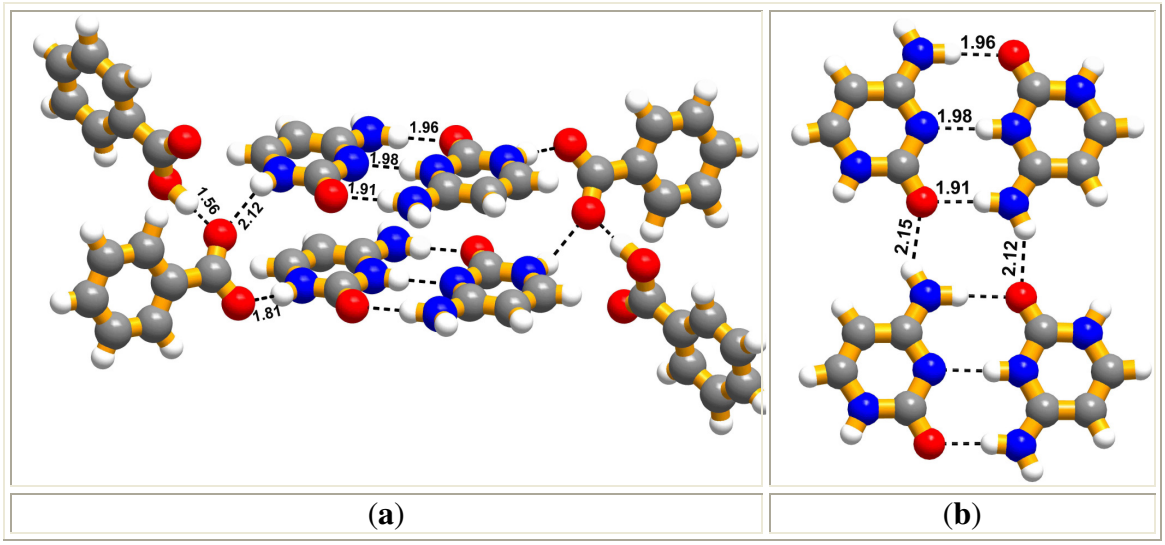

Figure 2.10. (a) Recognition pattern between cytosine, **C** and benzoic acid, **BA** in the molecular adduct. (b) Duplexes of cytosines connected together by $N\text{-}H^{\cdots}O$ hydrogen bonds.

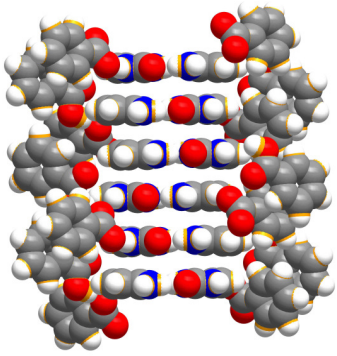

Figure 2.11. Three-dimensional packing of **C** and **BA** in the molecular adduct forming a supramolecular ladder.

2.2.4 Molecular adduct of cytosine with phthalic acid

Cytosine and phthalic acid in a 1:1 molar ratio, from DMF, gave block-like crystals, suitable for data collection by X-ray diffraction methods. Structure analysis revealed that a 2:1 adduct of cytosine and the acid is formed, as shown in ORTEP diagram below (Figure 2.12). The complete crystallographic information is given in Table 2.2.

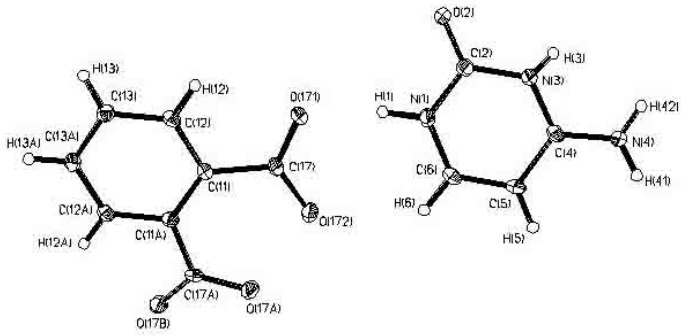

Figure 2.12. ORTEP (50% probability level) drawing of the molecular complex of cytosine and phthalic acid.

In the adduct, both the –COOH groups undergo proton transfer to N^3 of cytosine molecules, forming cytosinium ions, CH^+ and carboxylate. Interaction

between CH^+ molecules is established through triple hydrogen bonding pattern, forming a binary supramolecular unit. Further, such units are held together by two N-H···O hydrogen bonds with H···O distances of 2.01 and 2.01 Å, similar to the cytosine benzoic acid adduct, forming molecular tapes, as shown in Figure 2.13. Characteristics of hydrogen bonds are listed in Table 2.3.

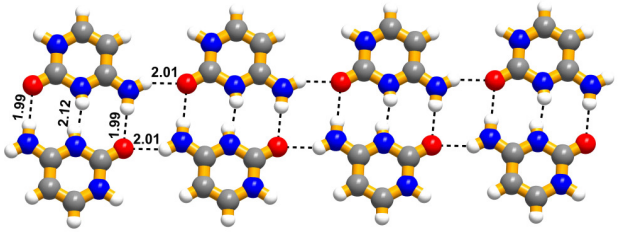

Figure 2.13. Interaction between cytosine molecules in cytosine-phthalic acid adduct.

Further, these tapes interact with the acid molecules through N-H···O and C-H···O hydrogen bonds, with H···O distances of 1.78 and 2.56 Å, respectively, forming crinkled tapes, as shown in Figure 2.14. Thus, in each sheet, the **PA** molecules appear as sandwiched between tapes of cytosine molecules. The three dimensional arrangement is shown in Figure 2.15.

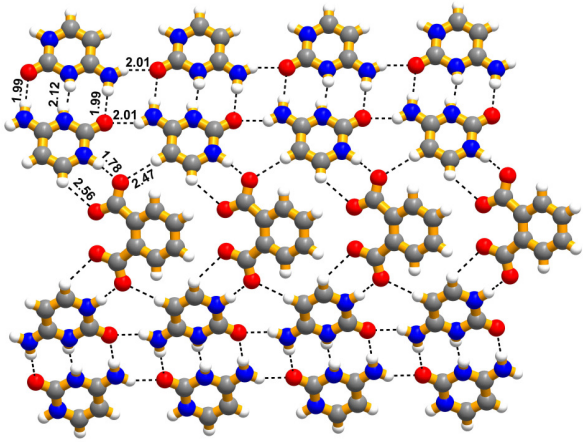

Figure 2.14. Arrangement of molecules of cytosine (**C**) and phthalic acid (**PA**) in the adduct forming a pillar-like structure.

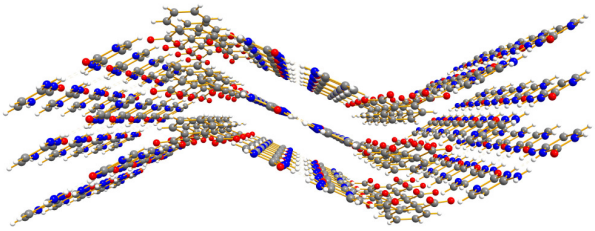

Figure 2.15. Three-dimensional arrangement of molecules in C-PA adduct.

2.2.5 Molecular adduct of cytosine with isophthalic acid

Co-crystallization between cytosine and isophthalic acid, from DMF solution, yielded good quality crystals, and structure determination by X-ray diffraction methods revealed that the asymmetric unit has a composition of the reactants in 1:1 ratio of cytosine and the acid, as shown in ORTEP drawing (Figure 2.16). Complete crystallographic details are given in Table 2.2. In this adduct also, proton transfer occurred between one of the –COOH groups and N^3 of the cytosine.

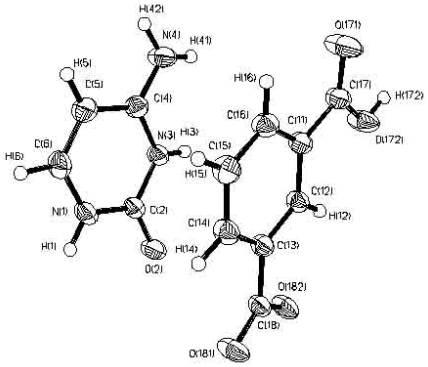

Figure 2.16. ORTEP (50% probability level) drawing of the molecular complex of cytosine and isophthalic acid.

Interaction between cytosine molecules is through the triple hydrogen bonding pattern, but, in contrast to the patterns observed in the complexes with **BA** and **PA**, the cytosine duplexes are further held together by cyclic hydrogen bonding patterns, consisting of centrosymmetric N-H···O hydrogen bonds (H···O, 1.95 Å, Table 2.3), as

shown in Figure 2.17(a). On the other hand, interaction between isophthalic acid molecules is established by O-H···O (H···O, 1.80 Å) and C-H···O (H···O, 2.69 Å) hydrogen bonds, with a quartet arrangement (see Figure 2.17(b)). Further, interaction between cytosine and the acid molecules is formed by C-H···O hydrogen bonds with hydrogen bond distances of 2.28 and 2.44 Å, forming a sheet like structure, in two dimensional arrangement (see Figure 2.17(c)). This arrangement has a close resemblance to the structure of cytosine and phthalic acid except that in the present case, the cytosine duplexes are being separated by two layers of dimers of acid molecules.

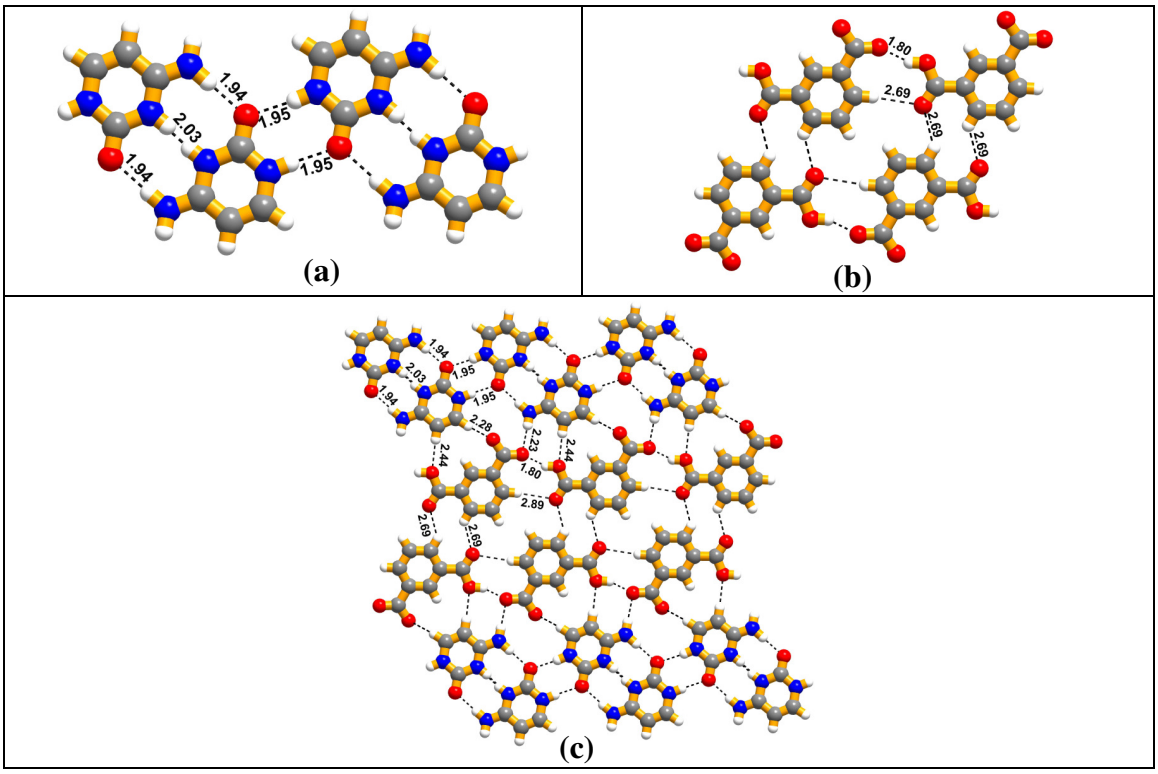

Figure 2.17. (a) Interaction of the adjacent triple hydrogen bonded duplexes of cytosine through dimeric hydrogen bonds pattern, (b) Quartet arrangement of **IA** molecules and (c) 2D arrangement of cytosine and isophthalic acid (**IA**) in the crystal lattices of their adduct.

2.2.6 Molecular adduct of cytosine with terephthalic acid

Co-crystallization of cytosine with terephthalic acid from various solvents such as methanol, ethanol, DMF, DMSO etc., yielded microcrystalline material, which could not be used for structure determination by single crystal X-ray diffraction methods. However, analysis by powder X-ray diffraction methods suggest the formation of complex, as evident from the different peak positions in powder pattern compared with the powder X-ray diffraction patterns of the reactants, as shown in Figure 2.18. It is clearly evident from Figure 2.18(c) that new peaks appeared at 2θ angles of 7.1, 14.1 and 20.9 º, while the characteristic peaks corresponds to cytosine (13.7, 16.6, 20, 26 and 27.1 º) and terephthalic acid (25.2 and 28.1 º) are absent.

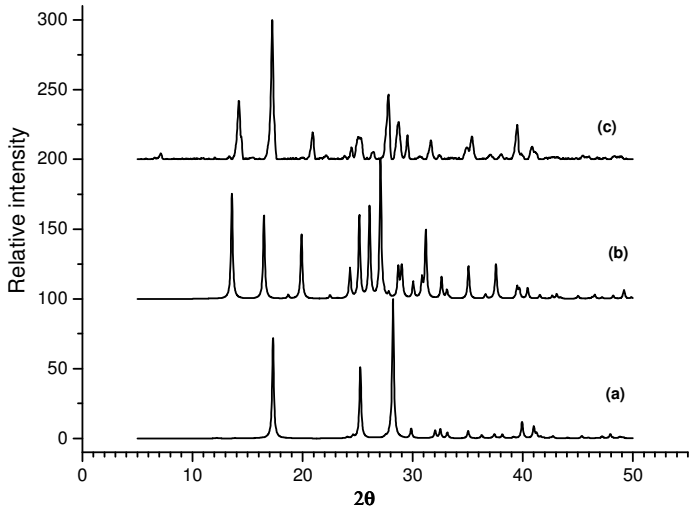

Figure 2.18. Powder X-ray diffraction patterns of (a) terephthalic acid (b) cytosine and (c) molecular adduct of cytosine-terephthalic acid.

Comparison of the three adducts of cytosine discussed above, it is evident that in all the cases, cytosine forms duplexes, connected together by triple hydrogen bonding patterns, and yield molecular tapes. These molecular tapes are arranged in the

crystal lattice as rungs in the ladder structure with **BA** but sandwiched in the two-dimensional arrangement in the adducts of **PA** and **IA**. A schematic representation of systematic variations in the arrangement of molecules in the adducts is shown in Figure 2.19.

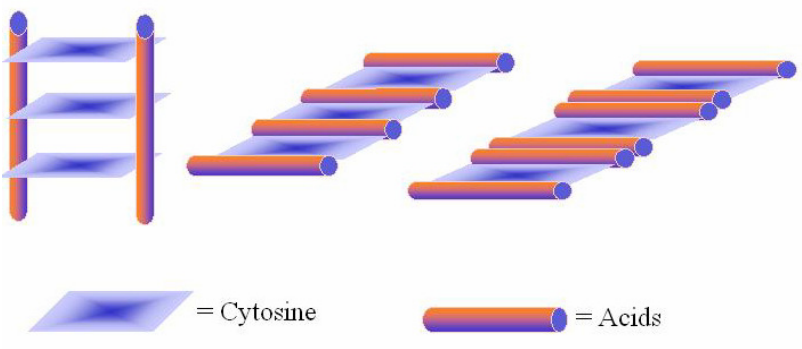

Figure 2.19. Schematic representation of the packing of molecules in the adducts of cytosine with (left) benzoic acid, (middle) phthalic acid and (right) isophthalic acid.

2.2.7 Co-crystallization experiments of guanine with benzoic acid, phthalic acid, isophthalic acid and terephthalic acid

Among the all nucleobases, guanine shows very low solubility in many of the solvents such as methanol, ethanol, water, DMF, DMSO, etc. All the experiments that were carried out between guanine and benzoic acid as well as its other acid derivatives yielded only precipitates. The powder patterns, thus, recorded are shown in Figure 2.20. An analysis revealed that complexes were not formed as no new peaks except the sum of the both the reactants peaks, are present in the powder patterns of the residues. For example, in **G-BA** the prominent peaks at 8.1, 14, 17.2 and 27.9 ° are same as observed in the patterns of **BA** and **G**. Similarly, in the case of **G-TPA**, the peaks at 14, 17.2, 25.1 and 28.1 ° corresponds to **G** and **TPA** (see Figure 2.20(i)).

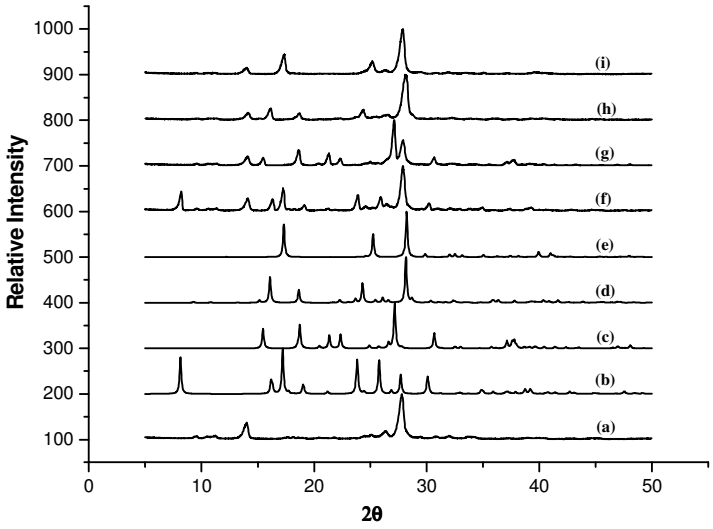

Figure 2.20. Powder X-ray diffraction patterns of (a) guanine, (b) benzoic acid, (c) phthalic acid, (d) isophthalic acid, (e) terephthalic acid, (f) guanine - benzoic acid, (g) guanine- phthalic acid, (h) guanine-isophthalic acid and (i) guanine-terephthalic acid.

However, the residues obtained from co-crystallization experiments of thymine and uracil with benzoic acid and its derivatives were not crystalline enough even to evaluate by powder X-ray diffraction methods.

Thus, in this study, it was noted that cytosine and adenine both did show tendency to form molecular complexes, irrespective of the nature of the other species in the recognition process. The cytosine-cytosine interactions with triple hydrogen bonding pattern is observed in biological environment, which is referred as I-motifs in structural biology.[21] Systematic analysis of these moieties are further discussed in Chapter 3. Also, this study indicates that in the co-crystallization experiments with –COOH functionality, adenine binds with the other molecules, utilizing N^1 and N^7 sites, as it binds to thymine in DNA structure. However, cytosine participated in the molecular recognition preferentially through N^1 position, which is generally connected

to sugar moiety in DNA, but mimics the hydrogen bonding pattern that it forms with guanine in G-C base pair, by *homomeric* process.

Selective recognition features observed in this study employing acid functionalities directed to further investigate molecular recognition studies of nucleobases with compounds, which are basic in nature. For this purpose, ligands like melamine, which is quite well known to form molecular adducts with many organic substrates,[22] have been chosen to co-crystallize with all the nucleobases. For example, melamine with hydrogen bonding capabilities as shown below, in principle can form aggregation of different compositions. In a typical example with thymine or uracil, the possible patterns are shown in Scheme 2.10.

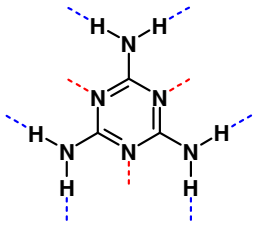

Melamine, M

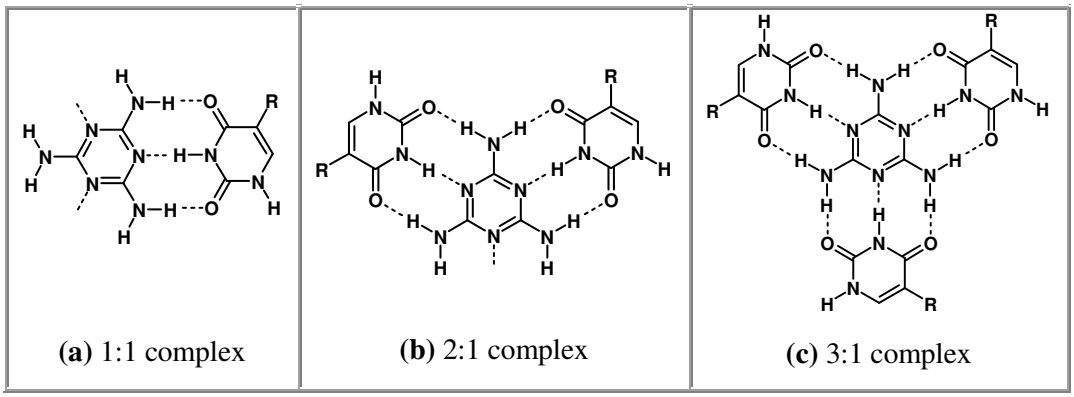

(a) 1:1 complex **(b)** 2:1 complex **(c)** 3:1 complex

Scheme 2.10. Anticipated recognition patterns between melamine and thymine (uracil) i.e., (a) Binary unit, (b) triplet arrangement and (c) quartet arrangement.

Co-crystallization of melamine with different nucleobases from various solvents have yielded either single crystals or precipitates. The analysis by X-ray diffraction methods revealed that only thymine and uracil form molecular complexes with melamine, which were inert to carboxylic acids as observed in the earlier sections. Complexes, thus, obtained in these experiments by varying solvents and concentrations have been labeled as **1**, **2**, **3**, **4**, **5** and **6** (see Scheme 2.11).

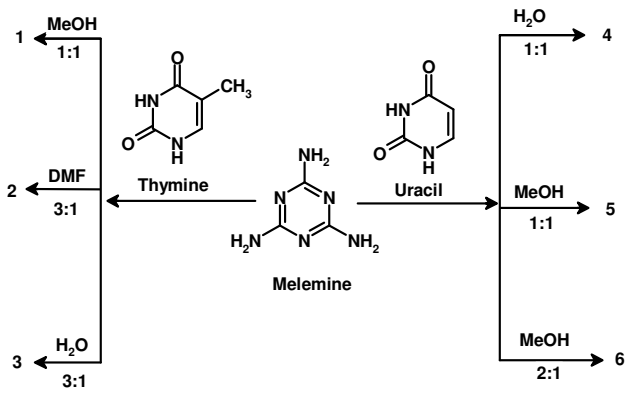

Scheme 2.11

2.3. Molecular adducts of thymine and melamine

2.3.1 Molecular adduct of thymine and melamine from methanol, 1

Co-crystallization of thymine and melamine from a methanol solution yielded a 1:1 adduct along with solvent of crystallization, as shown in Figure 2.21. The complete crystallographic information is given in Table 2.2.

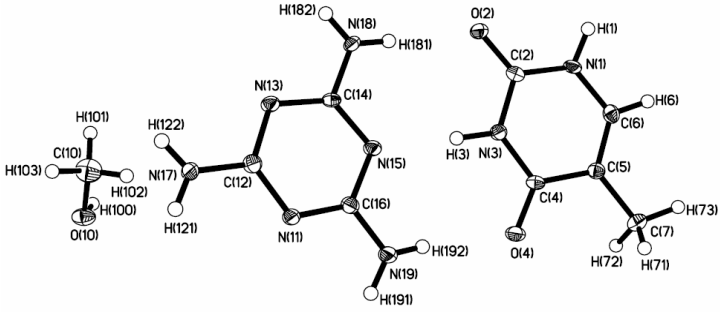

Figure 2.21. ORTEP (50% probability level) drawing of the adduct **1**.

In the adduct **1,** the recognition pattern between thymine and melamine (See Figure 2.22b) is through the formation of triple hydrogen bonding pattern, comprising of N-H···O and N-H···N hydrogen bonds. The hydrogen bond distances in the binary unit are H···O, 2.05, 2.14 Å and H···N, 1.93 Å. Further, these binary units are held together by N-H···O (H···O, 2.06 Å) hydrogen bonds, yielding a quartet arrangement, as shown in Figure 2.22(b). Four such quartets, aggregate by homomeric melamine···melamine and thymine···thymine interactions to yield channels of dimension 11.6 Å x 7.2 Å, which are being occupied by solvent molecules (CH_3OH), as depicted in Figure 2.22(b). The hydrogen bonds in melamine···melamine dimers is H···N, 2.13 Å while in thymine···thymine, it is H···O, 1.87 Å. The interaction between the host structure of melamine-thymine and the solvent is through the formation of N-H···O hydrogen bonds, between melamine and CH_3OH molecules, with H···O distances of 2.30, 2.22 Å.

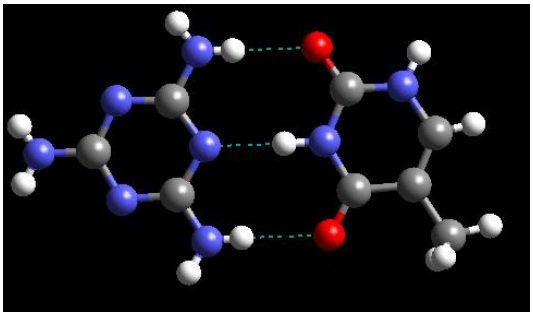

(a)

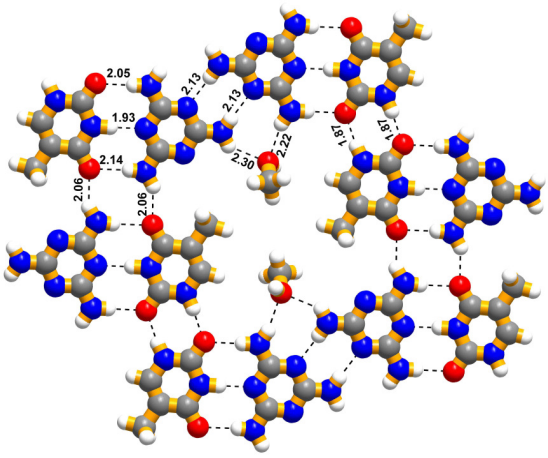

(b)

Figure 2.22. (a) Molecular recognition between thymine and melamine in the crystal structure **1**. (b) Packing arrangement of the binary supramolecular units with the channels being occupied by CH_3OH molecules.

Although, in two-dimensional arrangement void space is observed, that is being filled by CH_3OH molecules, however, no channel structure is observed in three-dimensional arrangement. Since the nature of molecules in voids can also direct the ultimate supramolecular assembly, co-crystallization of thymine and melamine from other solvents have been carried out from different solvents. In the process, good quality single crystals were obtained from DMF and H_2O and structural features are discussed in the following section.

2.3.2 Molecular adducts of thymine and melamine from dimethyl formamide and water, 2 and 3

Thymine and melamine in 1:1 ratio dissolved in dimethyl formamide (DMF) gave single crystals of suitable quality for the structure determination by X-ray diffraction methods. Complete crystallographic details are given in Table 2.2. Structure analysis reveals that thymine and melamine formed 3:1 adducts along with the solvent of crystallization (DMF). In the adduct, basic recognition between the reactants is established through the interaction of each melamine molecule with three thymine molecules, held together by triple hydrogen bonding pattern, consisting of one N-H···N and two N-H···O hydrogen bonds, as shown in Figure 2.23. The hydrogen bond distances in the adduct **2** are H···O, 2.08, 2.13 Å and H···N, 2.07 Å. Complete hydrogen bond details are listed in Table 2.3. Further, each supramolecular unit is held to a molecule of solvent of crystallization, as shown in Figure 2.24, by forming N-H···O hydrogen bonds with H···O, 1.89 Å.

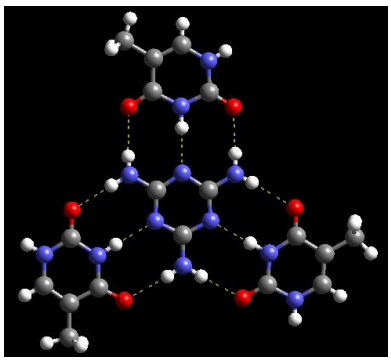

Figure 2.23. Molecular recognition between melamine and thymine in the 3:1 adducts obtained from *N*,*N*-dimethylformamide (DMF).

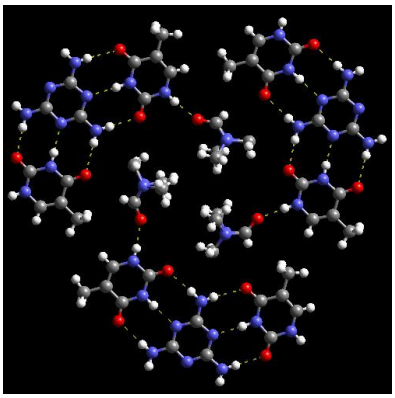

Figure 2.24. Two-dimensional arrangement of supramolecular units of melamine and thymine in the crystal structures of **2**.

In two-dimensional arrangement, the units are arranged in planar sheets such that each of three units are closely packed through hydrophobic interactions (H···H) yielding void space of diameter ~ 15 Å. In three-dimensional arrangement, the sheets are, however, aligned yielding a channel structure, as shown in Figure 2.25(a), in which the solvents of crystallization are embedded. The solvent incorporated channels are shown in Figure 2.25(b). Thus, in the adduct, six molecules of DMF are present in each channel.

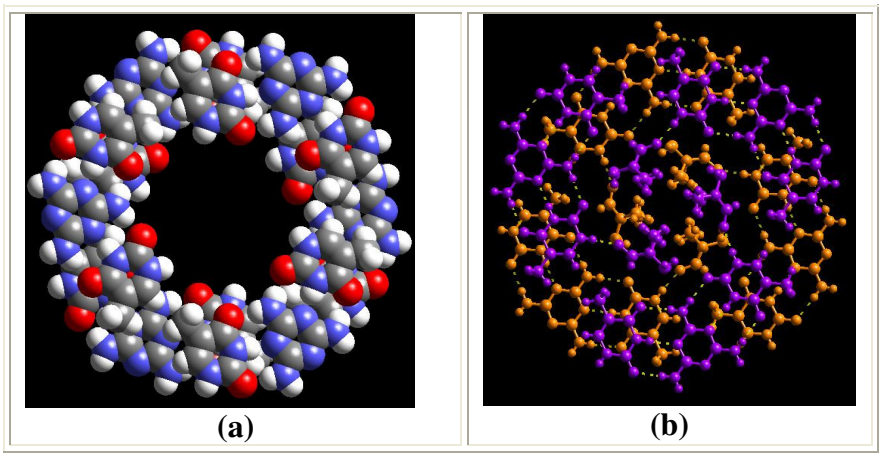

Figure 2.25. (a) Representation of the channels observed in the adduct **2**, in close-pack model. (b) The channels embedded with the solvent molecules.

The co-crystals of thymine and melamine obtained from water, in fact, are isostructural to that of **2**, except that DMF molecules are being replaced by water molecules. We labelled this adduct as **3**. Two-dimensional arrangement of molecules and also packing in three-dimension are shown in Figure 2.26. It is, indeed, interesting to note that, water molecules in the channels aggregate mimicking cyclohexane topology.

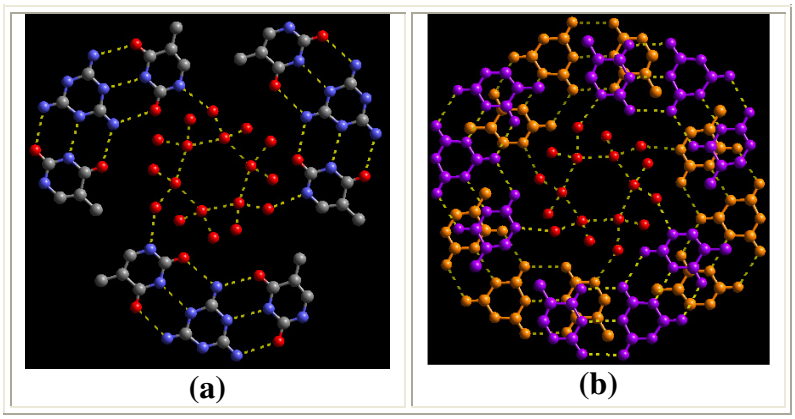

Figure 2.26. (a) Two-dimensional arrangement of supramolecular units of melamine and thymine in the crystal structures of **3**. (b) Three-dimensional arrangement of melamine and thymine in the crystal structure of **3**.

Thus, it is interesting to note that nucleobases with basic molecule like melamine, form not only molecular complexes but also exotic supramolecular structures with voids and channels, which may have extensive potential applications and may also address interactions of drugs, toxic moieties etc., with the species represent for biological processes. This is further, reflected in the experiments of co-crystallization of melamine with uracil.

2.4 Molecular adducts of uracil and melamine

Co-crystallization experiments between melamine and uracil, however, gave different complexes with the change of solvents and composition of the reactants. The salient features of all the obtained complexes are discussed in detail in the following sections.

2.4.1 Uracil with melamine from dimethyl formamide or water, 4

Uracil and melamine dissolved in water gave a needle shaped crystals suitable for data collection, by X-ray diffraction methods. In asymmetric unit, melamine, uracil and one water molecules are present, as shown in Figure 2.27(a). Interaction between uracil and melamine is established through triple hydrogen bonding pattern comprising of two N-H···O (H···O, 2.09 and 2.09 Å) and one N-H···N (H···N, 2.10 Å) hydrogen bond, yielding an ensemble (Figure 2.27(b)), which is similar to the one observed in thymine-melamine adduct, except for the variation in the hydrogen bond distances.

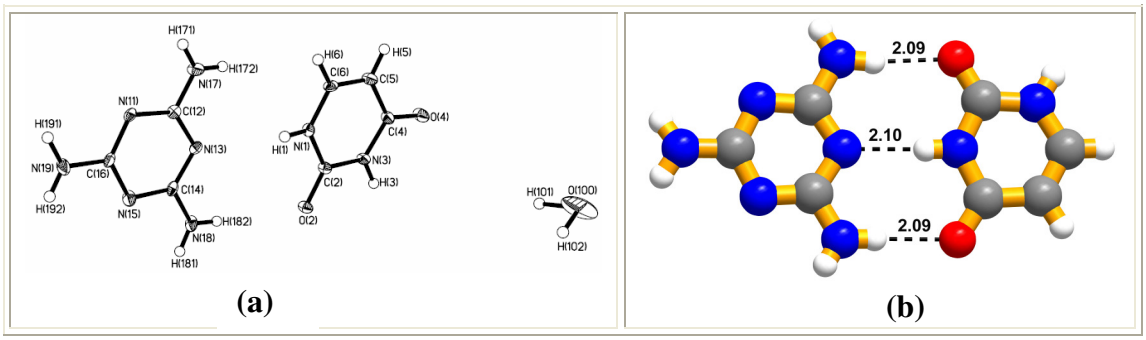

Figure 2.27. (a) ORTEP (50% probability level) drawing of the adduct **4** (b) binary supramolecular adduct formed in the adduct **4**.

Further, the adjacent supramolecular units interact through melamine···melamine and uracil···uracil interactions by centrosymmetric N-H···N and N-H···O hydrogen bonds, with hydrogen bond distances 2.26 and 2.04 Å respectively. In this process, aggregation of six units constituted void space, as shown in Figure 2.28(a), which is being occupied by water molecules. Interaction between water molecules with melamine and uracil is found to be through the O-H···O, N-H···O and C-H···O hydrogen bonds, with hydrogen bond distances 2.07, 2.20 and 2.98 Å, respectively. Such an aggregation form sheets in two-dimensional arrangement, which, in turn, are stacked in three-dimensional arrangement (see Figure 2.28(b)). As it was observed in the complexes **1**-**3** discussed in the earlier sections for the co-crystals of melamine and thymine, wherein, solvent played a significant role to yield different assemblies, co-crystallization of melamine and uracil also have been carried out from different solvents. It was noted that from DMF and many other solvents, the same structure as that of **4** was obtained, except from CH_3OH.

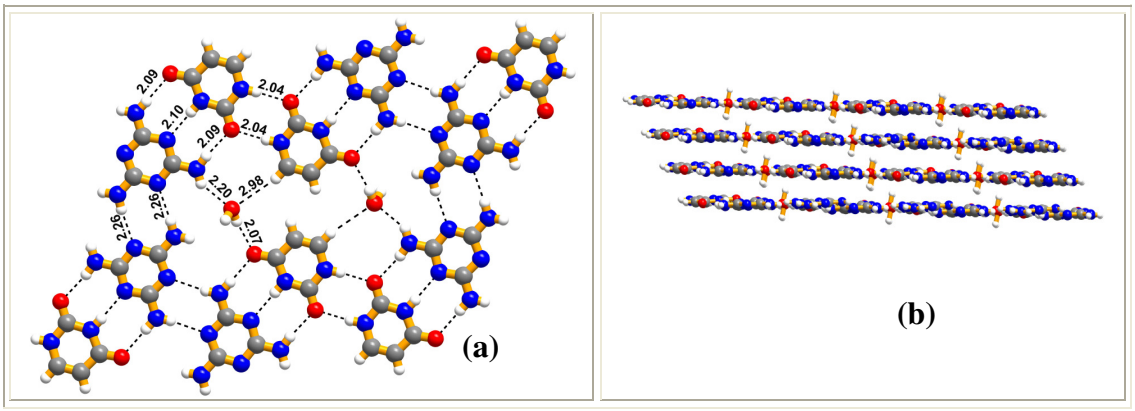

Figure 2.28. (a) 2D structure showing the formation of channels being occupied by H_2O molecules. (b) 3D structure showing the stacking of the layers connected through H_2O molecules.

2.4.2 Uracil with melamine from methanol in 1:1 ratio, 5

Crystallization of uracil and melamine in 1:1 ratio from methanol solution gave a block like colorless crystals, suitable for X-ray diffraction studies. The structure determination by X-ray diffraction methods reveals that 1:1 adduct, **5**, of uracil and melamine is formed. The ORTEP diagram of asymmetric unit is shown in Figure 2.29. The complete crystallographic details are given in Table 2.2. Interestingly, there is no solvent of crystallization in the crystal lattice.

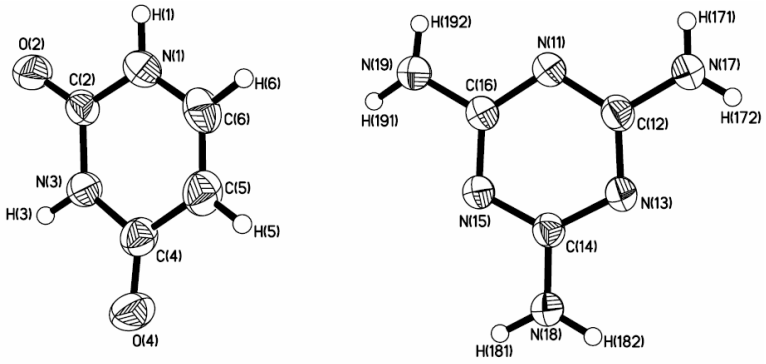

Figure 2.29. ORTEP (50% probability level) drawing of the adduct **5**.

Packing analysis revealed that uracil interacts with the melamine with triple hydrogen bonding pattern, similar to the one observed in the adduct **4**, with hydrogen bond distances of H···O, 1.99 and 2.02 Å while H···N is 1.94 Å. Further, in two-dimensional arrangement, these supermolecules aggregate through melamine···melamine and melamine···uracil by cyclic hydrogen bonding patterns possessing two hydrogen bonds (see Figure 2.30). While the melamine···melamine is formed through N-H···N hydrogen bond of H···N, 2.27 Å, in melamine···uracil, N-H···N and C-H···N hydrogen bonds with H···N, 1.94 Å and 2.20 Å, respectively, are observed. However, when co-crystallization was carried out with variable composition of uracil and melamine from CH_3OH, it has been observed that reactants in 2:1 and 3:1 molar ratios gave same structures, which are entirely different from that of **5**.

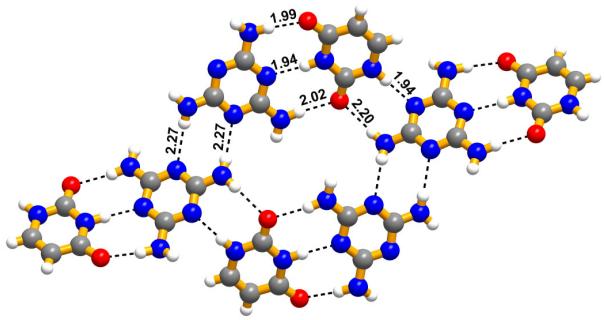

Figure 2.30. Arrangement of molecules of uracil and melamine in the adduct forming a hexameric network.

2.4.3. Uracil with melamine from methanol in 2:1 ratio, 6

X-ray diffraction analysis of single crystals of **6** reveals that, it also gave an asymmetric unit without any solvent of crystallization (see Figure 2.31) like in **5**.

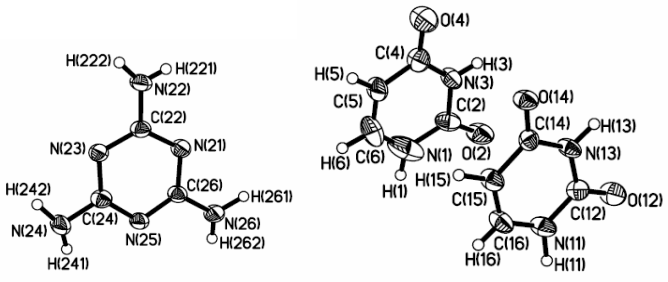

Figure 2.31. ORTEP (50% probability level) drawing of the adduct **6**.

The packing analysis reveals that, two types of layers are present in the crystal lattice, that are labeled as **A** and **B**. Stacking of these layers are shown in Figure 2.32(a). In the layer **A** both the reactants are present, where as only uracil molecules are present in the layer **B**.

In the layer **A**, recognition between uracil and melamine is through the association of two N-H···O (H···O, 2.16, 1.96 Å) and one N-H···N (H···N, 2.09 Å) hydrogen bonds, similar to the adduct **4** and **5**, forming a binary supramolecular unit. Arrangement and interaction between the molecules are shown in Figure 2.32(b). Such units, further, aggregate to constitute hexagonal network, comprising of three of each melamine and uracil. Interactions between uracil···uracil and melamine···melamine are established by N-H···O, C-H···O and N-H···N hydrogen bonds with H···O and H···N distances of 2.33, 1.96 and 2.16, 2.20 Å, respectively.

In the layer **B**, uracil molecules also form hexagonal network, as shown in Figure 2.32(c), through cyclic hydrogen bonding pattern comprising of N-H···O and C-H···O, with H···O distances of 2.02, 1.95 and 2.94, 2.64 Å, respectively. Thus, it has been observed that even in the complexes between uracil and melamine, solvent and

composition of the reactants played a crucial role in the final supramolecular assembly.

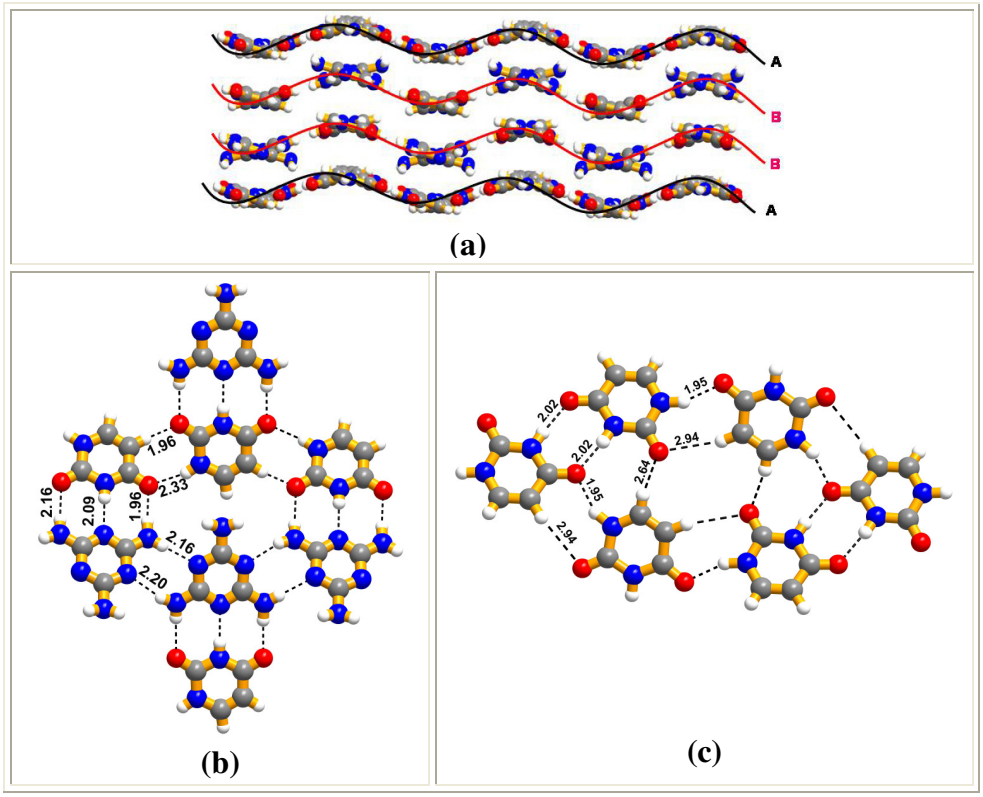

Figure 2.32. (a) Stacking of the planar sheets in three dimensional arrangement of adduct **6**, (b) Molecular arrangement of uracil and melamine in the sheet A and (c) interaction between the uracil molecule with N-H···O and C-H···O interactions forming hexameric network in sheet B.

2.5 Conclusions

Thus, supramolecular assemblies of melamine with thymine and uracil could be represented as host-guest complexes, with encapsulation of solvent molecules or close-packed hexagonal network structures, which are shown schematically in Figure 2.33. Except in adduct **2** and **3**, in all the cases recognition pattern between melamine and thymine/uracil is formed through triple hydrogen bonding interaction. It is

interesting to note that uracil only formed different complexes depending upon the concentration of the reactants. However, in none of the cases the three molecular component ensembles, as shown in Scheme 2.9(b), is not observed.

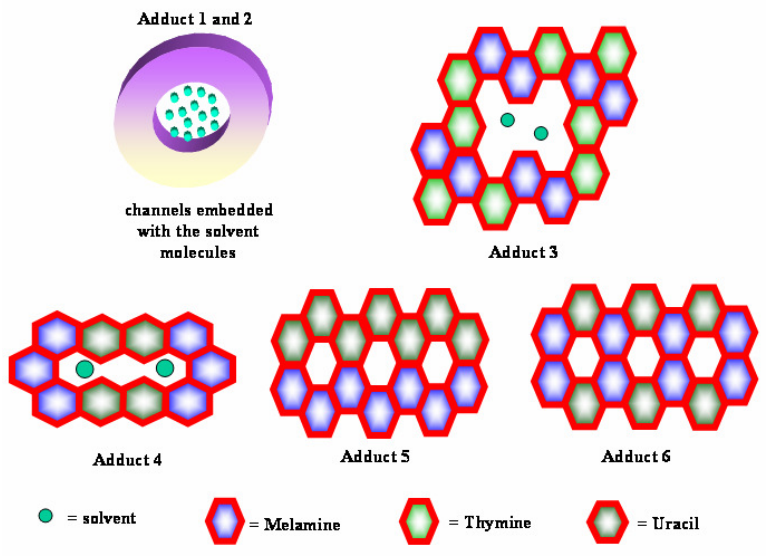

Figure 2.33. Schematic representation of arrangement of molecules in molecular adducts of thymine/uracil with melamine.

2.6 Experimental details

All the chemicals used in this study were obtained commercially and used without purification. HPLC grade solvents were used for carrying out experiments. For a typical crystallization, 0.0252 g (0.2 mmol) of adenine and 0.0270 g (0.2 mmol) of benzoic acid were dissolved (in 25 mL conical flask) in methanol, by heating, and then subsequently cooling to room temperature at ambient conditions. Colorless block type single crystals of good quality were obtained within one week, which were used for single crystal structure determination studies by X-ray diffraction methods.

2.7 Crystal structure determination

Good quality single crystals were chosen after viewing through a Leica microscope supported by a rotatable polarizing stage and a CCD camera. The crystals were glued to a thin glass fiber using an adhesive (cyano acrylate) and mounted on a diffractometer equipped with an APEX CCD area detector. The data collection was smooth in all the cases, and no extraordinary methods have been employed expect in case of melamine-thymine water adduct being collected at 133K. The intensity data were processed using Bruker's suite of data processing programs (SAINT), and absorption corrections were applied using SADABS. The structure solution of all the complexes have been carried out by direct methods, and refinement were performed by full matrix least squares on F^2 using the SHELXTL-PLUS suite of programs. All the structures converged to good R factors. All the non-hydrogen atoms were refined anisotropically, and the hydrogen atoms abstained from Fourier maps were refined isotropically. All the refinements were smooth in all the structures. The details of data collection and crystallographic information for all the structures are given in table. All the intermolecular interactions were computed using PLATON are given in the table.

Table 2.2: Crystallographic information of molecular adducts

	Adenine-Benzoic acid complex	Cytosine-Benzoic acid complex	Cytosine-Phthalic acid complex	Cytosine-Isophthalic acid complex
Empirical formula	$C_{19}H_{17}N_5O_4$	$C_{22}H_{22}N_6O_6$	$C_{16}H_{16}N_6O_6$	$C_{12}H_{11}N_3O_5$
Formula wt.	379.38	466.46	388.35	277.24
Crystal system	Triclinic	Monoclinic	Monoclinic	Triclinic
Space group	$P\bar{1}$	$P2(1)/c$	$P2(1)/m$	$P\bar{1}$
T [K]	298(2)	298(2)	298(2)	298(2)
a [Å]	6.949(2)	22.410(1)	3.684(1)	8.588(1)
b [Å]	10.324(3)	7.450(1)	29.770(4)	8.963(2)
c [Å]	14.286(5)	13.060(1)	7.338(1)	9.061(2)
α [°]	80.46(1)	90.00	90.00	100.81(1)
β [°]	76.40(1)	91.92(1)	92.76(1)	105.20(1)
γ [°]	71.21(1)	90.00	90.00	113.08(1)
Z	2	4	2	2
Volume [Å^3]	938.6(5)	2179.2(1)	803.8(3)	585.1(2)
D_{calc} [g/cm^3]	1.342	1.422	1.604	1.574
F (000)	396	976	404	288
μ [mm^{-1}]	0.097	0.106	0.126	0.125
$2\theta_{max.}$	56.66	56.58	56.44	56.56
Range h	-9 to 9	-29 to 24	-4 to 4	-11 to 11
Range k	-13 to 13	-9 to 9	-28 to 38	-11 to 11
Range l	-18 to 18	-10 to 17	-9 to 9	-12 to 11
N-total	8200	12642	4517	5071
N-independent	4268	5066	1847	2651
N-observed	2329	2166	1611	2437
R_1 [I>2σ(I)]	0.0699	0.0791	0.0565	0.0401
wR_2	0.1755	0.2023	0.1954	0.1126
GOF	1.008	0.994	1.113	1.114

Table 2.2 continued...

	Adduct 1	Adduct 2	Adduct 3
Empirical formula	$C_9H_{16}N_8O_3$	$C_{27}H_{33}N_{15}O_9$	$C_{18}N_{12}O_{18}$
Formula wt.	284.30	711.68	672.30
Crystal system	Triclinic	Hexagonal	Hexagonal
Space group	$P\bar{1}$	$P\,6_3/m$	$P\,6_3/m$
T [K]	133(2)	133(2)	298(2)
a [Å]	7.235(9)	17.487(9)	17.041(13)
b [Å]	7.997(9)	17.487(9)	17.041(13)
c [Å]	12.801(2)	6.478(9)	6.413(7)
α [°]	75.60(1)	90.00	90.00
β [°]	78.83(1)	90.00	90.00
γ [°]	68.06(1)	120.00	120.00
Z	2	2	2
Volume [Å^3]	661.2(1)	1716(3)	1613(2)
D_{calc} [g/cm^3]	1.428	1.378	1.384
F (000)	300	744	672
μ [mm^{-1}]	0.111	0.107	0.127
$2\theta_{max.}$	56.70	56.50	50.58
Range h	-9 to 9	-22 to 19	-20 to 17
Range k	-10 to 7	-8 to 23	-20 to 20
Range l	-16 to 16	-8 to 8	-7 to 7
N-total	3898	9490	8600
N-independent	2873	1486	1078
N-observed	2243	1245	158
R_1 [I>2σ(I)]	0.0565	0.1116	0.0956
wR_2	0.2176	0.2936	0.3108
GOF	1.065	1.403	0.857

Table 2.2 continued...

	Adduct 4	Adduct 5	Adduct 6
Empirical formula	$C_7H_{12}N_8O_3$	$C_7H_{10}N_8O_2$	$C_{11}H_{14}N_{10}O_4$
Formula wt.	256.25	238.23	350.32
Crystal system	Triclinic	Monoclinic	Monoclinic
Space group	$P\bar{1}$	$C2/c$	$P2(1)/c$
T [K]	298(2)	298(2)	298(2)
a [Å]	7.273(1)	14.371(3)	10.145(2)
b [Å]	8.937(2)	7.543(2)	12.012(2)
c [Å]	9.443(2)	19.006(4)	12.161(2)
α [°]	66.87(1)	90.00	90.00
β [°]	80.29(1)	91.85(1)	95.33(1)
γ [°]	72.49(1)	90.00	90.00
Z	2	8	4
Volume [Å^3]	537.4(2)	2059.2(8)	1475.6(5)
D_{calc} [g/cm^3]	1.584	1.537	1.577
F (000)	268	992	728
μ [mm^{-1}]	0.127	0.120	0.125
$2\theta_{max.}$	56.56	46.56	52.16
Range h	-6 to 9	-15 to 14	-12 to 12
Range k	-11 to 11	-8 to 8	-14 to 14
Range l	-11 to 12	-19 to 21	-14 to 15
N-total	3165	4212	11366
N-independent	2673	1474	2927
N-observed	1541	1243	2375
R_1 [I>2σ(I)]	0.0739	0.0410	0.1090
wR_2	0.2581	0.1076	0.2269
GOF	1.049	1.042	1.294

Table 2.3. Characteristic hydrogen bonds (distances/Å and angles/°)[#]

D-H···A	A-BA			C-BA			C-PA			C-IPA		
N-H···O	2.15	3.02	175	1.64	2.66	170	1.78	2.71	167	1.95	2.84	176
	2.09	2.96	173	2.09	2.87	160	2.01	2.80	152	2.23	3.11	168
				2.13	2.90	153	1.99	2.84	178	1.95	2.87	178
				1.65	2.77	179						
				2.15	2.90	141						
				1.94	2.91	177						
N-H···N	1.97	2.86	169	1.84	2.84	173	2.12	2.86	164	2.02	2.83	175
C-H···O	2.68	3.41	136	2.80	3.48	131	2.81	3.62	147	2.43	3.35	164
	2.60	3.51	167	2.66	3.66	156	2.56	3.20	126	2.28	3.20	156
				2.37	3.29	163	2.46	3.39	175	2.68	3.65	173
				2.40	3.24	141				2.69	3.35	126
				2.79	3.59	149						
				2.80	3.59	140						
O-H···O				1.52	2.57	175				1.80	2.62	156
O-H···N	1.83	2.64	170									
	1.86	2.68	171									

Table 2.3 continued.....

D-H···A	Adduct 1			Adduct 3			Adduct 4			Adduct 5			Adduct 6		
N-H···O	2.05	2.90	170	2.13	2.99	180	1.92	2.81	173	2.20	3.01	165	2.33	3.07	144
	2.14	2.96	169	2.08	2.94	179	2.05	2.90	176	2.02	2.93	173	1.94	2.87	156
	2.06	2.87	150	1.89	2.74	175	1.97	2.92	174	2.00	2.86	164	2.02	2.93	175
	1.87	2.78	169				2.12	2.90	150	1.99	2.94	175	2.37	3.16	155
	2.30	2.98	140										2.28	3.13	160
	2.22	3.05	163										2.17	2.97	177
													1.96	2.88	173
N-H···N	1.93	2.90	177	2.07	2.93	178	1.92	2.87	169	1.94	2.84	173	2.08	2.88	175
	2.13	2.97	179				2.17	2.99	159	1.93	2.88	178	2.20	3.01	163
							2.18	3.04	173	2.27	3.08	168	2.17	3.00	179
										2.54	3.33	152			
C-H···O				2.05	3.25	147							1.96	2.86	164
O-H···O							1.96	2.77	163						
O-H····N	1.99	2.79	166				1.89	3.11	167						

the three numbers for each structure indicate H···A, D···A and D-H···A angles respectively.

2.8 References

[1] Watson, J. D.; Crick, F. H. C. *Nature* **1953**, *171*, 964-967.

[2] Sanger, W. *Principles of Nucleic Acid Structure* Springer Verlag, New York **1984**.

[3] (a) Nielsen, P. E.; Egholm, M.; Berg, R. H.; Buchardt, O. *Science*, **1991**, *254*, 1497-1500. (b) Ray. A.; Norden. B. *FASEB J*, **2000**, *14*, 1041-1060. (c) Corradini. R.; forza, S. S.; Tedeschi, T.; Totsingan. F.; Marchelli. R. *Curr. Top. Med. Chem.* **2007**, *7*, 681-694. (d) Egholm, M.; Buchardt, O.; Christensen, L.; Behrens, C.; Freier, S. M.; Driver, D. A.; Berg, R.H.; Kim, S. K.; Nordon, B.; Nielsen, P. E. *Nature*, **1993**, *365*, 566-567. (e) Jensen, K. K.; Qrum, H.; Nielsen, P. E.; Norden, B. *Biochemistry,* **1997**, *36*, 5072-5077. (f) Kumar, V. A.; Ganesh, K. N. *Acc. Chem. Res.* **2005**, *38*, 404-412.

[4] (a) Niemeyer, C. M. *Angew. Chem. Int. Ed.* **1997**, *36*, 585-587. (b) Seeman, N. C. *Nature* **2003**, *421*, 427-431. (c) Yan, H. *Science* **2004**, *306*, 2048-2049. (d) Samor, B.; Zuccheri, G. *Angew. Chem. Int. Ed.* **2005**, *44*, 1166-1181. (e) Cheng, M. M. C.; Cuda, G.; Bunimovich, Y. L.; Gaspari, M.; Heath, J. R.; Hill, H. D.; Mirkin, C. A.; Nijdam, A. J.; Terracciano, R.; Thundat, T.; Ferrari, M. *Current Opinion in Chemical Biology* **2006**, *10*, 11-19.

[5] (a) Choo, H.; Chen, X.; Yadav, V.; Wang, J.; Schinazi, R. F.; Chu, C. K. *J. Med. Chem.* **2006**, *49*, 1635-1647. (b) Bouazza, A. H.; Zerrouki, R.; Krausz, P.; Laumond, G.; Aubertin, A. M.; Champavier, Y. *Nucleosides, Nucleotides, and Nucleic Acids* **2005**, *24*, 1249-1263. (c) Malik, V.; Singh, P.; Kumar, S. *Tetrahedron* **2005**, *61*, 4009-4014. (d) Ichikawa, S.; Matsuda, A. *Nucleosides, Nucleotides, and Nucleic Acids* **2005**, *24*, 319-329. (e) Exall, A. M.; Jones, M. F.; Mo, C.-L.; Myers, P. L.; Paternoster, I. L.; Singh, H.; Storer, R.; Weingarten, G. G.; Williamson, C.; Brodie, A.

C.; Cook, J.; Lake, D. E.; Meerhok, C. A.; Turnbull, P. J.; Highcock, R. M. *J. Chem. Soc. Perkin Trans. 1* **1991**, *1*, 2467-2477. (f) Uschinsky, R.; Pleven, E.; Eidelherger, C. *J. Am. Chem. Soc.* **1957**, 4559-4560. (g) Katiyar, S. B.; Srivastava, K.; Puri, S. K.; Chauhan, M. S. *Bioorg. Med. Chem. Lett.* **2005**, *15*, 4957-4960. (h) Agarwal, A.; Srivastava, K.; Puri, S. K.; Chauhan, P. M. S. *Bioorg. Med. Chem.* **2005,** *13*, 6226-6232. (i) Pathak, T. *Chem. Rev.* **2002**, *102*, 1623-1667. (j) Hanessian, S.; Huang, G.; Chenel, C.; Machaalani, R.; Loiseleur, O. *J. Org. Chem.* **2005**, *70*, 6721-6734. (k) Niedballa, U.; Vorbruggen, H. *Angew. Chem. Int. Ed.* **2006**, *9*, 461-462. (l) Torii, T.; Yamashita, K.; Kojima, M.; Suzuki, Y.; Hijiya, T.; Izawa, K. *Nucleosides, Nucleotides, and Nucleic Acids* **2006**, *25*, 625-634. (m) Agrofoglio, L. A.; Gillaizeau, I.; Saito, Y. *Chem. Rev.* **2003**, *103*, 1875-1916. (n) Torii, T.; Onishi, T.; Izawa, K.; Maruyama, T.; Demizu, Y.; Neyts, J.; Clercq, E. D. *Nucleosides, Nucleotides and nucleic acids* **2006**, *25*, 655-665.

[6] (a) Sivakova, S.; Wu, J.; Campo, C. J.; Mather, P. T.; Rowan, S. J. *Chem. Eur. J.* **2006**, *12*, 446-456. (b) Burke, K. A.; Sivakova, S.; Mckenzie, B. M.; Mather, P. T.; Rowan, S. J. *J. Poly. Sci. A* **2006**, 5049-5059. (c) Burke, K. A.; Sivakova, S.; McKenzie, B. M.; Mather, P. T.; Rowan, S. J. *J. Poly. Sci. A* **2006**, *44*, 5049-5059. (d) Ghoussoub, A.; Lehn, J. M. *Chem. Commun.* **2006**, 5763-5765.

[7] (a) Sivakova, S.; Bohnsack, D. A.; Mackay, M. E.; Suwanmala, P.; Rowan, S. J. *J. Am. Chem. Soc.* **2005**, *127*, 18202-18211. (b) Rowan, S. J.; Suwanmala, P.; Sivakova, S. *J. Poly. Sci. A* **2003**, *41*, 3589-3596. (c) Ghoussoub, A.; Lehn, J. M. *Chem. Commun.* **2006**, 5763-5765.

[8] (a) Murata, T.; Nishimura, K.; Saito, G. *Molecular Crystals and Liquid Crystals* **2007**, *466*, 101-112. (b) Murata, T.; Saito, G. *Chem. Lett.* **2006**, *35*, 1342-1343.

[9] (a) Sessler, J. L.; Wang, B.; Harriman, A. *J. Am. Chem. Soc.* **1995**, *117*, 704-714. (b) Torres, T.; Gouloumis, A.; Garcia, D. S.; Jayawickramarajah, J.; Seitz, W.; Guldi, D. M.; Sessler, J. L. *Chem. Commun.* **2007**, 292-294. (c) Sessler, J. L.; Sathiosatham, M.; Brown, C. T.; Rhodes, T. A.; Wiederrecht, G. *J. Am. Chem. Soc.* **2001**, *123*, 3655-3660. (d) Sessler, J. L.; Jayawickramarajah, J.; Gouloumis, A.; Torres, T.; Guldi, D. M.; Maldonado, S.; Stevenson, K. J. *Chem. Commun.* **2005**, 1892-1894.

[10] (a) Ise, T.; Shiomi, D.; Sato, K.; Takui, T. *Chem. Commun.* **2006**, 4832-4834. (b) Tanaka, H.;Shiomi, D.; Ise, T.; Sato, K.;Takui, T. *CrystEngComm***. 2007**, *9*, 767-771.

[11] Shimizu, T.; Iwaura, R.; Masuda, M.; Hanada, T.; Yase, K. *J. Am. Chem. Soc.* **2001**, *123*, 5947-5955.

[12] Sivakova, S.; Rowan, S. J. *Chem. Commun.* **2003**, 2428-2429.

[13] Schall, C. F.; Gokel, G. W. *J. Am. Chem. Soc.* **1994**, *116*, 6089-6100.

[14] Furuta, H.; Furuta, K.; Sessler, J. L. *J. Am. Chem. Soc.* **1991**, *113*, 4706-4707.

[15] Mascal, M.; Hext, N. M.; Warmuth, R.; Moore, M. H.; Turkenburg, J. P. *Angew. Chem. Int. Ed. Engl.* **1996**, *35*, 2204-2206.

[16] Sessler, J. L.; Jayawickramarajah, J.; Sathiosatham, M.; Sherman, C. L.; Brodbelt, J. S. *Org. Lett.* **2003**, *5*, 2627-2630.

[17] Allen, F. H.; Kennard, O. *Chem. Des. Automat. News*. **1993**, *8*, 31-37.

[18] Hoogsteen, K. *Acta Cryst.* **1963**, *16*, 907-916.

[19] (a) Pedireddi, V. R.; Prakasha Reddy, J. *Tetrahedron Lett.* **2003**, *44*, 6679-6681. (b) Varughese, S.; Pedireddi, V. R. *Chem. Eur. J.* **2006**, *12*, 1597-1609. (c) Varughese,

S.; Pedireddi, V. R. *Tetrahedron Lett.* **2005**, *46*, 2411-2415. (d) Arora, K. K.; PrakashaReddy, J.; Pedireddi, V. R. *Tetrahedron* **2005**, *61*, 10793-10800. (e) Bhogala, B. R.; Nangia, A. *New J. Chem.* **2008**, *32*, 800-807. (f) Bhogala, B. R.; Basavoju, S.; Nangia, A. *Cryst. Growth Des.* **2005**, *5*, 1683-1686. (g) Bhogala, B. R.; Nangia, A. *Cryst. Growth Des.* **2003**, *3*, 547-554. (h) Bhogala, B. R.; Vishweshwar, P.; Nangia, A. *Cryst. Growth Des.* **2002**, *2*, 325-328. (i) Koshima, H.; Nakagawa, T.; Matsuura, T.; Miyamoto, H.; Toda, F. *J. Org. Chem.* **1997**, *62*, 6322-6325. (j) Zhang, J.; Li, Z.-J.; Kang, Y.; Cheng, J.-K.; Yao, Y. G. *Inorg. Chem.* **2004**, *43*, 8085-8091. (k) Paz, F. A. A.; Klinowski, J. *CrystEngComm* **2003**, *5*, 238-244. (l) Inoue, K.; Itaya, T.; Azuma, N. *Supramolecular Science* **1998**, *5*, 163-166. (m) Bensemann, I.; Gdaniec, M.; Lakomecka, K.; Milewska, M. J.; Polonski, T. *Org. Biomol. Chem.* **2003**, *1*, 1425-1434. (n) Venkataramanan, B.; Ning, Z.; Vittal, J. J.; Valiyaveettil, S. *CrystEngComm* **2005**, *7*, 108-112. (o) Sharma, C. V. K.; Broker, G. A.; Szulczewski, G. J.; Rogers, R. D. *Chem. Commun.* **2000**, 1023-1024. (p) Curtis, S. M.; Le, N.; Fowler, F. W.; Lauher, J. W. *Cryst. Growth Des.* **2005**, *5*, 2313-2321. (q) Nguyen, T. L.; Fowler, F. W.; Lauher, J. W. *J. Am. Chem. Soc.* **2001**, *123*, 11057-11064. (r) Aakeroy, C. B.; Desper, J.; Urbina, J. F. *CrystEngComm* **2005**, *7*, 193-201. (s) Bhattacharya, S.; Dastidar, P.; Guru Row, T. N. *Chem. Mater.* **1994**, *6*, 531-537.

[20] Perumalla, S. R.; Suresh, E.; Pedireddi, V. R. *Angew. Chem. Int. Ed. Engl.* **2005**, *44*, 7752-7757.

[21] Gehring, K; Lorey, J.-L.; Gueron, M. *Nature* **1993**, *363*, 561-565.

[22] (a) Lazar, A. N.; Danylyuk, O.; Suwinska, K.; Coleman, A. W. *New J. Chem.* **2006**, *30*, 59-64. (b) Marchewka, M. K.; Baran, J.; Pietraszko, A.; Haznar, A.; Debrus,

S.; Ratajczak, H. *Solid State Sciences* **2003**, *5*, 509-518. (c) Janczak, J.; Perpetuo, G. J. *Acta Crystallogr., Sect. C: Cryst. Struct. Commun.* **2004**, *60*, o211-o216. (d) Zhang, X.-L.; Chen, X.-M. *Cryst. Growth Des.* **2005**, *5*, 617-622. (e) Tanbug, R.; Kirschbaum, R.; Pinkerton, A. A. *J. Chem. Cryst.* **1999**, *29*, 45-55. (f) Roy, A.; Choudhury, A.; Rao, C. N. R. *J. Mol. Struct.* **2002**, *613*, 61-66. (g) Brodski, V.; Peschar, R.; Schenk, H.; Brinkmann, A.; van Eck, E. R. H.; Kentgens, A. P. M.; Coussens, B.; Braam, A. *J. Phys. Chem. B* **2004**, *108*, 15069-15076. (h) Zhang, X.-L.; Ye, B.-H.; Chen, X.-M. *Cryst. Growth Des.* **2005**, *5*, 1609-1616. (i) Brodski, V.; Peschar, R.; Schenk, H.; Brinkmann, A.; Bloemberg, T. G.; van Eck, E. R. H.; Kentgens, A. P. M. *J. Phys. Chem. B* **2008**, *109*, 13529-13537. (j) Du, Z. X.; Han, M.-L.; Feng, X. *Z. Kristallogr. -New Cryst. Struct.* **2006**, *221*, 313. (k) Tukada, H.; Mazaki, Y. *Chem. Lett.* **1997**, *26*, 441-442. (l) Kabir, M. K.; Tobita, H.; Matsuo, H.; Nagayoshi, K.; Yamada, K.; Adachi, K.; Sugiyama, Y.; Kitagawa, S.; Kawata, S. *Cryst. Growth Des.* **2003**, *3*, 791-798. (m) Marchewka, M. K.; Pietraszko, A. *J. Phys. Chem. Solids* **2003**, *64*, 2169-2181. (n) Hughes, E. W. *J. Am. Chem. Soc.* **1941**, *63*, 1737-1752. (o) Ridder, D. J. A. D.; Goubitz, K.; Brodski, V.; Peschar, R.; Schenk, H. *Helv. Chim. Acta* **2004**, *87*, 1894-1905.

CHAPTER THREE

Cytosine duplexes

3.1 Introduction

In telomere DNA, repeating sequences are generally enriched by guanine (*G*) and cytosine (*C*) clusters at chromosome ends.[1] Under such environment, those *G* and *C* nucleobases, instead of pairing to yield *GC* base pairs, well known in the duplex structure of DNA, undergo *homomeric* aggregation. For example, *G*-rich strands self-assemble to yield *G*-quadruplexes by *Hoogsteen* hydrogen bonding, in association with alkali/alkali-earth metal ions, as shown in Figure 3.1(a).[2] Several synthetic strategies were formulated to mimic such *homomeric* aggregations in the laboratory environment,[3] and in this direction, the *G*-quadruplexes have been shown to obtain, at ease, even in the absence of metal ions also.[4] In fact, the *G*-quadruplexes have been found to be of highly valuable in the preparation of material with desired properties.[5]

On the other hand, the complementary cytosine rich strands form $\mathbf{C}.\mathbf{CH}^+$ duplexes in acidic conditions, which ultimately yield quadruplex arrangement with the intercalation of $\mathbf{C}.\mathbf{CH}^+$ duplexes (Figure 3.1(b)), which is defined as *i*-motif. A schematic representation of *i*-motif observed in the tetramer of d(TCCCCC) is shown Figure 3.1(c).[6] In fact, first ever $\mathbf{C}.\mathbf{CH}^+$ duplex was initially observed in the structure of small organic compound, acetyl cytosine,[7] but it was explored thoroughly in macromolecules only, as part of *i*-motif. Like *G*-quadruplexes, *i*-motif structures also have been found to be of great utility in various applications, especially in the contemporary frontier areas, nano materials and devices.[8] Some of the representative examples of *G*-quadruplexes and *i*-motifs are discussed in the following sections.

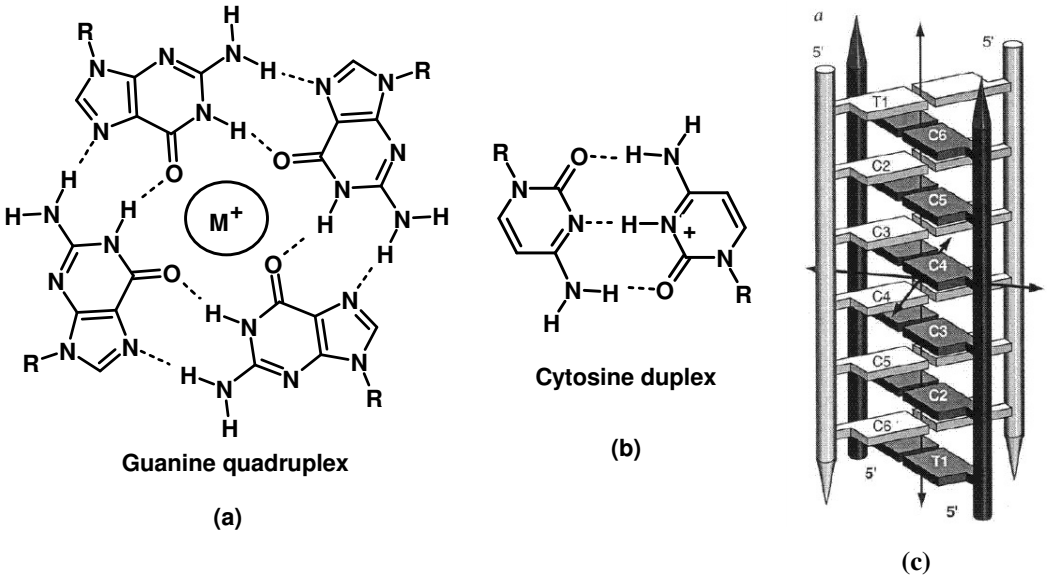

Figure 3.1. Schematic representation of (a) *G*-quadruplexes in presence of metal ions, (b) cytosine duplexes with **C.CH$^+$** interactions and (c) *i*-motifs observed in a DNA polymer.

3.1.1 *G*-quadruplexes

Wu and co-workers have reported X-ray crystallographic results for a self-assembled *G*-quadruplex formed by a guanine nucleoside, 5'-*tert*-butyl-dimethylsilyl-2',3'-*O*-isopropylidene guanosine (G1).[3d]

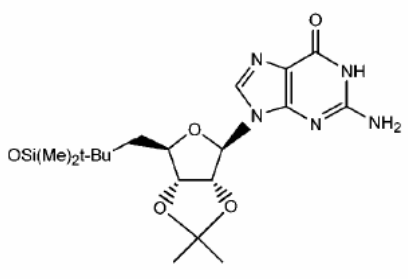

5'-*tert*-butyl-dimethylsilyl-2', 3'-*O*-isopropylidene guanosine (G1)

Crystallization of G1 in the presence of Na and Cs salts of picrate, in CH_3CN solution, yielded a complex of composition $[G1]_{16}\cdot[3Na/CsPic_4]$, characterized by

single crystal X-ray diffraction methods. Packing analysis reveals that a *G*-quadruplex structure consists of four *G*-quartets, which stack to form channels, being occupied by three collinear Na^+ ions and one Cs^+ ions, as shown in Figure 3.2.

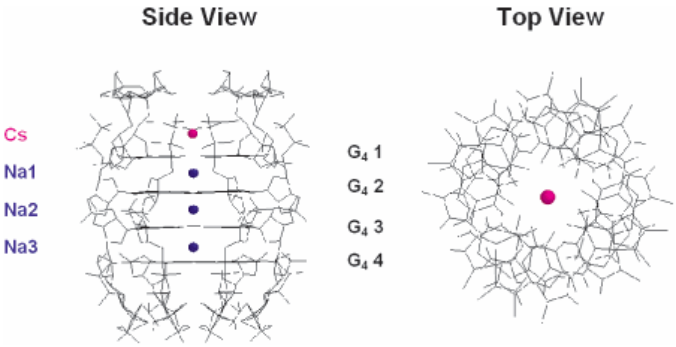

Figure 3.2. Crystal structure of $[G1]_{16}$·$[3Na/CsPic_4]$. Picrate molecules and hydrogen atoms are omitted for clarity. Only G-quartets are shown in the top view diagram to illustrate the ion channel structure.[3d]

Davis and co-workers have studied the effect of charge on the metal ions for the formation of *G*-quartets. For this purpose, D, L and (D,L)-5'-silyl-2',3'-*O*-isopropylidene guanosine (G2) were chosen as a guanosine moiety and K^+ and Ba^{+2} were chosen as metal centers.[3b]

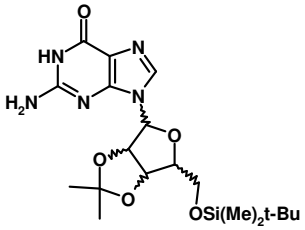

5'-silyl-2',3'-*O*-isopropylidene guanosine (G2)

Since octacoordinated K^+ (r = 1.51 Å) and Ba^{2+} (r = 1.42 Å) have similar ionic radii, it was believed that comparing the K^+ and Ba^{+2} complexes formed with G2 would reveal how the charge of cation affects *G*-quadruplex structure and dynamics.

It was observed that, in the presence of Ba^{+2}, (D,L)-G2 formed a homochiral self assembly whereas in the presence of K^+ it formed heterochiral self-assembly, as shown schematically in Scheme 3.1, which were confirmed by NMR studies.

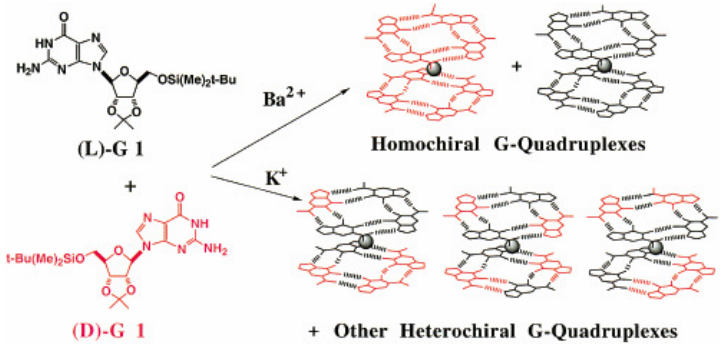

Scheme 3.1[3b]

Further, *G*-quartet formation of (D)-G2 in the presence Ba^{+2} is also confirmed by X-ray diffraction methods. A snapshot of arrangement of molecules in the crystal structure is shown in Figure 3.3.

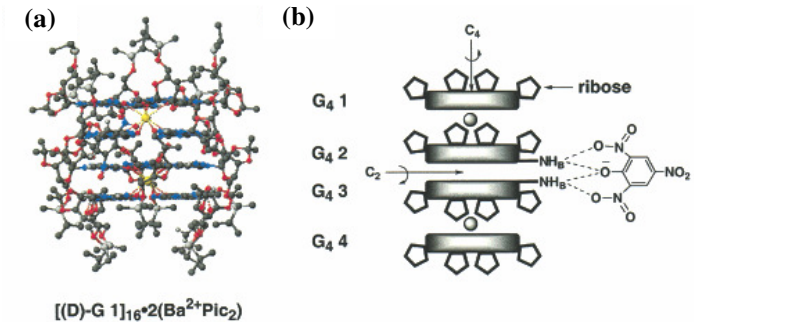

Figure 3.3. (a) A side view of the crystal structure of the G-quadruplex formed from (D)-G2 and Ba^{2+} picrate. The picrate counterions are deleted for clarity. (b) Four G-quartets, G_4 1-G_4 4, make up the G-quadruplex. The two Ba^{2+} cations are indicated, as are the picrate hydrogen bonds with the amino N_2 HB proton of G_4 2 and G_4 3.[3b]

Although cations are, usually, essential for the templation of *G*-quartets, there have been examples of *G*-quartets formed even in the absence of cations. Sessler and

co-workers reported a crystal structure of 8-(*N*,*N*-dimethylaniline)guanosine derivative (G3) that revealed an "empty" *G*-quartet.[4] G3 was shown to self-assemble into a *G*-quartet even without the assistance of a templating cation. Attachment of sterically bulky groups, a dimethylaniline unit, at the C_8 position of the guanine ring gave a conformationally constrained nucleoside that prefers to adopt a *syn* glycosidic bond conformer in the solid state as well as in solution. This *syn* conformation precluded the formation of hydrogen-bonded ribbon by the nucleoside and, thus, favoring the formation of the macrocyclic *G*-quartet (Scheme 3.2).

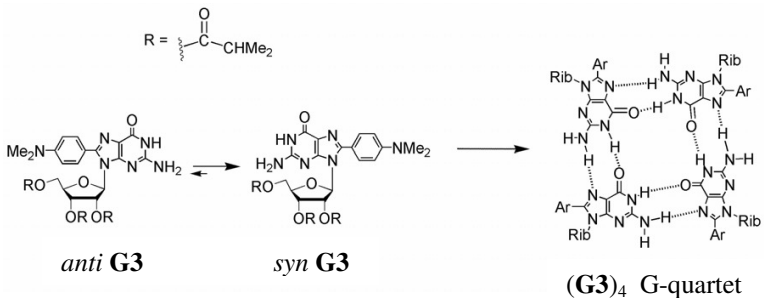

Scheme 3.2. Conformationally constrained G3 forms a G-quartet without presence of a templating cation.

Further, Lehn and co-workers have reported the formation of liquid crystal supramolecular assembly directed by guanine quadruplex formation, through the preparation of bis-guanine monomer G-G based hydrogel in the presence of K^+ ions.[9] The gelation properties of G-G may be attributed to the formation of extended supramolecular polymeric assemblies by hydrogen bonded *G*-quartet macrocycles, stabilized by binding of K^+ cations. The stabilization of the G_4 structure by K^+ offered the possibility of inducing gel-sol interconversion by sequential removal and addition of the K^+ ions controlled externally (see Figure 3.4) by a cryptand [2.2.2].

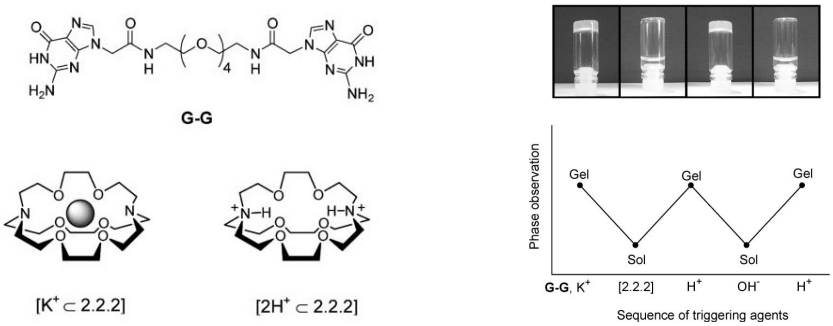

Figure 3.4. (Top) Visual observation of the reversible gel–sol interconversion of the hydrogel formed by a sample of G-G (10 mM) in 100 mM (10 eq.) KCl. From left to right: initial sample; addition of 10 eq. cryptand [2.2.2]; addition of 10 eq. HCl; addition of 10 eq. NaOH; all samples at room temperature (22 ºC). (Bottom) Schematic representation of the modulation of the gel–sol status induced by the sequence of triggering agents. The samples were warmed and cooled after each addition to ensure homogeneity; total dilution is less than 3%.[9]

3.1.2 *i*-motifs

Liu and co-workers have utilized the conformational flexibility of DNA for the preparation of a light-induced natural DNA conformational switch between close-packed quadruplex and random-coil structures with a reversible photo irradiated pH-jump system.[10] For this purpose a 21 mer **DNA-X**: 5'-CCCTAACCCTAACCCTAACCC-3', a light-induced hydroxide ion emitter, molecular malachite green carbinol base (MGCB) and a surfactant, cetyltrimethylammonium bromide (CTAB) were chosen.

The initial solution was prepared, with DNA-X, MGCB and CTAB, shows a slightly acidic pH value that facilitated the formation of the *i*-motif formation by DNA**-** X. Further, in the presence of 302-nm UV light, MGCB gives out OH^- ions, as well as showing an obvious color change, and this leads to an increase in the pH value.

Thus, the *i*-motif structure deforms into random coils with deprotonation of the **C.CH$^+$** base pairs. After the light is turned off, the malachite green (MG) cation recombines with the OH^- ions and return to the MGCB form to complete the cycle. Consequently, the pH value decreases and the DNA-X switches back to the *i*-motif conformation again. Accordingly, the conformational switch of DNA-X could be cycled by turning the UV light on and off alternately. The schematic representation of the sequence of reaction is shown in Figure 3.5.

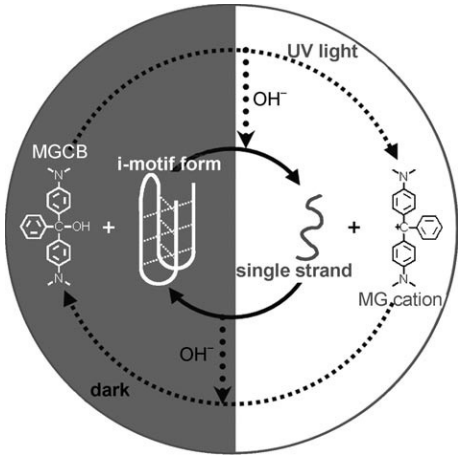

Figure 3.5. Working mechanism of the light-induced conformational switch of DNA-X. Inner cycle: The DNA conformational switch between the *i*-motif and random-coil structures. Outer cycle: The light-induced malachite green based pH jump. The conformational switch of DNA-X was associated with the on and off phases of UV light through the translation of photo induced hydroxide-group release by MGCB.[10]

Krishnan and co-workers have synthesized the higher order structures (HOS), also referred as *i*-wires, based on conformational flexibility of *i*-motif DNA, through poly-cytosine sequence 5'CCCCCCC3' ($d(C_7)$).[11]

For the preparation of *i*-wires, 500 μm $d(C_7)$ in 100 mM phosphate buffer at pH 5.5 was annealed, to promote formation of the *i*-motif and checked for HOS

formation by atomic force microscopy (AFM). It was observed that uniform 1D structures with lengths on the micrometer scale were formed, which are in good agreement with those of *i*-motifs, as confirmed by X-ray crystallography and solution NMR spectroscopy. Snapshot of the HOS recorded, using AFM, is shown in Figure 3.6. Further, the formation of the *i*-motif structures were also confirmed by using surface enhanced Raman spectroscopy.

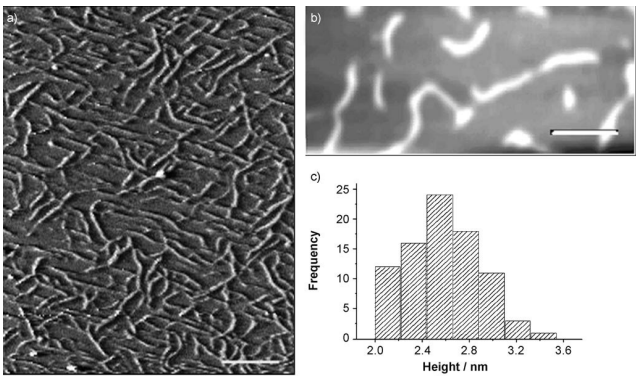

Figure 3.6. (a) and (b) Tapping mode AFM images of 500 μm d(C_7) pH 5.5 deposited on mica. Scale bar: (a) 1 μm; (b) 0.5 μm. (c) Histogram showing the height of a sample with 85 distinct wires.[11]

Kang *et al* have reported a crystal structure of the telomeric cytosine rich strand repeating sequence, d(TAACCC), crystallized from a solution containing 5% (vol/vol) 2-methyl-2,4-pentanediol (MPD), 20 mM $MgCl_2$, 0.10 mM spermine, 80 mM KCl, 40 mM potassium cacodylate buffer (pH 6.0), and 2 mM DNA (single-strand concentration) equilibrated against a reservoir of 35% MPD. Structure analysis revealed that four strands associate *via* the cytosine-containing parts to form a four-stranded intercalated structure held together by **C.CH$^+$** hydrogen bonds. Further, it was observed that, the base-paired strands are parallel to each other and the two duplexes are intercalated into each other in opposite orientations. Snapshot of

arrangement of molecules in the crystal structure of a d(TAACCC) sequence DNA is shown in Figure 3.7.[12]

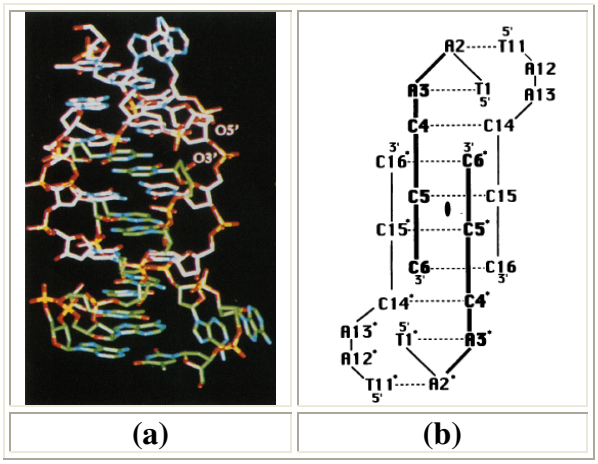

Figure 3.7. (a) Arrangement of molecules in the crystal structure of a telomeric cytosine rich strand repeating sequence, d(TAACCC). (b) Schematic representation of arrangement of molecules in the crystal structure.[12]

Balasubramanian and co-workers have reported a novel molecular machine based on a four stranded DNA structure, *i*-motif, formed by 21mer single-stranded oligonucleotide X containing four stretches of CCC.[13] In this structure protonated C forms a noncanonical base pair with an unprotonated C (i.e., a **C.CH$^+$** base pair), and these base pairs interlock to form a quadruple helix that is stable under slightly acidic conditions, as characterized by CD spectroscopy and fluorescence emission spectroscopy.

As illustrated in Figure 3.8, the system comprises a 21mer single-stranded oligonucleotide X containing four stretches of CCC. The second component is a 17 mer DNA strand Y, whose sequence is complementary to X with the exception of two bases. At acidic pH (pH 5.0) strand X folds into the closed *i*-motif structure. In this

closed state, complementary strand Y adopts a floppy random-coil conformation. When the pH value is raised to 8.0, strand X unfolds and is captured by hybridization to Y with formation of an extended duplex structure (the open state). Interconversion of the closed and open states of the machine is thus mediated by alternating addition of H^+ and OH^-.

To visualize the open and closed states of this machine, a doubly labeled version of X (i.e., X*) was synthesized with a rhodamine green fluorophore at the 5' end and a dabcyl quencher at the 3' end. When the 5' and 3' ends of strand X* are nearby, the fluorescence of rhodamine green is quenched by dabcyl, whereas rhodamine green fluorescence is strong when it is held away from the dabcyl moiety.

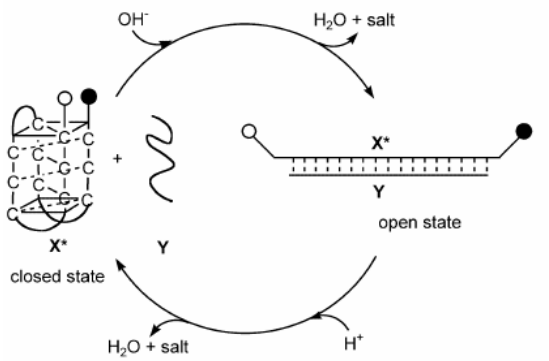

Figure 3.8. Oligonucleotide sequences and working cycle of the pH driven DNA machine. The underlined DNA bases indicate the mismatched nucleotide positions in the duplex. The open circle represents rhodamine green dye, and the filled circle the dabcyl group.[13]

Recently, we reported molecular complexes of benzoic acid derivatives and cytosine as described in Chapter 2, wherein, a variety of supramolecular structures

were obtained through the self assembly process governed by **C.CH$^+$** species, the fundamental moiety in *i*-motifs, depending upon the substrates co-crystallized with cytosine.[14]

In this context, we are interested to study the versatility of **C.CH$^+$** in the design and synthesis of myriad of molecular complexes that can yield exotic supramolecular architectures through self assembly. For this purpose, a search on Cambridge Structural Database (CSD, version 1.10) has been performed for a systematic analysis of the earlier reports known in the literature. The search has retrieved 109 entries possessing cytosinium ions (**CH$^+$**),[15] in which, only 28 entries have **C.CH$^+$** recognition pattern, and the CSD refcodes are listed in Table 3.3.[16] However, in none of those 28 examples, no reference to the significant contribution of **C.CH$^+$** towards observed structural features was made, including in our structure reports.[14] Hence, various co-crystallization experiments of cytosine with various aliphatic dicarboxylic acids, as shown in Scheme 3.3, have been carried out, to evaluate the role of **C.CH$^+$** in the formation of supramolecular assemblies.

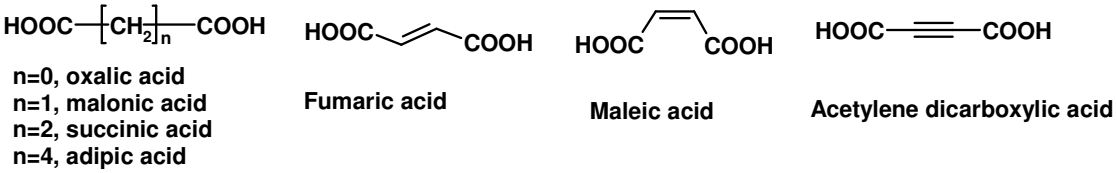

Scheme 3.3

The aliphatic dicarboxylic acids have been chosen, essentially, as they possess two –COOH groups, which would serve as proton source for cytosine to yield **CH$^+$**, a primary step to obtain **C.CH$^+$**, as shown in the following Scheme 3.4.

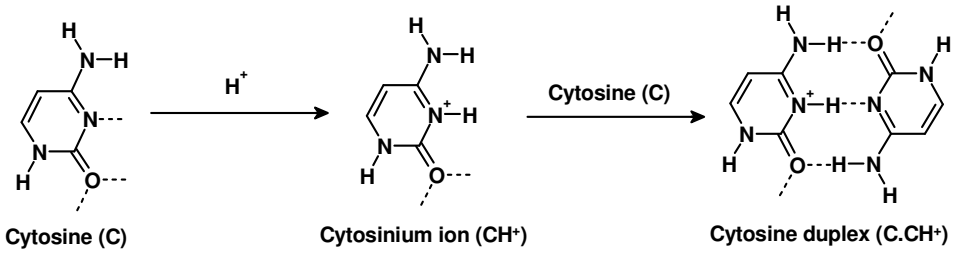

Scheme 3.4

3.2 Molecular adducts of cytosine and aliphatic dicarboxylic acids

Different aliphatic dicarboxylic acids, for example, oxalic, malonic, succinic, adipic, fumaric, maleic and acetylenedicarboxylic acids (as listed in Scheme 3.3), in which the two –COOH groups are being separated by different lengths of $–CH_2-$, C=C and C≡C etc., have been co-crystallized with cytosine in a 1:1 ratio. It has been observed that in all the complexes, **CH^+** is formed through the proton transfer from –COOH to cytosine. But the **CH^+** species, further, interact with complimentary molecules present in the lattice, yielding hetero assembly, without **$C.CH^+$** moiety. Structural features of these complexes would be described in the following sections.

3.2.1 Cytosine and oxalic acid, COX11[17]

In the asymmetric unit, cytosine and oxalic acid, in a 1:1 ratio, along with one water molecule are present, as shown in Figure 3.9.

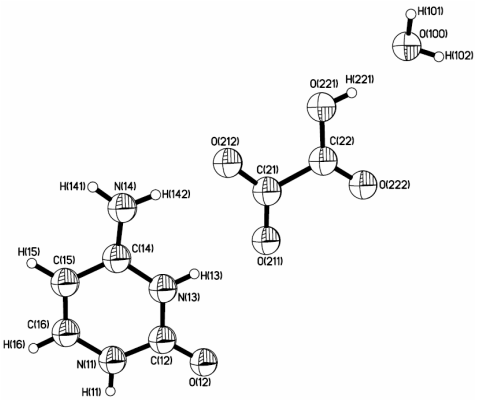

Figure 3.9. ORTEP (50% probability level) drawing of the 1:1 molecular complex COX11.

A proton from one of the –COOH groups is transferred to N^3 atom of cytosine forming cytosinium ion (**CH^+**), which further interacts with oxalate molecules through a cyclic hydrogen bonding pattern N-H···O and N^+-H···O^- hydrogen bonds with the corresponding hydrogen bond distances being, 1.87 and 1.94 Å, respectively. The recognition pattern is shown in Figure 3.10(a). Further, these units are held together by centrosymmetric N-H···O (H···O, 2.09 Å) hydrogen bonds, as shown in Figure 3.10(b).

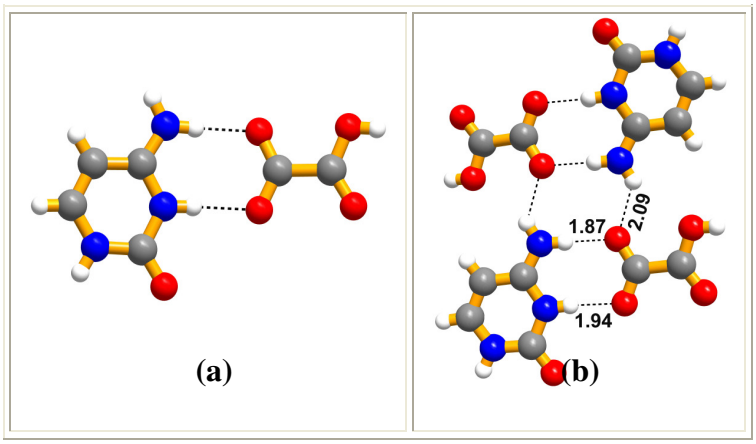

Figure 3.10. (a) Molecular recognition between cytosine and oxalic acid in its 1:1 adduct and (b) Quartet arrangement of molecules in cytosine-oxalic acid 1:1 complex.

3.2.2 Cytosine and malonic acid, CMA11

Cytosine and malonic acid in a 1:1 molar ratio gave good quality single crystals, from methanol solution, suitable for X-ray structure determination. Structure analysis reveals that in the obtained complex also, the composition of the reactants is 1:1. However, three molecules of each, denoted as A, B and C (cytosine) and i, ii and iii (malonic acid), are present in asymmetric unit, as shown in Figure 3.11. Crystallographic information is given in Table 3.1.

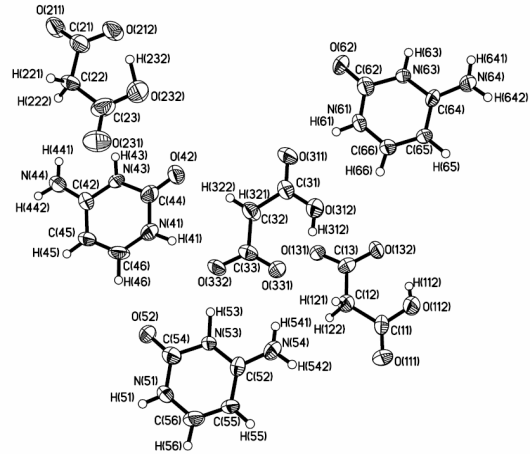

Figure 3.11. ORTEP (50% probability level) showing three molecules each of cytosine and malonic acid in the complex CMA11.

As observed in COX11, cytosinium ions (**CH**$^+$) are formed through the transfer of a proton from all the three acid molecules. Further, the second –COOH group on each malonic acid form intramolecular hydrogen bond, which is a general characteristic of malonic acid. Further, all the cytosinium and malonate molecules interact with each other through a similar hydrogen bonding pattern comprising of N-H$^{\cdots}$O and N$^+$-H$^{\cdots}$O$^-$ as observed in COX11. Such hetero molecular units, related by specific symmetry, are further held together by C-H$^{\cdots}$O hydrogen bonds, with H$^{\cdots}$O

distances of 2.37, 2.60 and 2.58 Å and constitute molecular tapes. These molecular tapes, thus, formed corresponding to each symmetry independent molecules, are arranged alternately in two-dimensional arrangement, to form a sheet structure, as shown in Figure 3.12. Further, the adjacent tapes in a typical sheet are held together by different types of hydrogen bonding networks. While the layers between A and B establish interaction through *homomeric* as well as *heteromeric* interactions, between either B and C or C and A occurs only through *heteromeric* interactions. The hydrogen bonds are given in Table 3.2.

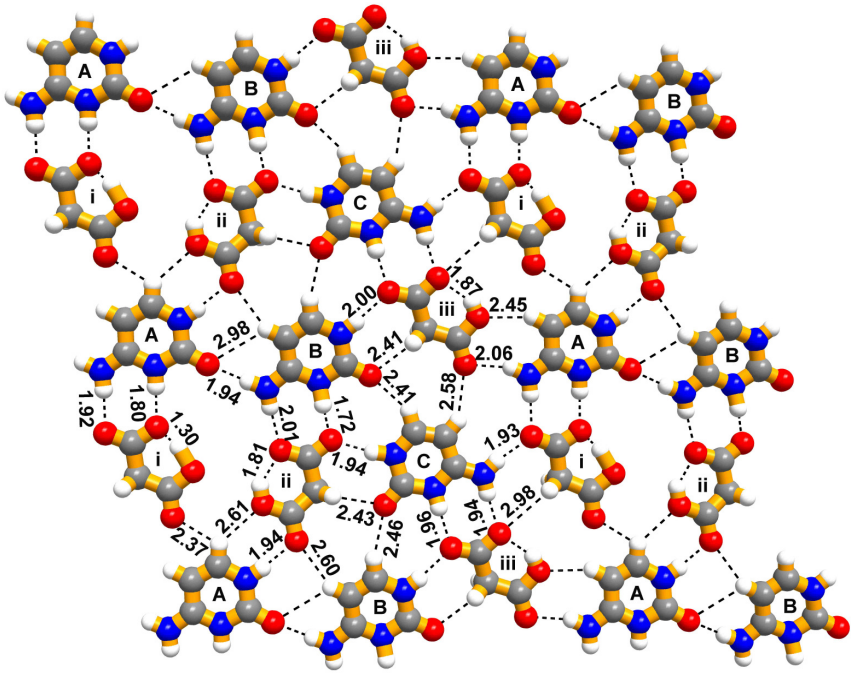

Figure 3.12. Two-dimensional arrangement molecules in CMA11.

3.2.3 Cytosine and succinic acid, CSU11

Co-crystallization of cytosine and succinic, acid in 1:1 ratio, gave an adduct, with an asymmetric unit as shown in Figure 3.13.

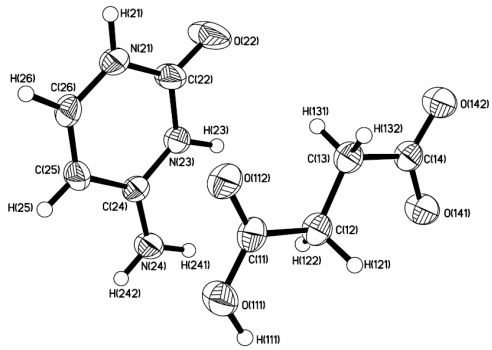

Figure 3.13. ORTEP (50% probability level) of the 1:1 molecular complex CSU11.

Like in the earlier examples, a proton is transferred from one of the –COOH functional groups to N^3 of the cytosine. In three-dimensional arrangement, the molecules are packed to give stacked layers structure, as shown in Figure 3.14.

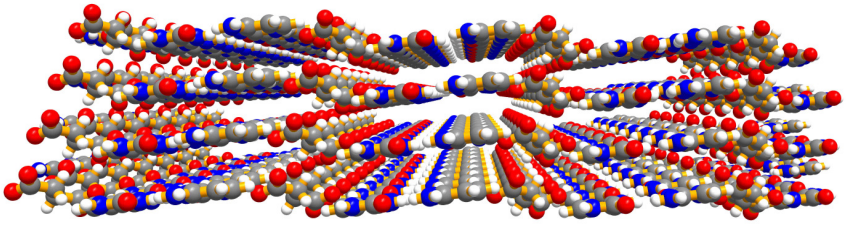

Figure 3.14. Stacked layers formed in the crystal structure of CSU11.

In a typical layer, the arrangement of molecules is shown in Figure 3.15(a). In each layer, the cytosinium and succinate molecules form an ensemble through N-H···O and N^+-H···O^- with corresponding hydrogen bonding distances being 1.99 and 1.58 Å, respectively. However, unlike in COX11 and CMA11, in the present structure, the succinate and cytosinium ions arrange in such a manner that a ladder type structure is formed with cytosinium ions being rods and succinate molecules as rungs. A schematic representation is shown shown in Figure 3.15(b).

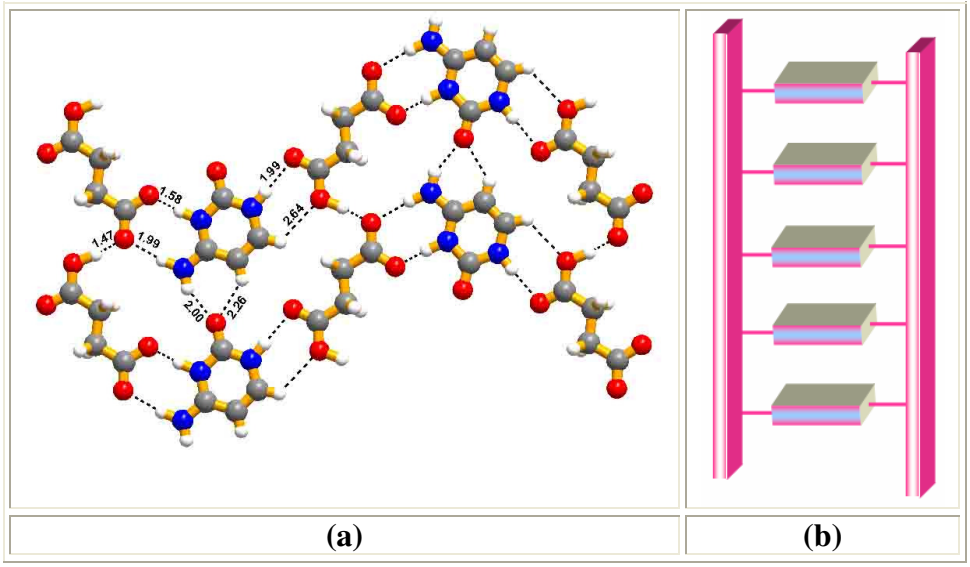

Figure 3.15. (a) Arrangement of succinic acid and cytosine in the molecular complex CSU11 in two dimension and (b) Schematic representation of ladder-like structure observed in the complex CSU11.

However, attempts to obtain single crystals of molecular complex of cytosine and glutaric acid were not successful as the mixture always gave only precipitate. Further, interestingly co-crystallization of cytosine and adipic acid gave always a 2:1 ratio molecular complex.

3.2.4 Cytosine and adipic acid, CAD21

Co-crystallization of cytosine and adipic acid in 1:1 molar ratio yielded good quality single crystals from a methanol solution. X-ray structure analysis revealed that the adduct obtained, indeed, is in 2:1 ratio (see Figure 3.16(a)), rather than 1:1.

However, the cytosine molecule converts to cytosinium with the aid of protons from the –COOH of adipic acid, but in a sharing mode, as the hydrogen atom has partial occupancy residing on both cytosine and adipic acid. Further, the cytosinium molecules establish interaction with acid molecules by N-H···O and C-H···O hydrogen

bonds, with corresponding H···O distances being 1.96 and 2.43 Å respectively, such an arrangement is shown in Figure 3.16(b). These ensembles are further arranged in two-dimensions, establishing *homomeric* interactions between cytosinium ions, yielding the desired **C.CH**$^{+}$,[18] as shown in Figure 3.16(c).

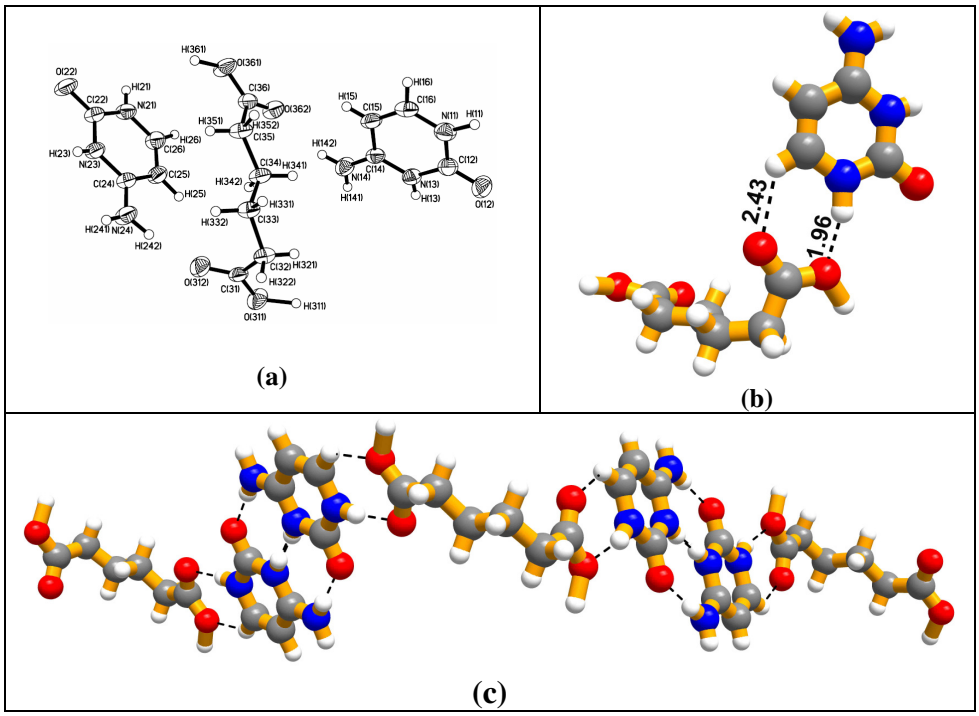

Figure 3.16. (a) ORTEP of the asymmetric unit of CAD21. (b) Basic recognition pattern formed between cytosine duplexes and the acid molecules in the adduct CAD21.

Further, in three-dimensional arrangement, the aggregates are arranged to yield a ladder type structure, in which adipic acids form rods, while cytosinium ions constitute rungs (see Figure 3.17), resembling the complex of cytosine and benzoic acid.

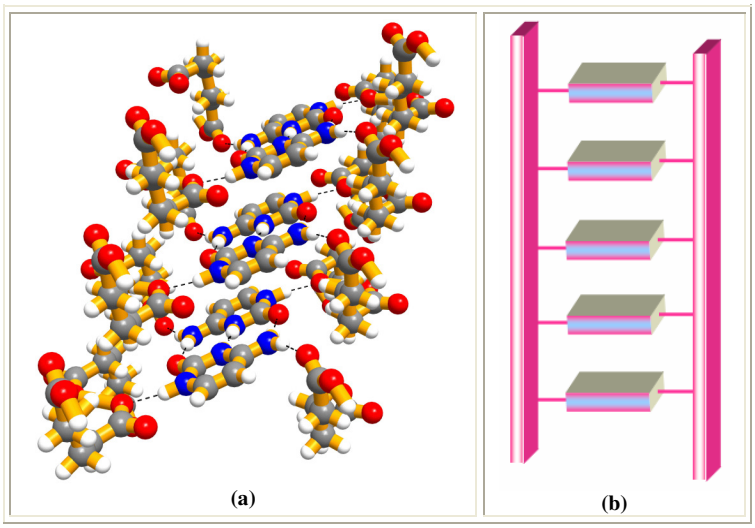

Figure 3.17. (a) Arrangement of the acid and cytosine molecules forming a ladder. (b) Cartoon of the three dimensional arrangement of CAD21 with ladder-like topology.

The 2:1 complex, CAD21 is, indeed, quite intriguing with the formation of **C.CH$^+$** species. In fact, with benzene dicarboxylic acids also, although such **C.CH$^+$** species were observed (Chapter 2), the reaction mixture of co-crystallization was, in fact, is in 1:1 ratio. However, such a change of composition was not observed in COX11, CMA11 and CSU11. However, from scheme 3.4 it is apparent that formation of **C.CH$^+$** indeed requires excess cytosine than the complementary molecules and also the prerequisite in the formation of *i*-motifs in the macromolecular structure is the cytosine rich region. Thus, co-crystallization experiments of cytosine with oxalic acid, malonic acid and succinic acid have been carried out deliberately in 2:1, 3:1 and 4:1 ratios, to maintain the excess cytosine for the preparation of structures with **C.CH$^+$** species. In each case, good quality crystals were obtained and the composition is found to be always 2:1 even from 3:1 and 4:1 ratios of the reaction mixtures. The structural features of the complexes are as described in the following sections.

3.2.5 Cytosine and oxalic acid, COX21

Cocrystallization of cytosine and oxalic acid in a 2:1 molar ratio, from ethanol: water (in 70:30 v/v), by slow evaporation, yielded 4:2 complex, as an hydrate. Constituents of asymmetric unit are shown in Figure 3.18(a). Complete crystallographic details are given in Tables 3.1. Both the –COOH groups transfer hydrogen atoms to two cytosines, yielding oxalate dianion and cytosinium ions. As observed in CAD21, in the present structure also, cytosinium molecules interact with each other yielding cytosinium duplex as shown in Figure 3.18(b). This duplex show its significant influence in the ultimate supramolecular assembly by interacting with water and acid molecules, separately, in two-dimensional arrangement. The molecular interactions are shown in Figure 3.19.

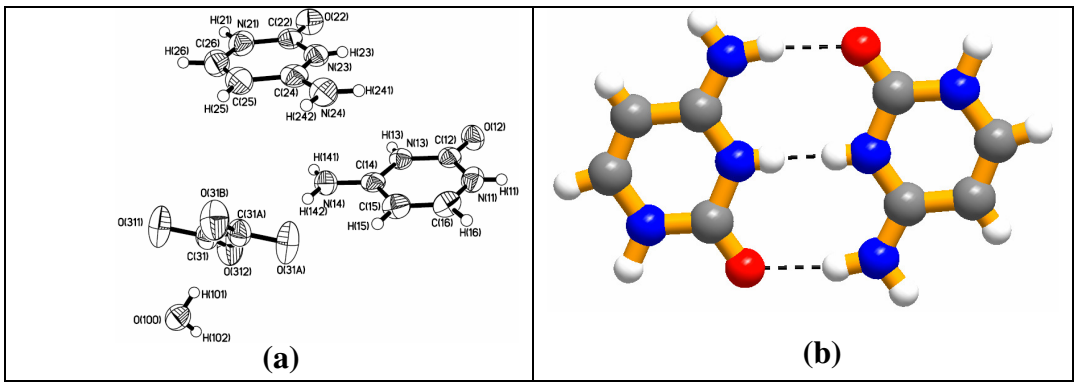

Figure 3.18. (a) ORTEP (50% probability level) of the 2:1 molecular complex **COX21**, of cytosine and oxalic acid and (b) homomeric interactions between cytosine molecules forming duplexes.

Thus, in the layers of oxalate molecules, cytosinium duplexes are being held together by oxalate molecules through N-H···O$^-$ (H···O$^-$, 2.03 Å) and C-H···O$^-$ (H···O$^-$, 2.71 Å) hydrogen bonds, constituting molecular tapes, which, in turn, are held together

again by N-H···O$^-$ and C-H···O$^-$ hydrogen bonds but of different topology, in two-dimensional arrangement (see Figure 3.19(a)). Similarly, in the layers of water, cytosinium duplexes are connected to each other through water molecules by N-H···O hydrogen bonds with H···O distance being 1.76 Å (Figure 3.19(b)).

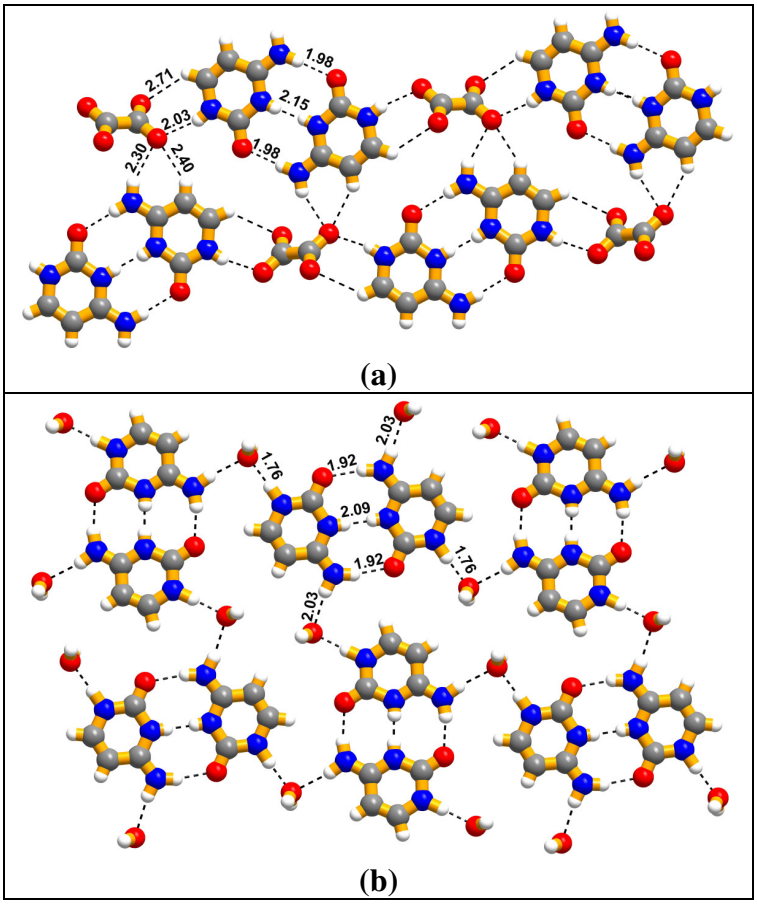

Figure 3.19. Interaction of **C.CH$^+$** duplexes with (a) oxalic acid and (b) water molecules in a typical sheet structure.

In the crystal lattice, such layers are stacked with acid and water layers being arranged alternately, as shown in Figure 3.20(a). Interestingly, the layers are being held together by the interactions, established between oxalate and water molecules,

through, O-H···O$^-$ hydrogen bonds (1.86 and 2.38 Å) arranged in a diamond topology, as shown in Figure 3.20(b).

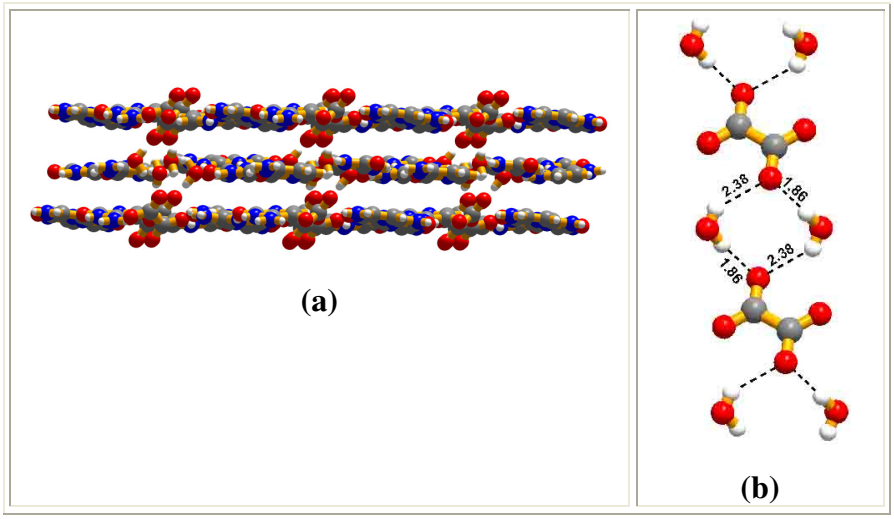

Figure 3.20. Interaction of **C.CH$^+$** duplexes with (a) Stacked sheet arrangement in three-dimension and (b) linear strands formed by oxalic acid and water molecules across the sheets in the adduct **COX21**.

3.2.6 Cytosine and malonic acid, CMA21

Co-crystallization of cytosine and malonic acid, in 2:1 ratio, from a methanol solution, yielded complex CMA21. Structure determination revealed that in the crystal lattice, cytosine and malonic acid molecules are present in a 2:1 ratio, as shown in the Figure 3.21. The complete crystallographic details are given in Table 3.1.

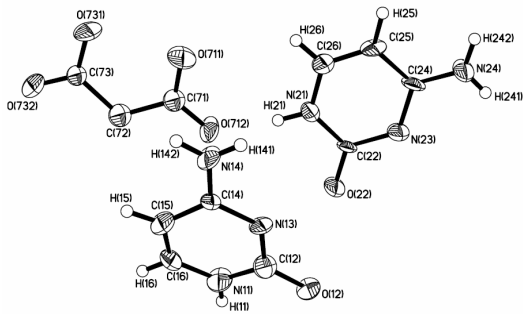

Figure 3.21. ORTEP (50% probability level) of the 2:1 molecular complex of cytosine and malonic acid, CMA21.

In this complex also, both the –COOH groups donate protons to cytosine. Although, the location of hydrogen atoms on –COOH could not be established, the protons transfer has been concluded with the overall packing, wherein cytosine molecules are connected together, yielding duplexes, as observed in the other 2:1 complexes discussed above. Further, the arrangement in both two and three-dimensions is similar to the structure of CMA21. Thus, malonate molecules connects the cytosinium duplexes through N-H···O$^-$ (H···O$^-$, 1.90 Å)and C-H···O$^-$ (H···O, 2.94 Å) hydrogen bonds, yielding molecular tapes in one-dimensional arrangement, which, in turn constitute layers by establishing interaction between the adjacent tapes through different types of C-H···O, N-H···O$^-$, C-H···O$^-$ hydrogen bonds. The hydrogen bond distances areannotated in Figure 3.22(a) and full characteristics are listed in Table 3.2. These sheets stack in three-dimensional arrangement, as shown in Figure 3.22(b).

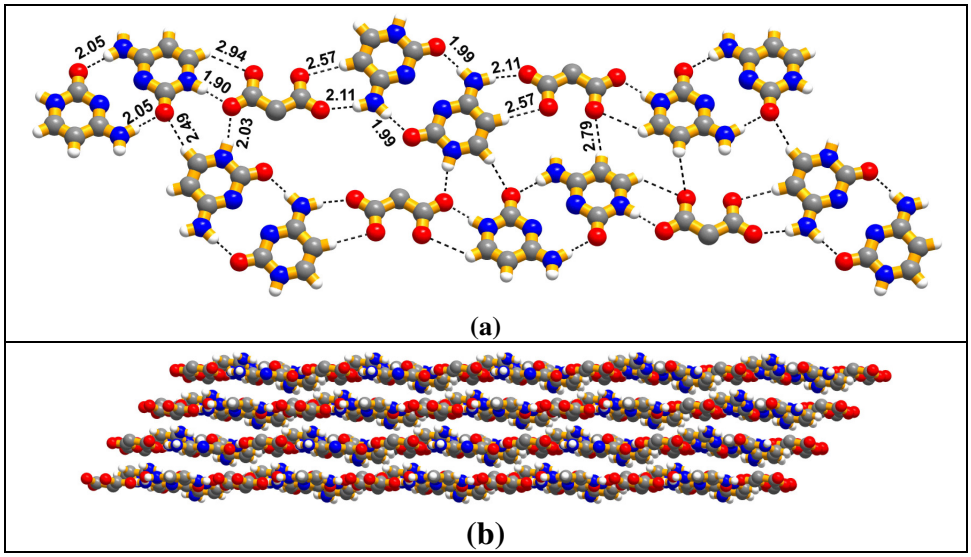

Figure 3.22. (a) Recognition between the cytosine duplexes and malonic acid molecules in the adduct CMA21 and (b) Stacking of sheets in three-dimensional arrangement of the complex CMA21.

3.2.7 Cytosine and succinic acid, CSU21

In CSU21 also, obtained by co-crystallization of cytosine and succinic acid in a 2:1 ratio from a CH_3OH solution, cytosinium duplexes are formed as observed in COX21 and CMA21, but only one of the –COOH groups transfers proton, which is being shared by two cytosine molecules. These duplexes, further, interact with each other through monosuccinate molecules, by N-H···O and C-H···O hydrogen bonds with the corresponding H···O distances being 1.81 and 2.44 Å, yielding molecular tapes (see Figure 3.23(a)). These tapes, are held together in two-dimensional arrangement, mainly by N-H···O (H···O, 2.11 Å) hydrogen bonds formed between cytosine duplexes (see Figure 3.23(b)), as observed in cytosine and benzoic acid complex, discussed in Chapter 2.

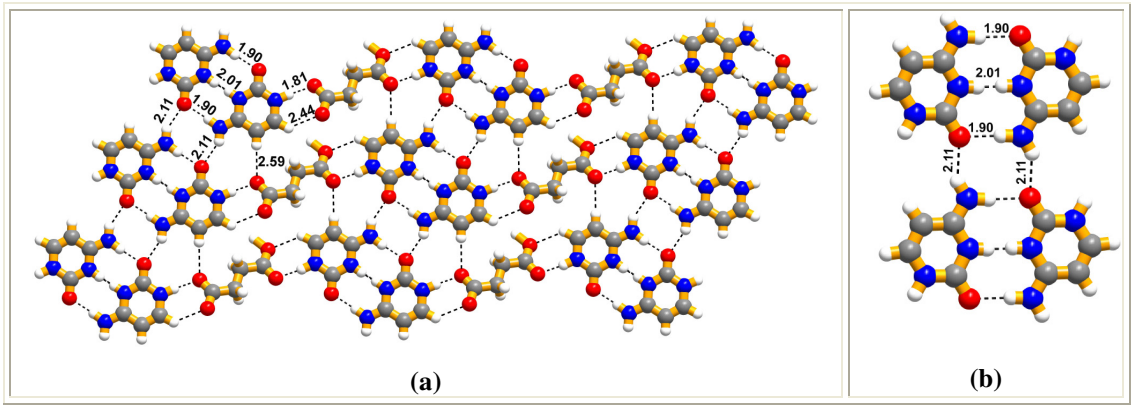

Figure 3.23. (a) Arrangement of molecules in a typical sheet structure of co-crystals of cytosine and succinic acid. (b) Interactions between the cytosine duplexes forming a quartet hydrogen bonding pattern.

These sheets are stacked in three-dimensional arrangement, with the acid molecules in the adjacent sheets interacting with each other through O-H···O (H···O, 1.23 Å) hydrogen bonds, thus, constituting a ladder structure, as shown in Figure 3.24,

resembling the structure of CAD21, a molecular complex of cytosine and adipic acid, discussed in section 3.2.4.

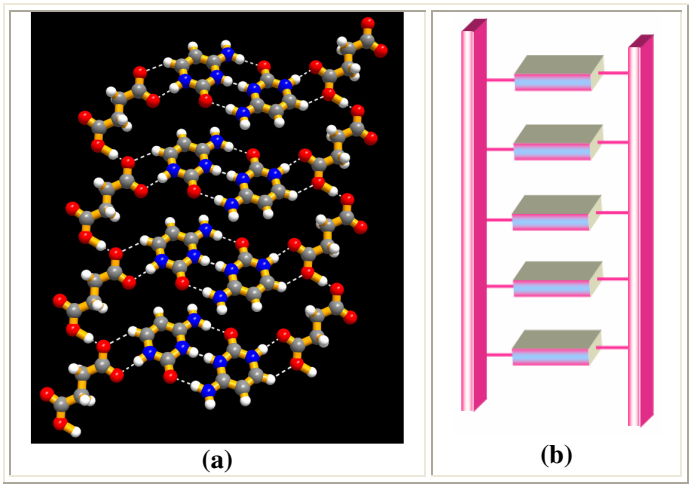

Figure 3.24. (a) Arrangement of molecules in the form a ladder in the crystal structure of cytosine and succinic acid. b) Schematic representation of cytosine duplexes and acid molecules in the adduct CSU21.

In further explorations, cytosine and glutaric acid in 2:1 molar ratio also did not yield single crystals as observed in the experiments with 1:1 ratio reaction mixtures. However, to illustrate the features of cytosinium duplexes in a variety of supramolecular assemblies, and also to demonstrate the dependence of its formation upon the distinct composition of the reaction mixtures, co-crystallization of cytosine with other dicarboxylic acids like maleic, fumaric, acetylene dicarboxylic acid have been carried out in different ratios (1:1 and 2:1) as discussed below.

3.2.8 Cytosine and maleic acid, CMAL11[19]

As observed in the 1:1 complexes of other dicarboxylic acids, in CMAL11 also, the maleic acid transfers one of its protons to cytosine, and forms cytosinium,

while the other –COOH forms intramolecular O-H···O$^-$ hydrogen bond. The asymmetric unit of the adduct is shown in Figure 3.25(a).

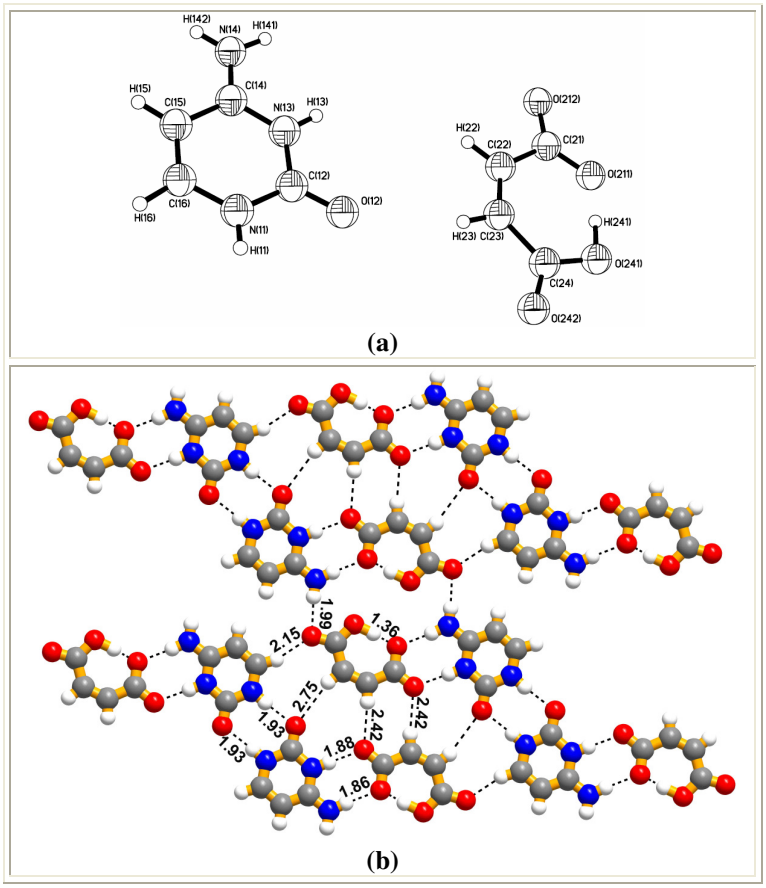

Figure 3.25. (a) The ORTEP (50% probability level) showing the 1:1 molecular complex of cytosine-maleic acid and (b) The two-dimensional layer formed by cytosine and maleic acid in CMAL11.

In the crystal lattice, the molecules self assemble to yield stacked layers and typical arrangement within a layer is shown in Figure 3.25(b). Thus, each cytosinium interacts with maleiate through N-H···O (H···O, 1.86 Å) and N$^+$-H···O$^-$ (H···O, 1.88 Å) hydrogen bonds, yielding binary units, which are further held together by C-H···O hydrogen bonds of H···O distance, 2.15 Å, to constitute molecular tapes. Arrangement of molecules connected by hydrogen bonds is shown in Figure 3.25(b). Further, such

adjacent tapes are held together by different types of hydrogen bonds yielding dimers of cytosinium and maleiates, leading to the formation of binary tapes, which are further held together in two-dimensional arrangement through N-H···O hydrogen bonds, with a H···O distance of 1.99 Å (see Figure 3.25(b)).

3.2.9 Cytosine and fumaric acid, CFU11

Slow evaporation of ethanol-water solvent mixture with cytosine and fumaric acid in a 1:1 molar ratio gave an adduct CFU11 as shown in Figure 3.26.

In the crystal lattice, while cytosinium formation and arrangement in three-dimensions in the form of layers (see Figure 3.26(a) and (b)), is as same as observed in the earlier examples.

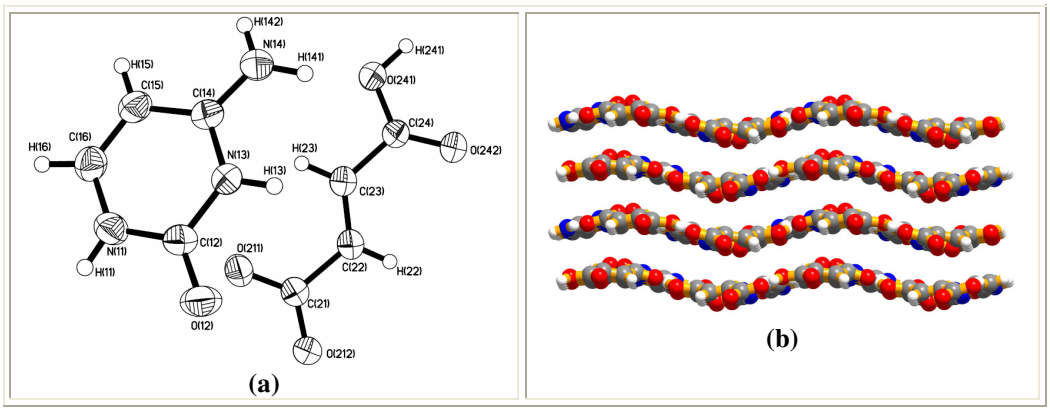

Figure 3.26. **(a)** ORTEP (50% probability level) of the 1:1 molecular complex CFUMA11, of cytosine-fumaric acid and (b) the three-dimensional arrangement forming sheet structure in complex CFUMA11.

However, within a layer, the interactions among the molecules show some differences to the other structures described earlier. In CFU11, the binary units of cytosinium and fumarate connect to each other to give an arrangement in two-

dimensions such that chains of each molecule are arranged alternately, as shown in Figure 3.27.

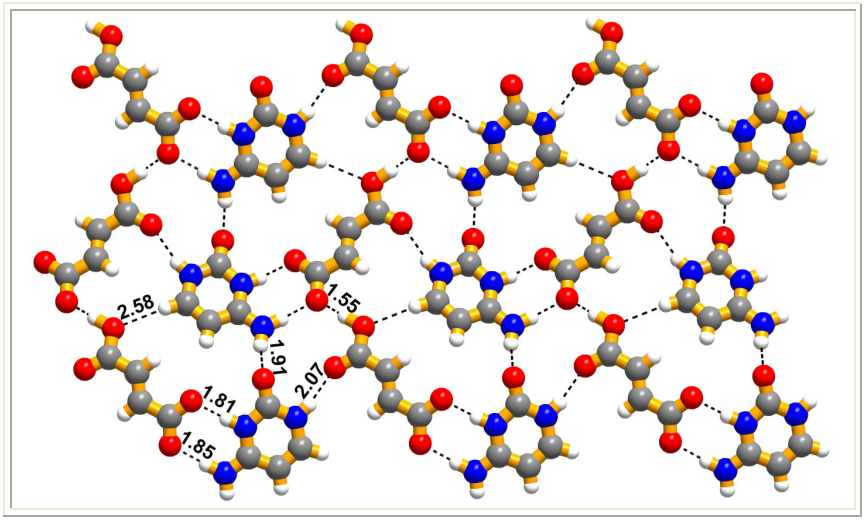

Figure 3.27. Arrangement of cytosine and the acid molecules, in the adduct CFU11, in an individual sheet.

3.2.10 Cytosine and acetylene dicarboxylic acid, CAC21

Cytosine and acetylene dicarboxylic acid, ACDCA, in a 1:1 molar ratio, from methanol, gave good quality single crystals by slow evaporation process. However, structure analysis reveals that a molecular adduct is formed in a 2:1 ratio as shown in Figure 3.28.

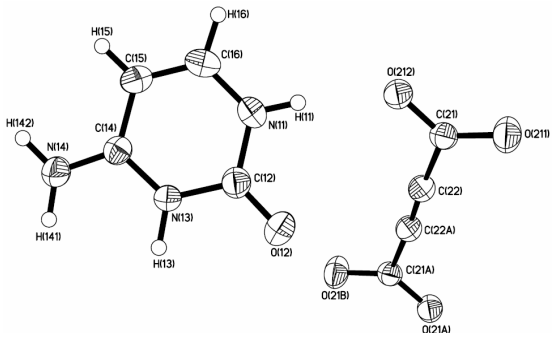

Figure 3.28. ORTEP (50% probability level) of the 2:1 molecular complex CAC21, of cytosine and acetylene dicarboxylic acid.

In the complex, the *in situ* generated cytosinium and carboxylate interact each other, by a cyclic hydrogen bonding pattern, through N-H···O (H···O, 2.03 Å) and N^+-H···O^- (H···O, 1.72 Å) hydrogen bonds, yielding a binary unit, as shown in Figure 3.29. Complete details of hydrogen bonds are listed in Table 3.2.

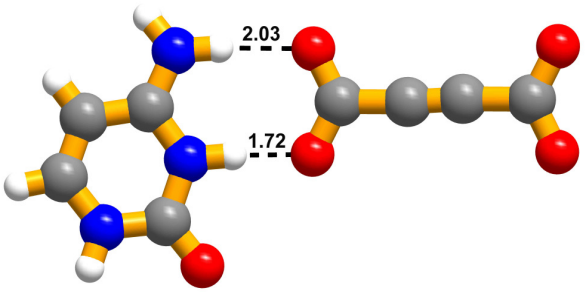

Figure 3.29. Binary supramolecular unit formed between C and ACDCA in the molecular adduct CAC21.

Such binary units aggregate in two-dimensional arrangement by N-H···O and C-H···O hydrogen bonds with a H···O distance of 1.97 and 2.70 Å, respectively, as shown in Figure 3.30.

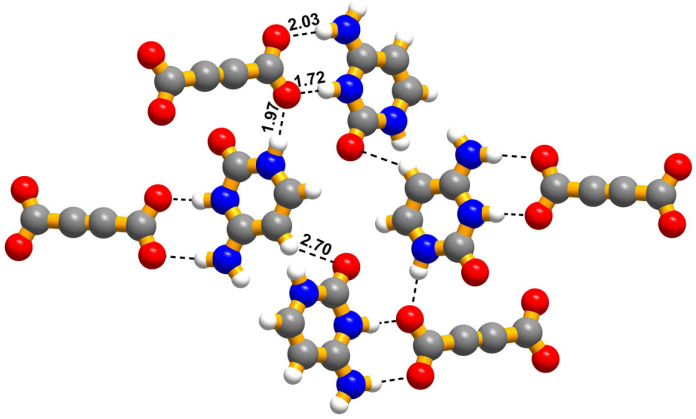

Figure 3.30. Cyclic network observed in the molecular adduct CAC21.

Thus, even the dicarboxylic acids, wherein, the –COOH are being separated by other than $–CH_2$ moieties, still preferentially formed complexes with cytosine is the

same ratio as of the composition of the reaction mixtures, except in the complex with acetylene dicarboxylic acid. But, in the absence of excess cytosine, CH^+ generated, *in situ*, established interaction with the complimentary ligands rather than forming **C.CH$^+$** even in 2:1 complexes of acetylene dicarboxylic acid, supporting the importance of excess cytosine conditions, to obtain **C.CH$^+$** duplexes. Thus, co-crystallization of maleic acid, fumaric acid[20] and acetylene dicarboxylic acids with cytosine in 1:2 ratios have been carried out to obtain the complexes mediate by **C.CH$^+$** duplexes. The obtained crystals have been analyzed by X-ray diffraction methods to evaluate the arrangement of molecules in the crystal lattices and the salient features are described below.

3.2.11 Cytosine and maleic acid, CMA21

Co-crystallization of cytosine and maleic acid, in a 2:1 ratio, from a CH_3OH solution gave single crystals of good quality suitable for X-ray diffraction studies. In the asymmetric unit, as expected, one maleic acid and two molecules of cytosine molecules are present, as shown in Figure 3.31. In CMA21 also, without any exception, cytosinium is formed by the proton transfer from one of the –COOH groups to cytosine at N^3 position.

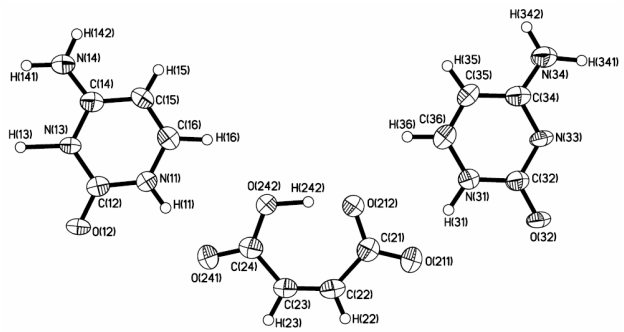

Figure 3.31. ORTEP (50% probability level) of the 2:1 molecular complex CMA21.

In the crystal lattice, the molecules are arranged in stacked layers, as shown in Figure 3.32(a), and typical arrangement of molecules is shown in Figure 3.32(b). It is evident that cytosinium and malonate ions form aggregates, through N-H···O (H···O, 1.73 Å) and C-H···O (H···O, 2.49 Å) hydrogen bonds, which, in turn, are held together by *homomeric* interactions between cytosinium molecules, thus yielding expected **C.CH$^+$** moiety. Such a network gave molecular tapes, which are further held together by interactions being established between the cytosinium duplexes by N-H···O hydrogen bonds, with H···O distances of 2.02 and 2.07 Å.

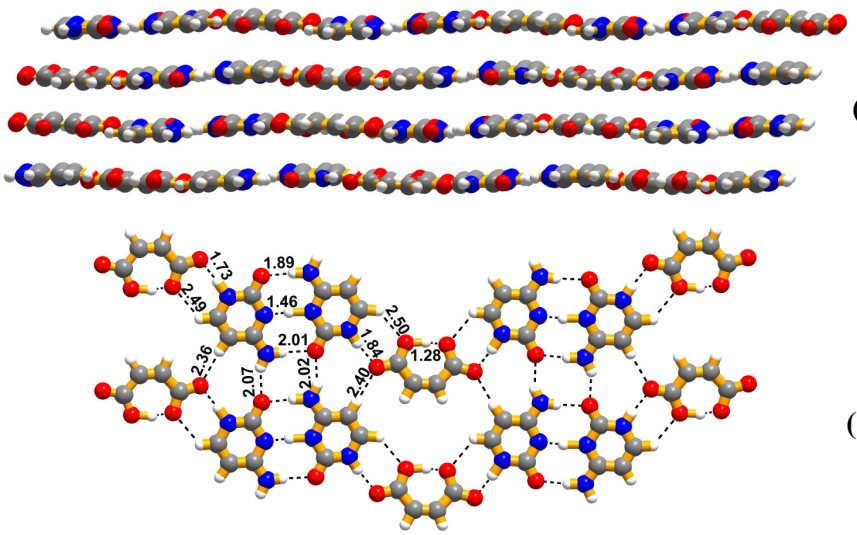

Figure 3.32. (a) Stacked sheet structure formed in complex CMA21 and (b) two-dimensional arrangement of cytosine duplexes and the acid molecules existing in an individual sheet.

3.2.12 Cytosine and acetylenedicarboxylic acid, CAC41

Co-crystallization of cytosine and acetylenedicarboxylic acid in a 2:1 ratio, in a methanol solution, gave good quality single crystals for X-ray diffraction studies.

Structure determination, however, reveals that the complex is in 4:1 ratio of cytosine and the acid. In addition, one water molecule also present in the asymmetric unit (see Figure 3.33).

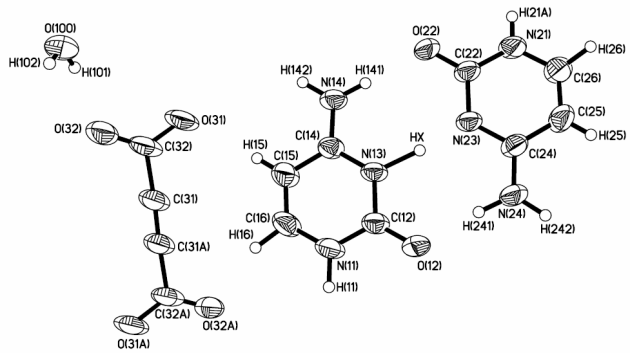

Figure 3.33. ORTEP (50% probability level) of the 4:1 molecular complex of cytosine and acetylene dicarboxylic acid (CAC41).

Both the hydrogen atoms form –COOH groups are transferred to two cytosine molecules, leading to the formation of the cytosinium molecules, while two other neutral cytosine molecules remains intact. Cytosine and cytosinium molecules form duplexes, as expected in the cytosine excess complexes. In three-dimensional arrangement, molecules are arranged as stacked layers, as shown in Figure 3.34(a). Within the layers, the arrangement of **C.CH$^+$** moieties is shown in Figure 3.34(b). Thus, adjacent **C.CH$^+$** moieties interact with water on one end and with carboxylates on the other end, in one-dimensional arrangement, through N-H$^{\cdots}$O and C-H$^{\cdots}$O hydrogen bonds, yielding molecular tapes. Such tapes are held together by cyclic N-H$^{\cdots}$O hydrogen bonds formed between cytosinium duplexes. However, stacking direction, the adjacent layers are held together by interactions formed between carboxylates and water molecules, as shown in Figure 3.34(c). Such an arrangement

resembles a ladder type structure with carboxylate and water constituting rods, while cytosinium duplexes as rungs (see Figure 3.34(d)).

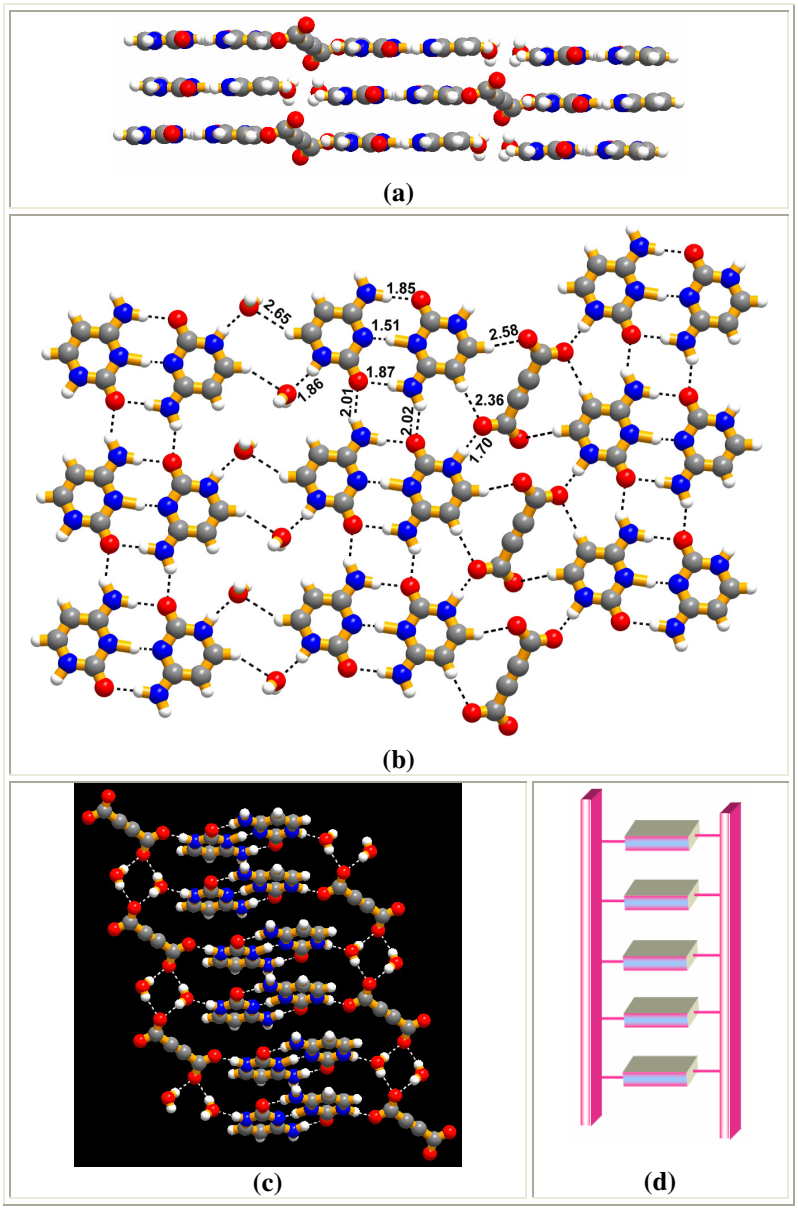

Figure 3.34. (a) The three-dimensional arrangement of molecules in the adduct CAC41, (b) the two-dimensional representation of the recognition patterns existing in sheets, (c) interaction between cytosine duplexes and ACDCA molecules and water molecules in three-dimension and (d) Schematic representation of cytosine duplexes and acid molecules in the crystal structure.

The molecular complexes, thus, so far been described in this chapter illustrate the significance of cytosine in the molecular recognition studies with the formation of different types of assemblies. In particular, the distinct dependence of composition of ligands in the co-crystal towards aggregation of **CH$^+$** either to yield *hetero* assembly directly or through **C.CH$^+$** is quite intriguing. Since, in all the co-crystals discussed so far have only carboxylic acids, it is noteworthy to study the co-crystals of cytosine and aromatic compounds of different types. Especially, the experiments will have great significance as previous study (chapter 2) with benzoic acids always formed **C.CH$^+$** by yielding 2:1 complexes irrespective of the initial of the reaction mixture. Thus, we have initiated preparation of large number of molecular complexes of various aromatic compounds, as listed in Scheme 3.4, in different ratios, and the structural features of the obtained complexes are discussed in the following sections.

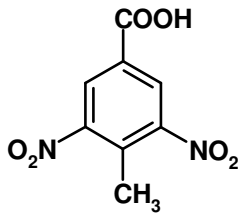

3,5-dinitro-4-methyl benzoic acid

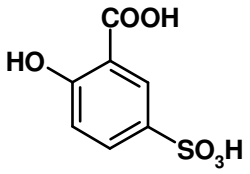

5-sulphosalicylic acid

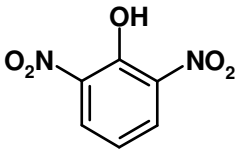

2,6-dinitrophenol

Scheme 3.4

3.3 Molecular adducts of some aromatic compounds with cytosine

Different aromatic compounds, 3,5-dinitro-4-methylbenzoic acid, 5-sulphosalicylic acid and 2,6-dinitrophenol with acidic hydrogens of variable strength have been co-crystallized with cytosine, in a 1:1 ratio, from a suitable solvent. The crystals obtained were characterized by single crystal X-ray diffraction methods and

the structures were evaluated for the molecular recognition features between cytosine and the complementary compound, with an emphasis on the packing in three-dimensional arrangement, as described below.

3.3.1 Cytosine and 3, 5-dinitro-4-methylbenzoic acid, CDMB11

Co-crystallization of cytosine and 3,5-dinitro-4-methybenzoic acid in a 1:1 molar ratio, from DMF solution, gave block like crystals suitable for structure elucidation by X-ray diffraction methods. In asymmetric unit, the composition of the reactants is also found to be in 1:1 ratio, as shown in Figure 3.35.

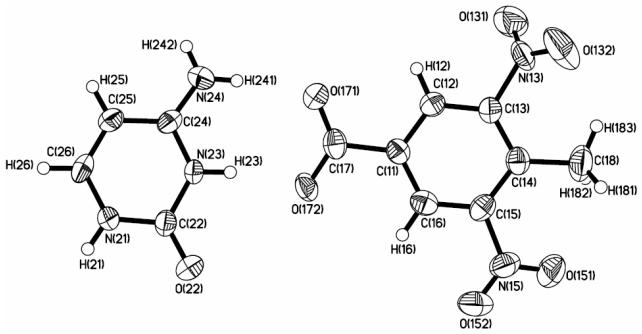

Figure 3.35. ORTEP (50% probability level) of the molecular complex CDMB11.

Packing analysis of molecules reveals that, in CDMB11, three-dimensional arrangement is in the form of stacked sheets, as shown in Figure 3.36(a). Arrangement of molecules in a typical layer is shown in Figure 3.36(b). Thus, in CDMB11, the cytosinium molecules which are formed due to the transfer of the proton from –COOH of the acid, interacts with the carboxylate through N^{+}-H···O^{-} (H···O, 1.92 Å) and N-H···O (H···O, 1.96 Å) hydrogen bonds, as shown in Figure 3.36(b). Further, these entities are held together by cyclic hydrogen bonding patterns, consisting of N-H···O (H···O, 2.63 Å) and C-H···O (H···O, 2.61 Å) hydrogen bonds, yielding molecular tapes. The adjacent tapes, are held together by different C-H···O (H···O, 2.28 Å) hydrogen bonds (see

Figure 3.36(b)), yielding binary tapes, which, in turn, are extended in two-dimensional arrangement by C-H···O (H···O, 2.87 Å) hydrogen bonds formed by CH_3 groups.

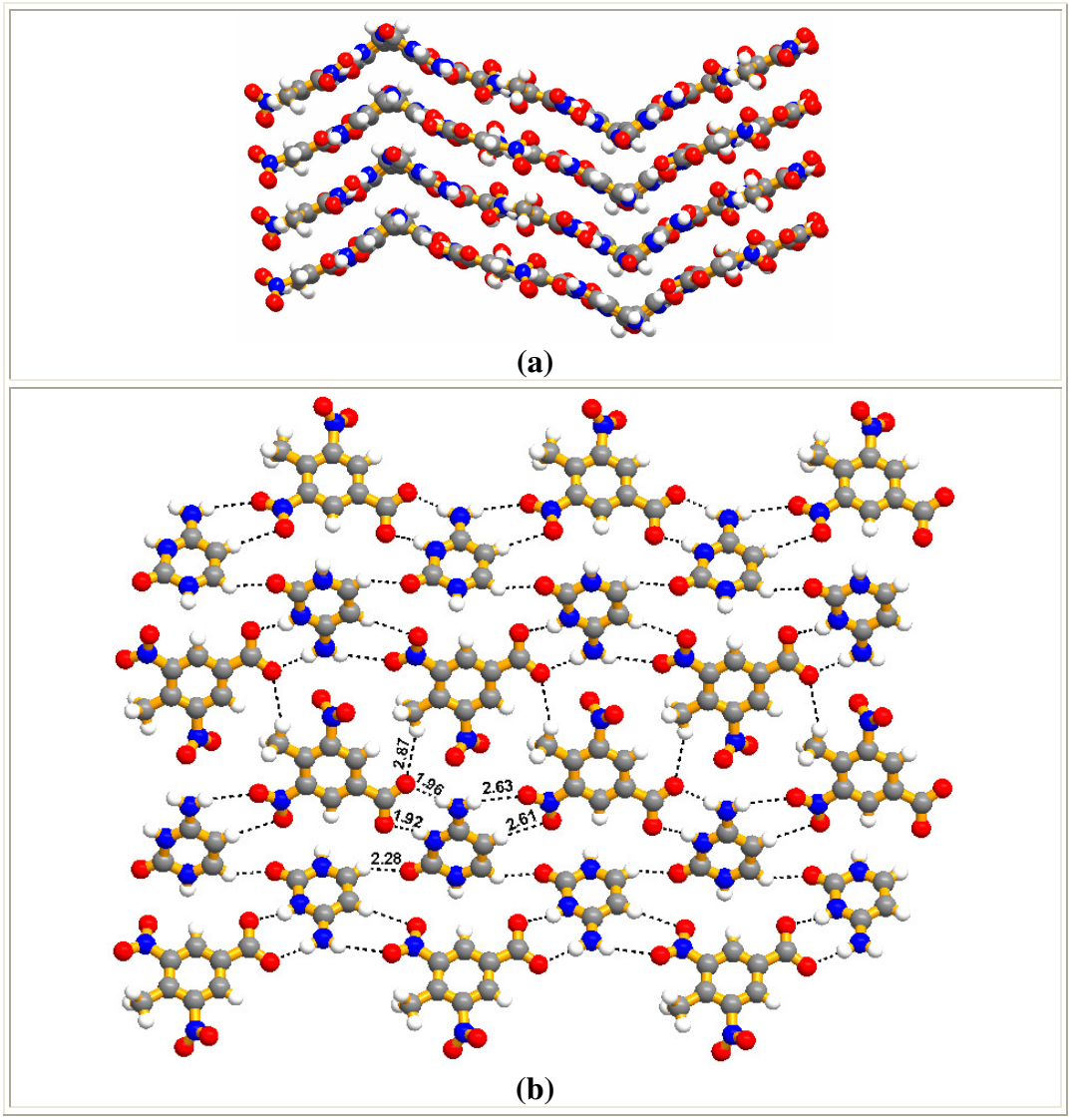

Figure 3.36. (a) Stacking of layers in three-dimension. (b) Arrangement of cytosine and the acid molecules in CDMB11, existing in a sheet.

3.3.2 Cytosine and 5-sulphosalicylic acid, CSUL11

Co-crystallization of cytosine and 5-sulphosalicylic acid in a 1:1 molar ratio, from methanol solution, yielded crystals suitable for data collection. Structure

determination by X-ray diffraction methods revealed that the composition of the contents of the asymmetric unit is also 1:1 and in addition it has two water molecules, as shown in Figure 3.37.

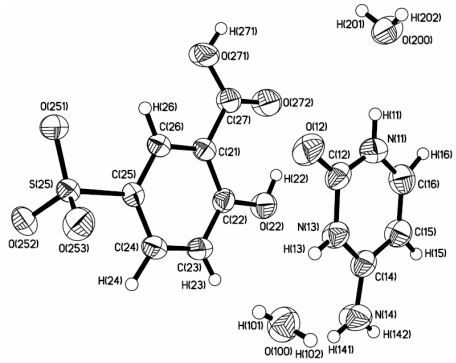

Figure 3.37. ORTEP (50% probability level) of the molecular complex of CSUL11.

It is noteworthy to mention that the –OH group on salicylic acid form intramolecular hydrogen bond with the –COOH group, while proton from the sulphonic acid group is transferred to cytosine. Further, in three-dimensional arrangement, the molecules pack in the form of stacked sheets, as shown in Figure 3.38(a). However, the alternate sheets comprise of molecules of only either sulphonic acid or cytosinium molecules. Thus, there is no interaction between the constituent molecules in the two-dimensional arrangement.

In a typical cytosinium layer, molecular tapes are formed through N-H···O (H···O, 1.97 Å) and C-H···O (H···O, 2.52 Å) hydrogen bonds, which in turn, are held together by water molecules present in the same layers (see Figure 3.38(b)). However, the acid molecules, in a typical layer, are held together by O-H···O (H···O, 1.85 Å) and C-H···O (H···O, 2.55 Å) hydrogen bonds, formed between –COOH and $–SO_3^-$ groups,

yielding molecular tapes. Such tapes are further held together by C-H···O (H···O, 2.67 Å) hydrogen bonds, as shown in Figure 3.38(c).

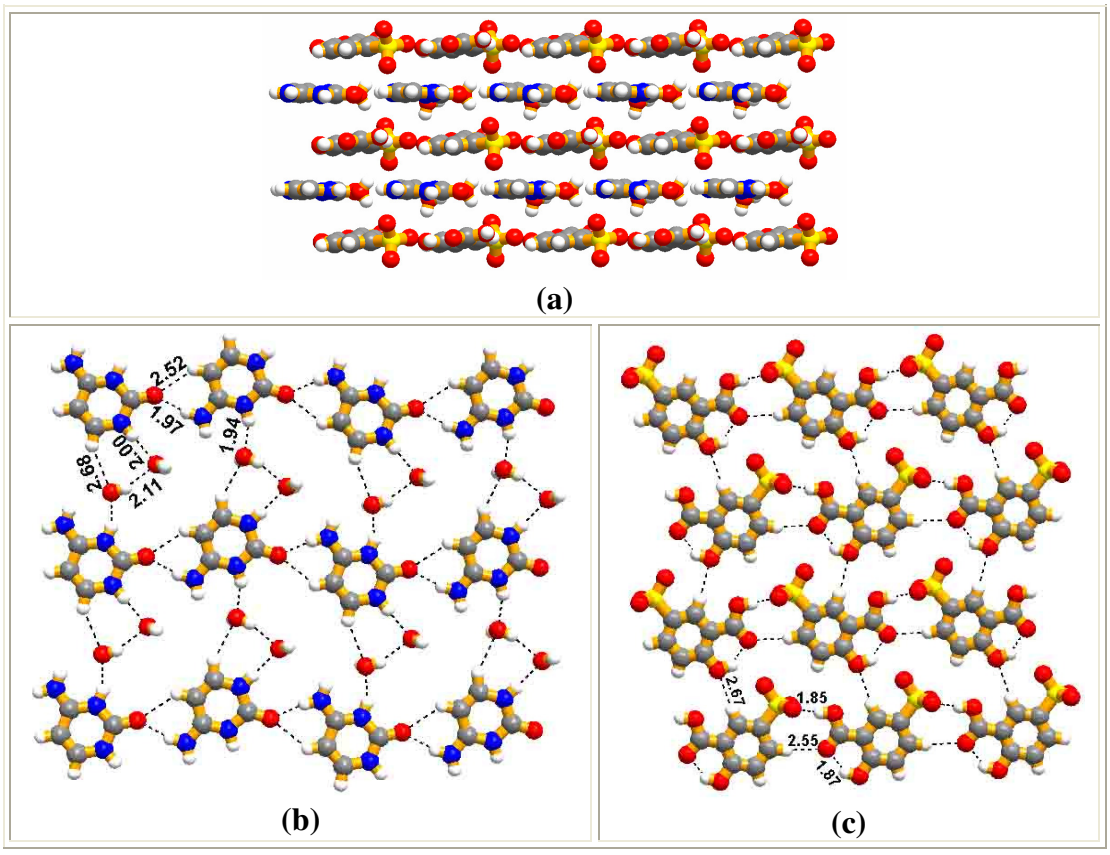

Figure 3.38. (a) Stacking of the planar sheets in three dimensional arrangement of complex CSUL11. (b) Arrangement of cytosine and water molecules in one layer. (c) Arrangement of the salicylic acid molecules in a layer.

3.3.3 Cytosine and 2,6-dinitrophenol, CDNP11

Co-crystallization of cytosine and 2,6-dinitrophenol, in a 1:1 molar ratio, from a DMF solution, gave a 1:1 molecular complex, with two molecules of each in the asymmetric unit. The hydrogens of the both the phenol moieties are transferred to the cytosines, yielding cytosinium species. ORTEP diagram of asymmetric unit is shown

in Figure 3.39(a). In the crystal lattice, the molecules are arranged, as stacked layers, as shown in Figure 3.39(b).

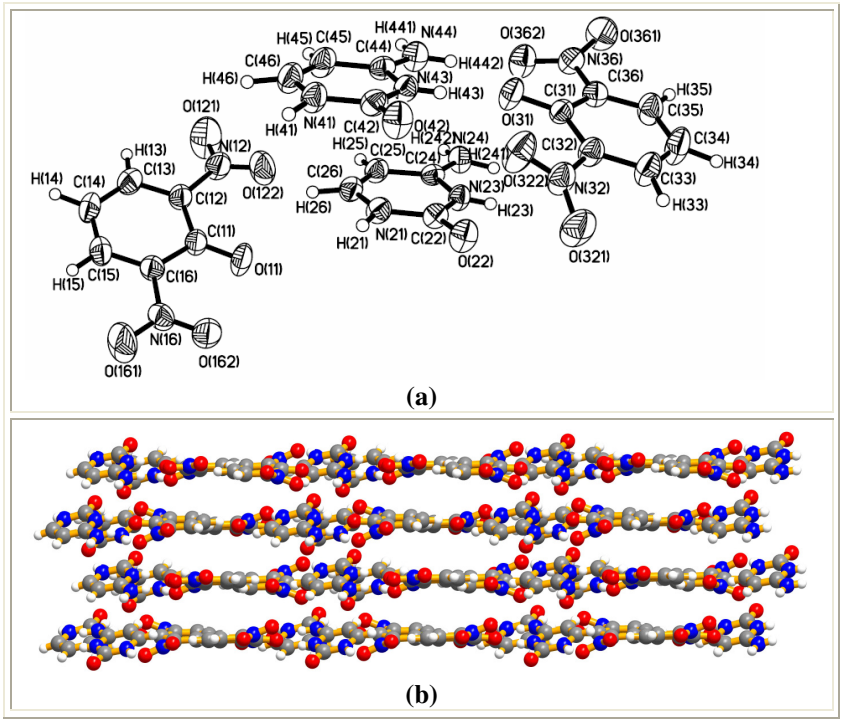

Figure 3.39. (a) ORTEP (50% probability level) of the molecular complex of CDNP11. Note that two molecules of each are present and (b) Stacking of the planar sheets in three dimensional arrangement of complex CDNP11.

Within a typical layer, the cytosinium molecules of each symmetry interacts with phenolates through, N^{+}-H···O^{-} and N-H···O hydrogen bonds, as shown in Figure 3.40. Such adjacent symmetry independent binary units are further held together by N-H···O and C-H···O hydrogen bonds (see Figure 3.40) and form quartet units, which, in turn, are held together by cyclic C-H···O hydrogen bonds with H···O distances of 2.51 and 2.63 Å. Further, such one-dimensional networks are connected to each other by different types of C-H···O hydrogen bonds, with H···O distances of 2.60 and 2.65 Å, as depicted in Figure 3.40.

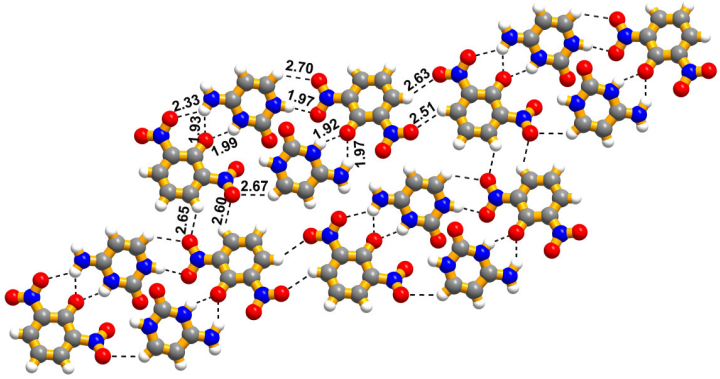

Figure 3.40. Interactions existing between the molecules of cytosine and the phenol in the molecular complex CDNP11.

Thus, even aromatic compounds with various functional groups retained in composition of the reaction mixture in the co-crystals evolved. And also, the resultant **CH**$^+$ species did form *hetero* assemblies with complimentary ligands, as observed in the complexes of the 1:1 assemblies of cytosine and aliphatic dicarboxylic acids, rather than yielding **C.CH**$^+$. Hence, further experiments have been carried out by changing the composition of the reaction mixture, by dissolving cytosine and aromatic compounds in a 2:1 ratio. The additional structural features of the obtained complexes are discussed below.

3.3.4 Cytosine and 3,5-dinitro-4-methylbenzoic acid, CDMP22

Co-crystallization of cytosine and 3,5-dinitro-4-methybenzoic acid, in 2:1 molecular ratio, gave single crystals, from a CH_3OH solution. Analysis by X-ray diffraction methods reveals that the components are in 2:2 ratio, with one hydrogen transferred from one of the acid molecules is being shared by two cytosine molecules. Further, the cytosinium molecules undergo dimerisation to form **C.CH**$^+$ duplexes. The packing of molecules in three-dimensional arrangement is in the form of sheets, as

shown in Figure 3.41(a). Interestingly, the adjacent cytosinium duplexes are held together by centrosymmetric N-H···O hydrogen bonds, yielding molecular tapes, with acid molecules being stuffed, as dimers, in between the tapes, as shown in Figure 3.41(b).

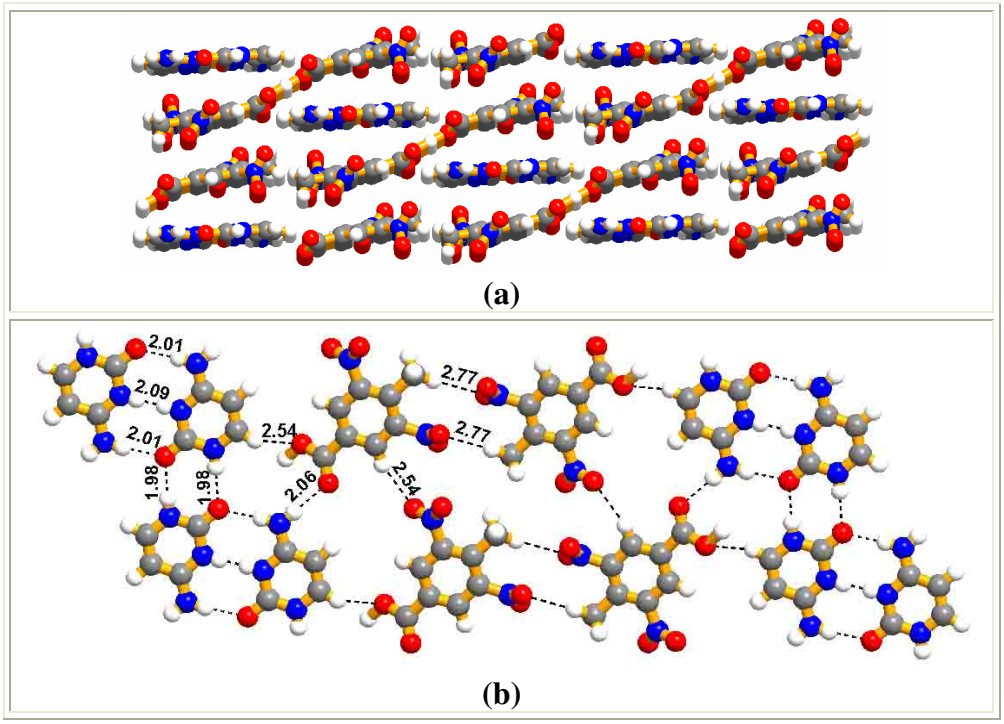

Figure 3.41. (a) Pictorial representation of the arrangement of molecules in three-dimension and (b) Sheet-like arrangement of cytosine duplexes and acid molecules in two-dimension.

3.3.5 Cytosine and 5-sulphosalicylic acid, CSUL21

Cytosine and 5-sulphosalicylic acid form a molecular complex in a 2:1 ratio along with a water molecule, from a 2:1 reaction mixture in methanol. Contents of asymmetric unit are shown in Figure 3.42.

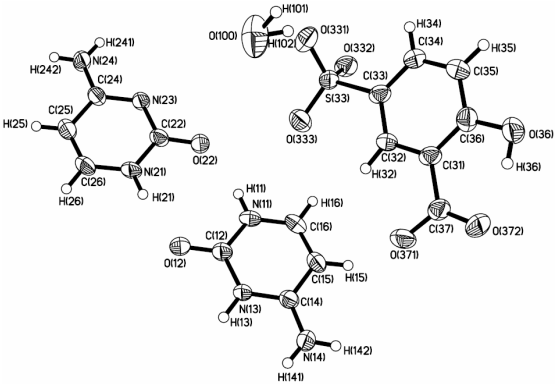

Figure 3.42. ORTEP (50% probability level) of the molecular complex of CSUL21

As observed in 1:1 complex (CSUL11), an intramolecular O-H···O (H···O, 1.80 Å) hydrogen bond is formed between –OH and –COOH groups, and -SO_3H group transfers its proton to one of the cytosine molecules, thus forming cytosinium. The molecules in the crystal lattice are arranged in stacked layers, as shown in Figure 3.43.

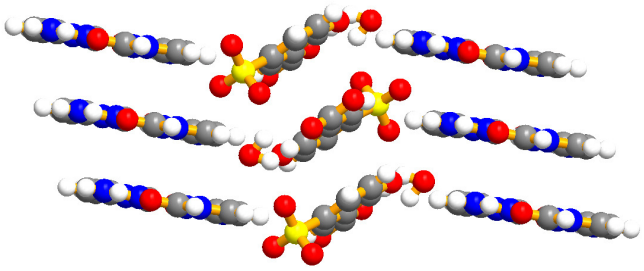

Figure 3.43. View of the arrangement of molecules in three-dimension.

In a typical layer, as shown in Figure 3.44, the arrangement of molecules is such that CH^+ moiety form *homomeric* interactions with cytosine yielding **C.CH$^+$**, that can be attributed to the cytosine excess environment, as observed in the similar complexes described above. Further, such cytosinium duplexes are held together by centrosymmetric N-H···O hydrogen bonds, with a H···O distance of 2.02 Å, constituting one-dimensional tapes of cytosinium molecules. In between such tapes, chains of acid

molecules as well as water molecules are embedded, which interact with cytosinium duplexes through different C-H···O (H···O, 2.67, 2.88 Å) hydrogen bonds, as shown in Figure 3.44.Within the chains, the acid molecules aggregates through the interaction formed between –COOH and SO_3^- group. In addition, a C-H···O (H···O, 2.69 Å) hydrogen bond is also present.

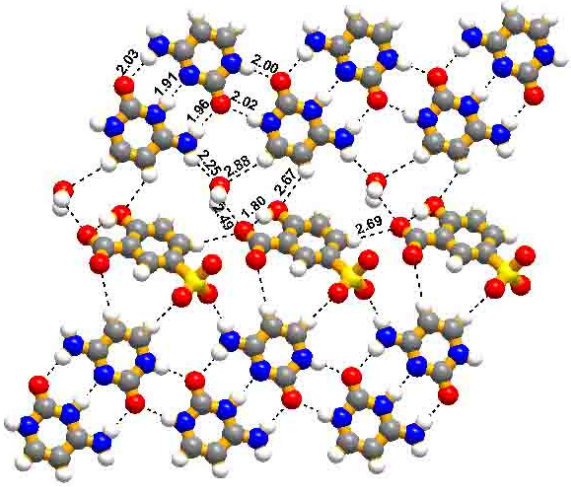

Figure 3.44. Arrangement of molecules in CSUL21 complex, forming sheet-like structure in two-dimension.

3.3.6 Cytosine and 2,6-dinitrophenol, CDNP21

In asymmetric unit of CDNP21, cytosine and phenol molecules are present in a 2:1 ratio and also proton transfer occurs between –OH and cytosine, as observed in the corresponding 1:1 ratio complex (see Figure 3.45(a)). In two-dimensional arrangement, packing of molecules is very much similar to the arrangement observed in CDNP22 and CSUL21. Thus, cytosinium duplexes are held together by centrosymmetric N-H···O (H···O, 1.95 Å) hydrogen bonds, yielding molecular tapes. Between such tapes, the phenolate molecules, in the form of dimers being formed

through C-H···O (H···O, 2.82 Å) hydrogen bonds, are intercalated, as shown in Figure 3.45(b).

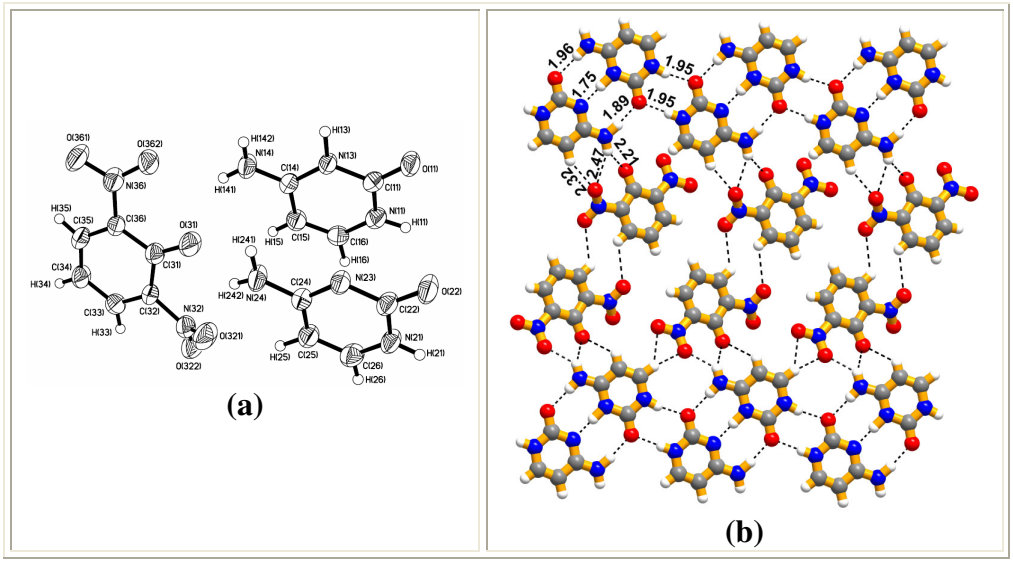

Figure 3.45. (a) ORTEP (50% probability level) of the 2:1 molecular complex of cytosine and 2,6-dinitrophenol. (Note that two molecules of cytosine and one phenol are present in asymmetric unit.) (b) Arrangement of molecules in the adduct CDNP21, forming a sheet-like structure.

Such a distinct dependence of molecular ratio towards formation of specific molecular complexes, indeed, would be a great advantage with versatile applications in pharmaceutical industry, in particular, in the process of controlled drug delivery, formulation etc. In order to develop such protocols, co-crystallization experiments with drug molecules (often referred as active pharmaceutical ingredients (API's)), placebo materials (additives, often salt makers like halides, saccharides, etc., used to make the API's to strengthen the physical properties like mechanical strength) would be of great importance. Hence, co-crystallization of cytosine with different slat formers, like mineral acids, and saccharine have been carried out. Thus, 2:1 complexes

formed between cytosine and different aromatic compounds show different structural features than 1:1 complexes, especially demonstrating the propensity of **CH^+** to form **$C.CH^+$** in the excess cytosine environment.

3.3.7 Cytosine with hydrochloric acid (CHCL11)[21] and hydrobromic acid (CHBR11)

The asymmetric unit of co-crystals of 1:1 ratio of cytosine with hydrochloric acid and hydrobromic acid are shown in Figure 3.46.

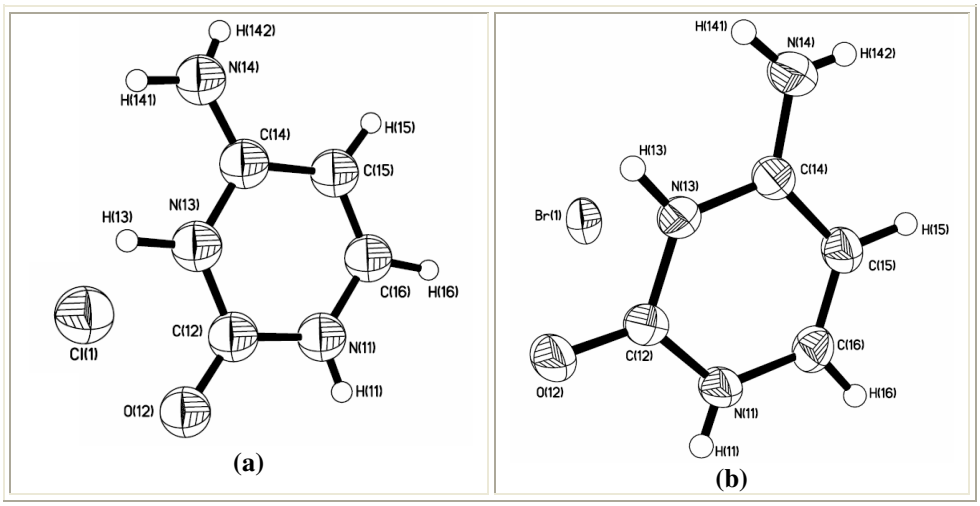

Figure 3.46. ORTEPs (50% probability level) of the 1:1 molecular complexes of (a) CHCL11 and (b) CHBR11.

As expected, cytosinium is formed with the aid of H^+ form HCl. In the crystal lattice, the cytosinium and counter anion, Cl^- are packed to form layers, as shown in Figure 3.47. Within a layer, cytosinium molecules are aggregated by C-H···O (H···O, 2.40 Å) hydrogen bonds forming chains. The chains are further stabilized by a variety of C-H···Cl^- hydrogen bonds formed with Cl^-. Halogen mediated hydrogen bonds play significant role in the structure stabilization, as reviewed, recently, by Orpen and co-

workers.[22] The distances of intermolecular interactions are shown in Figure 3.47 and full characteristic hydrogen bonds are given in Table 3.2.

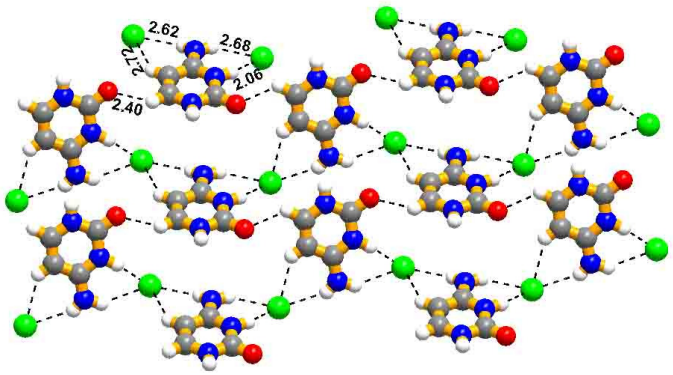

Figure 3.47. Interactions formed between the molecules in 1:1 adduct of CHCL11

A noteworthy point is that, as observed in the earlier examples, in CHCL11 also, **C.CH**$^{+}$ species are not formed. Interestingly, replacing HCl by HBr, the obtained 1:1 molecular complex, CHBR11 is found to be isostructural (see Figure 3.48) with CHCL11, in all respects, except for the change of halide ion. Hence, for the reasons discussed in the earlier section, 2:1 complexes of cytosine with HCl and HBr have been carried out.

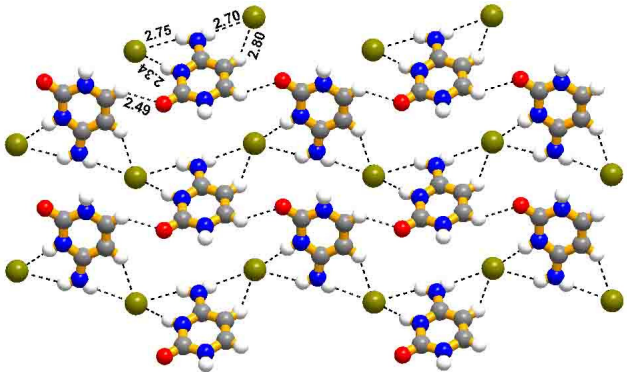

Figure 3.48. Interactions existing between the molecules in 1:1 adduct of CHBR11, an isostructural complex (see Figure 3.47) with CHCL11.

3.3.8 Cytosine and hydrochloric acid 2:1 complex, CHCL21

Structure analysis of data obtained for the single crystals, grown from a 2:1 mixture of cytosine and HCl, indeed, show that, the complex CHCL21 has asymmetric with the reactants in a 2:1 ratio. Further, one of the cytosine converts to cytosinium with the proton obtained from HCl. The **CH^+**, thus, formed interacts with cytosine yielding **$C.CH^+$**, as shown in Figure 3.49, demonstrating the importance of specific composition, in particular, cytosine excess, to form **$C.CH^+$** species. Adjacent duplexes are bridged by Cl^- ions through N-H···Cl^- (H···Cl^-, 2.09 and 2.29 Å) and C-H···Cl^- (H···Cl^-, 2.79 Å) interactions, as shown in Figure 3.49.

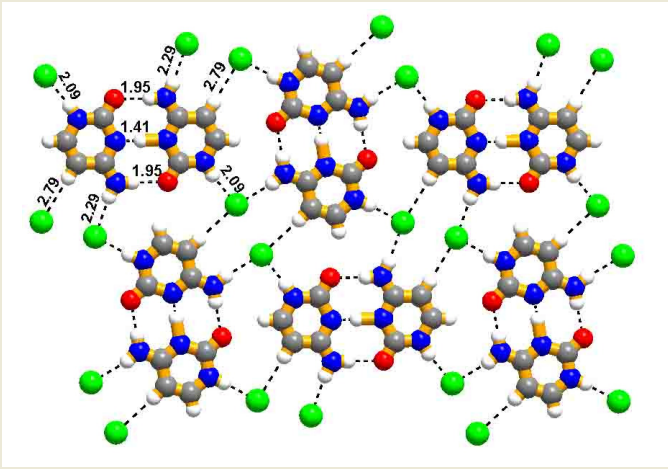

Figure 3.49. Two-dimensional arrangement and interactions between the molecules in the adduct CHCL21.

3.3.9 Cytosine and hydrobromic acid 2:1 complex, CHBR21

X-ray diffraction studies on the single crystals of CHBR21, obtained from water, by co-crystallization of cytosine and HBr in a 2:1 ratio, revealed the retention of molar ratios along with one water molecule. ORTEP diagram of contents of the

asymmetric unit is shown in Figure 3.50(a). The complex CHBR21 forms stacked sheets structure, in three-dimensions, as shown in Figure 3.50(b).

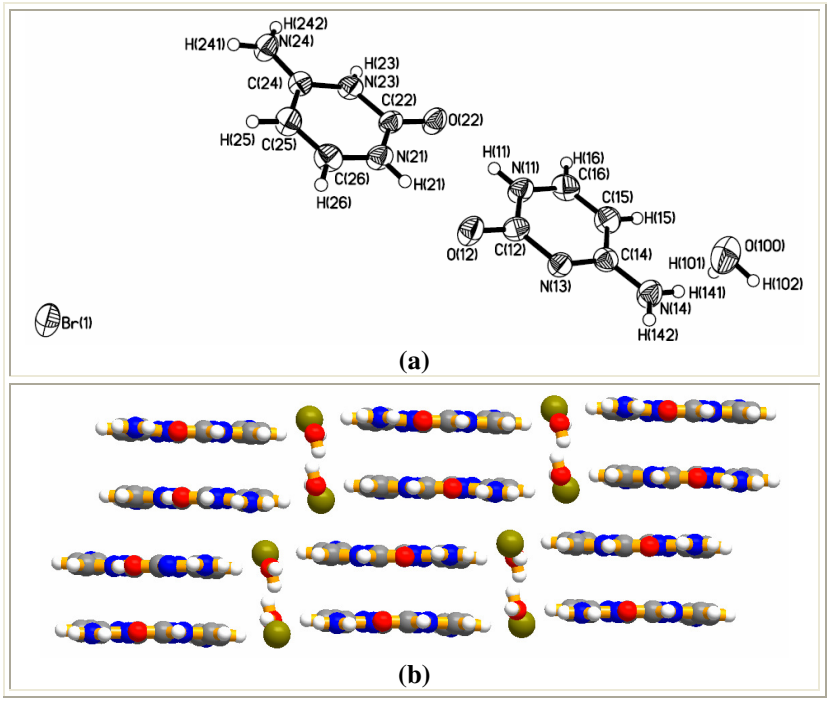

Figure 3.50. (a) ORTEP (50% probability level) of the 2:1 molecular complex CHBR21, of cytosine and hydrobromic acid, (b) Arrangement of molecules in two-dimension forming sheet-like structure.

In a typical layer, cytosinium duplexes are stabilized through cyclic N-H···O (H···O 1.95 and 1.99 Å) hydrogen bonds, forming molecular tapes. Such adjacent tapes are further held together by water and Br^- through different type of interactions like N-H···Br^-, O-H···Br^-, C-H···O, N-H···O in two-dimensional arrangement (see Figure 3.51). All the intermolecular interactions are annotated in Figure 3.51 and complete characteristics are listed in Table 3.2.

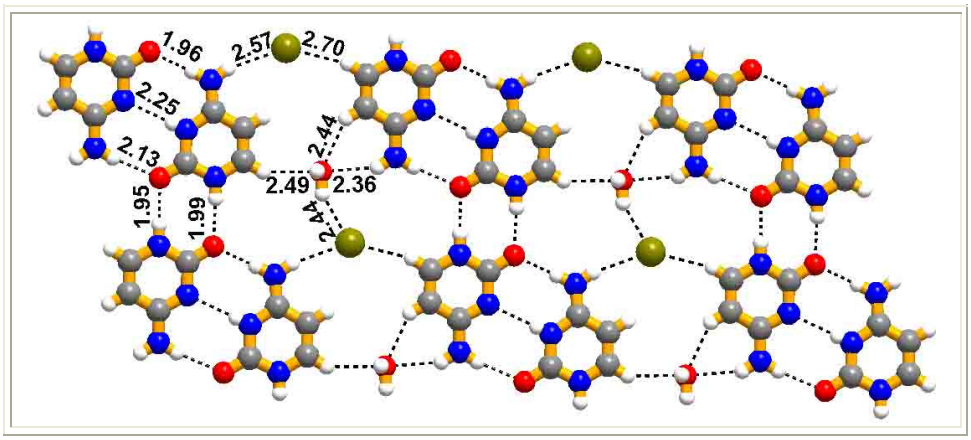

Figure 3.51. Stacked sheet arrangement in three-dimension.

The successful endeavors with the mineral acids in the formation of different types of complexes with varied composition of the reactants, co-crystallization of cytosine and saccharin (another well known salt former) in the formulation process of drugs, has been carried out, as described below.

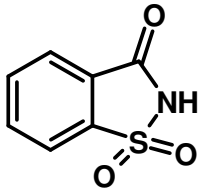

Saccharin

3.3.10 Cytosine and saccharin, CSAC11

Co-crystallization of cytosine and saccharin, in 1:1 molar ratio, from a ethanol solution, yielded crystals suitable for structure determination by X-ray diffraction methods. The contents of the asymmetric unit are shown in Figure 3.52, which confirms the formation of 1:1 complex, thus, retaining the composition of the reaction mixture.

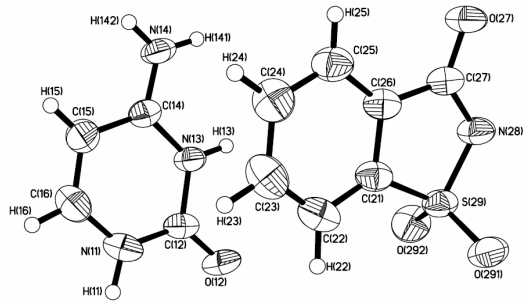

Figure 3.52. ORTEP (50% probability level) of the adduct CSAC11.

Cytosine is converted into cytosinium ion and interacts with saccharine as shown in Figure 3.53(a), through, N-H···N$^-$ (H···N, 1.96 Å) and N$^+$-H···O (H···O, 1.88 Å) hydrogen bonds. Such aggregates are, further, held together in two-dimensional arrangement through N-H···O (H···O, 2.01 and 1.89 Å) hydrogen bond, as shown in Figure 3.53(b).

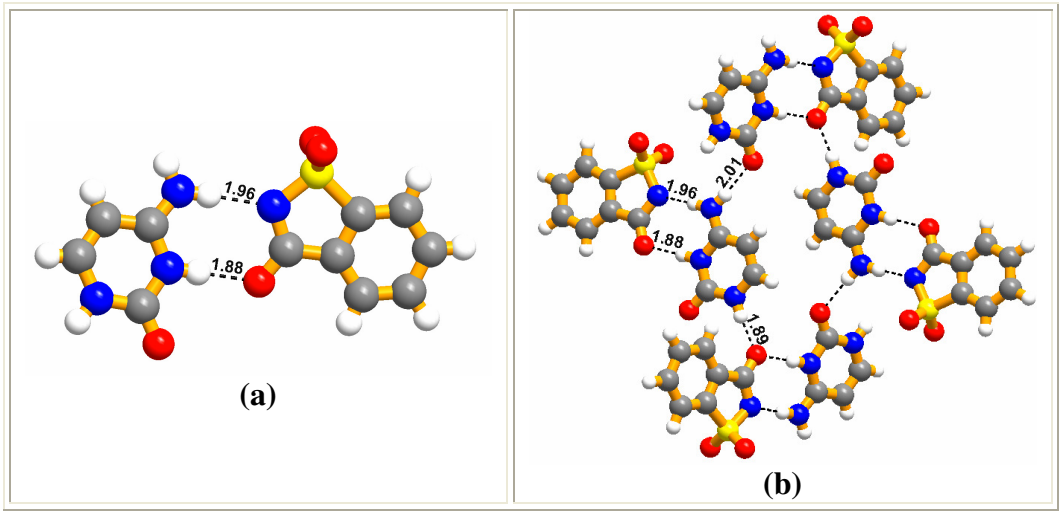

Figure 3.53. (a) Basic recognition pattern formed between cytosine and saccharin molecules in CSAC11 and (b) hexagonal arrangement of saccharin and cytosine molecules in CSAC11.

3.3.11 Saccharin 2:1 complex, CSAC21

Following the same strategy applied for the preparation of 2:1 complexes as described in the earlier sections, co-crystallization of cytosine and saccharin in a 2:1 ratio has been carried out. In the asymmetric unit of CSAC21, water molecule is also present along with a 2:1 ratio of the reactants, as shown in Figure 3.54(a).

Cytosine forms **CH**$^{+}$ with the proton transferred from saccharin and it further interacts with cytosine to yield **C.CH**$^{+}$ species. Thus, saccharin also has shown ability to form different assemblies with the varied composition of the reaction mixtures. The duplexes are further connected to each other through cyclic N-H···O hydrogen bonds, similar to the feature observed in the complexes formed by aromatic compounds with cytosine, as described in Chapter 2 (section 2.2.5). Further, the molecular tapes of cytosinium duplexes are connected to each other through saccharin and water molecule, as shown in Figure 3.54(b), by different types of N-H···O and C-H···O hydrogen bonds.

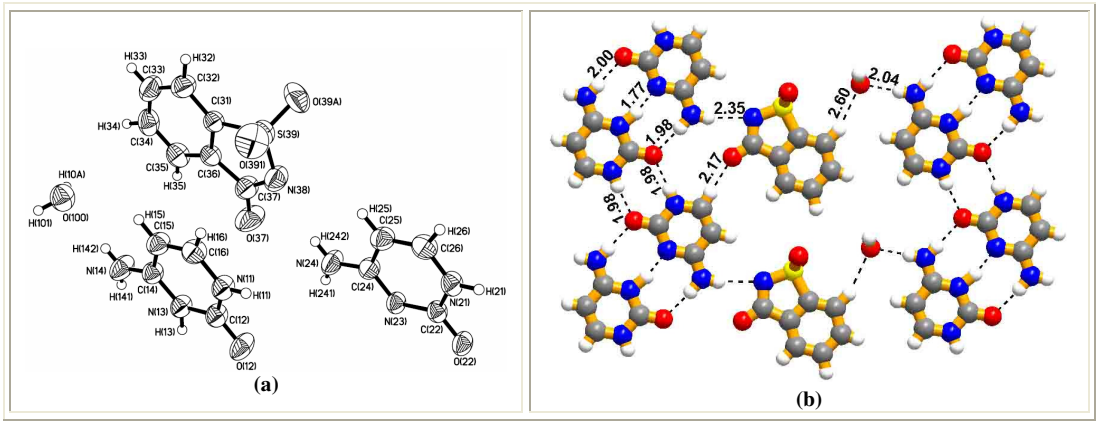

Figure 3.54. (a) ORTEP of the asymmetric unit of CSCA21 and (b) two-dimensional arrangement of molecules in the crystal structure of cytosine and saccharin adduct, CSCA21.

Observing the ability of salt formers to give different molecular complexes with cytosine, these salt formers have been further employed to co-crystallize with cytosine based drug molecules, for example halocytosines. In this respect, since 5-fluorocytosine is well know as an antifungal drug,[23] co-crystallization of it with HCl, HBr and saccharin in varied composition have been carried out and the obtained results are as given below and the experimental details are shown in Scheme 3.5.

3.4 Preparation of salts of 5-fluorocytosine, FC

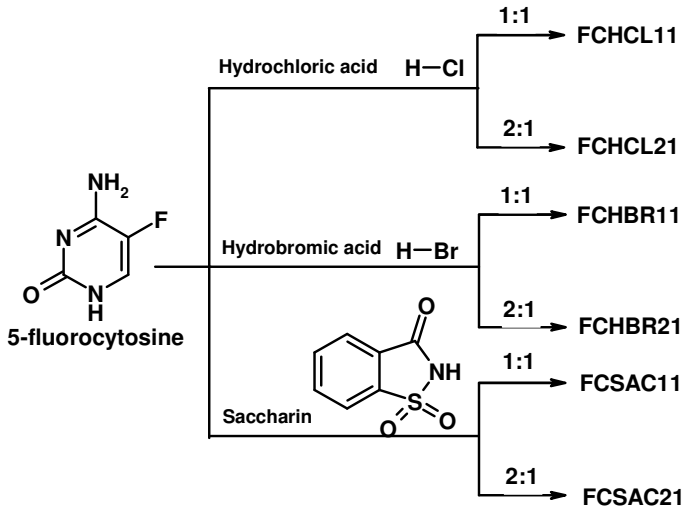

Scheme 3.5

3.4.1 5-fluorocytosine and hydrochloric acid, FCHCL11 and FCHCL21

5-fluorcytosine (**FC**) and hydrochloric acid (HCl), in a 1:1 and 2:1 ratios, were grown, by co-crystallizing **FC** and HCl in the required compositions. The structure determination reveals that hydrated salts are formed from both 1:1 and 2:1 compositions and the complexes have been labeled as FCHCL11 and FCHCL21,

respectively. Further, it reveals that, in both the complexes, composition of the reaction mixture is retained in the asymmetric units, as shown in Figure 3.55.

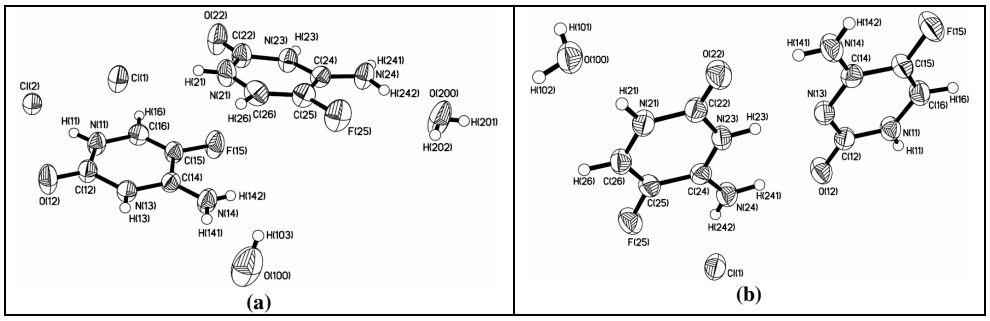

Figure 3.55. ORTEP (50% probability level) of the molecular complexes (a) FCHCL11 and (b) FCHCL21.

Further, cytosine form **FCH$^+$** species with the H^+ provided by HCl. While in FCHCL11, the fluorocytosinium molecules form chains, through C-H$^{\cdots}$O hydrogen bonds, with H$^{\cdots}$O distance of 2.32 Å, as observed in 1:1 complex of cytosine and HCl. Further, the adjacent chains are bridged by Cl^- and H_2O molecules, which are arranged alternately in a columnar pattern. Thus, in FCHCL11 also, Cl^- interact with **FCH$^+$** through N-H$^{\cdots}$$Cl^-$ and H_2O molecules through N-H$^{\cdots}$O and O-H$^{\cdots}$O hydrogen bonds. However, in FCHCL21, the **FCH$^+$** form duplexes known for the 2:1 complexes, as shown in Figure 3.56(b). The adjacent duplexes are further held together by N-H$^{\cdots}$O (H$^{\cdots}$O, 1.95 Å) hydrogen bonds, as shown in Figure 3.56(b).

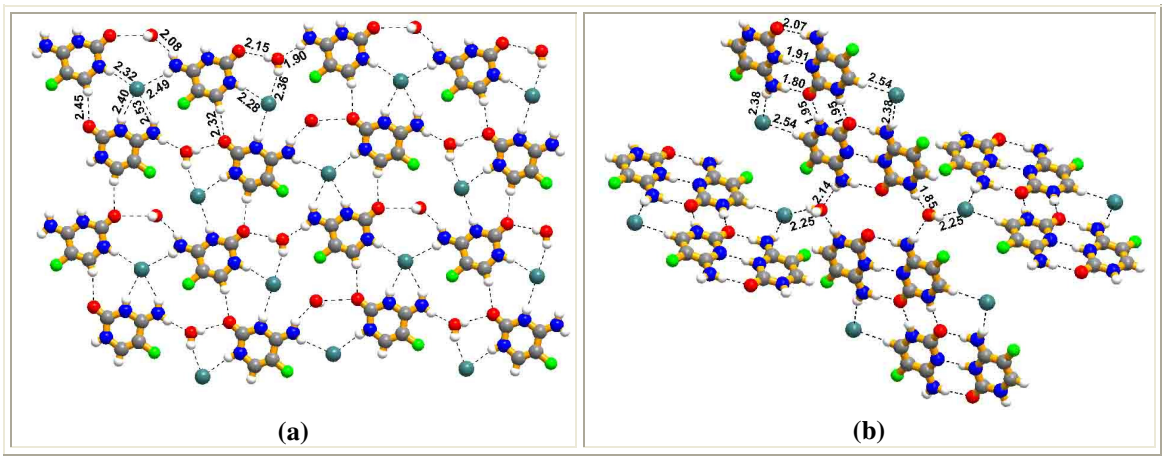

Figure 3.56. Representation of the intermolecular interactions existing in the salts (a) FCHCL11 and (b) FCHCL21.

Thus, we have observed variant structures, even for drug molecule, **FC**, by simply changing its composition, while co-crystallizing with salt formers. The concept is further strengthened with similar observation made with HBr as described below.

3.4.2 Complexes of 5-fluorocytosine and hydrobromic acid, FCHBR11 and FCHBR21

As observed in FCHCL11 and FCHCL21, in the complexes of FCHBR11 and FCHBR21 also, obtained by co-crystallization of **FC** and HBr in 1:1 and 2:1 ratios, respectively, the composition in the crystal structures is as same as the reaction mixtures. Also, **FC** molecules are converted to $\mathbf{FCH^+}$ with the protons obtained from HBr. While molecules pack in the crystal lattice by interactions established between $\mathbf{FCH^+}$ and Br^- in FCHBR11, in the complex FCHBR21, the interaction was through the formation of $\mathbf{FC.FCH^+}$, as shown in Figure 3.57(a) and Figure 3.57(b), respectively.

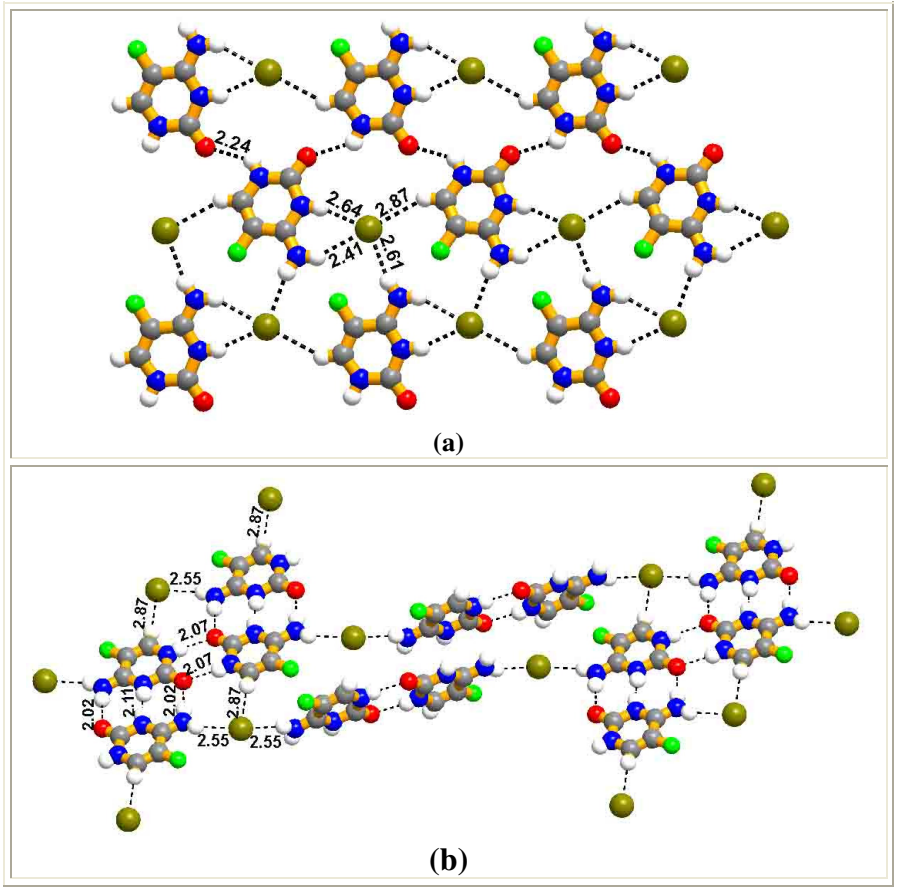

Figure 3.57. Arrangement of molecules in the salts (a) FCHBR11 and (b) FCHBR21.

In FCHCR11, **FCH**$^{+}$ molecules form chains in one-dimensional arrangement, by interacting with Br^{-} and forms N-H$^{\cdots}Br^{-}$ and C-H$^{\cdots}Br^{-}$ interactions (see Figure 3.57(a)). Further, those chains are held together through N-H$^{\cdots}$O hydrogen bonds. However, in FCHBR21, the duplexes are held together by cyclic N-H$^{\cdots}$O (H$^{\cdots}$O, 2.07 Å) hydrogen bonds, which are further held together by Br^{-} (see Figure 3.57(b)).

3.4.3 5-Fluorocytosine and saccharin complexes, FCSAC11 and FCSAC21

5-fluorocytosine and saccharine, in a 1:1 and 2:1 molar ratios, gave good quality crystals. Structure determination reveals that the composition of the reactants

in FCSAC11 and FCSAC21 are in 1:1 and 2:1, respectively. ORTEP diagram of asymmetric units are shown in Figure 3.58(a) and Figure 3.58(b).

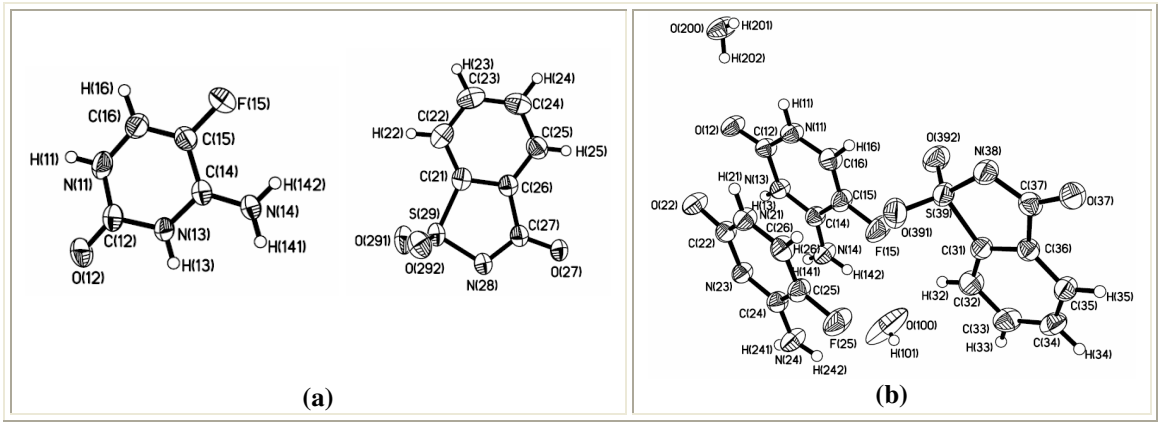

Figure 3.58. ORTEP (50% probability level) of the molecular adducts (a) FCSAC11 and (b) FCSAC21.

As expected, in both the complexes, **FCH**$^{+}$ moieties are formed and it interacts with saccharinates by N-H$^{\cdots}$N^{-} and N^{+}-H$^{\cdots}$O hydrogen bonds, as observed in CSAC11. Thus, the adjacent binary units are held together by N-H$^{\cdots}$O hydrogen bonds, as shown in Figure 3.59.

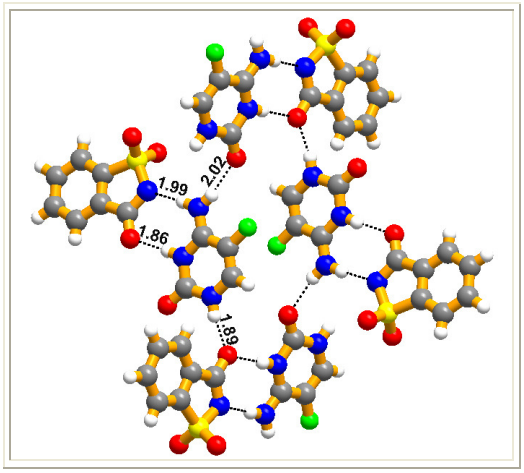

Figure 3.59. Arrangement of saccharin and 5-fluorocytosine molecules in 1:1 co-crystals.

However, in the 2:1 crystals, apart from the observation of exotic duplexes formed by 5-fluorocytosine, the packing of molecules in two-dimensional arrangement is quite intriguing, as shown in Figure 3.60.

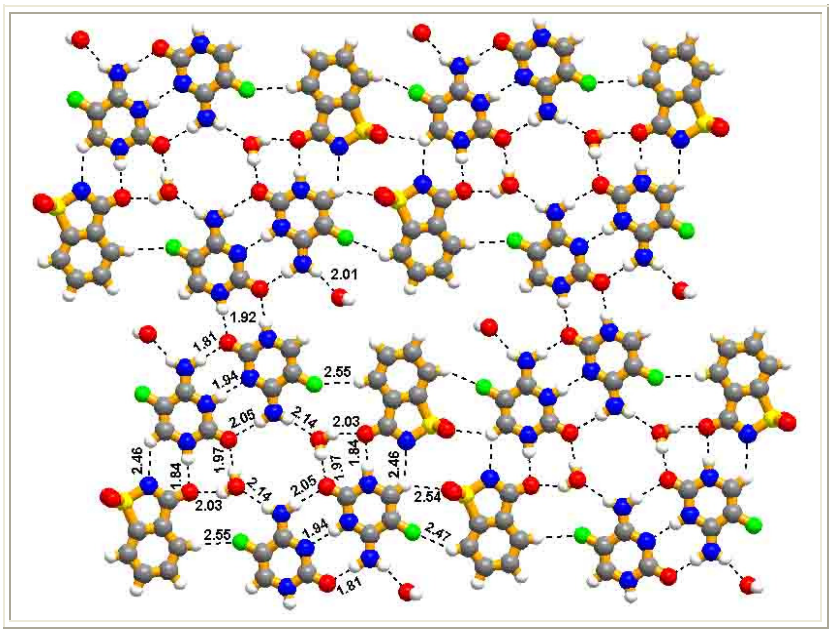

Figure 3.60. Hexagonal arrangement in the 2:1 5-fluorocytosine - saccharin adduct with void spaces being filled by water molecules.

Each duplex interacts with saccharin molecules through cyclic hydrogen bonding pattern comprising of N-H···O (H···O, 1.84 Å) and C-H···N (H···N, 2.46 Å) hydrogen bonds, which are, further, held together by C-H···F (H···F, 2.55 Å) hydrogen bonds, forming a hexagonal network with void space, which is being occupied by water molecules. The adjacent hexagons, in turn, are held together by C-H···F and C-H···O hydrogen bonds constituting one-dimensional columnar moiety. In two-dimensional arrangement, the columnar units are connected to each other through centrosymmetric N-H···O hydrogen bonding formed between the duplexes of 5-flurocytosine molecules. As a result, further, another void space is being created,

which is being occupied by other water molecules present in the crystal lattice, which are connected to 5-fluorocytosine by O-H···O hydrogen bonds with an H···O distance of 2.01 Å. Thus, FCSAC21 complex is not only been excellence to highlight the pharmaceutical co-crystallization, but also have exotic host-guest features, which may further be useful for several other application studies.

3.5 Conclusions

In conclusion, this study has demonstrated the feasibility of formation of **C.CH$^+$** duplexes, through molecular recognition process between **CH$^+$** and cytosine in excess cytosine environment, and its significance in the formation of different structural arrangements like in different forms like sheet like structures, simple ladders, etc., in the ultimate supramolecular assemblies. Further, it has been demonstrated that the importance of cytosine rich environment even in the supramolecular synthesis in comparison with the macromolecular structures as 2:1 complexes only gave the desired **C.CH$^+$** duplexes, while 1:1 complexes did not. In all the 1:1 complexes proton from acid molecules is transferred to N^3 atom of cytosine, which further undergo *heteromeric* interactions with other ligands used for co-crystallization. According to our best of the knowledge, this is the first study towards the understanding of duplex conditions. The duplex formation is demonstrated with aliphatic carboxylic acids, aromatic compounds with various functional groups, saccharin and mineral acids etc. Since **C.CH$^+$** duplexes are observed in four stranded DNA structures in the form of *i*-motifs, understanding of these interactions through model systems may be important towards understanding biological relevance and also

to find various applications. Towards the applications, a distinct variations in the structural features with the change of composition of cytosine has been demonstrated to form different types of assemblies for one of the well known pharmaceutical compounds, 5-fluorocytosine (antifungal drug). It may provide opportunity to use such co-crystals for further bio-active studies in the directions of controlled drug delivery and bioavailability etc.

3.6 Experimental section

All the chemicals used in this study were obtained commercially and used as such without any further purification. HPLC grade solvents were used for carrying out experiments. The synthesis of molecular complexes was carried out, by dissolving the reactants in the appropriate solvents either at room temperature or by warming on a water bath and subsequently cooling by a slow-evaporation method. Some of the typical examples are discussed herein.

COX21 adduct was prepared by dissolving 111 mg (1 mmol) of cytosine and 63 mg (0.5 mmol) of oxalic acid, in a methanol solution, on water bath and then subsequently cooled to room temperature. Colorless rectangular block shaped single crystals of good quality were obtained over a period of one week and were used for X-ray diffraction studies.

CHCL21 adduct was prepared by dissolving CHCL11 adduct (173.5 mg, 0.5 mmol) and cytosine (56 mg, 0.5 mmol) in DMF. Slow evaporation of solvent gave good quality single crystals suitable for X-ray diffraction.

FCHCL11 adduct was prepared by dissolving 13 mg (0.1 mmol) of 5-fluorocytosine in concentrated hydrochloric acid solution. Slow evaporation of solvent gave good quality single crystals suitable for X-ray diffraction.

FCHCL21 adduct was prepared by dissolving FCHCL11 adduct (0.10 mmol of 5-fluorocytosine in concentrated HCl) and 5-fluorocytosine (13 mg, 0.5 mmol) in water. Slow evaporation of solvent gave good quality single crystals suitable for X-ray diffraction.

3.7 Crystal structure determination

Good quality single crystals of all complexes, grown as described above were carefully chosen with the aid of polarized optical microscope and glued to glass fiber to mount on the X-ray diffractometer goniometer, equipped with CCD area detector. The data collection proceeded without any complication and processed using the Bruker suite of software. The structures were determined and refined using SHLEXTL suite of programmes and absorption corrections were made on all the crystals using SADABS. All the non-hydrogen atoms were refined anisotropically. The hydrogen atom positions were taken from a difference Fourier maps and were refined isotropically. The structural parameters were given in Tables 4.1 and 4.2. All the intra and intermolecular distances were computed using PLATON software. The packing drawings were generated either by XP package of SHELXTL or diamond software.

Table 3.1

	COX21	**CMA11**	**CMA21**	**CSU11**
Empirical formula	$C_9H_{14}N_6O_5$	$C_7H_9N_3O_5$	$C_{11}H_{10}N_6O_6$	$C_8H_{11}N_3O_5$
Formula wt.	286.26	215.17	322.25	229.20
Crystal system	Monoclinic	Triclinic	Triclinic	Monoclinic
Space group	$P2_1/c$	$P\bar{1}$	$P\bar{1}$	$C2/c$
T [K]	298	298	298	298
a [Å]	6.447(3)	8.315(2)	8.819(4)	15.717(2)
b [Å]	15.020(6)	11.853(2)	8.952(4)	6.712(1)
c [Å]	12.487(5)	14.964(3)	9.086(4)	18.711(3)
α [°]	90.00	79.180(1)	95.830(7)	90.00
β [°]	102.03(1)	76.690(1)	96.210(7)	100.58(1)
γ [°]	90.00	76.820(1)	98.867(7)	90.00
Z	4	6	2	8
Volume [Å^3]	1182.6(9)	1383.1(5)	699.5(5)	1940.3(5)
D_{calc} [g/cm^3]	1.608	1.550	1.530	1.569
F (000)	600	672	332	960
μ [mm^{-1}]	0.133	0.133	0.127	0.132
$2\theta_{max.}$	4.30 – 50.66	2.82 – 50.56	4.54 – 50.54	4.42 – 50.54
Range h	-7 to 7	-9 to 9	-10 to 10	-18 to 18
Range k	-17 to 18	-14 to 14	-10 to 10	-8 to 8
Range l	-15 to 14	-17 to 17	-10 to 10	-22 to 22
N-total	8373	13797	5143	6835
N-independent	2147	5005	2519	1760
N-observed	1584	1501	1845	1273
R_1 [I>2σ(I)]	0.0535	0.0376	0.2064	0.0403
wR_2	0.1361	0.0680	0.6063	0.1059
GOF	1.018	0.653	3.982	0.973

Continued...

	CSU21	**CFU11**	**CFU21**	**CMAL21**
Empirical formula	$C_{12}H_{16}N_6O_6$	$C_8H_9N_3O_5$	$C_{12}H_{12}N_6O_6$	$C_{12}H_{14}N_6O_6$
Formula wt.	340.31	227.18	336.28	338.29
Crystal system	Triclinic	Monoclinic	Triclinic	Monoclinic
Space group	$P\bar{1}$	$P2_1/c$	$P\bar{1}$	$C2/c$
T [K]	298	298	298	298
a [Å]	3.829(1)	8.590(2)	3.778(1)	27.376(1)
b [Å]	6.526(2)	13.125(3)	6.506(2)	7.375(4)
c [Å]	14.290(4)	8.765(2)	14.252(4)	14.748(7)
α [°]	90.56(1)	90.00	89.61(1)	90.00
β [°]	91.77(1)	98.96(1)	88.51(1)	94.12(1)
γ [°]	92.79(1)	90.00	87.35(1)	90.00
Z	1	4	1	8
Volume [Å^3]	356.5(2)	976.1(4)	349.9(2)	2970(3)
D_{calc} [g/cm^3]	1.585	1.546	1.596	1.513
F (000)	178	472	174	1408
μ [mm^{-1}]	0.129	0.131	0.131	0.124
$2\theta_{max.}$	2.86 – 50.54	4.80 – 50.54	2.86 – 50.54	5.54 – 50.64
Range h	-4 to 4	-10 to10	-4 to 4	-32 to 32
Range k	-7 to 7	-15 to15	-7 to 7	-8 to 8
Range l	-17 to 17	-10 to 10	-17 to 17	-17 to 17
N-total	3499	9174	3081	13552
N-independent	1294	1771	1271	2693
N-observed	1005	1706	611	1206
R_1 [I>2σ(I)]	0.0484	0.0336	0.2105	0.0653
wR_2	0.1233	0.0902	0.4763	0.1825
GOF	1.095	1.078	1.881	0.881

Continued...

	CAC11	**CAC21**	**CAD21**	**CDMB11**
Empirical formula	$C_6H_6N_3O_3$	$C_{10}H_{13}N_6O_5$	$C_{14}H_{20}N_6O_6$	$C_{12}H_{11}N_5O_7$
Formula wt.	168.14	297.26	368.36	337.26
Crystal system	Monoclinic	Triclinic	Triclinic	Orthorhombic
Space group	$P2_1/n$	$P\bar{1}$	$P\bar{1}$	$Pbca$
T [K]	298	298	298	298
a [Å]	6.946(7)	6.779(1)	5.315(1)	12.937(2)
b [Å]	9.759(1)	7.438(1)	10.100(1)	7.599(1)
c [Å]	10.537(1)	13.828(2)	16.313(2)	28.304(4)
α [°]	90.00	79.63(1)	74.48(1)	90.00
β [°]	99.27(2)	77.90(1)	83.97(1)	90.00
γ [°]	90.00	73.94(1)	81.01(1)	90.00
Z	4	2	2	8
Volume [Å^3]	704.9(1)	649.6(2)	831.6(2)	2782.5(7)
D_{calc} [g/cm^3]	1.584	1.520	1.471	1.610
F (000)	348	310	388	1392
μ [mm^{-1}]	0.130	0.124	0.117	0.135
$2\theta_{max.}$	5.72 – 50.58	3.04 – 50.46	2.60 – 50.56	2.88 – 50.54
Range h	-7 to 8	-8 to 8	-6 to 6	-15 to 15
Range k	-11 to 11	-8 to 8	-12 to 12	-9 to 9
Range l	-12 to 12	-16 to 16	-19 to 19	-33 to 33
N-total	4172	6411	8063	19065
N-independent	1271	2334	3001	2521
N-observed	915	1276	2676	925
R_1 [I>2σ(I)]	0.0331	0.0599	0.0594	0.0456
wR_2	0.0823	0.1785	0.1754	0.1425
GOF	0.925	0.949	1.077	0.777

Continued...

	CDMB21	**CDNP11**	**CDNP21**	**CHCL21**
Empirical formula	$C_{24}H_{22}N_{10}O_{14}$	$C_{10}H_9N_5O_6$	$C_{14}H_{14}N_8O_7$	$C_8H_{11}Cl_2N_6O_2$
Formula wt.	674.52	295.22	406.33	294.13
Crystal system	Triclinic	Triclinic	Triclinic	Orthorhombic
Space group	$P\bar{1}$	$P\bar{1}$	$P\bar{1}$	*I*bam
T [K]	298	298	298	298
a [Å]	8.337(1)	9.068(2)	8.423(3)	15.295(2)
b [Å]	9.263(1)	9.865(2)	10.229(3)	12.497(2)
c [Å]	10.322(2)	13.410(3)	10.986(3)	6.369(1)
α [°]	67.27(1)	91.75(1)	64.45(1)	90.00
β [°]	83.58(1)	94.62(1)	82.50(1)	90.00
γ [°]	76.26(1)	93.84(1)	74.22(1)	90.00
Z	1	4	2	4
Volume [Å^3]	713.9(2)	1192.2(4)	821.7(4)	1217.5(3)
D_{calc} [g/cm^3]	1.569	1.645	1.642	1.605
F (000)	348	608	420	604
μ [mm^{-1}]	0.132	0.139	0.135	0.538
$2\theta_{max.}$	4.28 – 50.56	3.04 – 50.58	4.10 – 50.52	4.20 – 50.04
Range h	-9 to 10	-10 to10	-10 to 10	-18 to 17
Range k	-11 to 11	-11 to 11	-12 to 12	-14 to 14
Range l	-12 to 12	-16 to 16	-13 to 13	-7 to 7
N-total	6906	11705	7989	4180
N-independent	2570	4313	2962	598
N-observed	1991	2976	1334	563
R_1 [I>2σ(I)]	0.0460	0.0760	0.0494	0.1330
wR_2	0.1225	0.2084	0.1212	0.4465
GOF	0.971	0.991	0.822	4.124

Continued...

	CHBR11	**CHBR21**	**CSAC11**	**CSAC21**
Empirical formula	$C_4H_6Br_1N_3O_1$	$C_8H_{13}Br_1N_6O_3$	$C_{11}H_{10}N_4O_4S_1$	$C_{15}H_{17}N_7O_6S_1$
Formula wt.	192.03	321.15	294.29	423.42
Crystal system	Monoclinic	Monoclinic	Monoclinic	Monoclinic
Space group	$P2_1/n$	$C2/c$	$P2_1/n$	$P2_1/m$
T [K]	298	298	298	298
a [Å]	8.335(2)	23.444(4)	8.574(8)	8.389(3)
b [Å]	7.014(1)	8.488(1)	11.200(1)	6.538(2)
c [Å]	11.511(2)	13.370(2)	13.733(1)	16.884(5)
α [°]	90.00	90.00	90.00	90.00
β [°]	98.18(1)	110.79(1)	104.82(2)	93.14(1)
γ [°]	90.00	90.00	90.00	90.00
Z	4	8	4	2
Volume [Å^3]	666.1(2)	2487.2(7)	1275(2)	924.7(5)
D_{calc} [g/cm^3]	1.915	1.715	1.533	1.521
F (000)	376	1296	608	440
μ [mm^{-1}]	6.090	3.318	0.274	0.227
$2\theta_{max.}$	5.66 – 50.54	3.72 – 50.56	4.76 – 50.84	4.84 – 50.54
Range h	-9 to 9	-28 to 28	-10 to 10	-10 to 8
Range k	-8 to 8	-10 to 10	-11 to 13	-7 to 5
Range l	-13 to 13	-16 to 16	-16 to 12	-20 to 20
N-total	4609	11261	6244	4650
N-independent	1200	2246	2317	1827
N-observed	1015	1561	1956	1623
R_1 [I>2σ(I)]	0.0224	0.0315	0.0336	0.0488
wR_2	0.0543	0.0969	0.0977	0.1385
GOF	0.963	0.950	1.087	1.046

Continued...

	CSUL11	**CSUL21**	**FCHCL11**	**FCHCL21**
Empirical formula	$C_{11}H_{15}N_3O_9S_1$	$C_{15}H_{17}N_6O_9S_1$	$C_8H_{14}Cl_2F_2N_6O_4$	$C_8H_{11}Cl_1F_2N_6O_3$
Formula wt.	365.32	457.41	366.14	312.68
Crystal system	Monoclinic	Triclinic	Monoclinic	Monoclinic
Space group	*P*c	*P*$\bar{1}$	$P2_1/c$	$P2_1/n$
T [K]	298(2)	298	298	298(2)
a [Å]	9.386(3)	7.375(3)	9.823(9)	7.075(1)
b [Å]	8.583(3)	8.477(4)	12.559(1)	8.395(1)
c [Å]	12.909(3)	15.666(7)	13.093(1)	21.597(3)
α [°]	90.00	77.75(1)	90.00	90.00
β [°]	132.68(1)	83.271(1)	108.87(1)	92.669(2)
γ [°]	90.00	88.70(1)	90.00	90.00
Z	2	2	4	4
Volume [Å^3]	764.6(4)	950.5(8)	1528(2)	1281.4(3)
D_{calc} [g/cm^3]	1.587	1.598	1.591	1.621
F (000)	380	474	748	640
μ [mm^{-1}]	0.267	0.237	0.473	0.342
$2\theta_{max.}$	4.74 – 50.60	2.68 – 50.76	4.38 – 50.58	5.20 – 50.52
Range h	-11 to 11	-8 to 8	-11 to 11	-8 to 8
Range k	-10 to 10	-10 to 10	-15 to 15	-10 to 9
Range l	-14 to 15	-18 to 18	-15 to 15	-25 to 25
N-total	6656	9155	10316	8980
N-independent	2804	3425	2767	2321
N-observed	2696	2268	2455	2014
R_1 [I>2σ(I)]	0.0281	0.0826	0.0326	0.0364
wR_2	0.0737	0.2086	0.0922	0.1014
GOF	1.061	1.269	1.079	1.056

Continued...

	FCHBR11	**FCSAC11**	**FCHBR21**	**FCSAC21**
Empirical formula	$C_4H_5Br_1F_1N_3O_1$	$C_{11}H_9F_1N_4O_4S_1$	$C_8H_{10}Br_1F_2N_6O_2$	$C_{15}H_{16}F_2N_7O_7S_1$
Formula wt.	210.02	312.28	340.13	476.41
Crystal system	Monoclinic	Monoclinic	Monoclinic	Triclinic
Space group	*C*2/*c*	$P2_1/n$	*C*2/*c*	$P\bar{1}$
T [K]	298	298	298	298
a [Å]	16.008(3)	8.698(7)	15.800(3)	8.828(4)
b [Å]	11.369(3)	10.591(8)	5.117(8)	11.183(5)
c [Å]	9.174(2)	14.381(1)	15.040(2)	11.354(5)
α [°]	90.00	90.00	90.00	103.70(1)
β [°]	122.95(4)	107.14(1)	94.53(4)	109.35(1)
γ [°]	90.00	90.00	90.00	99.16(1)
Z	8	4	4	2
Volume [Å^3]	1401.0(5)	1265.9(16)	1212(3)	992.3(8)
D_{calc} [g/cm^3]	1.991	1.639	1.864	1.595
F (000)	816	640	676	490
μ [mm^{-1}]	5.820	0.292	3.426	0.238
$2\theta_{max.}$	4.70 – 50.56	4.86 – 50.72	5.08 – 50.60	3.88 – 50.62
Range h	-19 to 19	-10 to 10	-18 to 18	-10 to 10
Range k	-13 to 13	-11 to 12	-6 to 6	-13 to 13
Range l	-10 to 11	-17 to 17	-18 to 17	-13 to 13
N-total	4962	6246	5368	9368
N-independent	1270	2300	1086	3581
N-observed	911	1964	1014	3326
R_1 [I>2σ(I)]	0.0371	0.0316	0.0247	0.0431
wR_2	0.0959	0.0919	0.0669	0.1146
GOF	0.980	1.067	1.090	1.062

Continued...

Table 2.3. Characteristic hydrogen bonds (distances/Å and angles/º)[#]

D-H···A	COXA21			CMA11			CMA21			CSU11		
N-H···O	2.03	2.76	161	1.94	2.90	167	2.03	2.86	163	1.99	2.92	179
	1.76	2.75	174	1.96	2.81	161	1.90	2.75	167	1.58	2.60	174
	1.98	2.82	175	2.00	2.85	168	1.99	2.85	176	1.99	2.99	172
	2.30	3.06	154	1.72	2.74	154	2.11	2.96	169	2.00	2.82	152
	2.46	3.11	138	1.93	2.80	174	2.05	2.90	169			
	1.92	2.79	167	1.81	2.71	178	2.24	3.07	160			
	2.03	2.90	170	1.93	2.79	177						
				1.93	2.79	171						
				2.01	2.86	171						
				1.94	2.80	173						
				1.92	2.78	176						
				2.06	2.88	160						
N-H···N	2.15	2.83	176									
	2.09	2.80	177									
C-H···O	2.40	3.13	145	2.58	3.39	147	2.57	3.48	166	2.26	2.98	135
				2.42	3.29	146	2.49	3.35	155			
				2.60	3.43	149						
				2.46	3.33	154						
				2.45	3.35	152						
				2.45	3.35	152						
				2.41	3.24	143						
				2.53	3.44	156						
				2.43	3.14	130						
O-H···O	1.86	2.73	167	1.86	2.51	146						
	2.30	2.99	150	1.21	2.49	163				1.47	2.53	172
	2.38	2.97	135	1.82	2.52	140						

Continued...

D-H···A	CSU21			CFU11			CMAL21			CAC11			CAC21		
N-H···O	1.81	2.77	174	2.06	2.90	168	1.85	2.74	173	1.97	2.86	171	1.70	2.71	178
	1.90	2.84	176	1.81	2.69	175	1.73	2.77	167	1.72	2.68	176	1.86	2.69	164
	2.11	2.90	146	1.85	2.78	175	1.89	2.86	173	2.03	2.97	174	1.88	2.84	179
				1.91	2.77	165	2.02	2.84	152	2.05	2.94	161	2.03	2.90	149
							2.01	2.86	174				1.84	2.85	176
							2.07	2.86	153				2.01	2.90	153
N-H···N	2.01	2.84	178				1.47	2.84	175				1.51	2.83	175
C-H···O	2.59	3.47	157	2.58	3.56	171	2.40	3.31	176				2.36	3.29	173
	2.44	3.20	131				2.50	3.34	133				2.58	3.52	149
							2.36	3.35	168						
							2.49	3.20	126						
O-H···O	1.23	2.45	180	1.55	2.55	179	1.16	2.43	169				2.00	2.74	160
													1.98	2.77	167

Continued...

D-H···A	CAD21			CAD21			CDMP11			CDMP21			CSUL11		
N-H···O	1.96	2.92	161	1.97	2.83	166	1.97	2.82	168	1.97	2.83	176	2.00	2.8640	174
	1.97	2.87	172	1.89	2.76	172	1.92	2.75	161	2.00	2.87	170	1.94	2.7532	156
	1.97	2.82	177	1.92	2.78	175	1.96	2.81	170	2.07	2.93	178	2.47	3.0506	131
	2.21	3.02	159	2.04	2.87	160							1.97	2.8058	166
	2.06	2.87	178	1.96	2.95	175									
	1.94	2.86	173	2.14	3.01	166									
N-H···N	2.05	2.79	174	1.76	2.84	179				2.09	2.85	178			
	2.13	2.85	175												
C-H···O	2.42	3.09	132	2.48	3.38	168	2.27	3.09	146	2.54	3.50	163			
	2.43	3.14	130	2.30	3.20	160	2.58	3.44	149	2.54	3.30	137			
	2.28	3.07	135	2.55	3.20	122	2.35	3.00	124	2.58	3.42	148			
	2.59	3.34	137												
O-H···O	1.24	2.48	180	1.58	2.65	172				1.22	2.44	180	1.87	2.6268	143
	1.23	2.45	180	1.83	2.85	166							2.44	3.0695	129
				2.42	2.90	124							2.10	2.8304	160
													2.13	2.9016	155
													1.97	2.7707	166
													2.09	2.8141	167
													1.85	2.6737	161

Continued...

D-H···A	CSUL21			CDNP11			CDNP21			CSAC11			CSAC21		
N-H···O	2.02	2.87	169	1.97	2.85	162	1.96	2.83	169	1.89	2.79	174	1.98	2.79	176
	2.00	2.85	171	1.92	2.63	150	1.95	2.81	179	1.88	2.79	179	1.98	2.79	177
	1.96	2.82	175	1.96	2.87	171	2.15	2.84	137	2.01	2.88	174	2.01	2.83	178
	2.25	3.03	150	1.99	2.68	146	2.19	2.85	133				2.05	2.84	180
	2.03	2.89	175	1.97	2.77	148	1.96	2.81	169				1.98	2.87	175
	2.08	2.90	159	2.07	2.84	163	1.89	2.90	173				2.37	3.01	133
				2.21	3.04	163	2.21	2.95	139						
				1.93	2.68	145									
				2.33	3.02	136									
N-H···N	1.91	2.85	175	2.60	3.47	160	1.74	2.83	178	1.96	2.85	174	1.77	2.84	167
				2.60	3.47	160							2.34	3.18	170
C-H···O	2.48	3.31	149	2.60	3.31	135	2.54	3.30	132	2.32	3.02	133	2.16	3.08	178
				2.56	3.25	136	2.25	3.23	160	2.52	3.20	132			
				2.51	3.28	140	2.32	3.23	152						
O-H···O	1.79	2.64	160										2.06	2.86	161
	2.12	2.88	135												
	2.49	3.15	126												
	2.22	2.87	125												

Continued...

D-H···A	CHCL21		
N-H···O	1.95	2.81	178
N-H···N	1.41	2.82	180
C-H···O	2.54	3.42	157
N-H···Cl	2.09	2.95	173
	2.29	3.15	172
C-H···Cl	2.79	3.72	180

Continued...

D-H···A	CHBR11			CHBR21			FCHCL11			FCHCL21		
N-H···O	2.00	2.79	176	1.95	2.81	178	2.07	2.77	148	1.95	2.79	174
				1.99	2.85	174	1.90	2.73	170	1.85	2.76	171
				2.13	2.98	170				2.07	2.93	178
				2.36	3.15	154				2.14	2.92	166
				1.96	2.82	175				1.80	2.75	176
N-H···N				2.25	2.89	179				1.91	2.83	178
N-H···Br	2.33	3.18	169	2.57	3.40	163						
	2.75	3.52	149									
	2.70	3.42	162									
	2.80	3.65	142									
N-H···Cl							2.28	3.12	163	2.38	3.17	158
							2.46	3.17	170			
							2.32	3.11	166			
							2.39	3.10	158			
							2.49	3.21	164			
							2.53	3.26	148			
N-H···F							2.47	3.00	123			
C-H···O	2.49	3.24	136	2.44	3.24	144						
				2.49	3.31	147						
O-H···Cl							2.36	3.17	158	2.28	3.12	172
										2.25	3.07	161
O-H···Br				2.50	3.32	159						
				2.44	3.25	147						
C-H···Cl										2.54	3.54	173
C-H···Br				2.70	3.57	156						
O-H···O							2.15	2.83	178			

Continued...

D-H···A	FCHBR11			FCHBR21			FCSAC11			FCSAC21		
N-H···O	2.24	2.89	133	2.07	2.79	172	1.89	2.75	169	1.84	2.75	178
				2.02	2.81	174	1.87	2.73	168	1.92	2.79	178
							2.02	2.85	163	1.81	2.75	178
										2.01	2.80	159
										2.05	2.95	175
										2.14	2.93	163
N-H···N				2.11	2.81	173	1.99	2.88	176	1.94	2.84	179
N-H···Br	2.41	3.23	160	2.55	3.34	161						
	2.63	3.40	148									
	2.61	3.44	162									
C-H···O							2.29	2.99	131	2.54	3.31	137
C-H···F										2.46	3.25	145
										2.55	3.48	171
C-H···Br	2.87	3.68	146	2.87	3.79	177						
C-H···N										2.45	3.14	128
O-H···O										2.31	2.88	156
										2.03	2.81	155
										1.97	2.82	177

the three numbers for each structure indicate H···A, D···A and D-H···A angles, respectively.

Table 3.3

Refcodes for cytosine salts

ACUHIP	ADALAS	ARACYP	ARFCYT10	BEHLIJ	BOMHEQ
BOQBAK	BZCYTN	CASCIJ	CCYTMP	CCYTMP01	CTBGLU
CTSGLM	CYCYPH10	CYTBGL	CYTBGL01	CYTCUC	CYTFGL
CYTIAC	CYTIAC01	CYTICL	CYTIDN	CYTOSC	CYTOSC01
CYTOSC02	CYTPIC	CYTSPD	DCYTCA10	DOCYPO	DOCYPO01
DOCYPO02	DOCYPO03	DOCYPO04	DOCYPO05	DOCYTC	EDATOS
FICXIZ	FUDYIM	FUQHEE	GIFWAT	HABKEA	HEBTOX
HEXWEN	JAPPEV	JAWLUI	JAYNIG	JEJLEQ	JIBDIH
KAYXUD	KEQPEC	KOGBOX	KOGBOX01	LAVYUD	LAVZAK
LEZHON	MCYHBR	MCYTOS	MCYTRI	MECYTO10	MHCYTC
MUWPUP	MUWQAW	MUWQEA	NUJNEL	NUZKEY	OCIRAT
OJERIE	QOCTOR	ROFLAZ	SEGZUZ	TAZZUP	UMIBUN
VAWPIT	VUYMAD	WUFKUD	XAVGAD	XFURCC	XFURCC10
YIDKIF	ZEXGUE	ZEXJOB			

Refcodes for cytosine duplexes

ACAMEX	ACITEM	CIYTOT
CYACET	CYTRES10	CYTZNC
DINYII	DINYII10	FIZLUW
GITYEN	GOXCOL	JOGHES
JOGHES01	JOMCOD	JOQCAT
MCYTIM10	MECTSI	POGGAT
QOCTUX	RADKOX	RADKOX01
SUMDAF	TAZWUN	TAZXAU
TAZXEY	YILYAT	JETHAS
KEVSAG		

3.8 References

[1] Blackburn, E. H. *Nature* **1991**, *350*, 569-573.

[2] Gellert, M.; Lipsett, M. N.; Davies, D. R. *Proc. Natl. Acad. Sci. USA* **1962**, *48*, 2013– 2018.

[3] (a) Davis, J. T. *Angew. Chem. Int. Ed. Engl.,* **2004**, *43*, 668-698. (b) Shi, X.; Fettinger, J. C.; Davis, J. T. *J. Am. Chem. Soc.* **2001**, *123*, 6738-6739. (c) Shi, X.; Fettinger, J. C.; Davis, J. T. *Angew. Chem. Int. Ed. Engl.,* **2001**, *40*, 2827-2831. (d) Wong, A.; Fettinger, J. C.; Forman, S. L.; Davis, J. T.; Wu, G. *J. Am. Chem. Soc.* **2002**, *124*, 742-743. (e) Forman, S. L.; Fettinger, J. C.; Pieraccini, S.; Gottarelli, G.; Davis, J. T. *J. Am. Chem. Soc.* **2000**, *122*, 4060-4067.

[4] Sessler, J. L.; Sathiosatham, M.; Doerr, K.; Lynch, V.; Abboud, K. A. *Angew. Chem. Int. Ed.* **2000**, *39*, 1300-1303.

[5] (a) Kotlyar, A. B.; Borovok, N.; Molotsky, T.; Cohen, H.; Shapir, E.; Porath, D. *Adv. Mater.* **2005**, *17*, 1901-1905. (b) Marsh, T. C.; Vesenka, J.; Henderson, E. *Nucleic Acids Res.* **1995**, *23*, 696-700. (c) Yan, H.; Park, S. H.; Finkelstein, G.; Reif, J. H.; LaBean, T. H. *Science* **2003**, *301*, 1882-1884. (d) Ghodke, H. B.; Krishnan, R.; Vignesh, K.; Kumar, G. V. P.; Narayana, C.; Krishnan, Y. *Angew. Chem. Int. Ed. Engl.,* **2007**, *46*, 2646-2649. (e) Wang, D.; Chen, L. *Nano Lett.* **2007**, *7*, 1480-1484. (f) Li, X.; Peng, Y.; Ren, J.; Qu, X. *Proc. Natl. Acad. Sci. USA* **2008**, *103*, 19658-19663. (g) Alberti, P.; Bourdoncle, A.; Sacca, B.; Lacroix, L.; Mergny, J. L. *Org. Biomol. Chem.* **2006**, *4*, 3383-3391. (h) Liu, H.; Xu, Y.; Li, F.; Yang, Y.; Wang, W.; Song, Y.; Liu, D. *Angew. Chem. Int. Ed. Engl.,* **2007**, *46*, 2515-2517. (i) Beissenhirtz, M. K.; Willner, I. *Org. Biomol. Chem.* **2006**, *4*, 3392-3401. (j) Liedl, T.; Sobey, T. L.;

Simmel, F. C. *Nano Today* **2007**, *2*, 36-41. (k) Alberti, P.; Mergny, J. L. *Proc. Natl. Acad. Sci. USA* **2003**, *100*, 1569-1573. (l) Miyoshi, D.; Inoue, M.; Sugimoto, N. *Angew. Chem. Int. Ed. Engl.,* **2006**, *45*, 7716-7719. (m) Murata, T.; Saito, G.; Nishimura, K.; Enomoto, Y.; Honda, G.; Shimizu, Y.; Matsui, S.; Sakata, M.; Drozdova, O. O.; Yakushi, K. *Bull. Chem. Soc. Jpn.* **2008**, *81*, 331-344. (n) Murata, T.; Nishimura, K.; Saito, G. *Mol.Cryst.Liq.Cryst.,* **2007**, *466*, 101-112. (o) Murata, T.; Saito, G. *Chem. Lett.* **2006**, *35*, 1342-1343.

[6] Gehring, K.; Lorey, J. –L.; Gueron, M. *Nature* **1993**, *363*, 561-565.

[7] Marsh, R. E.; Bierstedt, R.; Eichhorn, E. L. *Acta Cryst.* **2008**, *15*, 310-316.

[8] (a) Li, X.; Peng, Y.; Ren, J.; Qu, X. *Proc. Natl. Acad. Sci. USA* **2008**, *103*, 19658-19663. (b) Liedl, T.; Simmel, F. C. *Nano Letters* **2005**, *5*, 1894-1898. (c) Liu, D.; Balasubramanian, S. *Angew. Chem. Int. Ed. Engl.,* **2003**, *42*, 5734-5736. (d) Xu, Y.; Hirao, Y.; Nishimura, Y.; Sugiyama, H. *Bioorg. Med.Chem.* **2007**, *15*, 1275-1279. (e) Liu, D.; Bruckbauer, A.; Abell, C.; Balasubramanian, S.; Kang, D. J.; Klenerman, D.; Zhou, D. *J. Am. Chem. Soc.* **2006**, *128*, 2067-2071. (f) Beissenhirtz, M. K.; Willner, I. *Org.Biomol.Chem.* **2006**, *4*, 3392-3401. (g) Liedl, T.; Sobey, T. L.; Simmel, F. C. *Nano Today* **2007**, *2*, 36-41. (h) Alberti, P.; Mergny, J. L. *Proc. Natl. Acad. Sci. USA* **2003**, *100*, 1569-1573. (i) Miyoshi, D.; Inoue, M.; Sugimoto, N. *Angew. Chem. Int. Ed. Engl.,* **2006**, *45*, 7716-7719. (j) Alberti, P.; Bourdoncle, A.; Sacca, B.; Lacroix, L.; Mergny, J. L. *Org. Biomol. Chem.* **2006**, *4*, 3383-3391. (k) Liu, H.; Xu, Y.; Li, F.; Yang, Y.; Wang, W.; Song, Y.; Liu, D. *Angew. Chem. Int. Ed. Engl.,* **2007**, *46*, 2515-2517. (l) Seela, F.; Budow, S. *Helv. Chim. Acta* **2006**, *89*, 1978-1985. (m) Liedl, T.; Simmel, F. C. *Nano Letters* **2005**, *5*, 1894-1898. (n) Ghodke, H. B.; Krishnan, R.;

Vignesh, K.; Kumar, G. V. P.; Narayana, C.; Krishnan, Y. *Angew. Chem. Int. Ed. Engl.,* **2007**, *46*, 2645-2649.

[9] Ghoussoub, A.; Lehn, J. M. *Chem. Commun.,* **2006,** 5763-5765.

[10] Liu, H.; Xu, Y.; Li, F.; Yang, Y.; Wang, W.; Song, Y.; Liu, D. *Angew. Chem. Int. Ed.* **2007,** *46,* 2515 –2517.

[11] Ghodke, H. B.; Krishnan, R.; Vignesh, K.; Kumar, G. V. P.; Narayana, C.; Krishnan, Y. *Angew. Chem. Int. Ed.* **2007**, *46*, 2645-2649.

[12] Kang, C.; Berger, I.; Lockshin, C.; Ratliff, R.; Moyzis, R.; Rich, A. *Proc. Natl. Acad. Sci. USA* **1994**, *91*, 11636-11640.

[13] Liu, D.; Balasubramanian, S. *Angew. Chem. Int. Ed.* **2003**, *42*, 5734-5736.

[14] Perumalla, S. R.; Suresh, E.; Pedireddi, V. R. *Angew. Chem. Int. Ed. Engl.,* **2005**, *44*, 7752-7757.

[15] (a) Bruning, W.; Freisinger, E.; Sabat, M.; Sigel, R. K. O.; Lippert, B. *Chem. Eur. J.* **2002**, *8*, 4681-4692. (b) Jaskolski, M. *Acta Crystallogr. ,Sect. C:Cryst. Struct. Commun.* **2008**, *45*, 85-89. (c) Sivalakshmidevi, A.; Vyas, K.; Reddy, G. O.; Sivaram, S. D. V. N.; Swamy, P. V.; Puranik, R.; Sairam, P. *Acta Crystallogr. , Sect. E:Struct. Rep. Online* **2008**, *59*, o1435-o1437. (d) Gdaniec, M.; Brycki, B.; Szafran, M. *J. Mol. Struct.* **1989**, *195*, 57-64. (e) Salam, M. A.; Aoki, K. *Inorg. Chim. Acta* **2000**, *311*, 15-24. (f) Wang, Z.; Cheng, Y.; Liao, C.; Yan, C. *CrystEngComm* **2001**, *3*, 237-242. (g) Trus, B. L.; Marsh, R. E. *Acta Crystallogr. , Sect. B: Struct. Crystallogr. Cryst. Chem.* **1972**, *28*, 1834-1840. (h) Rossi, M.; Marzilli, L. G.; Kistenmacher, T. J. *Acta Crystallogr. ,Sect. B: Struct. Crystallogr. Cryst. Chem.* **1978**, *34*, 2030-2033. (i) Nowak, I.; Cannon, J. F.; Robins, M. J. *J. Org. Chem.* **2007**, *72*, 532-537. (j)

Viswamitra, M. A.; Reddy, B. S.; Lin, G. H. Y.; Sundaralingam, M. *J. Am. Chem. Soc.* **1971**, *93*, 4565-4573. (k) Ohki, M.; Takenaka, A.; Shimanouchi, H.; Sasada, Y. *Bull. Chem. Soc. Jpn.* **1975**, *48*, 848-852. (l) Takenaka, A.; Ohki, M.; Sasada, Y. *Bull. Chem. Soc. Jpn.* **1980**, *53*, 2724-2730. (m) Vijay-Kumar, S.; Sakore, T. D.; Sobell, H. M. *Nucleic Acids Res.* **1984**, *12*, 3649-3657. (n) Swamy, K. C. K.; Kumaraswamy, S.; Kommana, P. *J. Am. Chem. Soc.* **2001**, *123*, 12642-12649.

[16] Allen, F. H.; Kennard, O. *Chem. Des. Automat. News.* **1993**, *8*, 31 – 37.

[17] This structure was reported in literature by *Bouchouit et al.* The coordinates retrived from the CSD have been used for the description of structural aspects, to facilitate comparision with other dicarboxylic acids. Bouchouit, K.; Benali-Cherif, N.; Dahaoui, S.; Bendeif, E.-E.; Lecomte, C. *Acta Crystallogr., Sect. E: Struct. Rep. Online* **2005**, *61*, o2755-o2757.

[18] In the majority of the structures, in this study, duplexes are shown as cytosinium....cytosinium ($CH^{+}\cdots CH^{+}$), due to the crystallographic symmetry requirements, difficulty to locate hydrogen positions from Fourier maps, etc. However, we refer in the description of text, all such situations as **C.CH^{+}** species/moieties/duplexes, for a meaningful and factual chemical representation.

[19] Molecular complex of cytosine and maleic acid in a 1:1 ratio was reported by Balasubramanian and co-workers. The information was retrieved for further structure analysis. Balasubramanian, T.; Muthiah, P. T.; Robinson, W. T. *Bull. Chem. Soc. Jpn.* **1996**, *69*, 2919-2922.

[20] The complex obtained between cytosine and fumaric acid in 2:1 ratio is not discussed herein in detail, as it is isostructural with the 2:1 complex formed between cytosine and succinic acid (discussed in section 3.2.7).

[21] Molecular complex of cytosine and hydrochloric acid, HCl, in a 1:1 ratio was reported by Mandel *et al.* the information was retrieved for further structure analysis. Mandel, N. S. *Acta Crystallogr.,Sect.B: Struct. Crystallogr. Cryst. Chem.* **1977**, *33*, 1079-1082.

[22] (a) Adams, C. J.; Angeloni, A.; Orpen, A. G.; Podesta, T. J.; Shore, B. *Cryst. Growth Des.* **2006**, *6* , 411-422. (b) Angeloni, A.; Crawford, P. C.; Orpen, A. G.; Podesta, T. J.; Benjamin, J. S. *Chem. Eur. J.* **2004**, *10*, 3783-3791

[23] (a) Tassel, D.; Madoff, A. *J. Am. Med. Assoc.* **1968**, *206*, 830-832. (b) Vermes, A.; Guchelaar, H.-J.; Dankert, J. *J. Antimicrob. Chemother.* **2000**, *46*, 171-179.

CHAPTER FOUR

Molecular recognition studies of nucleosides with 5-halouracils

4.1 Introduction

Macromolecules that bind to DNA regulate cellular functions, such as replication and gene expression, etc., often, leading to the unfavorable biological process. However, a few small molecules that block these processes, in general, are potential therapeutic agents.[1] Critical to the understanding of the function of such molecules is the characterization of their binding modes, which are usually investigated through molecular aggregation processes. Such knowledge also may give an account of how recognition processes influence both the structural and mechanical properties of DNA and may also provide a key to more rational drug design.

In this direction, understanding the bioproperties of various molecules, within chemical sciences, is a long standing research goal for the pioneers in chemical biology.[2] Interestingly, many drug molecules have structural similarities to the nucleobases,[3] for example, glutarimides, barbiturates, succinimides, and hydantoins have similarities to uracil and thymine, as shown in Scheme 4.1.

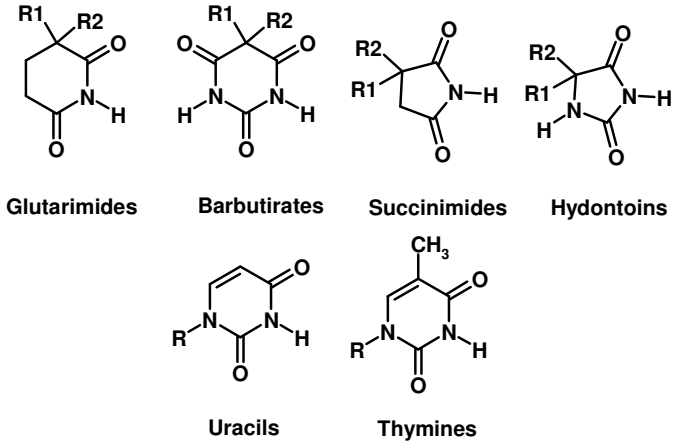

Scheme 4.1. General structure of classes of heterocyclic compounds of pharmacological interest and the structures of bases thymine, uracil.

The molecules, listed above, are well known as metabolic depressants and function as competitive inhibitors in oxidative metabolism, through molecular recognition process between drug substrate and biological macromolecules by following certain reaction pathways. For instance, it is known from the literature that barbiturate drugs form aggregates with adenine derivatives, similar to those found in the base pairs of adenine-thymine and adenine-uracil, and such associations have been suggested to be, in part, the basis of the pharmacological activity of these drugs.[4] If such aggregation is being presented, the biological process may be different, as it was noted that barbiturate derivatives are physiologically effective as sedative-hypnotic agents only when the ($–CH_2$) group is substituted by two nonpolar groups of at least the size of ethyl groups.[5] However, no pairing of the barbiturates was detected with the other nucleobases. Thus, for a through understanding of relation between such bioproperties and functional groups, molecular recognition studies are imminent between the possible drug targets and the constituents of DNA, for example, nucleobases. Thus, several co-crystallization experiments between barbiturates and adenine derivatives were reported and structural elucidations have been carried out for the analysis of molecular geometry and packing of molecules as described below.

Voet *et al.* have studied the molecular recognition between 9-ethyladenine and 5,5-diethylbarbituric acid,[6] and it was noted that the adenine and the barbiturate derivatives associate by the formation of extended hydrogen-bonded strips that contain adenine and barbiturate residues, as shown in Figure 4.1. The layers of hydrogen-bonded strips appear to be held together by a series of stacking interactions, such as π - π, C-H$^{\cdots}$π etc.

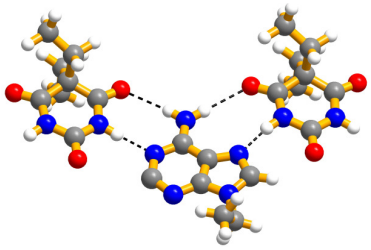

Figure 4.1. Interaction between 9-ethyladenine and 5,5-diethylbarbutiric acid in the solid state.

This strong association has been demonstrated by infrared studies as well, and by the formation of a number of crystalline intermolecular complexes containing derivatives of adenine and barbiturates.[7] The molecular basis of extremely varied pharmacological effects of these molecules might, therefore, be understood in terms of the strong association of the barbiturates with adenine-containing coenzymes as well as with molecules, such as cyclic adenosine monophosphate (**AMP**) that play an important role in controlling various metabolic activities.

Further, similar studies have been carried out on metallo-based drug molecules as well. For example, *cis*-platin (see Scheme 4.2) is a clinically important anticancer drug, being especially effective for the management of testicular, ovarian, head and neck cancers.[8]

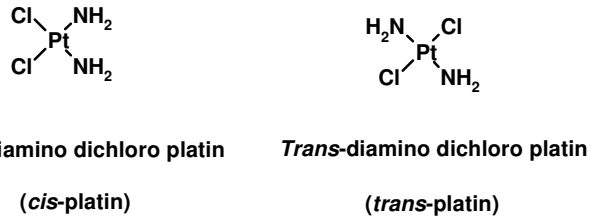

Cis*-diamino dichloro platin** (cis*-platin**)

Trans*-diamino dichloro platin** (trans*-platin**)

Scheme 4.2. Structure of *cis* and *trans*-platin.

While *cis*-platin is one of the most widely used antitumor drugs at the present time, the *trans* isomer is inactive. Considerable evidence points that *cis*-platin directly

binds to the tumor cell. Attention is, therefore, focused on the nature of the adducts formed by *cis* and *trans*-platin with DNA. By using a variety of enzymatic mapping techniques, Lippard and co-workers and others have shown that the most common binding mode of *cis*-platin with DNA involves loss of two chloride ions and formation of two Pt-N bonds to the N^7 atoms of two adjacent guanosine nucleosides on the same strand.[9] For stereochemical reasons, this intrastrand d(GpG) cross-link cannot be formed by *trans*-platin. In general, structural information about the adducts of *cis*-platin with synthetic oligonucleotides was deduced through different analytical techniques like NMR spectroscopic investigations, FT-IR, X-ray diffraction, etc.[10]

The X-ray structural work on Pt-nucleobase complexes[11] provided the structural insights towards its activity, as reported by Sherman *et al.,* with complete details of molecular geometry of the anticancer drug bound to its assumed biological target on DNA (Figure 4.2).[12] In addition, recent molecular mechanics calculations on *cis*-[$Pt(NH_3)_2${d(GpG)}] adducts in two oligonucleotide duplexes and two single-stranded oligomers have provided theoretical insights about the structure.[13]

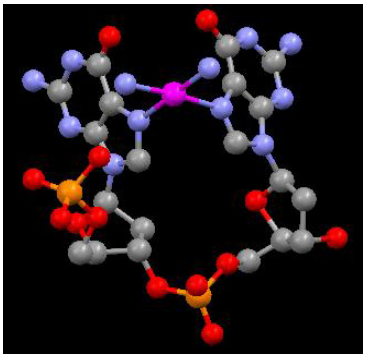

Figure 4.2. Interactions of *cis*-platin in the crystal structure of *cis*-[$Pt(NH_3)_2${d(pGpG)}].

Among many nucleobases derivatives, nucleosides (sugar substituted nucleobase) play a crucial role in various functions and structural aspects of macromolecules through molecular recognition processes. However, such molecular recognition studies in laboratory conditions are not well explored, especially in the co-crystallization experiments that can make significant effect to understand bioactivity of drug targets, as evident from literature search performed using CSD.[14]

For this purposes, the known five nucleosides, i.e., adenosine, cytidine, guanosine, thymidine and uridine (see scheme 4.4), have been chosen to co-crystallize with different drug substrates. In this context, 5-halouracils which are known for drug activity, have been chosen to co-crystallize with the nucleosides and the obtained results are discussed in the following section.

From the literature, halo uracils (XU, X = any halogens, U = uracil) are well known as chemical mutagens, antiviral agents, radio-sensitizers and anticancer drugs etc.,[15] (see in box 1). Although the mechanism of the biological activity of these halouracils is not well understood, it is likely that they inhibit the proper replication of DNA, in tumor and infected cells. Further, towards the understanding of radiosensitisation properties, Sevilla and co-workers studied, by using density functional theory (DFT), the base pair configuration, as shown in Scheme 4.3, which mimics the environment in double-stranded DNA.[16]

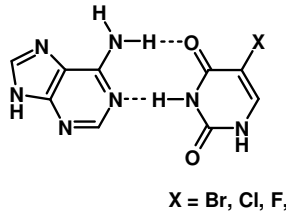

Scheme 4.3. Molecular recognition between adenine and derivatives of uracil.

Box 1

History of 5-halouracils

The 5-halouracils and their derivatives have been extensively investigated as potential anticancer drugs, each exhibiting a different spectrum of inhibitory effects in different animals. For example, 5-fluorouracil, a common anticancer drug, this has been used for cancer treatment for more than 40 years. 5-chlorouracil and 5-bromouracil have been studied to treat inflammatory tissue. Complexes of 5-iodouracil with a variety of transition metal ions (e.g., Mn^{+2}, Co^{+2}, Cu^{+2}, Zn^{+2}, and Cd^{+2}) have been shown to have antitumor activity. The 5-halouracils have also been investigated as a possible class of radio-sensitizers, which are used to control damage to healthy tissues in radiation therapy. Although the mechanism of the antitumor and antiviral action of these complexes is not well understood, it is likely that they inhibit the proper replication of DNA in tumor and infected cells.

Early studies showed that 5-halouracils can be incorporated in DNA and RNA and enhance the sensitivity of these important biomolecules to ionizing radiation. These properties leads to the therapeutic benefits by eventually halting DNA or RNA replication in tumor cells. Elegant experiments have recently been performed to identify the early steps in the enhancement process. One plausible mechanism involves the formation of halouracils anions, which dissociates to form halide anions plus reactive uracil radicals. The latter lead to a multitude of DNA damage, including dimerisation, cross linking and base and sugar radicals.

To intricate the role of nucleobase anions and cations in the reactions initiated by radiation of DNA and RNA has been widely studied. Theoretical studies have also examined the radicals formed after DNA is subjected to ionizing radiation. More recent investigations highlight the calculation of the electron affinities and the ionization potentials of the DNA and RNA bases in order to obtain information about the important initial steps in the radiation damage process.

Further, from the CSD analysis it is apparent that co-crystallization experiments employing halouracils are also very much limited. Indeed, the analysis reveals that only two co-crystals of 5-fluorouracil (with cytosine and 1-methylcytosine) and one with 5-bromouracil (with adenosine) were reported in the literature,[17] and salient structural features of those complexes are described below.

5-fluorouracil complex with cytosine is the first example reported in literature between pyrimidine and pyrimidine bases.[17a] In this complex as well as with 1-methylcytosine, 5-flourouracil establish interactions by cyclic hydrogen bonding network through N-H···N and N-H···O interactions, yielding a quartet arrangement. The arrangement of molecules in the complexes are shown in Figure 4.3.

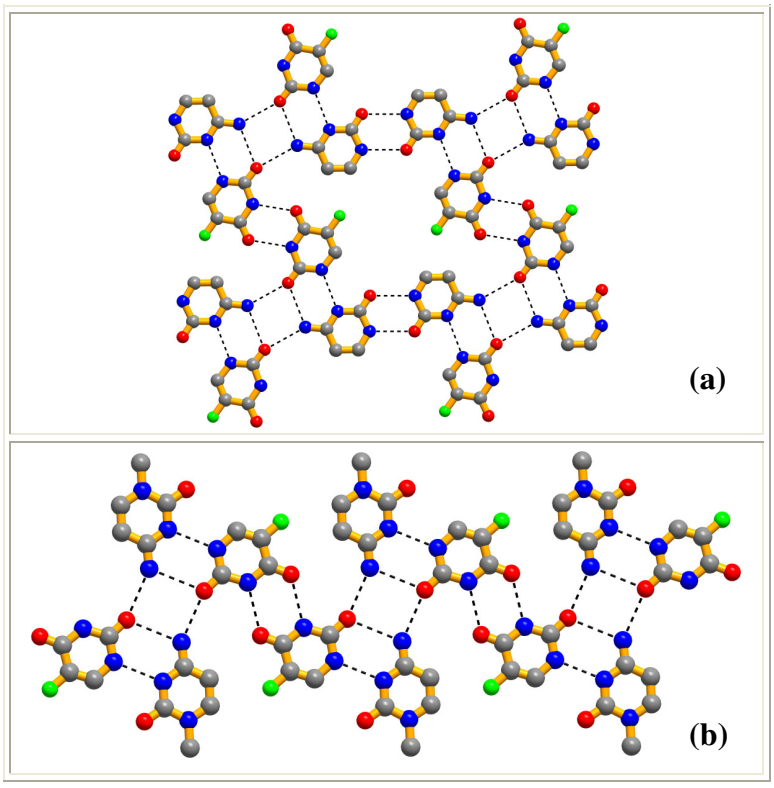

Figure 4.3. Molecular recognition in the complexes of 5-fluorouracil with (a) cytosines and (b) 1-methyl cytosine.

Thus, different halouracils have been chosen for molecular recognition studies with different nucleosides (see Scheme 4.4) to understand, further, the intrinsic nature of interactions between drug targets and biomolecules.

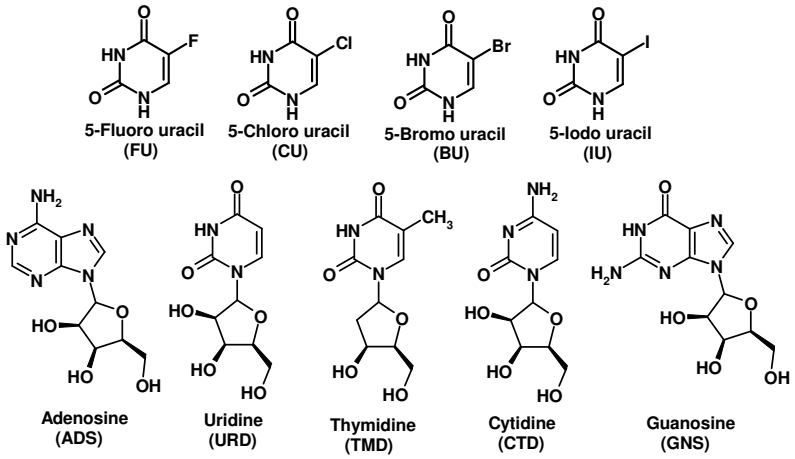

Scheme 4.4

X-ray diffraction (XRD) analysis of the resulting crystals/precipitates revealed that, as observed in the study of nucleobases with –COOH group, as discussed in Chapter 2, nucleosides also did show selectivity in such a manner that adenosine (ADS) and cytidine (CTD) only form molecular complexes with the 5-halouracils, whereas guanosine (GNS) and thymidine/uridine (TMD/URD) remain inert towards the halouracils (XU). The exotic features of the complexes in their recognition patterns, self-assembly and three dimensional packing etc., would be presented in the following sections.

4.2 Molecular adducts of adenosine with 5-halouracils

Adenosine form molecular complexes with each halouracil (5-flourouracil, 5-cholorouracil, 5-bromouracil and 5-iodouracil), upon co-crystallization, by dissolving it in ethanol-water (80:20 v/v %) solution of the halouracil, as the case may be, and

subsequently allowing for slow evaporation at ambient conditions. All the complexes gave good quality single crystals suitable for the analysis by X-ray diffraction methods.

The analysis reveals that the composition of adenosine and the corresponding haloruacil is in 1:1 ratio. Further all the complexes are isomorphous with similar unit cell dimensions and same space group $P2_1$. The complete crystallographic information is given in Table 4.1. The ORTEP diagrams for all the complexes are shown in Figure 4.4. In all the complexes, ADS forms N-H···O intramolecular hydrogen bonding. Other characteristics of hydrogen bonds are given in Table 4.2

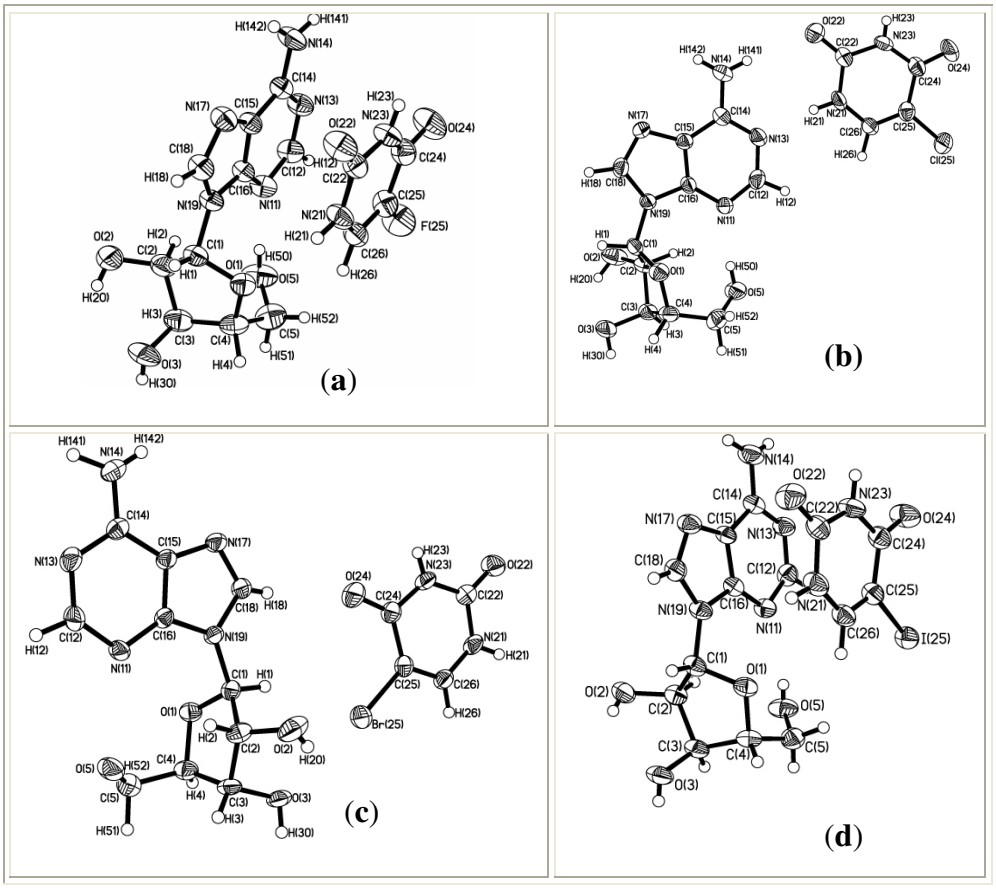

Figure 4.4. Asymmetric unit of complexes of adenosine with a) 5-fluorouracil, b) 5-chlorouracil, c) 5-bromouracil and d) 5-iodouracil.

In addition, packing analysis reveals that all the complexes are also isostructural adopting identical packing arrangement both in two-dimensions as well as in three-dimensions. The arrangement of molecules is shown in Figure 4.5, for a typical complex formed between adenosine and 5-fluorouracil, FU.

In crystal lattice, ADS interact with FU molecules through a cyclic hydrogen bonding patterns comprising of N-H···O (H···O, 2.19Å) and N-H···N (H···N, 1.96 Å), hydrogen bonds, as shown in Figure 4.5(a). Such adjacent binary units are held together, by another cyclic hydrogen bonding patterns, formed due to the C-H···O (H···O, 2.10 Å) and C-H···F (H···F, 2.67 Å) hydrogen bonds, yielding molecular tapes. In two-dimensional arrangement, such tapes are held together by different types of hydrogen bonds, for example O-H···N, N-H···O, C-H···O, etc., as vividly shown in Figure 4.5(b).

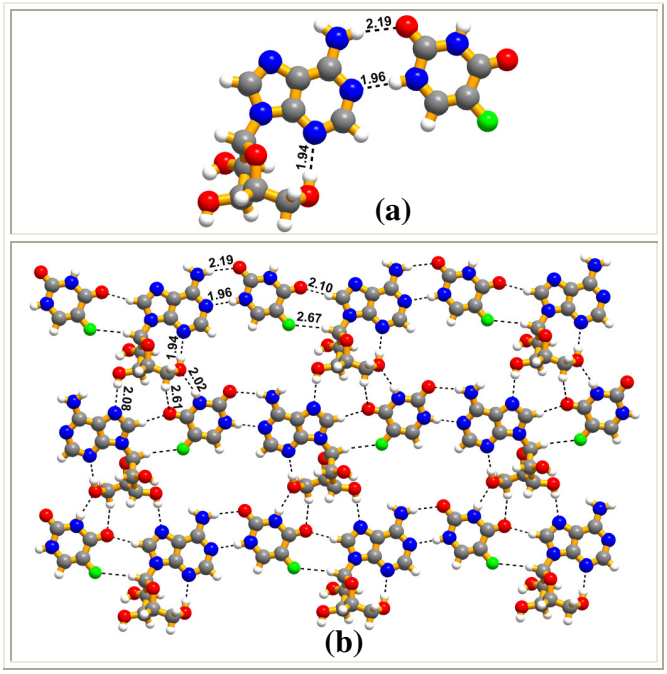

Figure 4.5. (a) Recognition between ADS and a FU and (b) 2D arrangement of ADS-FU adducts forming sheet like structure.

In three-dimensional arrangement, however, the sheets are stacked (see Figure 4.6(a)) in such a way that sugar moieties from the adjacent molecules are held together by forming C-H···O (H···O, 2.71Å) hydrogen bonds, as shown in the Figure 4.6(b). Such an organization mimic a ladder structure, with sugar moieties of ADS molecules function as rods, while cyclic moieties of ADS and uracil constituting rungs, as shown in Figure 4.6. Similarly, in the complexes of ADS with other halouracils also (5-cholorouracil, 5-bromouracil and 5-iodouracil) three-dimensional arrangements represent ladder-type structures. In addition, hydrogen bonding patterns also remain the same except for the bond distances and angles. The two-dimensional structural features of the complexes formed by ADS with 5-chlorouracil (CU), 5-bromouracil (BU) and 5-iodouracil (IU) are shown in Figure 4.7.

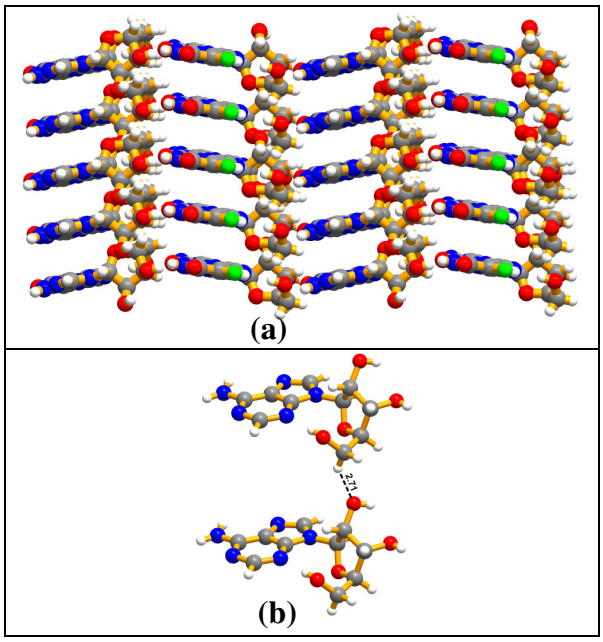

Figure 4.6. (a) Ladder like structure formed in ADS-FU complex and (b) Interaction between sugar moieties exist with C-H···O hydrogen bonds forming rods in the ladders.

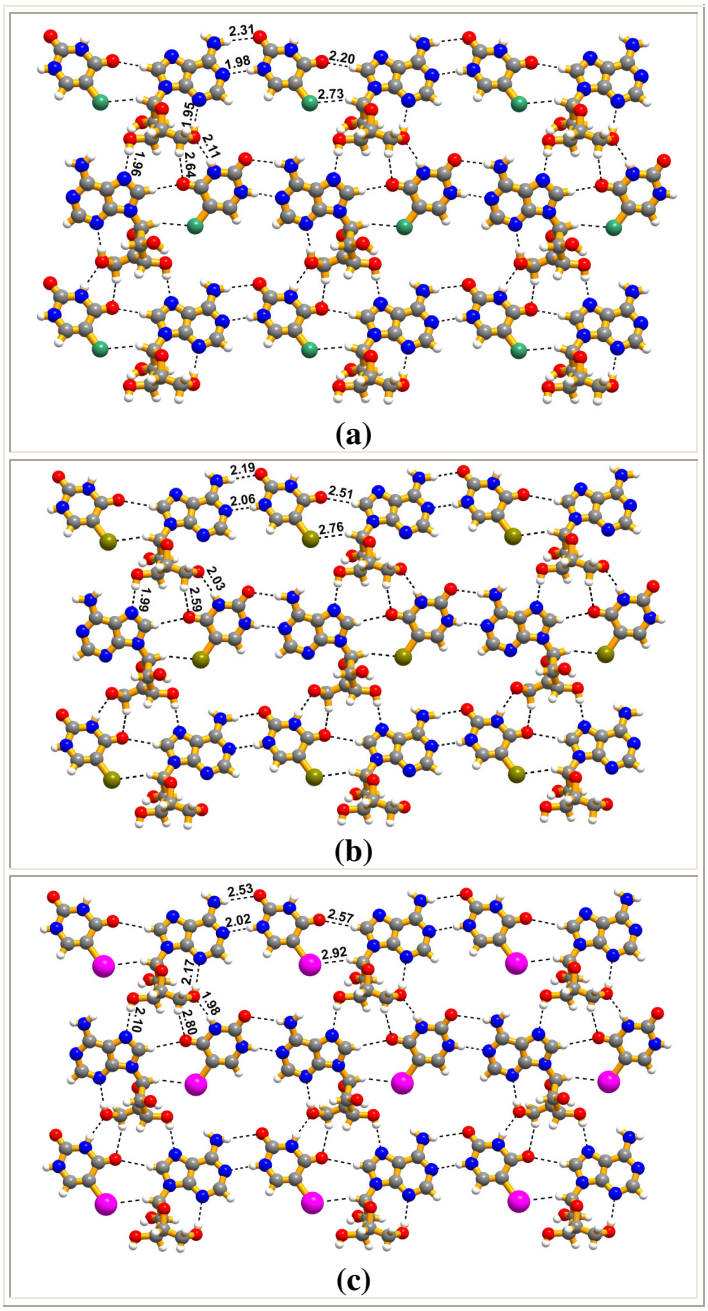

Figure 4.7. Recognition patterns between adenosine and (a) 5-chlorouracil, (b) 5-bromouracil and (c) 5-iodouracils in the crystal structures.

Thus, observing the versatility of all the halouracils to interact with adenosine, further experiments were carried out to evaluate the functional features of halouracils with other nucleosides as well, especially whether any selectivity can be established to

understand the differences in the bioproperties of the halouracils. Interestingly, the experiments reveal that cytidine only formed co-crystals with halouracils as described below.

4.3 Molecular adduct of cytidine with 5-fluorouracil

Cytidine and 5-fluorouracil in a 1:1 ratio, upon dissolving in ethanol and subsequently allowing for slow evaporation of the solvent, gave single crystals of good quality for analysis by x-ray diffraction methods. ORTEP drawing of the asymmetric unit is shown in Figure 4.8. In fact, the structural features of the complex has large similarities with the complex of ADS and 5FU, with respect to the topological features as described below.

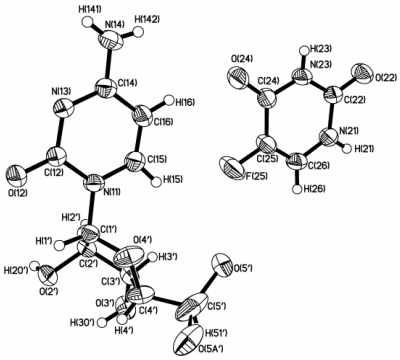

Figure 4.8. ORTEP (50% probability level) drawing of the molecular complex of cytidine and 5-fluorouracil.

In the crystal structure, the constituent molecules interact with each other through the formation of a triple hydrogen bonding network, consisting of N-H···O (H···O, 2.21 Å), N-H···N (H···N, 1.96 Å), and C-H···O (H···O, 2.66 Å), yielding a binary unit (see Figure 4.9(a)). Such adjacent units are held together by a cyclic network of the hydrogen bonds, C-H···O (H···O, 2.26 Å) and C-H···F (H···F, 2.55 Å), constituting

molecular tapes as it was observed in the adenosine complex also. In fact, arrangement in two dimensions also resembles with that of the complex of ADS and FU in terms of topological aspects but with different hydrogen bonding features. In the complex of cytidine and FU, the adjacent molecular tapes are held together by N-H···O (H···O, 2.17, 2.52 Å) and O-H···O (H···O, 1.98 Å) hydrogen bonds (see Figure 4.9(b)). Similarly, in three-dimensional arrangement also, the adjacent sheets are stacked and interact with each other through O-H···O (H···O, 1.98 Å) hydrogen bonds formed by sugar moieties (See Figure 4.10). Thus a ladder type structure is noted in the complex of CTD and FU as well.

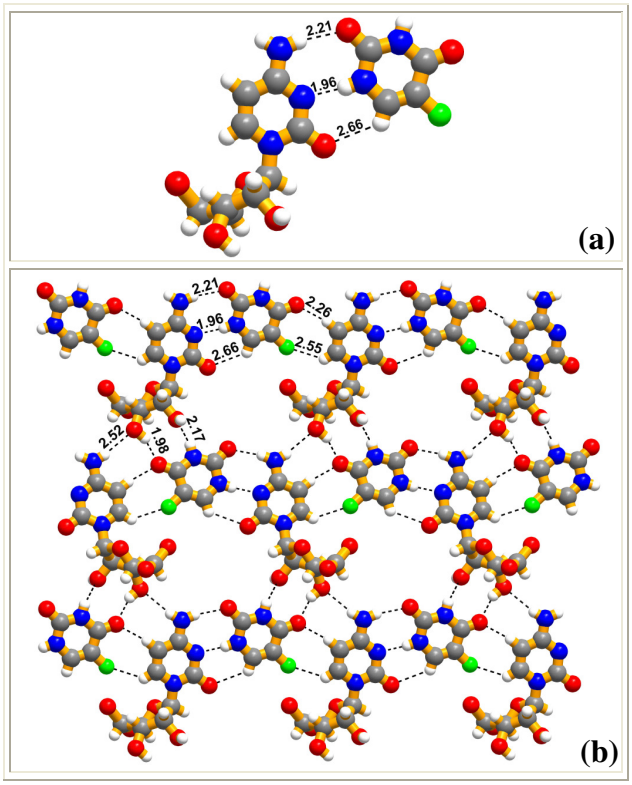

Figure 4.9. (a) Recognition pattern between FU and CTD in the molecular adduct. (b) 2D arrangement of CTD-FU adduct forming sheet like structure.

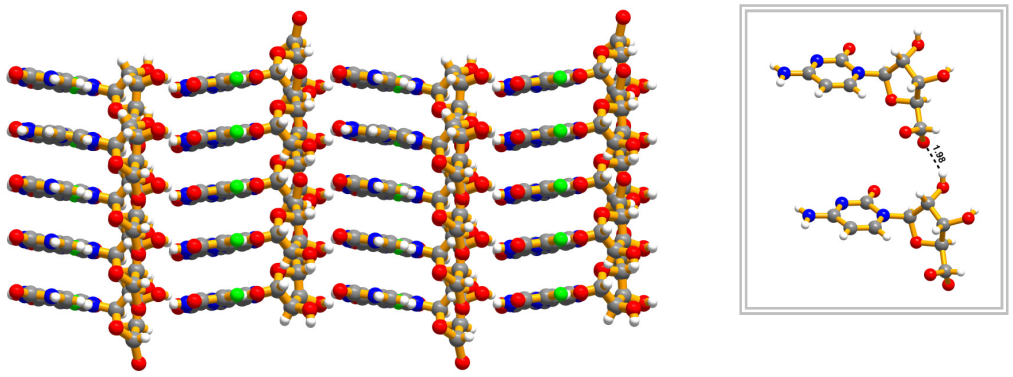

Figure 4.10. Ladder like structure formed in CTD-FU complex. Inset figure shows the interaction between sugar moieties exist with O-H···O hydrogen bonds forming rods in the ladders.

In continuation of co-crystallization experiments with other halouracils (chloro, bromo and iodo uracils), the single crystals could not be obtained, hence, three-dimensional structure elucidation by x-ray diffraction methods, could not be carried out. However, the obtained precipitates were characterized by powder diffraction methods, to evaluate the formation of complexes.

4.4 Powder diffraction analysis of complexes of cytidine with chloro, bromo and iodo uracils

The powder patterns recorded on the residues obtained from co-crystallization experiments of cytidine with chloro, bromo and iodo uracils are shown in Figure 4.11. It is evident that the major peaks of cytidine and also of uracils are present in the residual patterns shown in Figure 4.11(e,f,g). It is evident that there are some new peaks at 12.7, 13.6, 19.4, 22, and 22.7 °, as shown in Figures 4.11(e,f,g), that may be accounted for the formation of complexes. However, intensities are very low, perhaps indicate that the complexes are formed in very small quantities, between cytidine and corresponding halouracils, this is substantiated indeed with the observation of peaks

corresponding to both the reactants in the residue peaks. For example, in Figure 4.11(f), the peaks at 8.8, 12.4, 15.7, 18, 22.8, 25, 26, 27.8, 30.4 and 36.2 º are same as observed as characteristic peaks in Figure 4.11(a) and (c) corresponds to cytidine and bromouracil.

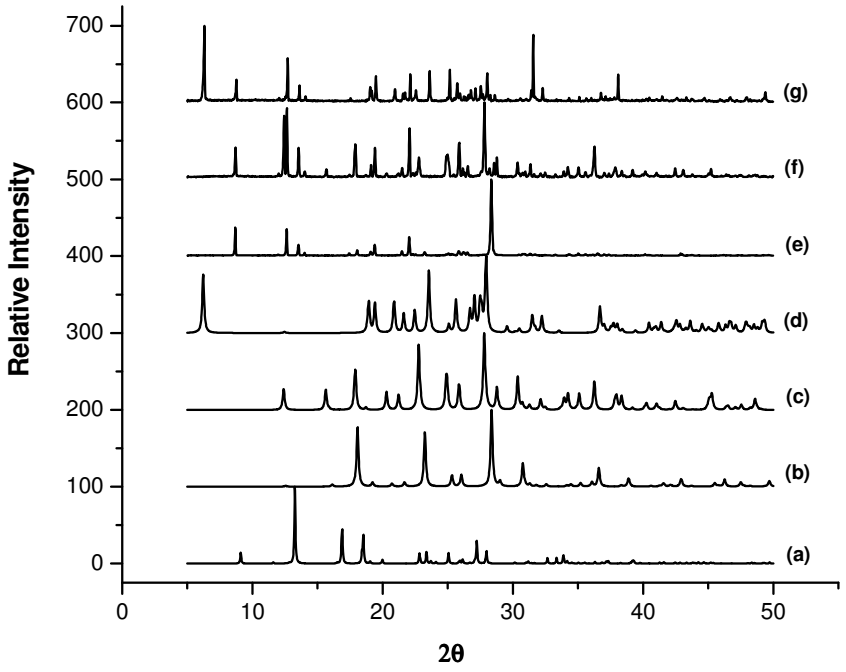

Figure 4.11. Powder X-ray diffraction patterns of (a) cytidine, (b) chlorouracil, (c) bromouracil, (d) iodouracil, (e) cytidine-chlorouracil, (f) cytidine-bromouracil and (g) cytidine-iodouracil.

4.5 Uridine, thymidine and guanosine with 5-halouracils

Co-crystallization of other nucleosides, i.e., uridine, thymidine and guanosine, with 5-halouracils from various solvents such as ethanol, methanol, water, etc., also gave only polycrystalline material. However, analysis by powder x-ray diffraction methods, as shown in Figure 4.12, 4.13, and 4.14, for the residues obtained for uridine,

thymidine and guanosine, respectively, during the course of co-crystallization experiments, indicates that in neither of the cases molecular complexes did form. For example, in the Figure 4.12, the peaks corresponding to uridine at 14, 19, 22 and 26 º etc., and peaks correspond to fluorouracil 16 and 29 º etc., are also present in the residue patterns (Figure 4.12(f)), with the only difference being absolutely no. Peak intensity, which may be due to the variation in the crystallinity nature of the residues.

In other patterns of the residues corresponding to different uracils, the situation is similar with the patterns are the mixture of the reactant peaks without any additional peaks. Thus, in Figure 4.13 and 4.14 also the patterns are additive patterns of the either thymidine/guanosine and corresponding uracils.

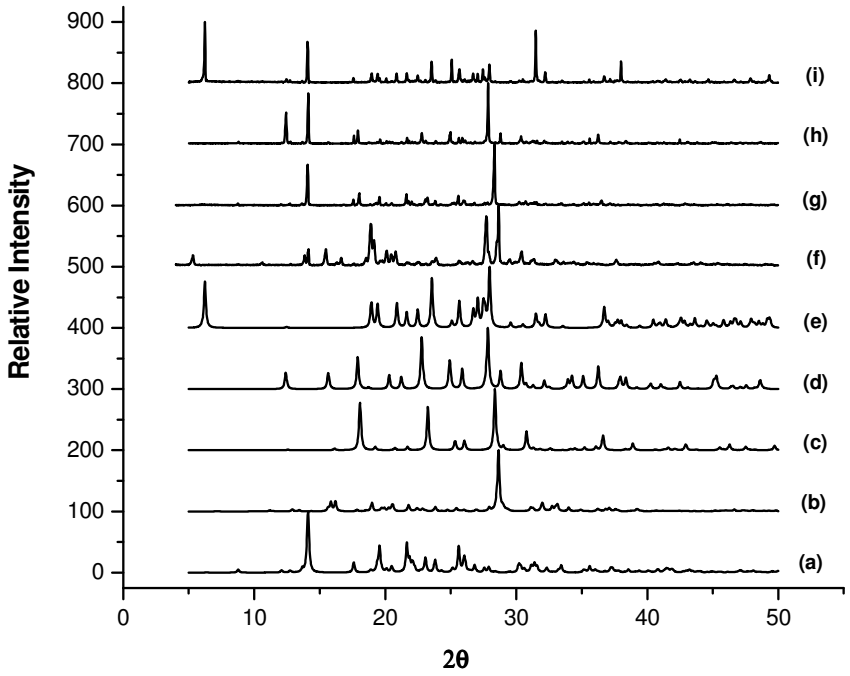

Figure 4.12. Powder X-ray diffraction patterns of (a) uridine, (b) fluorouracil, (c) chlorouracil, (d) bromouracil, (e) iodouracil, (f) uridine - fluorouracil, (g) uridine - chlorouracil, (h) uridine - bromouracil and (i) uridine - iodouracil.

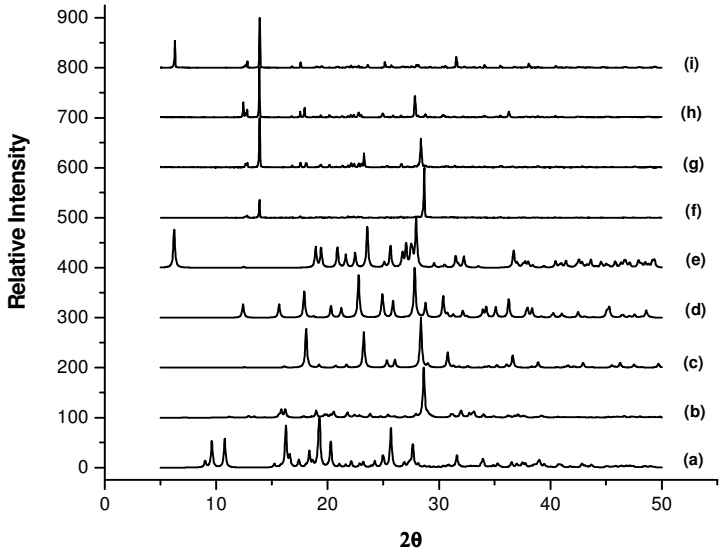

Figure 4.13. Powder X-ray diffraction patterns of (a) thymidine, (b) fluorouracil, (c) chlorouracil, (d) bromouracil, (e) iodouracil, (f) thymidine - fluorouracil, (g) thymidine -chlorouracil, (h) thymidine - bromouracil and (i) thymidine - iodouracil.

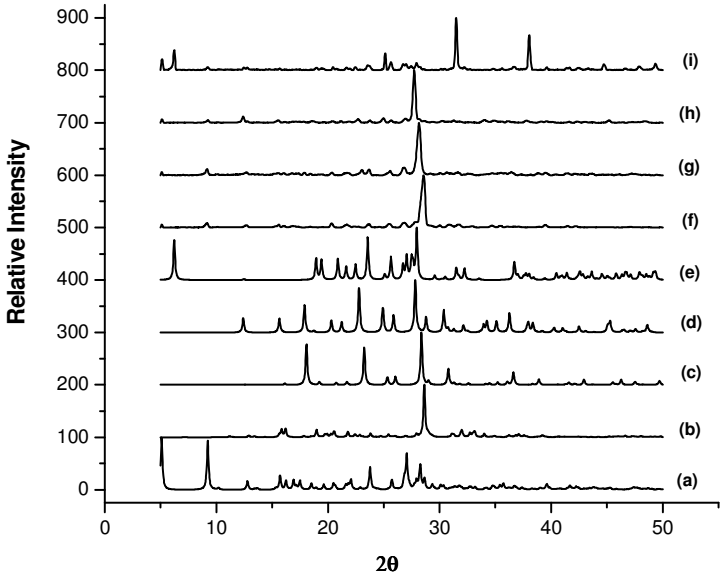

Figure 4.14. Powder X-ray diffraction patterns of (a) guanosine, (b) fluorouracil, (c) chlorouracil, (d) bromouracil, (e) iodouracil, (f) guanosine - fluorouracil, (g) guanosine -chlorouracil, (h) guanosine - bromouracil and (i) guanosine - iodouracil.

4.6 Conclusions

In conclusion, the molecular recognition features have been discussed for the complexes formed by ADS and CTD with different halouracils and the noted selectivity of FU towards ADS and CTD may be of significant in further understanding of bio-processes related to the nucleosides. To supplement these findings, molecular recognition features of nucleobases and nucleosides with various bioactive compounds need to be further explored, which could be utilized as model interactions towards understanding many biological processes.

4.7 Experimental section

All the chemicals used in this study were obtained commercially and used as such without any further purification. HPLC grade solvents were used for carrying out experiments. The synthesis of molecular complexes was carried out, by dissolving the reactants in the appropriate solvents either at room temperature or by warming on a water bath and subsequently cooling by a slow-evaporation method. In a typical experiment, 133.5 mg (0.5 mmol) of adenosine and 65 mg (0.5 mmol) of 5-fluorouracil were dissolved in ethanol solution on water bath and then subsequently cooled to room temperature. Colorless rectangular block shaped single crystals of good quality were obtained over a period of one week and were used for X-ray diffraction studies.

Cytidine-5-fluoruracil adduct was prepared by dissolving cytidine (122 mg, 0.5 mmol) and 5-fluoruracil *(*65 mg, 0.5 mmol) in ethanol/water (v/v 60:40). Slow evaporation of solvent gave good quality single crystals suitable for X-ray diffraction.

Powder X-ray diffraction (PXRD) was recorded on a PNAlytical 1712 (Philips Systems Inc) diffractometer using Cu Kα X-radiation at 40 kV and 30 mA. Diffraction patterns were collected over a range of 5-50° 2θ at a scan rate of 10° / min^{-1}. 40-50 mg of samples was ground and loaded in glass sample holder at room temperature. The programs X'Pert High Score were used for processing and comparing powder patterns.

4.8 Crystal structure determination

Good quality single crystals of all complexes, grown as described above were carefully chosen with the aid of polarized optical microscope and glued to glass fiber to mount on a X-ray diffractometer goniometer equipped with CCD area detector. The data collection proceeded without any complication and processed using the Bruker suite of software. The structures were determined and refined using SHLEXTL suite of programmes, and absorption corrections were made on all the crystals using SADABS. All the non-hydrogen atoms were refined by anisotropically. The hydrogen atom positions were taken from a difference Fourier maps and were refined isotropically. The structural parameters were given in Tables 4.1 and 4.2. All the intra and intermolecular distances were computed using PLATON software. The packing drawings were generated either by XP package of SHELXTL, or diamond software.

Table 4.1

	ADSFU	ADSCU	ADSBU	ADSIU	CTDFU
Empirical formula	$C_{14}H_{16}F_1N_7O_6$	$C_{14}H_{16}Cl_1N_7O_6$	$C_{14}H_{15}Br_1N_7O_6$	$C_{14}H_{16}I_1N_7O_6$	$C_{13}H_{14}F_1N_5O_7$
Formula wt.	397.34	413.79	457.24	505.24	371.29
Crystal system	Monoclinic	Monoclinic	Monoclinic	Monoclinic	Monoclinic
Space group	$P2_1$	$P2_1$	$P2_1$	$P2_1$	$P2_1$
T [K]	298	298	298	298	298
a [Å]	6.990(1)	7.033(2)	7.068(1)	7.102(1)	5.114(1)
b [Å]	17.345(2)	16.994(4)	16.917(3)	16.842(3)	20.041(5)
c [Å]	7.122(1)	7.276(2)	7.367(1)	7.519(1)	7.783(2)
α [°]	90.00	90.00	90.00	90.00	90.00
β [°]	103.50(1)	103.02(1)	103.07(1)	102.66(1)	101.10(1)
γ [°]	90.00	90.00	90.00	90.00	90.00
Z	2	2	2	2	2
Volume [Å^3]	839.6(2)	847.3(4)	858.0(2)	877.5(2)	782.8(3)
D_{calc} [g/cm^3]	1.572	1.622	1.770	1.912	1.575
F (000)	412	428	462	500	384
μ [mm^{-1}]	0.132	0.279	2.448	1.876	0.137
$2\theta_{max.}$	4.70-50.48	4.80-50.52	4.82-50.50	4.84-46.54	5.34-50.54
Range h	-8 to 8	-8 to 8	-7 to 8	-5 to 7	-6 to 6
Range k	-17 to 20	-20 to 18	-19 to 20	-18 to 18	-24 to 24
Range l	-8 to 6	-8 to 8	-8 to 6	-8 to 8	-9 to 9
N-total	4362	4370	4311	3774	7624
N-independent	2536	2461	2946	2302	2828
N-observed	2220	2005	2761	2274	2549
R_1 [I>2σ(I)]	0.0309	0.0365	0.0346	0.0163	0.0341
wR_2	0.0634	0.0644	0.0842	0.0404	0.0775
GOF	0.953	0.927	1.024	1.031	1.061

Table 4.2: Characteristic hydrogen bonds (distances/Å and angles/°)[#]

D-H···A	ADS-FU			ADS-CU			ADS-BU			ADS-IU			CTD-FU		
N-H···O	2.02	2.80	168	2.11	2.80	164	2.03	2.79	165	1.97	2.77	166	2.17	2.88	146
	2.19	3.05	169	2.31	3.15	175	2.19	3.18	178	2.53	3.26	179	2.21	3.07	168
													2.52	3.31	165
N-H···N	1.96	2.85	179	1.98	2.84	174	2.07	2.85	166	2.01	2.87	172	1.96	2.77	175
O-H···O	2.15	2.65	121	2.49	3.07	124	2.25	2.68	127	2.34	2.70	122	1.98	2.63	142
													2.44	2.97	127
													1.98	2.79	157
C-H···F	2.67	3.64	164										2.55	3.20	130
C-H···Cl				2.73	3.67	154									
C-H···Br							2.76	3.69	155						
C-H···I										2.92	3.75	155			
O-H···N	2.08	2.85	171	1.96	2.80	169	1.99	2.80	173	2.16	2.82	166			
	1.95	2.77	177	1.95	2.78	173				2.10	2.78	174			
C-H···O	2.60	3.36	129	2.20	3.17	173									
	2.10	3.08	171	2.40	3.26	144	2.51	3.24	172	2.55	3.13	120	2.57	3.48	163
	2.45	3.31	145				2.40	3.27	151	2.57	3.40	170	2.26	3.18	168
							2.59	3.42	134	2.56	3.36	142	2.59	3.29	136

the three numbers for each structure indicate H···A, D···A and D-H···A angles respectively.

4.9 References

[1] (a) Neidle, S.; Waring, M., Eds.; Molecular Aspects of Anticancer Drug-DNA Interactions; CRC: Boca Raton, **1993**; Vols. 1 and 2 (b) D'incalci, M.; Sessa, C. *Expert Opin. Invest. Drugs* **1997**, *6*, 875-884.

[2] (a) Spring, D. R. *Chem. Soc. Rev.* **2005,** *34*, 472-482. (b) Dervan, P. B. *Bioorg. Med. Chem.* **2001**, *9*, 2215-2235. (c) Hsu, C. F.; Phillips, J. W.; Trauger, J. W.; Farkas, M. E.; Belitsky, J. M.; Heckel, A.; Olenyuk, B. Z.; Puckett, J. W.; Wang, C. C. C.; Dervan, P. B. *Tetrahedron* **2007,** *63*, 6146-6151. (d) Dose, C.; Ho, D.; Gaub, H. E.; Dervan, P. B.; Albrecht, C. H. *Angew. Chem. Int. Ed. Engl.* **2007,** *46*, 8384-8387. (e) White, S.; Szewczyk, J. W.; Turner, J. M.; Baird, E. E.; Dervan, P. B. *Nature* **1998,** *391*, 468-471.

[3] (a) Simons, C. Nucleoside mimetics: Their chemistry and biological properties; Simons, C., Gordon and Breach science publishers, **2001**.

(b) http://www.accessdata.fda.gov/scripts/cder/drugsatfda/

[4] (a) Voet, D.; Rich, A. *J. Am. Chem. Soc.* **1972**, *94*, 5888-5891. (b) Camerman, A.; Mastropaolo, D.; Hempel, A.; Camerman, N. *Can. J. Chem.* **2000**, *78*, 1045-1051. (c) Epstein, R. H.; Zeiger, A. V.; Crocker, C.; Voet, D. *Acta Crystallogr., Sect. B: Struct. Crystallogr. Cryst. Chem.* **1976**, *32*, 2180-2188. (d) Kim, S. H.; Rich, A. *Proc. Nat. Acad. Sci. USA* **1968**, *60*, 402-408. (e) Bush, M. T. *Physiological Pharmacology;* Academic: New York, **1963**.

[5] (a) Sharpless, S. K. in "The Pharmacological Basis of Therapeutics," 3rd ed, Goodman, L. S.; Gilman, A. Ed., Macmillan, New York, **1965**.

[6] Voet, D. *J. Am. Chem. Soc.* **1972**, *94*, 8213-8222.

[7] (a) Buchet, R.; Sandorfy, C. *J. Phys. Chem.* **1983**, *87*, 275-280. (b) Kyogoku, Y.; Lord, R. C.; Rich, A. *Nature* **1968**, *218,* 69-72. (c) Buchet, R.; Sandorfy, C. *J. Phys. Chem.* **1984**, *88*, 3274-3282. (d) Kim, S. -H.; Rich, A. *Proc. Natl. Acad. Sci. U. S. A.* **1968**, *60*, 402-408.

[8] (a) Rosenberg, B.; VanCamp, L.; Trosko, J. E.; Mansour, V. H. *Nature* **1969**, *222,* 385-386. (b) Jamieson, E. R.; Lippard, S. J. *Chem. Rev.* **1999**, *99*, 2467 –2498.

[9] (a) Fichtinger-Schepman, A. M. J.; Veer, J. L. V.; Hartog, J. H. J. D.; Lohman, P. H. M.; Reedijk, J. *Biochemistry* **1985**, *24,* 707-713. (b) Plooy, A. C. M.; Fichtinger-Schepman, A. M. J.; Schutte, H. H.; Van Dijk, M.; Lohman, P. H. M. *Carcinogenesis* **1985**, *6*, 561-566. (c) Tullius, T. D.; Lippard, S. J. *J. Am. Chem. Soc.* **1981**, *103,* 4620-4622. (d) Royer-Pokora, B.; Gordon, L. K.; Haseltine, W. A. *Nucleic Acids Res.* **1981**, *9,* 4595-4609. (e) Pinto, A. L.; Lippard, S. J. *Proc. Natl. Acad. Sci. U.S.A.* **1985**, *82*, 4616-4619. (f) Pinto, A. L.; Lippard, S. J. *Biochim. Biophys. Acta.* **1984**, *780,* 167.

[10] (a) Hartog, J. H. J. D.; Altona, C.; Chottard, J. –C.; Girault, J. –P.; Lallemand, J. –Y.; Leeuw, F. A. A. M.; Marcelis, A. T. M.; Reedijk, J. *Nucleic Acids Res.* **1982**, *10*, 4715-4730. (b) Den Hartog, J. H. J.; Altona, C.; Van der Marel, G. A.; Reedik, J. *Eur. J. Biochem.* **1965**, *147*, 371 and references cited therein.

[11] (a) Lippert, B. *Coord. Chem. Rev.* **2000**, *200-202*, 487-516. (b) Lippert, B. "Cisplatin: Chemistry and Biochemistry of a Leading Anticancer Drug", VHCA and Wiley-VCH, Weinheim, **1999**.

[12] Sherman, S. E.; Gibson, D.; Wang, A. H. J.; Lippard, S. J. *Science* **1985**, *230*, 412-417.

[13] (a) Kozelka, J.; Petako, G. A.; Lippard, S. J.; Quigley, G. J. *J. Am. Chem. Soc.* **1985**, *107*, 4079-4081, (b) Kozelka, J.; Petako, G. A.; Quigley, G. J.; Lippard, S. J. *Inorg. Chem.* **1986**, *25*, 1075-1077.

[14] Allen, F. H.; Kennard, O. *Chem. Des. Automat. News*. **1993**, *8*, 31-37.

[15] (a) Boudaiffa, B.; Cloutier, P.; Hunting, D.; Huels, M. A.; Sanche, L. *Science* **2000**, *287*, 1658-1660. (b) Carime, H. A.; Huels, M. A.; Illenberger, E.; Sanche, L. *J. Am. Chem. Soc.* **2001**, *123*, 5354-5355. (c) Dugal, P. C.; Carime, H. A.; Sanche, L. *J. Phys. Chem. B* **2000**, *104*, 5610-5617. (d) Hanus, M.; Kabelac, M.; Nachtigallova, D.; Hobza, P. *Biochemistry* **2005**, *44*, 1701-1707. (e) Hu, X.; Hu, H.; Ding, J.; Han, S. *Biochemistry* **2004**, *43*, 6361-6369. (f) Li, X.; Sanche, L.; Sevilla, M. D. *J. Phys. Chem. A* **2002**, *106*, 11248-11253. (g) Cohen, S. S.; Flaks, J. G.; Barner, H. D.; Loeb, M. R.; Lichtenstein, J. *Proc. Nat. Acad. Sci. USA* **1958**, *44*, 1004-1012. (h) Lewis, C. W.; Tarrant, G. M. *Mutation,* **1971**, *12,* 349. (i) Aebersold, P. M. *Cancer Res.,* **1979**, *39,* 808-810. (j) Freese, E. *J. Mol. Biol.,* **1959**, *1,* 87. (k) Henderson, J. P.; Byun, J.; Takeshita, J.; Heinecke, J. W. *J. Biol. Chem.* **2003**, *278*, 23522-23528. (l) Jiang, Q.; Blount, B. C.; Ames, B. N. *J. Biol. Chem.* **2003**, *278*, 32834-32840. (m) Grem, J. L. *Invest. New Drugs* **2000**, *18*, 299-313.

[16] Li, X.; Sevilla, M. D.; Sanche, L. *J. Am. Chem. Soc.* **2003**, *125*, 8916-8920.

[17] (a) Voet, D.; Rich, A. *J. Am. Chem. Soc.* **1969**, *91*, 3069-3075. (b) Kim, S.-H.; Rich, A. *J. Mol. Biol.* **1969**, *42*, 87-95. (c) Aiba, K.; Hata, T.; Sato, S.; Tamura, C. *Acta Cryst. , Sect. B* **1978**, *34*, 1259-1263.

Publications

1) **"**Nucleobases in Molecular Recognition: Molecular Adducts of Adenine and Cytosine with COOH Functional Groups". **Sathyanarayana Reddy Perumalla,** E. Suresh, V. R. Pedireddi, *Angew. Chem. Int. Ed. Engl.* **2005**, *44*, 7752 – 7757.
2) "Molecular Recognition between Nucleobases and Bioactive Molecules: Supramolecular Assemblies of Thymine/Uracil and Melamine". **Sathyanarayana Reddy Perumalla,** E. Suresh and V. R. Pedireddi. (*Manuscript submitted*).
3) "Supramolecular Assemblies of Halouracils and Nucleosides". **Sathyanarayana Reddy Perumalla** and V. R. Pedireddi. (*Manuscript submitted*).
4) "Cytosine-Cytosine$^+$ Duplexes (Base Pairs in *i*-Motifs) in Supramolecular Synthesis". **Sathyanarayana Reddy Perumalla** and V. R. Pedireddi. (*Manuscript submitted*).
5) **"**Molecular recognition studies between cytosine with a molecules having acidic hydrogen". **Sathyanarayana Reddy Perumalla** and V. R. Pedireddi. (*Manuscript under preparation*).
6) **"**Pharmaceutical salts of an antifungal drug, 5-fluorocytosine".**Sathyanarayana Reddy Perumalla** and V. R. Pedireddi. (*Manuscript under preparation*).
7) **"**Review article: All about nucleobases and their derivatives". **Sathyanarayana Reddy Perumalla** and V. R. Pedireddi. (*Under preparation*).

Symposia/invited talk etc.

- Royal Society of Chemistry "West India Section" Ph.D. Students Symposium 19-20th October 2007, Goa University, INDIA
- International school of crystallography 39th course – Engineering of crystalline materials properties: State-of-the-art in modeling, design, applications held between 7th and 17th June 2007 at "Ettore Majorana" foundation and centre for scientific culture, Italy.

- Symposium on "Asia Academic Seminar on molecular and supramolecular materials with designed functions" held between 24th and 28th February 2007 at National Chemical Laboratory, Pune, India.
- Royal Society of Chemistry "West India Section" student symposium, 24-25th Sept 2004, IIT Bombay, INDIA.
- Symposium on "50 years of collagen triple helix: A celebration of science" 7th August 2004, Delhi, India.

Awards

- **ERICE VACIAGO AWARD 2007** in the International School of Crystallography 39th course – Engineering of Crystalline Materials Properties: State-of-the-art in Modeling, Design, Applications held between 7th and 17th June 2007 at "Ettore Majorana" Foundation and Centre for Scientific Culture, Italy.
- **Dr. Rajappa award** for the best paper in organic chemistry 2005; National Chemical Laboratory, Pune, INDIA. 2005.